

A. KALIN



**Euro Electromagnetics**  
30 May - 2 June 2000, Edinburgh

# **BOOK OF ABSTRACTS**

**EUROEM 2000**  
30 May - 2 June 2000, Edinburgh

Conference Secretariat, EUROEM 2000, c/o Concorde Services Ltd  
Suite 325, The Pentagon Centre, Washington Street, Glasgow G3 8AZ, Scotland, UK

Tel: +44 (0) 141 221 5411 Fax: +44 (0) 141 221 2411



**Euro Electromagnetics**  
30 May - 2 June 2000, Edinburgh

# **Oral Presentations**

# Programme Overviews

**Tuesday, 30 May 2000**

	<b>Pentland</b>	<b>Fintry</b>	<b>Sidlaw</b>	<b>Moorfoot</b>	<b>Kilsyth</b>	<b>Tinto</b>
0900 – 1040		HPEM-1: Sources 1	HPEM-2: Materials	S5 - Intentional EMI	S1 - Fundamental Solutions of Maxwell's Equations	UWB-2: Radar Systems
1040 – 1100	<b>Coffee Break</b>					
1100 – 1240		HPEM-1: Sources 1	HPEM-9: Measurement	S5 - Intentional EMI	S1 - Fundamental Solutions	UWB-2: Radar Systems
1240 – 1400	<b>Lunch Break</b>					
1400 – 1540		HPEM-3: Vulnerability 1	HPEM-4: Methods	S5 - Intentional EMI	S1 - Fundamental Solutions & UWB-1: EM Theory 1	UWB-2: Radar Systems & UWB-8: Target Identification & Propagation
1540 – 1600	<b>Coffee Break</b>					
1600 – 1740		HPEM-3: Vulnerability 1	HPEM-4: Methods	S5 - Intentional EMI	UWB-1: EM Theory 1	UWB-8: Target Identification & Propagation
1930 - 2100	<b>Millennium Reception at Edinburgh Castle</b>					

**Wednesday, 31 May 2000**

	<b>Pentland</b>	<b>Fintry</b>	<b>Sidlaw</b>	<b>Moorfoot</b>	<b>Kilsyth</b>	<b>Tinto</b>
0900 – 1035	Plenary Sessions					
1035 – 1055	<b>Coffee Break</b>					
1055 – 1235	Plenary Sessions					
1235 – 1400	<b>Lunch Break</b>					
1400 – 1540	S2 - EMC Modelling Tools			S6 - Basics of Detection	S9 - High Power Facilities	UWB-5: Antennas 1
1540 – 1600	<b>Coffee Break</b>					
1600 – 1740	S2 - EMC Modelling Tools			S6 - Basics of Detection	S9 - High Power Facilities	UWB-5: Antennas 1
1600 – 1740	<b>UWB &amp; UXO Poster Session (Cromdale)</b>					

# Programme Overviews

Thursday, 1 June 2000

	Pentland	Fintry	Sidlaw	Moorfoot	Kilsyth	Tinto
0900 – 1040		HPEM-11: Vulnerability 2	HPEM-5: Environments: Lightning, EMP	S4 - Geomagnetic Storms	S3 - UWB Polarimetry	UWB-3/ HPEM-8: Pulsed Power
1040 – 1100	<b>Coffee Break</b>					
1100 – 1240		HPEM-11: Vulnerability 2	UWB-4: EM Theory 2	S4 - Geomagnetic Storms	S3 - UWB Polarimetry	UWB-3/ HPEM-8: Pulsed Power
1240 – 1400	<b>Lunch Break</b>					
1400 – 1540		S7 - UWB & Transient Measurement	S4 - Geomagnetic Storms	UWB-7: Signal Processing	UWB-3/HPEM-8: Pulsed Power & HPEM-12/UWB-9 High Power Antennas	UXO-1: Detection/Sensor Technologies (Landmines)
1540 – 1600	<b>Coffee Break</b>					
1600 – 1740		S7 - UWB & Transient Measurement	S4 - Geomagnetic Storms	UWB-7: Signal Processing	HPEM-12/ UWB-9: High Power Antennas	UXO-1: Detection/Sensor Technologies (Landmines)
1600 - 1740	<b>HPEM Poster Session (Cromdale)</b>					
1930 - 2330	<b>Gala Ceilidh</b>					

Friday, 2 June 2000

	Pentland	Fintry	Sidlaw	Moorfoot	Kilsyth	Tinto
0900 – 1040		HPEM-6: Sources 2	HPEM-10: Biological Effects	UWB-6: Antennas 2	UWB-10: EM Theory 3	UXO-2: Detection/Sensors Technologies (UXO)
1040 – 1100	<b>Coffee Break</b>					
1100 – 1240		HPEM-6: Sources 2	HPEM-10: Biological Effects	UWB-6: Antennas 2	UWB-10: EM Theory 3	UXO-2: Detection/Sensors Technologies (UXO)
1240 – 1400	<b>Lunch Break</b>					
1400 – 1540		S8 - RF Interactions and Chaos	HPEM-7: Coupling	UWB-6: Antennas 2	UXO-4: Detection/Sensor Technologies (Mines)	UXO-3: ID, Signals, Discrimination
1540 – 1600	<b>Coffee Break</b>					
1600 – 1740		S8 - RF Interactions and Chaos	HPEM-7: Sources & Coupling			UXO-3: ID, Signals, Discrimination



# Programme Listings

HPEM-1: Sources 1	1.1 – 1.5 6.1 – 6.5	UWB-4: Theory 2	37.1 – 37.5
HPEM-2: Materials	2.1 – 2.5	S7: UWB and Transient Measurement	41.1 – 41.5 47.1 – 47.5
S5: Intentional EMI	3.1 – 3.5 8.1 – 8.5 13.1 – 13.4	UWB-7: Signal Processing	43.1 – 43.5 49.1 – 49.3
S1: Fundamental Solutions of Maxwell's Equations	4.1 – 4.5 9.1 – 9.5 14.1 – 14.2	HPEM-12/UWB-9: High Power Antennas	45.1 50.1 – 50.5
UWB-2: Radar Systems	5.1 – 5.5 10.1 – 10.5 16.1 – 16.2	UXO-1: Detection/Sensor Technologies (Landmines)	46.1 – 46.5 51.1 – 51.1
HPEM-9: Measurement	7.1 – 7.5	HPEM-6: Sources 2	52.1 – 52.5 57.1 – 57.5
HPEM-3: Vulnerability 1	11.1 – 11.5 18.1 – 18.5	HPEM-10: Biological Effects	53.1 – 53.5 58.1 – 58.5
HPEM-4: Methods	12.1 – 12.5 19.1 – 19.5	UWB-6: Antennas 2	54.1 – 54.5 59.1 – 59.5 64.1
UWB-1: EM Theory 1	15.1 – 15.3 21.1 – 21.5	UWB-10: EM Theory 3	55.1 – 55.5 60.1 – 60.5
UWB-8: Target Identification and Propagation	17.1 – 17.3 22.1 – 22.5	UXO-2: Detection/Sensor Technologies (UXO)	56.1 – 56.5 61.1 – 61.5
S2: EMC Modelling Tools	23.1 – 23.5 27.1 – 27.5	S8: Chaos	62.1 – 62.5 67.1 – 67.4
S6: Basics of Detection	24.1 – 24.5 28.1 – 28.3	HPEM-7: Sources and Coupling	63.1 – 63.5 68.1 – 68.5
S9: High Power Facilities	25.1 – 25.5 29.1 – 29.5	UXO-4: Detection/Sensor Technologies (Mines)	65.1 65.5
UWB-5: Antennas 1	26.1 – 26.5 30.1 – 30.6	UXO-3: ID, Signals, Discrimination	66.1 – 66.5 71.1 – 71.5
HPEM-11: Vulnerability 2	31.1 – 31.5 36.1 – 36.5	Plenary Sessions	PL1 - PL6
HPEM-5: Environments: Lightning, EMP	31.1 – 32.6	Late Submissions	6.5, 19.3 25.3, 28.3 32.2, 40.5 41.3, 54.1 54.2, 56.2 57.4, 57.5 58.1, 58.4 58.5, 61.2 61.3, 68.1 68.2, 68.3
S4: Geomagnetic Storms	33.1 – 33.5 38.1 – 38.5 42.1 – 42.4		
S3: UWB Polarimetry	34.1 – 34.5 39.1 – 39.5		
UWB3/HPEM-8: Pulsed Power	35.1 – 35.5 40.1 – 40.5 44.1 – 44.4		

## 1.1

### An Overview of Recent Advances in Intense Beam-Driven Relativistic Backward Wave Oscillators and Their Use in High Power Microwave Effects Studies

*Schamiloglu, E<sup>1</sup>; Hegeler, F<sup>1</sup>; Abdallah, C T<sup>1</sup>; Christodoulou, C G<sup>1</sup>*  
<sup>1</sup>University of New Mexico, USA

Much progress has been recently made regarding the understanding of the operation of intense relativistic electron beam-driven backward wave oscillators (BWO's). The issue of pulse shortening seems to be better understood, although its remediation has yet to be demonstrated. The energies radiated in X-band have yet to reliably reach the kiloJoule level, although operation at 10's to 100's of Joules has been established.

Recent results achieved at the University of New Mexico (F. Hegeler, M. Partridge, E. Schamiloglu, and C.T. Abdallah, "Studies of Relativistic Backward Wave Oscillator Operation in the Cross-Excitation Regime," submitted to the IEEE Trans. Plasma Sci. Special Issue on High Power Microwave Generation) have established that it is possible to operate a long pulse BWO in the so-called "Cross-Excitation" regime in a controlled manner. By this we mean that, by appropriately setting the diode voltage for a fixed impedance and for a fixed slow wave structure, one can demonstrate single mode operation in one of two adjacent axial modes, or operation when the two modes co-exist and compete for a period of time on the order of 10 ns.

In this presentation we review recent advances in the operation of intense beam-driven BWO's. We present increased understanding obtained through the use of sophisticated diagnostics, as well as novel experiments. We describe BWO operation in the cross-excitation regime and discuss intriguing possibilities on how this can be exploited for HPM effects studies.

## 1.3

### Progress on a High Power, Annular Beam Klystron with a Thermionic Cathode

*Fazio, M<sup>1</sup>; Carlsten, B<sup>1</sup>; Fortgang, C<sup>1</sup>; Habiger, K<sup>1</sup>; Nelson, E<sup>1</sup>; Arfin, B<sup>2</sup>; Caryotakis, G<sup>2</sup>; Haase, A<sup>2</sup>; Scheitrum, G<sup>2</sup>*

<sup>1</sup>Los Alamos National Laboratory, USA; <sup>2</sup>Stanford Linear Accelerator Center, USA

Los Alamos National Laboratory is developing a "hard-tube", repetitively pulsed, 1 GW annular beam klystron (ABK). The ABK will operate at 1.3 GHz and will have a thermionic cathode electron gun. The pulse length is 1ms and the pulse repetition frequency is 5 Hz. The beam voltage is 800 kV and the current is 4 kA. The development of the tube is being accomplished in collaboration with the Stanford Linear Accelerator Center (SLAC) where the tube will be fabricated to the same manufacturing standards used by the high power microwave tube industry for commercial klystrons. For reasonable extraction efficiency, a klystron operating in the high current regime must use an annular beam to avoid the electron kinetic loss caused by potential depression due to the high space charge. The production of a high current annular beam requires an aggressive cathode and electron gun design. The dispenser cathode will operate near the limit of what is considered the maximum emission current density for reasonable cathode lifetime. The electron gun has been modeled with DEMEOS, EGUN, and ISIS to ensure that the design produces a stable electron beam and that the peak electric fields in the gun are consistent with the levels used in commercial high power klystrons to achieve reliable electron gun operation. Because the beam must flow within a few millimeters of the drift tube wall to minimize beam potential depression, achieving beam stability with minimal scalloping is critical. High power RF conditioning over several million pulses and full power testing will be performed at Los Alamos on the Banshee modulator which has a 1ms pulse length and a 5 Hz PRF capability. The tube design, design issues, and status are presented.

## 1.2

### Two Dimensional (2D) Versus (1D) Co-Axial Bragg Reflectors; First Steps Towards a Gigawatt Level FEM

*Konoplev, Iv V<sup>1</sup>; Cross, A W<sup>1</sup>; Ginzburg, N S<sup>2</sup>; Peskov, N Yu<sup>2</sup>; Phelps, A D R<sup>1</sup>; Ronald, K<sup>1</sup>; Sergeev, A S<sup>2</sup>; He, W<sup>1</sup>; Whyte, C G<sup>1</sup>*

<sup>1</sup>University of Strathclyde, UK; <sup>2</sup>Russian Academy of Sciences, Russia

In recent years many successful experiments have been carried out on Free Electron Masers (FEMs) which utilise Bragg resonators. Such resonators are constructed by machining single periodic corrugations (1-D Bragg resonators) on the inner wall of the waveguide to select a single resonant cavity mode with the correct longitudinal index. However, in all previous experiments the diameter of the microwave systems used (D) did not exceed the wavelength of radiation ( $\lambda$ ) by more than  $D/\lambda \sim 2$  to 4. The electron energy available for conversion to radiation may be increased both by increased beam voltage or current. It is more attractive for most applications not to have to face the implications of size involved in all system components when high voltages are in use. In any case, whether one chooses to increase beam current or energy, if the transverse size of the system is not increased then the radiation power density becomes very high and RF pulse shortening results. In addition with very high current densities, beam instabilities may cause interruption of the beam transport. Therefore the most attractive solution is to increase the transverse size of the system to retain constant power and current densities. However maintaining coherence of radiation over such a large format electron beam is difficult and results in a decrease of the source efficiency and spectral purity. A new approach of using a 2-D Bragg resonator to provide additional mode selection over the transverse co-ordinate to permit scaling of the transverse size of the microwave system and gain medium whilst still retaining high efficiency will be presented. Theory has already given very promising predictions of 2-D Bragg resonator excitation by large diameter hollow electron beams to provide powerful spatially-coherent radiation in a system even when  $D/\lambda \sim 10$  to 1000. An experimental project to investigate an 8 mm Free Electron Maser (FEM) with a 2-D Bragg resonator with a  $D/\lambda \sim 10$  based on a high-current accelerator currently in operation at Strathclyde University will be presented. We will present a comparison between one and two dimensional Bragg mirrors. The results are based on the experimental cold measurements and theoretical predictions of the reflection and transmission coefficients of both reflectors. This work was supported in part by Grant No. 531 of the International Science and Technology Centre, Grant No. 97-02-17379 of the Russian Foundation for Basic Research, the United Kingdom DERA, the Royal Society and the Committee of Vice Chancellors and Principals of the Universities of the United Kingdom and Strathclyde University.

## 1.4

### Development of the Tapered MILO

*Eastwood, J<sup>1</sup>; Hook, M<sup>1</sup>; Hawkins, K<sup>1</sup>*

<sup>1</sup>AEA Technology, UK

This paper presents results from our studies of 15 Ohm and 30 Ohm Tapered MILOs; it will describe some of the technical challenges faced and their resolution, and conclude with an outline of potential future developments.

Tapered MILOs are relativistic high power microwave generators with potential for producing long pulses at power levels of several gigawatts and with frequencies up to several GHz. They operate like a linear magnetron, but need no external magnet; the regulating field is self produced by the internal currents. Consequently, their structure is lightweight, rugged and compact. Under certain conditions they exhibit problems similar to those encountered in relativistic magnetrons, such as mode hopping, gap closure, plasma discharge and pulse shortening.

Our work on the Tapered MILO has overcome problems of low efficiency and pulse shortening common to other tubes. Our designs, obtained using a combination of computer modelling and experiment, outperform reported best performance figures for other tubes in terms of peak power, energy per pulse and efficiencies at powers of over 1 GW and with frequencies close to 1GHz.

Computer modelling reaches over 25% efficiency and predicts a 30% bandwidth for the 1 GHz tubes, where tuning is realised by varying the geometry of the driver cavities. Frequency chirping and auto-modulation have also been obtained for certain configurations.

Single shot experiments have reproduced the performance predicted by computer simulation. Repeatable shots yielding over 250 J per shot at a mean power of over 1 GW and peak power of 2 GW have been obtained for the 15 Ohm MILO, with pulse length being limited to the 200 ns available from the power supply. The 30 Ohm MILO has delivered 1.7 GW and pulse energies of 220 J on the same power supply; on DERA power supplies, bursts of 300 ns rf pulses have been obtained.

Experimental results have been obtained in unconditioned tubes under modest vacuum conditions; more substantial power supplies and properly vacuum engineered tubes are expected to extend the performance of current designs to give repetitive multi-gigawatt pulses with pulse energies in excess of a kilojoule.

## 1.5

### Parametric Studies of Relativistic Magnetrons

Arter, W<sup>1</sup>; Eastwood, J<sup>1</sup>  
<sup>1</sup>AEA Technology, UK

The relativistic magnetron has for many years been regarded as a promising source of high power microwaves (J Benford and J Swegle, High Power Microwaves, Artech, 1992). Its basic physical principles are similar to those of the long-established cavity magnetron, but in practice it has proved more difficult to operate successfully. The move to higher power exacerbates the problems due to mode hopping, unwanted transients, plasma formation etc which may account for pulse shortening. The published literature therefore records a large number of experiments designed to improve relativistic magnetron operation. It has recently become possible to simulate most aspects of relativistic magnetron behaviour directly using 3-D particle-in-cell codes (W Arter and J W Eastwood, IEEE Trans Plasma Sci 26, 714-25, 1998). The 3DPIC software suite has been used to attempt to reproduce published data for the behaviour of both regular cavity (A6) and rising-sun magnetron designs operating at high voltage, with radial power extraction. This has enabled us to identify how accurately the numerical model agrees with experiment. With this information it is possible to set confidence levels for the computer predicted performance of novel magnetron designs. We have also gone on to investigate the sensitivity of high power relativistic magnetron operation with respect to changes in a large number of design parameters. Parameters studied include the geometry of both cathode and anode, the characteristics of the power supply and the method of power extraction. Such results are valuable for optimising novel designs of relativistic magnetron.

## 2.2

### Electromagnetic Properties of Ceramic Materials During Microwave Processing

Salmoria, G V<sup>1</sup>; Audhuy, M<sup>1</sup>; Silva Paula, M M<sup>2</sup>; Geronimo, R J<sup>3</sup>  
<sup>1</sup>ENSEEIH, France; <sup>2</sup>Universidade do Extremo Sul Catarinense, Brazil; <sup>3</sup>Universidade do Extremo Sul de Santa Catarina, Brazil

The use of microwave to the inorganic solid-state preparations, ceramics processing and the theoretical modelling of microwave interactions with ceramic and inorganic materials have been reported extensively in the literature; however, very few data have been published on the microwave heating characteristics of ceramics and inorganic compounds. Questions of enhanced reaction kinetics notwithstanding, processing of ceramic materials by microwave has traditionally been hampered by issues such as the formation of hot spots, cracking, thermal runaway, and other manifestations. In addition, the validity of the temperature measurements is often questioned, either on a macroscopic or microscopic scale. Modelling the interaction of a processed part with the electromagnetic fields present in the microwave applicator is desired to anticipated such problems. However, theoretical modelling of the process is hindered by the fact that the thermal profile in the sample during microwave heating is dependent on the dielectric and thermal properties of the sample. These properties, such as the complex permittivity and the thermal conductivity, are largely dependent on the density and the temperature.

This work presents the use of the resonant cavity technique to measure the temperature dependency of the dielectric properties of ceramic and inorganic materials to improve understanding the behaviour of the material to be processed. It is well known that a number of oxides, and a few halides absorb energy from microwaves very efficiently at low temperatures, but the majority of the inorganic materials absorb microwave energy only at high temperatures (>500°C). The positive slope of the loss factor vs. temperature response of the majority of the measured materials, mainly above the 400°C, result in a difficult control of rising temperature and thermal runaway effects. The use of hybrid heating which provides a better heating control is more indicated to the microwave processing of materials with this dielectric behaviour.

The average power absorbed during microwave heating is function of the applied electromagnetic field and the imaginary part of the relative permittivity (loss factor). Because the permittivity imaginary part varies strongly as a function of the temperature, the absorption of energy from electromagnetic field by the sample changes significantly as the process progresses. The measurement of the complex permittivity temperature dependency can provide knowledge of necessary parameters to a better modelisation and a optimisation of the microwave ceramic processing.

## 2.1

### Microwave Dielectric Properties Measurement as a Process Control of Wood Drying

Salmoria, G V<sup>1</sup>; Audhuy, M<sup>1</sup>; Zucco, C<sup>2</sup>  
<sup>1</sup>ENSEEIH, France; <sup>2</sup>Universidade Federal de Santa Catarina, Brazil

The SMI (Industrial, Scientific and Medical) applications of microwave energy in to the wood technology show many interesting work results in the manufacture, defrosting, glueing, reducing and modifications, bark and spruce needles removal, biological protection and drying process of lumbers, veneers, wooden ships, matches, composites and papers. The research of microwave wood and wood based materials processing demonstrated that the application of microwave energy create opportunities for intensification of existing processes and developing new methods of wood processing. The drying wood by microwave heating differs from conventional drying methods by the way energy is transferred into the material. A control over the microwave heating temperature profile and moisture developed within the material is required to reach the desired quality. The key to the optimisation of the process is to understand the temperature/composition dependency of the dielectric properties of the material to be processed. In this work we used the resonant cavity method to measure the dielectric properties of two wood samples (Pinus Elliotti and Pinus Taeda) and its relationships with temperature and moisture contents. The measurements showed that the course of the wood drying can be easily followed by measuring the dielectric properties versus time or temperature with successful control over the microwave process. The negative slope of the loss factor vs. temperature/composition response of wood samples, mainly during the water evaporation, result in a easy way to control of rising temperature and thermal effects such as carbonisations. This study shows how the desired temperature distribution, not necessarily uniform, may be implemented for a number of practical microwave processes with the effective monitoring over electromagnetic properties of the polymeric material heated and its applicability to the guides, multimode cavities or other kind of applicators using simple calibration curves.

## 2.3

### Energy and Failure Issues in Dielectrics

Kohlberg, I<sup>1</sup>; Sarjeant, W<sup>1</sup>; Blaise, G<sup>2</sup>  
<sup>1</sup>Energy System Institute, USA; <sup>2</sup>Laboratoire de Physique des Solides, France

**Background** This study attributes the cause of breakdown to instability in the polarization energy density contribution to the total energy in the medium. It focuses on charge distribution as the trigger for partial discharges observed in capacitors, as well as breakdown of the bulk material when charges are released disruptively. EMC issues will consider the fact that charge injection and charge trapping always occur for electric fields > 100 V/mm.

#### PURPOSE OF WORK

Electromagnetic Compatibility (EMC) issues in modern high density electronics are addressed through a new theory that seeks to explain sudden energy releases possible, even in powered-down states of systems, that could well create erroneous or misleading internal signals in such systems. This theory introduces the concept of localized stored energy at defects within insulating and semi-insulating materials that make up modern electronics.

This work addresses aspects of the nature of the physics of the breakdown process on the basis of an unsustainable increase in local internal energy within the material. This increase in local energy is due to charge trapping - the polarization around a trapped charge increases the local energy; the relaxation of the material lattice then follows a rapid de-trapping of charges from their sites, releasing the local excess site region energy into the material. Such a release executes transient virtual work on the material, producing macroscopic dielectric electrical breakdown when critical unstable conditions are achieved in the time domain. To illustrate the pervasiveness of the relevance of these results to the field of dielectrics, a fundamental approach to the limitations on storage of energy in dielectrics is formulated, with a special emphasis on charging of defects in spacecraft thermal dielectric blankets and the like. This relates, from first principles, the electromagnetic energy density stored directly to the intrinsic material constraints that limit the maximum energy density achievable.

## 2.4

### High Power Microwave Interface Breakdown

Krompholz, H<sup>1</sup>; Neuber, A<sup>1</sup>; Hemmert, D<sup>1</sup>; Hatfield, L L<sup>1</sup>; Kristiansen, M<sup>1</sup>

<sup>1</sup>Texas Tech University, USA

The knowledge of the behavior of solid dielectric/gas interface breakdown caused by microwaves is crucial for developing new design methods for highpower microwave windows. The physical mechanisms leading to breakdown for power levels on the order of 10 MW/cm<sup>2</sup> at 2.85 GHz and gas pressures varying from 10<sup>-4</sup> to 10<sup>3</sup> Torr are investigated, with emphasis on alumina/air interfaces. The high power microwaves are generated with a 4 MW magnetron having a 3.5 microseconds pulse width in conjunction with an S-band traveling wave resonator, resulting in a traveling wave power of 100 MW. This power level is sufficient to cause breakdown across the interface located in the pressure adjustable test region. The interface geometry comprises a thin ceramic alumina slab placed in the waveguide center. An almost purely tangential field and a localized breakdown are assured by orienting the alumina slab normal to the direction of the wave propagation and by making contact with two field enhancement tips placed in the middle of each waveguide broad wall. We monitor the pre-breakdown phase and the breakdown by recording the traveling and reflected power, and the luminosity, spatially integrated with high temporal resolution or imaged with a framing camera. Additionally, we gain information about the local field by placing electric field probes in the vicinity of the interface. An image intensifier, capable of a minimum gate time of 2.5 ns and in temporal correlation to the other phenomena enables us to take single shot photographs of the light emission. We compare the pressure dependent breakdown characteristics, such as appearance, breakdown field, and temporal behavior of electric signals to our solid dielectric/vacuum interface breakdown and volume breakdown results, all measured utilizing the same basic setup.

This work was solely funded by the High Energy Microwave Device MURI program funded by the Director of Defense Research & Engineering (DDR&E) and managed by the Air Force Office of Scientific Research (AFOSR).

## 3.1

### About Potential Possibility of Commitment of Large-Scale Terrorist Acts by Using Electrotechnical Devices

Loborev, V<sup>1</sup>; Parfenov, Yu<sup>1</sup>; Fortov, E<sup>1</sup>; Sini, L<sup>2</sup>

<sup>1</sup>Russian Academy of Sciences, Russia; <sup>2</sup>Research Institute for Pulse Technique, Russia

The report includes analysis of potential possibility of commitments of Large-scale terrorist acts by using electrotechnical devices. There are considered the following possibilities:

- 1). Irradiation of objects by ultra wide bands electromagnetic pulses;
- 2). Pulsed electric currents injection into the building power supply and earthing network;
- 3). High voltage impulses transference through the bulk electroconducting transient field from the high power source to the object

Analysis includes the description of electrotechnical devices, some theoretical and calculating results, and some experimental data.

The performed analysis shows that it is necessary to accept preventive protection measures. It is more profitable for the society than to liquidate the consequences of criminal action that is committed. In our opinion these standards must contain the following

- 1). The quantitative characteristics of potential threats
- 2). The recommendations about significant objects vulnerability testing by using relatively cheap experimental methods and means
- 3). The list of needed protection methods and means.

SINUS - 7 M 4x1x1 m<sup>3</sup> λ=0.1m 10GW 30ns  
 - 7 M 3cm 1.5GW 30ns

UWB Gen.: 100kV 3m diameter 100kHz mod. 120MW 200ns  
 1.57V 3ns 500Hz 10GW 1000ns

10<sup>-7</sup>...10<sup>-3</sup> | absorb. Energy → damage UWB: 100-200cm

## 2.5

### Microwave Giant-Magneto-Resistance and Inter-Layer Exchange Coupling in Ni/Cu Multilayer Films on Si(100)

Kuanr, B K<sup>1</sup>; Kuanr, A V<sup>2</sup>

<sup>1</sup>Forschungszentrum Juelich GmbH, Germany; <sup>2</sup>University of Delhi, India

We are reporting the first observation of Microwave-Giant-Magneto-Resistance (μW-GMR) and Inter-layer Exchange Coupling of Ni/Cu Multilayer (ML) thin-films (Ni=15 Å and Cu=5, 10, 15 Å) grown on Si(111) by a Varian UHV system. The microwave measurements were performed by a Hewlett Packard Vector Network Analyzer (HP-8510B) to observe the Ferromagnetic Resonance (FMR) of these samples by using a Reflection type transmission line. The surface resistance of the sample were measured through Scattering matrix (S<sub>11</sub>) parameters by sweeping the dc magnetic field at FMR. μW-GMR was calculated from the values of surface resistance at zero and saturation field and expressed as % unit. Interlayer exchange coupling (J) was calculated from relation  $J = M^* H_{sat} * t_w / 4$ .

We have observed maximum μW-GMR for the 5 Å Cu-layer sample (7.8%) and this decreases with the increase of Cu layer thickness (3.2 and 0.3 % for 10 and 15 Å samples). Interlayer exchange coupling are observed to be anti-ferromagnetic (AFM) type and show a similar behaviour to the GMR. It is observed to be 0.07, 0.045 and 0.037 erg/cm<sup>2</sup> at room temperature. Increase of temperature of the sample decreases the above values.

Our high-frequency data are comparable to the reported dc values (H. Kubota et al. J. Mag. Mag. Mater. **129**, p.383, 1994). The observed coupling strength is much less than that reported for MBE grown samples. it may be due to the fact that mixing at the interface in the e-beam evaporation technique used here reduces the coupling strength. The interface quality alter the degree of carrier confinement in the Cu-spacer layer. The observed μW-GMR can be explained by the spin dependent scattering of conduction electrons by the magnetic Ni atoms at the interface (J. Inoue, et al. J. Mag. Mag. Mater. **104-107**, p.1883, 1992). In addition to the interface scattering, we have added the contribution of bulk scattering due to phonon, magnon and lattice defects for this high value of observed μW-GMR in our samples.

We will also report the temperature dependent of these high frequency phenomenon presently under going.

## 3.2

### Requirements for a Program to Protect the Infrastructure from Illegal RF Attack

Stoudt, D C<sup>1</sup>; Latess, J<sup>1</sup>; Gardner, R L<sup>1</sup>

<sup>1</sup>Joint Program Office for Special Technology, USA

Counter RF prog. est.  
 DEW (RF) database

At their General Assembly in August 1999, the 41 member nations of the International Union of Radio Science issued a resolution that the potential illegal use of radio frequency (RF) devices against the civilian infrastructure was a potential problem. They further resolved that member nations should conduct research to determine the severity of the problem and uncover possible countermeasures. The JPO/STC is studying the consequences of the resolution and possible impact of RF devices on the U.S. high-technology infrastructure.

Assessing the impact of the RF threat requires that we consider who might threaten the infrastructure, what tools they might use, how they might employ them, and finally how effective those tools might be (RL Gardner, MW Wik, and DC Stoudt, Review of Radio Science 1996-1999, Ch 13). People considered here are normally not representatives of nations but are criminals, terrorists, or careless users of RF technology.

Finding the effectiveness of the various transmitters and antennas requires that we evaluate the access the criminal has to the target and the size and power requirements of his RF weapon. These characteristics are then compared to the RF weapons that are potential availability on the open market, and their overall effectiveness.

Judging the effectiveness of an RF weapon in this application requires the most careful experiment design. We must simulate each scenario and decide if the targeted system is vulnerable. The core, critical electronics of most businesses or similar organizations consists of computer networks and support systems. This talk, and the two following, will describe applied test and analysis methods used to draw conclusions about the potential RF threats.

→ injection into power lines: 10 - 100kV/Gen.

## 3.3

### The Threat of Intentional High Power EM Transients in the Information Age

Radasky, W<sup>1</sup>; Wik, M<sup>2</sup>  
<sup>1</sup>Metatech Corporation, USA; <sup>2</sup>Defence Materiel Administration, Sweden

This paper begins with a brief discussion of the age in which we live — the information age. The growth of fast, distributed computer power has allowed individuals, businesses and governments to use computers in ways that were not imagined thirty years ago. In addition, businesses in particular have devised new ways to use computers to offer new services or to make themselves more efficient. As a consequence, we are becoming more dependent on this information technology equipment (ITE) to perform even the most routine tasks.

Given this increased reliance on digital computers, the increasing density of transistors in integrated circuits, and the decrease in operating voltages of electronics in general, it is clear that electronic systems are potentially more vulnerable to electromagnetic interference. Fortunately, electronic manufacturers and standards developers have continued to upgrade their EMC standards to anticipate the types of transients that their products might observe during normal operations, and EM protection has been implemented in many cases.

While the above situation may seem like good news, there is the aspect of Intentional EMI. In this case criminals or terrorists may choose to introduce transient electromagnetic signals into a facility by radiated or conducted means. Because some of these methods can be done relatively covertly, the disturbances can be applied at very close range, thereby allowing the use of a fairly small energy source.

In this paper, after the threat conditions are discussed, the new standards program of the International Electrotechnical Commission (IEC) will be described. Its components will include a characterization of the threat environments, protection methods, test methods and surveillance techniques.

→ Critical functions not protected should not depend on normal operation of infrastructure

→ EMI-protection: shielding of facility or key enclosures  
use overvoltage protection and filtering on cable PCB's  
restrict access to cables

## 3.5

### Overview and Status of the International Electrotechnical Commission (IEC) High Power Electromagnetic Standardization Program

Wik, M<sup>1</sup>; Radasky, W<sup>2</sup>  
<sup>1</sup>Defence Materiel Administration, Sweden; <sup>2</sup>Metatech Corporation, USA

Over the past ten years, the International Electrotechnical Commission (IEC) headquartered in Geneva, Switzerland has been active in developing standards to define the electromagnetic environments produced from high altitude nuclear detonations. These environments are known as high-altitude electromagnetic pulse (HEMP). In addition to defining the environments themselves, most of the work of the IEC subcommittee (SC 77C) involves recommending protection methods that are flexible and affordable for civil systems. Five standards have been published, and seven others are in various stages of development.

This paper will begin by identifying the organization of the subcommittee and the countries that participate in the work. It will continue by reviewing the HEMP work accomplished to date and the ongoing projects. For each publication the project leader is identified, along with the schedule for developing the next phase of the document; in several cases, important aspects of documents are summarized. In addition, there is a discussion concerning how the HEMP standards have been organized to be consistent with the EMC publication strategy within the IEC.

In June of 1999, an expansion of the HEMP work in SC 77C was approved by the parent committee TC 77 (EMC) to consider other high power electromagnetic threats (HPE) that are intentionally produced. These environments include both radiated and conducted transient phenomena, typically produced by high power generators with attached antennas. These disturbances are considered serious threats to unprotected civil facilities such as computer centers, office buildings and factories. The future work of SC 77C will focus on protection methods against these types of threats. A companion paper will discuss the details of this new aspect of work of SC 77C.

## 3.4

### Lessons From Military EMP Hardening Relevant To Protecting Against Intentional EMI

Karzas, W J<sup>1</sup>  
<sup>1</sup>Metatech Corporation, USA

There has been a history of several decades during which military (and some civil) systems have been "hardened" to protect against the electromagnetic pulse (EMP). Many lessons have been learned, some of which can be relevant to coping with the threat of intentional EMI to various non-military systems.

**Testing:** Perhaps the most important lesson learned from our experience is that it is very difficult to predict how EMP or intentional EMI can couple to and damage or disrupt functional performance. Testing is critically important. In an ideal and not cost-driven world, each individual copy of the system in question would be tested. Since this may be impractical, some degree of control over system configuration is necessary so that the results of limited testing can be extrapolated to all copies. What is learned from the tests should be a guide toward what controls are relevant.

**Threats:** As important as the testing is a clear definition of the relevant EM threat or threats for which tests are to be conducted. (In the military case, threats are defined by considering various scenarios. The high altitude EMP (HEMP) being pervasive, it was possible to define EM criteria which applied to all systems.) For intentional EMI some imaginative thought may be required to generate the threats. This should involve a knowledge of the system functional workings.

**Retrofit:** Another lesson learned is that retrofitting protection into an existing system is far more costly than considering it in the initial design. Since EMI resistance is now usually a part of system design, some slight design modifications can often protect against (presumably more severe) intentional threats.

**Damage vs. Upset:** Damage to system components is more readily protected against than functional upset due to EM transients. Appropriate energy limiting components (diodes, surge arrestors, etc.) are available to restrict the magnitude of EM signals to those within the system operating levels. By definition, upset occurs when EM transients mimic operating signals within operating bandwidths and trigger, at unwanted times, disrupting system states. Protection against upset is thus not simply a matter of restricting energy content of transients but of excluding them even at lower levels, or of designing reset and recovery procedures (circumvention) which limit disruptions to acceptable outage times, etc. A combination of such practices is often warranted.

Testing - critical can not predict coupling  
comprehensive testing - end copy?  
- or configuration control required

Shielding:  
- protection costly  
- with EMI Resistance in initial design can easily be retrof.

Damage vs. Upset  
- Damage: limit magnitude of EMI signals  
- UPSET: signal paths allow operating levels or exclude from levels with wrong characteristics, or  
- Software Fix: "Circumvention"

1000-5-5 publ. → bundle  
→ Specs. for prot. devices: cond.



## 4.1

### From Maxwell to Einstein

*Van Bladel, J<sup>1</sup>*

<sup>1</sup>University of Ghent, Belgium

In 1931 Cambridge University published a volume commemorating the centenary of Maxwell's birth. The book contains contributions from former students and collaborators (H. Lamb, Fleming, Glazebrook, Garnett), which will be discussed briefly. More time will be devoted to Einstein's text. Einstein puts his own work squarely in the tradition of Maxwell's. He hails Maxwell's revolutionary transition from (unsuccessful) mechanical models to the primacy of fields and governing differential equations. In the same vein, Einstein dropped the concept "ether", and explained Physical Reality by requiring the equations of Physics, and in particular Maxwell's, to have the same form in every inertial frame. Coupled to Lorentz' space-time transformation laws, this requirement leads to the transformation laws for electromagnetic fields and sources. The power of this approach better to understand the electrodynamics of moving bodies will be illustrated by a few examples, such as slabs in uniform motion or the "blv" law. For accelerated bodies, the "instantaneous rest frame" hypothesis is fundamental. It helps evaluating currents and fields in, for example, rotating bodies, such as the Faraday disk, or in systems containing sliding contacts. It also serves as a basis for an appropriate use of the  $(D\Phi/Dt)$  induction law. Conceptually indispensable for a coherent presentation of fields in the presence of moving bodies, Relativity is also essential for a "clean" solution of many of the problems encountered in electromechanical applications. From a utilitarian point of view it is less relevant for the "radio" engineer, who may be satisfied with the quasi-stationary approach in analyzing phenomena such as the Doppler effect.

## 4.4

### Analytical Methods for Antenna Analysis and Synthesis in the Time Domain

*Heyman, Ehud<sup>1</sup>; Shlivinski, A<sup>1</sup>*

<sup>1</sup>Tel Aviv University, Israel

The ever-increasing interest in the radiation and detection of ultra-wideband (UWB) short pulses has made an impact on time domain (TD) analysis and design of short-pulse antennas. One way of analyzing the radiation and detection of these pulses would involve the traditional frequency domain (FD) antenna parameters on a frequency-by-frequency basis. FD parameterization lends itself conveniently to producing a comprehensive transmit - receive system description, yet because of the broad frequency band of the short-pulsed fields, direct treatment in the TD may lead to more efficient and physically transparent representations.

The present paper is a brief overview of two formulations which have been introduced recently for TD antenna characterization: The first one is based on plane wave analysis in the TD via the slant stack transform (SST) of the current distribution (A Shlivinski, E Heyman & R Kastner, IEEE Trans. Antennas Propag., AP-45, 1140-1149, 1997), while the other is based on a TD multipole expansion (A Shlivinski & E Heyman, IEEE Trans. Antennas Propag., AP-47, 271-286, 1999). The first formulation provides a complete far-zone characterization of transmit-receive antenna systems as a cascade of convolution operators of the antenna circuits and the TD effective heights (which are characteristics of the antennas, calculated from the current distributions via the SST). The TD multipole expansion, on the other hand, provides a convenient representation for the near zone properties of the field. Using this formulation we introduce new near field concepts such as TD radiative fields and energies, and introduce the ratio between them, termed the TD Q, as a measure of the radiation effectiveness. The theories described above will be used to evaluate and compare different realizations of collimated, short-pulse aperture distributions.

## 4.3

### The Maxwell Stress Dyadic

*Lindell, Ismo<sup>1</sup>; Jancewicz, B<sup>2</sup>*

<sup>1</sup>Helsinki University of Technology, Finland; <sup>2</sup>University of Wroclaw, Poland

The classical Maxwell stress tensor (or stress-energy-momentum tensor) is revisited in differential-form formalism by introducing the dyadic notation.

Differential-form formalism appears very elegant in combining basic electromagnetic quantities with geometrical concepts and minimal algebraic expressions. However, the long tradition of using vector calculus has been too suppressive to give way to this formalism in electromagnetics. The elegance was shown by Georges A. Deschamps a couple of decades ago in a basic article (Proc. IEEE, 69(6)676-696, 1981). More recently, there have been other articles and books trying to convince the reader about the advantage of the differential forms in electromagnetic theory. So far their success seems to be limited to geometrical interpretation of basic electromagnetic laws for undergraduate students. (A flourishing branch of computer electromagnetics making use of differential forms in the finite element method is outside the present scope.)

In spite of all the elegance, differential forms are not much used in practical electromagnetic field analysis. The reason of this may well be that, so far, the formalism has been lacking the counterpart of the Gibbsian dyadic algebra. However, being a coordinate-free notation, dyadics appear ideal to support the coordinate-free differential-form formalism. In the present paper it is shown that, by introducing dyadic notation to differential forms, the Maxwell stress tensor can be expressed in a very compact form, as the Maxwell stress dyadic. However, this requires that the quantity known as Lorentz force density (in 3D) or Lorentz force-energy density (in 4D) be first expressed in dyadic form as well. Finally, it is shown that, to be able to define the stress dyadic, the linear electromagnetic medium must satisfy a symmetry condition corresponding to the reciprocity condition for the time-harmonic fields.

## 4.5

### A Useful Property of Radiated and Scattered Fields: The Local Bandwidth

*Bucci, O.M<sup>1</sup>; Capozzoli, A<sup>1</sup>; D'Elia, G<sup>1</sup>*

<sup>1</sup>Dipartimento di Ingegneria Elettronica e delle, Italy

The idea of approximating the radiated (or scattered) fields on a given domain by means of a band-limited function dates back to 1981 [O.M.Bucci, G.Franceschetti, G.D'Elia, IEEE AP28, 306-310, 1980]. However, it was put on a satisfactory and general basis only with the introduction of the concepts of effective bandwidth and degrees of freedom of the electromagnetic field [O.M.Bucci, G.Franceschetti, IEEE AP37, 918-926, 1989]. During the last two decades, further advances concerned the exploitation of the effective bandwidth concept in developing non-redundant sampling representations of fields, also accounting for the geometry of the considered source or scatterer. Applications to near-field far-field transformation techniques, to fast analysis of large antennas, to antenna synthesis and inverse problems, showed the usefulness of the new concepts in solving electromagnetic practical problems. Basically, the efforts made on this subject aimed to find a suitable parametrisation of the observation domain and a proper phase factor to single out from the field, such that the corresponding "reduced" field can be expressed as a sampling series involving a minimum number of independent samples.

The criterion underlying the choice of the optimum parametrisation and phase factor is essentially based on the requirement that a particular function, called the "Local Field Bandwidth" (LFB), should be as small as possible and constant over the observation domain. This criterion relies on the ansatz that the LFB, while depends on the local behaviour of the field, determines the sampling rate required to approximate the field in the neighbourhood of an observation point. In particular, higher field derivatives in the neighbourhood of a point correspond to higher values of the LFB. According to this ansatz, the role played by the optimum parametrisation is to locate non-uniformly distributed field samples on the observation domain in an optimal way by increasing or decreasing their density in regions with higher or smaller LFB, respectively.

## 5.1

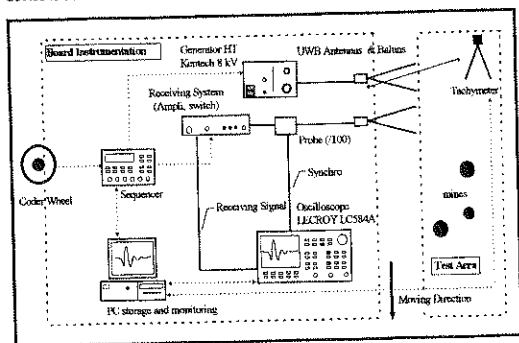
### A New Ultra Wideband, Short Pulse, Radar System for Mine Detection

Gallais, F<sup>1</sup>; Andrieu, J<sup>1</sup>; Beillard, B<sup>1</sup>; Imbs, Y<sup>1</sup>; Mallepeyre, V<sup>1</sup>; Jecko, B<sup>1</sup>; Le Goff, M<sup>2</sup>

<sup>1</sup>IRCOM Brive, France; <sup>2</sup>CELAR (DGA), France

An experimentation is described for measurement of UWB transient scattered responses from different targets. The measurements are performed using a new UWB synthetic aperture radar for the detection of buried in and placed atop soil targets.

The measurement configuration is an UWB (100 MHz - 1 GHz) transmission and reception system implanted on a mobile boom. This boom which can reach about ten meters high, is installed on a truck. Two identical antennas are used. The transmitting antenna is driven by a maximum 8 kV pulse generator with a risetime better than 150 ps. The generator is remote by a coder wheel behind the truck. A receiving system between receiving antenna and the digital sampling oscilloscope, is needed to protect the oscilloscope input from high level tension and to optimise the measurement dynamic. The oscilloscope can be synchronised with the coupling antenna signal. Data are sent to a PC work station for storage. An antennas location device is useful in motion compensation.



The purpose is to use lower frequencies for penetrating foliage, vegetation soil and ultra wide band for distance resolution. The measurements are possible in VV, HH, and HV polarisation. Different data processing are investigated. Some targets as metallic mines lied on the soil can be detected, based on a simple algorithm.

This facility is funded by the DGA (French General Armament Delegation) to meet CELAR requirement. It's the fruit of collaboration between CELAR and IRCOM.  
 - CELAR (French Defence Electronics Centre) : definition of requirement and experimentation  
 - IRCOM (Research institute in Microwave and Optical Communication): antennas conception and numerical modelisations.

## 5.3

### Ultra-Wideband Ground Penetrating Impulse Radar

Yarovoy, A G<sup>1</sup>; Van Genderen, P<sup>1</sup>; Ligthart, L P<sup>1</sup>

<sup>1</sup>Int. Res'ch Ctre for Tele-Comm Transmiss Radar, Netherlands

The International Research Centre for Telecommunications-transmission and Radar (IRCTR) of the Delft University of Technology has expertise in radar development and time-domain antenna measurements and performs since three years intensive research and development work in the area of Ground Penetrating Radar (GPR) systems. One of ongoing in IRCTR GPR-related projects is aimed to develop a cheap ultra-wideband GPR front-end suitable for accurate measurements of backscattering from subsurface. Accuracy of the measurements should be sufficient for the reconstruction of dielectric permittivity distribution.

The front-end comprises a pulse generator, an antenna system and a receiving unit. Flexibility of the construction allows to perform system optimization under different operational configurations and for different applications. A set of pulse generators (gaussian waveform with a duration of 350ps as well as monocycle waveform with duration of 0.8ns, 2.5ns and 5ns) permits measurements over an ultra-wide frequency band from 40MHz up to 3GHz with sufficient signal-to-noise ratio. The set was delivered by SATIS Co. (Russia). The receiving unit includes a signal conditioner and a sampling converter. The four channel sampling converter from GeoZondas Ltd. (Lithuania) has a repetition rate of 100kHz, a bandwidth of 6GHz and a RMS noise level below 2mV (without averaging). Time drift compensation circuits and algorithms results into an increased linear dynamic range of the receiver from 66dB up to 80dB. An amplitude measurement error depends on the amplitude of the signal but does not exceed 3%.

Significant efforts have been put in the design of the antenna system. For impulse GPR the antenna system should include separate transmit and receive antennas. Both antennas should be ultrawideband and have linear phase characteristics, constant polarization and possess short ringing. Two types of GPR antennas have been developed in close collaboration with SATIS Co.: a dielectric filled TEM horn and a dielectric embedded shielded dipole. It was shown experimentally that these antennas satisfy all above mentioned demands to a high extent. A set of dielectric embedded shielded dipoles have been manufactured for pulse generators with different pulse duration. The antennas have been experimentally matched to existing generators. The antenna configuration depends on the application. For deep subsurface sensing ground based dielectric embedded dipoles are used. The antenna system for high resolution imaging of surface and shallow subsurface includes elevated dielectric filled TEM horns. A principally new GPR antenna system has been developed for landmine detection.

One specific IRCTR-developed GPR system has been tested on different types of grounds (sand, clay, iron ore soil and woodland soil). The system has detected successfully surface laid, shallow and deep buried objects in different environmental conditions. Due to the high accuracy of the acquired data the system shows the potential of high-quality 3D subsurface imaging and reconstruction of 3D dielectric permittivity distribution.

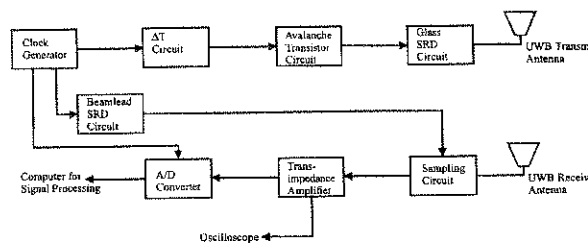
## 5.2

### An Extremely Cost-Effective Base-Band Microwave Pulsed Radar Head for an Existing Pulsed Laser System

Duzdar, A<sup>1</sup>; Kompa, G<sup>1</sup>

<sup>1</sup>University of Kassel, Germany

A pulsed laser radar system (G. Kompa, EuMC'96, 147-152) at our department was transformed into a base-band pulsed microwave radar sensor (figure below) for the purpose of near-range object detection and ranging based on the time-of-flight concept. The system transmits and receives ultra-short electrical pulses that are considered white noise by other frequency bands users. The new sensor is comparable in cost with existing ultrasonic-based radar systems with an advantage of millimeter ranging accuracy. A gaussian pulse for transmitting and receiving purposes was generated using the well known Step Recovery Diode (SRD). A pulse width (FWHM)  $\approx 150$ ps was achieved with a peak amplitude of 7V using a Metelics MMD-0153 axial-glass SRD. Using a Metelics MMD-35-B11 beamlead SRD, a FWHM  $< 70$ ps and a peak amplitude of 1.5V was generated for sampling purposes. The aperture of the sampling circuit was  $< 50$ ps since only the tip of the sampling gaussian pulse was used. The original system used an extended time sampling technique (G. Kompa, IEEE Trans. Instr. and Meas., Vol.33(2), No.1, 97, 1984) which transformed the received pulses from pico- to millisecond range. The electronics needed after sampling for amplification, signal processing and detection of signals were designed for kHz frequencies, which drastically minimized the overall system cost. The system is a bistatic radar sensor in which ultra-wide band antennas were used. A loaded inverted vertical trapezoidal antenna backed by an image plane and fed by a 50 $\Omega$  coaxial cable was designed, simulated and tested for that purpose. The radar sensor was tested with aluminum metal plates achieving millimeter range accuracy.



Base-band pulsed Microwave Radar sensor

## 5.4

### Object Shape Reconstruction at Small Base Ultrawideband Radar

Koshelev, V<sup>1</sup>; Shipilov, S<sup>1</sup>; Yakubov, V<sup>1</sup>

<sup>1</sup>Institute of High Current Electronics RAS, Russia

A new approach for radar objects shape reconstruction with use of time genetic functions is suggested. The parameters of the functions are determined by the reflected ultrawideband signals registered by four diverse receivers. The genetic functions are calculated for characteristic fragments of a radar objects selected type at various aspect angles of the radar surveillance. The algorithm for calculation of a structure of the genetic functions and the coordinates of the geometric fragments corresponding to these functions is realized. This algorithm allows to reconstruct the shape of the sounded objects using a radar system with a small angular base.

The error in the determination of the object aspect angle is shown to result in the essential deterioration of the reconstruction accuracy. The accuracy of the object shape reconstruction is directly proportional to the distance between the receivers in the receiving system and inversely proportional to the distance to the object. The shape reconstruction accuracy of a 4.5 m long three-dimensional model object was about 70 percent at a 1500 m distance to the object, a 50 m distance between the receivers, a 1 ns long sounding bipolar pulse, a 1 degree error of the aspect angle determination and a 10 percent noise level. The accuracy of the objects shape reconstruction is increased as the sounded pulses length is decreased.

The suggested approach allows only to solve the problem concerning the determination of the genetic function compositions in case when there is no possibility to determine the aspect angle with the required accuracy. The data about the composition of the genetic functions can be used for the object recognitions.

## 5.5

**UWB Subsurface Radar with Antenna Array for Imaging of Internal Structure of Concrete Structural Elements**

*Borysenko, A<sup>1</sup>; Borysenko, O<sup>2</sup>; Lishchenko, A<sup>2</sup>; Prokhorenko, V<sup>2</sup>*  
<sup>1</sup>Principal Engineer of Research Comp. Diascarb, Ukraine;  
<sup>2</sup>Engineer of Research Comp. Diascarb, Ukraine

Advanced UWB radar in the 0.5 - 1.5 GHz operation frequency band with multi-channel receiving array and full-polarimetric measurement opportunities will be considered in this presentation. The radar is installing on a moveable robotic platform for remote operation on the territory with radioactive pollution. The manufacturing and testing of the presented UWB radar in progress now. The radar should be employed in a half of year near the damaged power plant block No. 4 of the Chernobyl nuclear power plant. The following key tasks should be solved by radar on this site in the frame of international project: 1) determination of internal structure of concrete building elements; 2) localization of internal reinforcement elements in concrete; 3) searching nuclear-fuel contained elements of cylindrical shape under concrete shielding etc. Generally the presented UWB radar system includes two principal components, i.e. electronic and mechanical ones, the multi-channel radar and movable robotic platform. The multi-channel UWB radar consists of three main subsystems: 1) sensor receiving array (4 vertical and 4 horizontal receiving channels, 2 cross-polarized transmitters); 2) data and command transfer subsystem via optical line, 3) control of operation and data processing/storing subsystem. The sensor array is installed on the robotic platform for remote operation. This array is accomplished by using the transmitter and receiving modules with shielded antennas. Command for controlling the radar operation and to set the data acquisition modes as well as data transmission to the central computer from sensor array is implemented by the data/command transmission subsystem aforementioned. The last forms a local network between computer on robotic platform and the central computer installed on the safe distance up to 0.5 km from the working zone of radar.

The robotic platform is in fact a controlled distantly carrier of radar sensor array for its programmed replacement for scanning over

searching territory. There are also a video-control for visual monitoring of operation conditions and navigation subsystems. The last is necessary for exact spatial positioning of the sensor array on searching site and to give spatial coordinates in electronic format. In process of radar survey the sensor array is moving in discrete step-by-step or continuous mode over the searching area by the robotic platform. Antennas of the sensor array are close to the surface and operate in stand-on and stand-over modes. Multi-channel radar data are registered and stored with coordinate information and then post-processing for its visualization in form of B- and C-scan. 3-D reconstruction of sounding media for its imaging in electronic format will be considered and discussed.

## 6.1

**Virators and Virtodes - Current state and Perspectives**

*Didenko, A<sup>1</sup>; Magda, P<sup>2</sup>*  
<sup>1</sup>Russian Academy of Science, Russia; <sup>2</sup>Institute of Plasma Electronics Advanced, Ukraine

A modern state of HPM electronics based on overcritical beam current operation regimes is presented as an analysis of a variety of virtual cathode devices. In comparison to conventional HPM relativistic radiation sources virators have a number of essential advantages - design simplicity, high power microwave emission, wide tuning frequency band, and good adaptivity to variety of energy storage systems, which are attractive for numerous applications (A.N. Didenko Yu.G. Yushkov, Microwave High-Power Nanosecond Pulses, Moscow, 1984).

To increase the virator system efficiency and to extend a range of radiation parameter control some progressive virator configurations had been proposed for about 25 years (triode with reflex beam, waveguide system with traveling beam, cavity oscillator, reditron, etc). Given the supercritical current systems being associated with one class of HPM devices, one may notice the presence of a strong beam and electromagnetic feedback (BFB/EMFB) specific for every particular device. The complexity and means for providing both kinds of feedback are different for various virator configurations, detecting their basic features, operation regimes and performance.

The known practical and theoretical data witnesses the system sufficient efficiency improvement for cavity resonant VC-systems, which provides smaller start currents and larger increments. The highest performance (about 40 %) is shown for the reflex triodes (RT) with a high-Q resonator due to the possibility of electromagnetic field enhancement and the EMFB mode selection in the cavity. A different way for providing a high gain generation may be realized due to beam current preliminary modulation - a well known effect for systems with separated areas of beam formation and interaction. A kind of the traveling beam virator (TBV) with a controlled waveguide EMFB - the Virtode device demonstrated up to 17 % efficiency and the possibility of a wide-ranged radiation output

power control at the expense of the EMFB conditions variation (N.P. Gadetski, I.I. Magda, et al., Plasma Phys. Rep, 19, 273 1993). The Virtode basic difference from the traditional RT and TBV is associated with principally new control channel, based on an EMFB between the VC and REB acceleration regions. The presence of the EMFB signal in an area of REB formation also provides conditions for the system gain control over a wide frequency band given by the EMFB and original virator spectral characteristics. The last time projects developed the Virtode idea. A sufficient magnification of efficiency was shown for the virator-klystron configuration (W. Jiang, K. Masugata et al., SPIE, 2154, 124, 1994), and for the VC oscillator (S.D. Korovin, I.V. Pegel et al., Proc. 12-th Int. Conf. BEAMS'98, Haifa, Israel, 1998), which used an effect of a «thick» anode, incorporating resonant cavity, as an intermediate drift and interaction area.

In this report the basic virator systems are compared on efficiency, spectral characteristics and the possibility of the output radiation parameters control and the role of BFB and EMFB for the beam particle and system dynamics are analyzed.

## 6.2

### Study of Frequency-Tunable L-Band and S-Band Feedback Vircators

Pegel, I<sup>1</sup>; Kitsanov, S A<sup>1</sup>; Klimov, A I<sup>1</sup>; Korovin, S D<sup>1</sup>; Kurkan, I K<sup>1</sup>; Kutenkov, O P<sup>1</sup>; Polevin, S D<sup>1</sup>; Tarakanov, V P<sup>2</sup>; Wioland, R<sup>2</sup>; Rostov, V V<sup>3</sup>

<sup>1</sup>Institute of High Current Electronics SD RAS, Russia; <sup>2</sup>High Energy Density Research Investigation Center, Russia; <sup>3</sup>Centre d'Etudes de Gramat, France

In experiment, virtual-cathode HPM sources with a electrodynamic feedback are realized. The devices do not use external magnetic field. Employment of the feedback allows their operation at a small (20 - 50%) excess of current above the critical threshold. This distinguishes this type of devices from the traditional vircators operating at strongly (factor 2 - 3) supercritical current, improves the microwave production efficiency and the frequency stability, allows single-mode operation as well as continuous frequency tuning by means of changing of the feedback time delay.

The 3D computer modeling of 1.5-GHz and 2.7-GHz vircators (S. Korovin et al., Proc. PPC-97, 736 - 741) made with the completely electromagnetic PIC-code KARAT demonstrated the microwave production efficiency of up to 16% and the frequency tuning bandwidth of ~20% at the half-power level.

Based on the results of optimization made in numerical experiment, experimental mockups of vircators were produced. In experiments employing high-current electron accelerator SINUS-7 (pulse length 50 ns, maximum electron beam current and electron energy 20 kA and 2 MeV), microwave pulses of 1 GW and 500 MW peak power were produced at 1.5 GHz and 2.7 GHz, respectively. The frequency tuning rangewas ~7% at the half-power level. The operation mode of the vircators is TE<sub>10</sub>. The microwave production efficiency reaches ~10% with the radiation pulse length of 30 - 35 ns.

## 6.4

### Microwave Beam-Driven Propulsion Experiments for High-Speed Space Exploration

Benford, J<sup>1</sup>; Harris, H<sup>2</sup>; Benford, G<sup>3</sup>; Knowles, T<sup>4</sup>  
<sup>1</sup>Microwave Sciences Inc, USA; <sup>2</sup>Jet Propulsion Laboratory, USA;  
<sup>3</sup>Abbenford Inc, USA; <sup>4</sup>Energy Science Laboratories Inc, USA

We are conducting experiments and modeling to demonstrate the technique of using the photon pressure of a directed beam of microwave radiation to propel a sail of ultralight C-C material. In the future this method can be used to propel probes to very high speeds for science missions to the outer solar system, the interstellar region and the nearby stars.

Beam-driven scientific probes have the advantage that energy is expended only to send the payload and an attached sail in the region of scientific interest, not to accelerate the driving source itself. The beam source remains on Earth or in nearby space, so can be used to launch many such probes. The method has a substantial efficiency advantage over rockets for reaching speeds >100 km/sec. We report progress of a laboratory exploration to move 'photon-pushed' sails from paper concept to laboratory reality. We are using a 20 kW 7 GHz beam incident in a 10e-7 Torr vacuum chamber on new ultralight carbon-carbon microtruss fiber sails of mass density 1-10 g/m<sup>2</sup> at microwave power densities of ~kW/cm<sup>2</sup>. This should give accelerations of several gees. Sails under such accelerations reach ~2000 K, ruling out most materials. Diagnostics are optical and IR video photography, pyrometer, reflected microwave power and residual gas analysis. A predictive dynamic model of coupled differential equations is compared directly with the measurements.

We also discuss deep space exploration missions and concepts for building the infrastructure for space exploration using beamed microwave power systems.

## 6.3

### Power Extraction from the Tapered MILO

Hook, M<sup>1</sup>; Eastwood, J<sup>1</sup>; Hawkins, K<sup>1</sup>; Harbour, M<sup>2</sup>; Kerr, B<sup>2</sup>; Spark, S<sup>2</sup>; Douglas, S<sup>2</sup>

<sup>1</sup>AEA Technology, UK; <sup>2</sup>DERA, UK

This paper reports work on separating the dc and rf current in the output line of the Tapered MILO, and converting the rf output from TEM to a TE mode suitable for radiation.

The Tapered MILO is a crossed field device capable of providing Gigawatt-level rf power in the TEM mode in the output coaxial line. The problem to be resolved is to provide a dc current return path between the inner and outer conductor of the coaxial line and to convert the TEM mode to a TE mode in rectangular or circular guide for radiation. In addition, the mode converter needs to be sufficiently wide band to allow for the tuning of the MILO, and needs to avoid local field enhancements which may lead to breakdown at the high field levels it operates at.

A number of different current return and mode conversion scenarios will be considered, showing the rationale behind the options chosen for experimental demonstration. Experimental results showingsuccessful operation for high-power single-shot operation at Culham and for repetitively pulsed operation at DERA Pershore will be given.

## 7.1

### Envelope Power Sensors for HPM Measurement

Dagys, M<sup>1</sup>; Kancleris, Z<sup>1</sup>; Simniskis, R<sup>1</sup>; Schamiloglu, E<sup>2</sup>; Agee, F J<sup>3</sup>  
<sup>1</sup>Semiconductor Physics Institute, Lithuania; <sup>2</sup>University of New Mexico, USA; <sup>3</sup>AFOSR/INE, USA

Microwave pulses generated by HPM sources are, as a rule, non-rectangular. Therefore, the concept of a pulse's power - the power averaged over the pulse width - is not totally satisfactory to distinguish them. The power envelope or the instantaneous power allows one to more precisely characterize the generated pulses. When measuring the envelope power the averaging time is finite and limited. On the one hand, it must be small compared to the pulse length, on the other, the averaging time must be large in comparison with 1/f, where f is a carrier frequency of the microwave pulse. The response time of the particular device used for microwave pulse power measurement practically limits the minimal averaging time when measuring the power envelope.

In this contribution a series of waveguide type resistive sensors (RS) for HPM pulse measurement with short response time is presented. The performance of the RS is based on an electron heating effect in semiconductors. The sensing element is actually a resistor made from n-type Si with Ohmic contacts on the ends. It is placed within a waveguide where the HPM signal propagates. The HPM electric field heats the electrons in the volume of the semiconductor and its resistance increases. So, by measuring this resistance change the HPM pulse power can be determined. Electron heating inertia is the physical reason that limits the response time of the RS. It is a very fast process with a characteristic time of 2.9·10<sup>-12</sup> s for n-type Si at room temperature. Nevertheless, the actual response time of the sensor is limited by the current rise time in the DC circuit of the RS.

The RS for L, S, C, X, Ku and Ka-bands have been designed, manufactured, and calibrated. A 50 V DC pulse supply has been used for the RS feeding so that an output signal of a few tens of Volts has been obtained at maximum power level without any amplification. The response time of the RS has been estimated using a time-domain reflectometry method to be less than 10/f.

The RS has been tested under operational conditions at HPM facilities in the USA. The tests have revealed some advantages of the RS over traditional devices. They can detect directly about 60 dB greater pulsed microwave power, are resistant to larger power overloads, produce high output signals, and are sufficiently fast to measure the power envelope of nanosecond duration HPM pulses.

## 7.2

### The Investigation of the Effective Dielectric Measurement for Nondestructive Operation

Aksoy, S<sup>1</sup>; Tayyar, I.H<sup>1</sup>; Karaçuha, E<sup>1</sup>

<sup>1</sup>GIT, Gebze Institute of Technology, Turkey

#### Abstract

Microwave technology and electromagnetic wave theory have their conventional applications of telecommunications, radars, medical, military etc. which are rapidly expanding into new areas related to industrial measurements. Nevertheless, numerous techniques have been developed for measuring the dielectric properties of the materials at microwaves. Generally, most of these techniques like cavity method, open-ended transmission line, free-space method etc. need sample preparation before the dielectric measurement experiment on investigated objects. Because of the necessity of the destructive operation on sample, this is a big disadvantage for practical measurement. While making practical measurement of dielectric permittivity, it can not be possible to make destructive operation on every sample due to their structure, position, production cost, time and more man-power. In many industrial and medical applications, nondestructive measurement techniques are the only available options. To overcome all of these problems, an open-ended rectangular waveguide technique is described to measure dielectric coefficients of materials with a simple and effective numerical procedure which can be programmed on a personal computer. According to this procedure, a rectangular waveguide in which the dominant mode only can propagate is terminated by a flat large metallic flange which is placed in contact with the flat surface of the material to be tested. The amplitude and phase of the reflected wave are measured and compared to those produced by a flat metallic plate placed on the flange. This yields the complex reflection coefficient  $\Gamma$  from the relative permittivity ( $\epsilon = \epsilon' - j\epsilon''$ ) of the investigated material can be determined by using a personal computer program.

#### Conclusion

It is shown that the experimental results are satisfied according to some standard values of dielectric permittivity constant with an accuracy of %90. It means that extremely effective dielectric measurement method which is especially suitable for practical, easy and nondestructive measurement of the dielectric permittivity constant is investigated and applied to new materials such that different kind of sand, marble etc.

## 7.4

### The Measurement of Aperture Effective Area Using Mode Stirred Techniques

Watkins, S.P<sup>1</sup>

<sup>1</sup>DERA, UK

The experimental methods currently used for the assessment of screening performance of enclosures are based on the Mil Std 285 insertion loss technique. This method defines shielding effectiveness as the increase in insertion loss between two co-polarised antennas caused by the introduction of the enclosure into the test configuration. The technique has also been used to assess the relative screening performance of small samples of enclosure material by locating the sample under test in the dividing wall between a pair of anechoically lined or mode stirred test chambers. In both cases, however, the results are not determined solely by the shielding characteristics of the test object. Consequently the results are applicable to a predefined test configuration only and it is difficult to determine reliable information regarding the levels of shielding performance that could be expected in other environments. In the general case, this makes the accurate prediction of internal field levels very difficult even if the characteristics of the external threat are accurately known. To simplify matters, the measurement of an 'absolute' quantity which is defined solely in terms of the screening properties of the shield material itself is required. In theory this parameter could then be combined with factors describing variables such as internal loading, equipment configuration etc to predict the internal field level at any point within the enclosure.

This paper describes the measurement of the effective area of samples of enclosure material and whole enclosures within a statistically uniform electromagnetic environment. The technique uses a rotating conductive stirrer to perturb the transmitted field producing a uniform field distribution. Initially swept frequency measurements of effective area were performed on two Aluminium panels containing circular apertures of 5 and 10cm diameter respectively. In both cases the results were found to be independent of chamber loading. The measured effective area of each aperture, in combination with other parameters such as the Q factor and volume of the chamber, was then used to theoretically predict the aperture shielding effectiveness for various loading conditions. In all cases the shielding effectiveness predictions were compared to measurements and found to provide very good agreement.

## 7.3

### The Use of Direct Current Injection Techniques for EM Testing of Missile Systems

Barber, G.D.M<sup>1</sup>; McQuilton, D<sup>2</sup>

<sup>1</sup>DERA, UK; <sup>2</sup>Matra BAe Dynamics, UK

This paper describes a recent programme of work to investigate an alternative to whole platform free field illumination testing, employing direct current injection (DCI) techniques. The main objective of the research programme was to show equivalence between direct current injection and free field illumination techniques in terms of induced cable/loom transfer functions and comparisons between DCI and free field illumination at system upset.

The DERA have been actively involved in the research of alternative, more cost effective/efficient test techniques over the past 2 decades. More recently research effort has been concentrated on the development of the reverberation chamber technique for immunity, shielding effectiveness and emissions and the use of DCI for the EM clearance of whole aircraft and missile platforms. The missile DCI programme is being worked on jointly under a memorandum of Agreement between DERA and Matra BAe Dynamics.

The paper outlines the development of DCI applied to missile systems over the frequency range 10 kHz to several hundred MHz. Higher frequency EM transfer function measurements and susceptibility testing can be performed within reverberation chambers, sometimes known as mode stirred or mode tuned chambers. Most 'standard' shielded room sized reverberation chambers will operate from as low as 200 MHz, providing 'good' (time averaged) field uniformity. Low frequency EM transfer function measurements and susceptibility testing can be performed using DCI techniques, whereby the missile body/skin becomes the centre conductor of a coaxial transmission line system.

The paper also discusses the advantages of employing DCI, in terms of test costs and efficiency. In addition results are presented to show equivalence between measured free field cable transfer functions, employing OATS and the large (10\*8\*7m) reverberation chamber at DERA, Farnborough. The equivalence between free field and DCI measured transfer functions are also illustrated.

A target drone (Chukar II) was employed for both cable transfer function measurements and susceptibility measurements. Susceptibility measurement results are also illustrated showing equivalence between the reverberation chamber free field test and DCI at system upset. The target drone was powered and all control surface movements monitored via EM hardened cameras during testing.

## 7.5

### A Novel Near-Field Measurement Methodology for Random Emissions

Fourestié, B<sup>1,2</sup>; Altman, Z<sup>1</sup>; Wiart, J<sup>1</sup>; Bolomey, J Ch<sup>2</sup>; Brouaye, F<sup>2</sup>

<sup>1</sup>France Télécom R&D, France; <sup>2</sup>LSS-Supélec, France

Near-Field (NF) measurement facilities such as spherical compact range systems are widely used to accurately determine the deterministic fields radiated by antennas or scatterers in amplitude and phase. Well known NF to Far-Field (FF) transformation algorithms can then be applied to calculate the field at any point exterior to the measurement surface. However, in the context of EMC the fields radiated by a Device Under Test (DUT) are random and no reference of phase is available. Standard NF measurement techniques are therefore unsuited. The purpose of this paper is to introduce a novel NF methodology well suited to random emissions. Assuming that the radiated fields are weakly stationary in time and in space, it is possible to measure the spatial coherence function of the fields taken at two different points and for a particular frequency. We introduce the bimodal transform and the sub-space signal decomposition applied to NF coherence matrices to estimate up to the second order the fields radiated at any point exterior to the surface. The bimodal transform has been introduced in optics and is used in astronomy whereas the sub-space signal decomposition technique has been put forward in super resolution algorithms such as MUSIC. A new experimental spherical measurement facility has been designed and patented. It allows one to measure the coherence matrix of the NF radiated on a spherical surface enclosing the DUT and to apply the aforementioned processing technique. The following features of this measurement facility make it very advantageous compared to the measurement set up specified by standards: Absence of truncation in space, compactness, accuracy, and contingent identification of signals. Numerical simulations and measurement results validating the new technique will be included in the presentation.



## 8.1

HPM Coupling to Wire Structures Including Radiation Effects  
 Haase, H<sup>1</sup>; Nitsch, J<sup>1</sup>  
<sup>1</sup>Otto-von-Guericke-Universität Magdeburg, Germany

Nowadays, the coupling of high-frequency electromagnetic waves into complex electronic systems becomes more and more important, in particular for HPM and UWB. As soon as the electromagnetic energy has coupled into a system it will excite subsystem-cavities, wire structures as well as devices with their electronic components. Since the cabling in systems is a necessary means to transport signals, and the em interaction with cables is very effective, we concentrate our investigation on high-frequency coupling to general cable structures. This is done on the basis of an essentially modified transmission line theory.

Starting from the integral equation for the electric field a generalized transmission line theory for arbitrary wire structures, which can be considered as a nonuniform transmission line, is derived. While the general form of the telegraphers equation is preserved, new space dependent parameters are introduced that fully describe the behavior of the wire structures, independent of the current distribution on the wires. The solution of the resulting equations can be obtained using standard procedures to solve the telegraphers equation for nonuniform transmission lines.

In a first step quasi static parameters, strictly speaking, valid only for low frequencies, are determined by assuming a reasonable current distribution along the wires. These parameters already include information about the direction and the length of every individual wire. As opposed to traditional techniques where nonuniform lines are approximated by piecewise uniform lines, the new approach delivers accurate results for resonance frequencies as well as for the propagation speed of the electromagnetic wave, even for higher frequencies. However, radiation effects are not taken into account.

In a second step the general solution for the current distribution of the wires from step one will be used to determine new transmission line parameters. The idea behind this is that even at high frequencies, the currents from step one are a good approximation of the real current. Using this approximate solution, the electric field integral equation can be rewritten as a generalized telegraphers equation. In addition to the classical per unit length parameters other parameters occur that mainly account for radiation.

The results from the solution of the transmission line equation with the new parameters are in excellent agreement with results obtained using the Method of Moments or the PEEC Method and with measurements.

The main advantage of the proposed method over MoM or PEEC is to accomplish the solution of the telegraphers equation within a fraction of the time needed by others, except that the computational effort to determine the parameters is quite high. However, this has only to be done once for every wire configuration.

## 8.2

Modeling and Measurement of Internal H-fields of a Rebar Enclosure Excited by an External Current Source  
 Tesche, F M<sup>1</sup>; Ianoz, M V<sup>2</sup>; Nicoara, B<sup>2</sup>; Kálin, A<sup>3</sup>;  
<sup>1</sup>Electromagnetics Consultant, USA; <sup>2</sup>Ecole Polytechnique Federale de Lausanne, Switzerland; <sup>3</sup>NEMP Laboratory, Switzerland

The use of reinforced metal bars (rebar) in concrete is a common practice in modern construction. While not used primarily for electromagnetic (EM) field shielding, it is known that such a metallic structure will provide a modest amount of shielding for electronic equipment within such a concrete enclosure. The EM fields inside the enclosure can be produced by an externally incident propagating field (for example by a distant radio transmitter or from a nuclear electromagnetic pulse), or by the injection of current onto the rebar structure by a direct lightning strike or a power line fault. Moreover, the direct injection of current onto rebar shield by a portable pulser can be used to characterize the shielding properties of the facility -- and possibly even cause damage or upset to internal equipment.

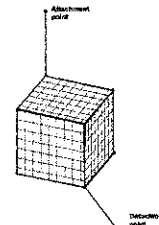


Figure 1. Geometry of rebar cage.

In this paper, a combined theoretical and experimental effort for characterizing the shielding properties of a rebar enclosure is described. This work involved connecting a lightning simulator at the EPFL laboratory in Switzerland to a 2x2x2 m cage constructed of 12 mm diameter welded bars, as the main bars, and 6 mm secondary bars, spaced at 25 cm in each direction on all sides of the cage, as shown in Fig. 1. The secondary bars were attached with thin iron wires (not welded) as is the practice in the actual construction. The attached pulser produced a 1 kA 2x10 μs simulated lightning current injected onto the rebar, and the internal H-field was measured within the enclosure at 99 different points. As described in the project report (Ianoz, M.V., and B. Nicoara, "L'étude sur les effets électromagnétiques dues à un coup de foudre sur un bâtiment ou à proximité d'un bâtiment", NEMP Lab., Spiez, Switzerland, Oct. 30, 1999), a cumulative probability distribution (CPD) for the internal field was generated.

For the same cage geometry, an analysis procedure was developed to evaluate the internal H-fields. Based on a transmission line model for individual currents flowing on the many rebar segments, this analysis first required the calculation of the rebar current and then evaluated the internal H-field by integrating over the rebar structure. As described in another report (Tesche, F.M., "Determination of the Internal and External H-fields for a Rebar Enclosure Excited by a Direct Lightning Strike", NEMP Lab., Spiez, Switzerland, Aug. 15, 1999), the CPD for the internal H-field was also calculated using 500 field samples. Figure 2 illustrates a comparison of the CPDs from the measurements and the calculated responses. Additional details of these results will be presented in the paper.

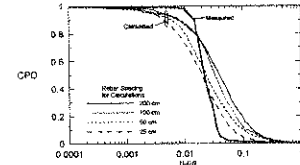


Figure 2. Measured and calculated CPD for the rebar enclosure.

Work sponsored by the Swiss Defense Procurement Agency under Contracts 151-186 and 152-200.

## 8.3

Estimation of Pulse Electromagnetic Disturbances Penetrating into Computers through Building Power and Earthing Circuits  
 Fortov, V<sup>1</sup>; Loborev, V<sup>1</sup>; Parfenov, Y<sup>1</sup>; Sizranov, V<sup>1</sup>; Yankovskii, B<sup>1</sup>; Radasky, W<sup>2</sup>

<sup>1</sup>Russian Academy of Sciences, Russia; <sup>2</sup>Metatech Corporation, USA

Over the past several years there has been increasing concern about the possibility of criminals or terrorists using electromagnetic interference (EMI) techniques to disrupt the operation of industrial or commercial facilities. The reasons for using these methods may be for blackmail purposes or to damage an important part of a communications or security system, thereby aiding general criminal activities. This paper examines, through experimental and analytic methods, the propagation of electromagnetic disturbances through a power supply system from locations outside of a building to locations where computers are found inside. The main objective of this effort is to establish the threat so that efficient, cost-effective protective methods can be developed.

In particular this paper considers a specific building power supply system beginning with a ground-mounted external 10 kV/380 V transformer. Experiments have been performed employing different methods of injecting voltage disturbances on to the three-phase power system. The propagation of these disturbances through the earthing system, protection devices, power cables, switchboards, and the wiring to power outlets is evaluated. Transfer functions are developed from the transformer secondary to specific equipment outlets for different types of injection techniques using both pulsed and cw waveforms.

In addition to the propagation aspects, computer vulnerability to pulse disturbances has also been examined and is discussed in this paper. Theoretical methods are used to predict the weak components in power supply filters in actual computers available to this project. For one of the computer power supplies, pulse testing is done to determine the consistency of the failures observed with the theoretical analyses performed.

This paper concludes with a list of future tests and analyses needed to complete the evaluation of this threat to computers in buildings.

## 8.4

Microwave Testing of a Computer: A Representative Example of the Susceptibility of Commercial System

Seow, T S<sup>1</sup>; Yeo, P C<sup>1</sup>; Jansson, L<sup>2</sup>; Backstrom, M<sup>2</sup>

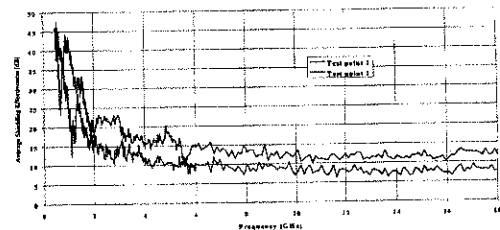
<sup>1</sup>DSO National Laboratories, Singapore; <sup>2</sup>FOA Defence Research Establishment, Sweden;

This paper describes the Low Power Microwave Test Methodology and the test result of Microwave susceptibility measurement on commercial PCs. In this research, we carried out two types of measurement on the PC. They are as follows:

- Shielding Effectiveness (SE) of the PC in Reverberation Chamber
- Low Power Microwave (LPM) Susceptibility Testing

For the SE measurement of the PC, it was performed in the FOA's Reverberation Chamber. The chamber size is 5.1 m X 2.46 m X 3 m. The Reverberation Chamber consists of two stirrers, one rotating vertically and the other horizontally. The field inside the computer was measured using two short "monopole" probes of length 4 mm. Such probe is constructed from a semi-rigid cable with the inner conductor exposed at the end. The figure below shows the average shield effectiveness level measured.

Average Shielding Effectiveness for Computer at TP1 & TP2. Measured in FOA Reverberation Chamber.



In the LPM susceptibility testing, the PC was broken down into seven sub-systems. Each sub-system was tested using the same test parameters (E-field = 100/200 V/m, CW, Horizontal and Vertical Polarisation). The objective of this measurement is to determine the impact of the PC sub-systems under Microwave radiation. The PC sub-systems were as follows:

- Power Supply
- Video Monitor Unit
- Keyboard
- Motherboard (Ram and Reset)
- Hard Disk / Floppy Disk
- Serial Communication Port
- Parallel Communication port

Preliminary investigation has shown that most of the sub-systems were more susceptible to low frequency than high frequency Microwave Radiation. It was also observed that field level of 200 V/m was unable to damage the PC (only caused degradation). The most susceptible sub-system was the Video Monitor and least susceptible was the Hard Disk.

## 8.5

### Structuring of data bus system response against unwanted electromagnetic signals

Carter, R J<sup>1</sup>; Kohlberg, I<sup>2</sup>;

<sup>1</sup>Operational Test & Evaluation, Office Sec, Defense, USA; <sup>2</sup>Institute of Defense Analysis, USA

→ BER caused bei EM-field

future: BER  $10^{-13}$  -  $10^{-14}$  required

if you know protocol: → put system to shutdown

## 9.1

### Complex Space-Time Solutions of Maxwell's Equations

Felsen, L B

<sup>1</sup>Boston University, USA

An important category of "fundamental solutions to Maxwell's equations" encompasses those carried out in complex space-time. The domain of complex space-time coordinates is accessed by analytic continuation of the field equations, with real physical fields generated by projection onto the real space-time subdomain. This process is systematized by formulating the Green's function  $G(\mathbf{r}, t; \mathbf{r}', t')$  excited by an impulsive point-source corresponding to  $\delta(\mathbf{r}-\mathbf{r}')\delta(t-t')$ , where  $\mathbf{r}'$  is the source location and  $t'$  is the impulse turn-on time. Analytic continuation of the coordinates  $(\mathbf{r}', t')$  to complex values  $(\hat{\mathbf{r}}', \hat{t}')$  yields complex-valued solutions  $\hat{G}(\mathbf{r}, t; \hat{\mathbf{r}}', \hat{t}')$  which continue to satisfy the field equations and boundary conditions for real  $(\mathbf{r}, t)$  in any physical environment, since  $(\hat{\mathbf{r}}', \hat{t}')$  are specified parameters.

The resulting solutions are of great interest and utility because the complex  $(\hat{\mathbf{r}}')$  or  $(\hat{t}')$ -generated wavefields in free space are time-harmonic Gaussian beam-type or time-dependent pulsed beam wave objects, respectively. Thus, at any given real observation point, the replacement of the real source point coordinates in any Green's function changes the response due to a spherically spreading time-harmonic or impulsive wave front to the response due to a spatially collimated beam or a spatially-temporally collimated pulsed beam wavepacket, respectively. The collimation is effected by evanescent spectra which are produced away from the real beam axis by the complex source displacement. The most general setting for performing the analysis is the eight-dimensional configuration (space-time)-spectrum (wavenumber-frequency) phase space, from which projections onto appropriate subdomains can be implemented.

At high frequencies or at observation times near the first arrival in the time domain, asymptotic methods can be employed to quantify and parameterize the wave dynamics. Paraxial approximations, restricted to strong collimation with weak evanescence in the vicinity of beam axis, allow beam or wavepacket tracking entirely in real space. Less collimated, more strongly evanescent wave objects require complex ray tracing, with each complex ray accommodating the single point  $(\mathbf{r}, t)$  at the intersection with the real configuration subdomain to generate a physical observable.

Various techniques and applications of phase space high frequency asymptotics are presented, with emphasis on open problems that need to be addressed.

## 9.2

### Diffraction by Arrays of Complex Source Point Beams

Jull, E; Cheong, H

<sup>1</sup>University of British Columbia, Canada

The complex source point (CSP) method converts an exact source diffraction solution to an exact beam source solution by a substitution of appropriate complex coordinates for the real source coordinates. An omnidirectional source pattern then becomes a beam pattern, paraxially Gaussian and with no sidelobes. Aperture antenna patterns, which have sidelobes, can be synthesized from arrays of Gaussian beams of appropriate spacing, direction and directivity with their amplitudes determined from the aperture distribution producing the field which they are to represent (P.Einziger, S.Raz and M.Shapira, JOSA A, 3, 508-522, 1986). This "Gabor" representation can be as accurate as desired if sufficient beam sources are used. The procedure is closely related to the use of wavelets in signal processing and, for efficiency, an arrangement which minimizes the required number of beams is chosen.

When the basis elements of this series are the elementary beam source solutions for a particular obstacle in the near field of an aperture antenna, the scattering pattern is obtained by summing the series. The great advantage of using CSP beams, rather than simply Gaussian beams, is that they permit the use of exact solutions as the basis elements, for the CSP beam solutions can rigorously satisfy the wave equation, while Gaussian beam solutions are approximations. This seems to be the most general and efficient method for accurately dealing with practical near field scattering problems for it can use the repertoire of line or point source low and high frequency diffraction solutions for canonical structures such as modal series and the uniform geometrical theory of diffraction, and, at least for the latter, combinations thereof.

The numerical examples given show that for apertures of moderate size very accurate results can be obtained with rather few beam sources. Accuracy is established by comparison with moment method results for scattering structures of moderate size. Beginning with semi-infinite two dimensional structures such as the half plane and wedge, we examine also results for small circular cylinders and larger rectangular cylinders in the presence of local aperture distributions which are both uniform and tapered.

## 9.3

### Application of Concepts of Advanced Mathematics and Physics to the Maxwell Equations

*Baum, C.E.*

*'Air Force Research Laboratory DEHP, USA*

Since the pioneering work of James Clerk Maxwell in establishing what we call the Maxwell equations, these have had a profound effect on the development of science and engineering. In addition some material-related parameters are needed to relate  $\vec{J}$ ,  $\vec{D}$  and  $\vec{B}$  to  $\vec{E}$  and  $\vec{H}$ , such as the constitutive parameters. More general (even nonlinear) forms are sometimes encountered. Various boundary conditions (e.g. perfectly conducting surfaces) are readily derived as limiting cases.

The role of the electromagnetic theorist concerns understanding what the Maxwell equations allow one to do in the way of analysis and synthesis of the performance characteristics of various electromagnetic devices as well as understanding the behavior of electromagnetic fields in natural environments. I would like to emphasize the concept of EM synthesis. One can analyze the interaction of EM waves with arbitrary geometries of various materials. While this is a challenging task, it is not synthesis. Synthesis starts with some desired performance characteristics and asks, "Is this possible within certain general constraints (e.g., passivity)?" If it is possible then one moves on to other questions such as: "What are the best possible values of the appropriate performance parameters?", and "What are the algorithms for designing (realizing) the device (antenna, scatterer, etc.) with the desired performance parameters?"

In 1976 I published a review paper concerning transient EM theory [C.E. Baum, Proc. IEEE, 1976, pp. 1598-1616]. In this I outlined some advanced analytic concepts used in mathematics and physics that are not commonly being used, or just beginning to be used, in EM theory for both analysis and synthesis. Since then considerable progress has been made in exploring these concepts and obtaining useful results. This gives new techniques for electromagnetic analysis, and especially for synthesis of new electromagnetic devices. This paper summarizes progress in this regard under five general headings: integral-operator diagonalization, complex variables applied to frequency, symmetry and group theory, differential geometry for transient lens synthesis, and electromagnetic topology for analysis and control of electromagnetic interaction with complex systems.

## 9.5

### Exact Solutions for Boundary-Value Problems Involving Isorefractive Media

*Uslenghi, P.*

*'University of Illinois at Chicago, USA*

Two media that are penetrable to electromagnetic radiation are called "isorefractive" (or "diaphanous") if they have the same refractive index, i.e. the same value of the product of electric permittivity and magnetic permeability; the intrinsic impedances of the two media have different values. If a plane wave is incident on the planar interface separating two isorefractive half spaces, the transmitted wave propagates in the same direction of the incident wave, and the reflection and transmission coefficients are independent of both direction of incidence and polarization of the incident wave. In particular, it follows that the critical angle is 90 degrees, hence the interface cannot support evanescent waves, but only lateral waves. These properties have been utilized by the author to solve exactly certain problems involving diffraction by multiple-wedge structures and by a paraboloid of revolution.

A second fundamental property of isorefractive media is the following: if the surface that separates two isorefractive media is a coordinate surface in an orthogonal coordinate system for which the wave equation is separable, an exact solution to the diffraction problem is obtained. This is possible because the eigenfunctions that appear in the representation of the electromagnetic field in each of the two media contain the propagation constant as a parameter (and this parameter has the same value in the two media), but not the intrinsic impedance. This property has made it possible to obtain the exact solution to the diffraction problem by a wedge, by elliptic and parabolic cylinders, and, for certain types of sources, by prolate and oblate spheroids, the paraboloid of revolution and the circular cone. Furthermore, we have solved exactly the problems of scattering by a slotted semielliptical cylindrical channel in a ground plane, by a semielliptical ribbon on a ground plane, by a gap in the corner of two metallic walls separating isorefractive media, and the problems of propagation inside a circular waveguide and a coaxial cable partially filled with isorefractive materials. All these exact solutions have been

## 9.4

### Fractional Operators and Solutions to Maxwell's Equations

*Engheta, N.*

*'University of Pennsylvania, USA*

Exploring the possible links between the mathematical field of fractional calculus and the electromagnetic theory has been one of the topics of our research interests in recent years. We have studied the possibility of bringing the tools of fractional calculus and electromagnetic theory together, and have explored and developed the topic of *fractional paradigm in electromagnetic theory* [see e.g., N. Engheta "Fractional Paradigm in Electromagnetic Theory" a chapter in *Frontiers in Electromagnetics*, D. H. Werner and R. Mitra (eds.), IEEE Press, New York, chapter 12, pp. 523-552, (2000)]. Fractional calculus is a branch of mathematics that addresses the mathematical properties of operation of fractional differentiation and fractional integration - operators involving derivatives and integrals to arbitrary *non-integer* orders [see e.g., K. B. Oldham and J. Spanier, *The Fractional Calculus*, Academic Press, New York, (1974)].

In our study, we have applied the tools of fractional calculus in various problems in electromagnetic fields and waves, and have obtained interesting results that highlight certain notable features and promising potential applications of these operators in electromagnetic theory. Moreover, since fractional derivatives/integrals are effectively the result of fractionalization of differentiation and integration operators, we have investigated the notion of fractionalization of some other linear operators in electromagnetic theory. Searching for such operator fractionalization has led us to interesting solutions to Maxwell's equations.

In this talk, we will describe how and under what conditions fractionalization of certain linear operators can provide us with interesting sets of solutions to Maxwell's equations. Such solutions, which can be interpretable as "intermediate solutions", may lead to interesting potential applications in mathematical treatments of some electromagnetic problems. Certain specific examples will be discussed in detail, and physical insights to these problems will be given.

obtained by separation of variables. The problem of a half space in contact with two isorefractive quadrants has been solved by Wiener-Hopf technique.

All the above exact solutions have been possible because of the following theorem: if the solution of a diffraction problem is known for perfectly conducting bodies, it is also known if the materials of these bodies are replaced with isorefractive media. In particular, it follows that the field scattered by an isorefractive cylinder of arbitrary cross section under oblique incidence is the sum of TE and TM fields.

## 10.1

### Selective Target Detecting UWB Radar Systems

*Taylor, J.D.<sup>1</sup>; Immoreev, I.<sup>2</sup>*

<sup>1</sup>J.D. Taylor Associates, USA; <sup>2</sup>Moscow State Aviation Institute, Russia

Future ultra-wideband (UWB) radar development will require understanding the interaction of fine resolution waveforms with both radar systems and targets. Short spatial waveforms will change during propagation, reflection and reception. Because the returned waveform will not be the same as when transmitted, prior knowledge, or estimation of the return signal characteristics will aid in building correlation filters to increase the detection probability. Because the length of the propagated signal will be smaller than the target, it will become many small reflectors at different ranges. A single transmitted short pulse will return as a series of overlapping returns. The resulting radar image will provide information about the target presence, location and structure. This new approach to signal detection can make UWB short pulse radar a powerful device for long-range target detection and identification. We will need time domain analyses of propagation, target scattering and reception.

1. Propagation measurement and analysis: Unlike conventional narrowband antennas, the UWB antenna and signal will interact to produce a time dependent antenna pattern. This effect is not well understood, but can yield valuable insights into building efficient, small beam with antennas for short pulse radar sensing systems. 2. Extended target characteristics measurement and analysis: When high-resolution waveforms interact with a large object, the target becomes a series of reflectors distributed along its length and width. The return will be many impulse responses from the different ranges. This leads to time and angle aspect angle dependent radar cross section concept. Understanding and using the unique high-resolution impulse scattering of extended targets can lead to target identification systems. 3. UWB radar range equation: The antenna and target characteristics of high-resolution waveforms lead to a new radar performance prediction equation. Time dependence of the signal waveform, antenna and target result in a time dependent

range equation. 4. Extended target detection: Building long-range, high-resolution UWB radar systems will require a new approach to signal detection. Extended targets will turn short pulse radar signals into a time shifted set of points, each point return may have a different waveform depending on the target geometry and materials. Simply detecting any of these point returns would result in limited radar range. We propose a different approach using a time delays and summation network to turn the time scattered returns into a single integrated return. Because target characteristics will drive the filter design, then the radar can be made sensitive to specific classes of objects. It would be possible to build radar systems for detecting only one class of targets and rejecting others. Computer control of the correlation interval and other parameters would give flexibility to selectively search for other types of targets.

## 10.2

### Experimental Results from an Ultra Wideband Precision Geolocation System

*Fontana, R.<sup>1</sup>*

<sup>1</sup>Multispectral Solutions Inc, USA

One of the most recent and unique applications of ultra wideband (UWB) technology has been to the determination of precision location in urban terrain and within building structures. In these applications, complex multipath and differential path loss often result in received waveforms in which the direct path is highly attenuated relative to subsequent multipath returns. As a consequence, UWB receiver processing techniques which provide high sensitivity and leading edge detection are critical to successful time-of-flight and, hence, true location measurements.

In this paper, we present experimental results taken with an ultra wideband precision geolocation system developed to track soldiers inside buildings and in open terrain. The UWB Precision Geolocation System utilizes a set of untethered, fixed position "Beacons" and an untethered mobile "Ranger". Three-dimensional positioning information is obtained by determining the round-trip time-of-flight from the UWB "Ranger" to each "Beacon" transponder. The system utilizes a 2 nanosecond (33% fractional bandwidth) burst waveform, and an unique tunnel diode receiver which is sensitive to the received pulse leading edge.

The paper begins with a discussion of the performance of the quantum tunneling device used as a leading edge detector, and proceeds to a description of the UWB Ranger hardware - UWB transmitter, antennas and receiver/processor. Experimental results are provided for both in-building and open terrain system configurations. RMS ranging errors of less than 1 foot are demonstrated for in-building propagation; while open terrain results produce RMS errors of better than a few inches due to leading edge detection of the received waveform.

## 10.3

### Recent Applications of Ultra Wideband Radar and Communications Systems

*Fontana, R.<sup>1</sup>*

<sup>1</sup>Multispectral Solutions Inc, USA

Ultra wideband (UWB) technology, well-known for its use in ground penetrating radar, has also been of considerable interest in communications and radar applications demanding low probability of intercept and detection (LPI/D), multipath immunity, high data rates and precision ranging and localization.

After a short introduction to the history and theory of ultra wideband technology, we describe the current state-of-the-art in this emerging field and provide descriptions of recently fielded UWB hardware and equipment. Applications to be discussed include: LPI/D transceivers for high data rate (video) communications and ad hoc wireless networking, non line-of-sight communications via surface wave propagation, precision geolocation, intrusion detection and alert, UWB tags, precision altimetry and obstacle/collision avoidance radars. A description of the short pulse measurement techniques used in these UWB systems will be presented, along with characterizations of the propagation modes unique to each specific application.

While UWB technology has recently received considerable attention in the U.S. press, many performance claims have been highly exaggerated. It is a further intent of this presentation to attempt to separate "fact from fiction" as well as to provide an overview of recent UWB research initiatives within the U.S. MSSl is a pioneer and an established industry leader in the development of ultra wideband systems (<http://www.multispectral.com>) and has been actively involved in UWB hardware and system development since 1984.

## 10.4

### A Low Power, Ultra-Wideband Radar Testbed

*Payment, T*

<sup>1</sup>Time Domain Corporation, USA

The availability of custom timer and correlator chips has enabled the design and development of a general purpose UWB research instrument by Time Domain Corporation. One configuration of this tool serves as a basic UWB Radar Testbed suitable for research on antennas and algorithms aimed at specific applications of UWB radar. The system includes the UWB radar unit, an antenna unit, and a personal computer for user interface and data storage.

The radar unit houses the UWB transmitter and receiver under the control of an embedded processor that accepts commands from and provides data to the controlling PC over an Ethernet link. The antenna unit consists of separate transmit and receive antennas mounted on a back reflector and cabled to the radar unit via connectors to allow use of alternate antennas. The system can be viewed as a radar response or received waveform capture device. The waveform is displayed and the user can save the waveform data to a file for post processing / application-specific algorithm development.

This radar is particularly useful as a design and development system where a commercial product is envisioned as the ultimate end goal. While the form factor of the Radar Testbed (with its PC, Ethernet, radar unit, and external antenna unit) does not resemble an end product, the fundamental UWB building blocks in this system are applicable to a variety of products.

Similar versions of this basic UWB radar research tool are in development to support research into communications and geo-location applications.

## 11.1

### German Forces Activities about HPM-Simulation/Experiments and Hardening Aspects

*Ruffing, K*

<sup>1</sup>Competence Center EME, Germany

The German Force (Bundeswehr) established a specific research and technology program in regard to find out eg the threshold on different EUT or SUT with several electromagnetic environments.

First step is to carry out a simulation approach about the susceptibility of components or PC's and to determine the transfer function (or shielding effectiveness) of the system in the time or frequency domain. After then, the experiment was done under functional response condition (different configuration and the behaviour of the electronic circuits).

This paper includes the framework of some EUT's and general results are available for the above research program eg

- Drone System
- Missile (foreign country)
- Center Line Travel Pod (CLT) with military equipment
- GENECS-System (Generic)
- Components threats

In the conclusion you will find a description some future activities, especially under the aspects of UWB / Vircator or and microwaves sources. (HPM puls generation utilizing chemical explosives).

direct } sources fixed/mobile (truck)  
 indirect } brought towards target ← Double

Ruffing: Technologiefeldverantwortliche Fachgebiet EME  
 Techn. Agreements - S-D, F-D, GB-D in prep.  
 Nation. Working Group HPM  
 in Testing \* EME incl. Ind.

## 10.5

### Ultra-Wideband Principles for Surface Penetrating Radar

*Sachs, J<sup>1</sup>; Peyerl, P<sup>2</sup>; Roßberg, M<sup>1</sup>; Rauschenbach, P<sup>1</sup>; Friedrich, J<sup>2</sup>*

<sup>1</sup>Ilmenau Technical University, Germany; <sup>2</sup>MEODAT GmbH, Germany

Surface Penetrating Radar (SPR) will be increasingly important in industrial and environmental application fields like mine detection etc. This technology uses electromagnetic scattering in inhomogeneous solid media. Its resolution in space is determined above all by the bandwidth of the sounding waves. Since the propagation loss of electromagnetic waves in solids decreases with increasing wavelength, this bandwidth has to be available at frequencies as low as possible. Thus a relative bandwidth near to one is required for the antennas and the RF-electronics.

Starting from the linear system theory some general requirements on the RF-electronics will be derived. Further some known principles will shortly explained and compared to a new UWB-technology, which is based on Maximum Length Binary Sequences having a bandwidth from DC to several GHz. The main parts of the electronics works on high speed digital circuits having a favourable effect on circuit integration, high speed data acquisition, multi-channel (array) capability, cost etc.

## 11.2

### Susceptibility of COTS PC to Microwave Illumination: Experiment and Modeling.

*Wilbers, A<sup>1</sup>; LoVetri, J<sup>2</sup>; Naus, R<sup>1</sup>*

<sup>1</sup>TNO-FEL, Netherlands; <sup>2</sup>University of Manitoba, Canada

The use of high power electromagnetic waves to intentionally disrupt and/or damage communications and information processing equipment is an area of concern which is receiving considerable attention in the electromagnetic compatibility community. The possibility of intentionally disrupting a communications or computing facility using a microwave burst of energy emitted by a directional antenna, coupled with the fact that there is little chance of detection, makes electromagnetic terrorism a real possibility. It is important to know the susceptibility of typical commercial computing equipment such as the personal computer in order to evaluate this threat.

We present results of susceptibility experiments on a PIII 450 MHz system working with two different operating systems. Also, some quick fixes to the susceptibility problem are presented.

The finite difference time domain (FDTD) method is used to analyze the penetration and coupling of electromagnetic energy into the PIII 450 MHz computer cabinet. Various configurations are investigated: case-cover off, case-cover on and installed quick fixes. The purpose of these investigations is to better understand the coupling mechanisms associated with the High Power Microwave (HPM) threat. That is: are there special frequencies which couple best; and are there any geometrical features of the problem which enhance or diminish the coupling of energy to the circuit board. Results of FDTD simulations performed on representative configurations are given.



## 11.3

### The Effects of the HPM Radiation on the Radio Fuze

Huang, J.S<sup>1</sup>; Deng, Q<sup>1</sup>; Liu, F<sup>1</sup>

<sup>1</sup>Beijing Research Inst. of Special Elect. Tech, China

The effects of two bands the High Power Microwave (HPM) on the fuze in different distance, different power density and different states of the fuze are investigated. The thresholds of power density to trig the fuze are studied. Many experiments to investigate the effects of the HPM on the signal of the high frequency of the fuze are carried out. The signals of the fuze are processed by a computer software. The time domain signals and the frequency domain signals such as the frequency spectrums and the power spectrums are analyzed.

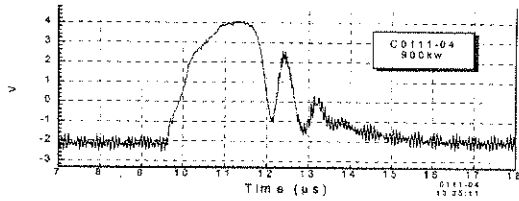


Fig. 1 The high frequency signal of the fuze radiated by HPM

Experimental results show that the HPM can influence the high frequent signals of the fuze seriously and even damaged the circuits of the fuze. The influenced high frequent signals of the fuze are very large than that of the normal signals and have several large short duration pulses (show in Fig.1). The duration is about 2 s. Fig. 2 shows the typical spectrum of the signals. The result shows the band of the signals is from 50kHz to 20MHz. The main frequency of the signal is 50 KHz and the signal amplitude is 1.5V.

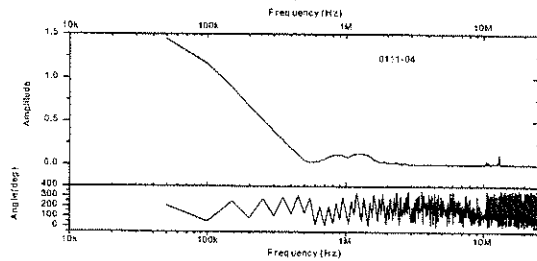


Fig. 2 The spectrum of the high frequency signal of the fuze radiated by HPM

## 11.5

### Radiated EMP Susceptibility Testing of COTS Electronics

Rooney, M<sup>1</sup>; Lubell, J<sup>2</sup>; Ma Pierre, J<sup>3</sup>

<sup>1</sup>Defense Threat Reduction Agency, USA; <sup>2</sup>JAYCOR, USA; <sup>3</sup>Defense Threat Reduction Agency

There is a requirement to use commercial electronics in United States military systems to the extent practical. As a consequence, commercial electronics are finding their way onto the modern battlefield. In addition, critical civilian infrastructure systems are becoming more reliant on electronic components. Thus, in both the commercial and military sectors, there is increasing interest in the capability of Commercial-Off-The-Shelf (COTS) electronics to operate during and after exposure to high-altitude electromagnetic pulse (HEMP) environments.

The capability of modern commercial electronics to operate through HEMP environments is largely unknown. Therefore, the Defense Threat Reduction Agency initiated a program to test COTS subsystems and to populate an immunity data base using the results. Several commercial electronic components, configured as operating subsystems, were exposed to simulated HEMP fields in the laboratory. Operation during and after exposure was monitored, and immunity/susceptibility levels determined. The specific objectives of this testing were:

1. Determine the EMP radiated susceptibility/immunity (modified RS105) for two COTS-based subsystems, a video equipment subsystem, and a CISCO Systems Router LAN subsystem.
2. Determine if radiated or conducted susceptibility is the dominant cause of any observed anomalies.
3. Determine the sensitivity of immunity/susceptibility to subsystem configuration.

The results of this COTS equipment testing show that COTS components configured as operating subsystems have upset and damage susceptibility levels below the peak HEMP fields that can be experienced on the battlefield. Upset was observed below 1 kV/m and damage in the range of 4 kV/m. Field coupling to interconnecting cables caused the anomalous response.

Immunity levels should be considered at least a factor of 2 below the corresponding susceptibility levels. Thus, there is risk that mission functions dependent on these COTS subsystems will be degraded upon exposure to HEMP fields if the subsystems are deployed without HEMP protection

## 11.4

### Interference of Smart Defence Systems (Ammunition and Missiles) caused by HPM- and UWB-irradiation

Bohl, J<sup>1</sup>; Ehlen, T<sup>1</sup>

<sup>1</sup>Diehl Munitionssysteme GmbH Co. KG, Germany

Smart ammunition and missile systems are characterized by the use of complex electronics, computers and sensors. On one side, these systems provide excellent performance regarding the mission they are designed and built for. On the other side, these systems are due to their design requirements especially vulnerable against electromagnetic fields radiated from HPM- and UWB-Sources. This vulnerability and susceptibility must be seen as a threat and as a chance as well. The friendly systems have to be hardened against this threat whereas the unfriendly smart defence systems should be combated using HPM- and UWB-Sources.

Coupling experiments with active smart defence systems are based on analytical and numerical results and also on coupling experiments with the passive systems. The introductory considerations provide information about frequency ranges, coupling paths, coupled currents and voltages on internal wirings. The provided analytical, numerical and experimental results of the passive system enables experiments with the active system in an effective way in respect of time as well as radiation parameters. Only susceptibility investigations with the active system show how the guidance and control loops including electronics and sensors can be interfered.

For the LPM-CW and LPM-Pulse Test Result the most interesting point is when we are looking at the susceptibility possibilities of smart defence systems, i.e. normally the systems are interferable in a broad frequency band. This means that you mustn't hit a very precise frequency for back door coupling. The various resonance peaks can be separated into structure (body) and wire resonances and into fin and slot resonances. It will be presented, that all investigated systems show the similar behaviour - the systems can be interfered on a wide frequency spectrum. Only a few narrow frequency ranges are relatively uncritical. The critical/uncritical frequencies will be shifted with varying the radiation parameters angle of incidence, rotation angle of the defence system and polarization the electromagnetic field.

Nevertheless, only a 6-degree-of-freedom (6-DOF) flightpath simulation is able to show, how the system's mission will be degraded due to interfered GC-signals. It will be shown, that already non-disturbing system interferences prevents a target hit of the investigated missiles.

Burn outs of electronic components within the GC Loops lead also to a target miss hit. Experiments showed, that the burn outs of electronic components occurred mainly with the first powerful HPM-Puls, if the critical frequency was used. Implemented processors into smart defence systems can even be reseted with a rather low electromagnetic fieldstrength. This leads also to a immediate flight interruption.

HPM weapon systems have to take into consideration, that using a single frequency with a narrow bandwidth can miss the systems' critical frequencies and show at the end no effect on the considered defence system. Finally a correlation of the experimentally gathered data with potential HPM/UWB Combat Scenarios will be presented. Advantages and disadvantages various applications are discussed especially in respect of stationary systems, compact systems, HPM systems, and UWB system.

*also for non-military, commercial equipment embedded in government infrastructure*

*Test: ~ Ans, up to 30kV/m*

*→ Primarily caused by conducted transients on unshielded cables*

*→ using COTS may require adding protection*

## 12.1

### Methodology and Results of System Simulation from the Farfield to Circuit Level at HPM Radiation

*Sonnemann, F.; Ehlen, T.; Bohl, J.; Whyman, N<sup>2</sup>*

<sup>1</sup>Diehl Munitionssysteme GmbH CoKg, Germany; <sup>2</sup>DERA Farnborough, UK

This paper describes a methodology to predict the generated distortion effects in electronic circuits caused by HPM radiation. For the calculation of the coupling behaviour from the farfield to the inner structure of a system and the determination of the induced currents on signal wires a FDTD simulation tool is used. Reasonable results are only available for the correct termination loads of the wire, that are specified by the frequency dependent and in general nonlinear input impedances of the connected electronic circuit. These impedances are considered as scattering parameters as a function of amplitude and frequency, measured by a network analyser and then implemented in the FDTD analysis.

Using a network simulation tool the induced currents and voltages are treated as additional independent input sources. The critical aspects of network modelling are the high simulation times resulting from the calculation of the High Frequency - Low Frequency conversion products. However, the main challenge is the implementation of high frequency suitable models.

Another way is to use the calculated induced currents from the FDTD and to create a direct current source in the network simulation program with identical frequency characteristics. Then, threshold values and burn-out values of electronic components can be determined experimentally. This enables the forward and backward system simulation to find out the susceptibility system behaviour.

## 12.3

### Mode-Matched Method in the Analysis of Waveguide-Loaded Cavity

*Hui, N<sup>1</sup>*

<sup>1</sup>Northwest Institute of Nuclear Technology, China

A waveguide-loaded cavity is a fundamental problem in the microwave electronics and accelerator technology. In recent years, a new type of microwave generator-virtual cathode oscillator has been developed. A cavity is also used to achieve narrow-band microwave output. The reign frequency and external Q value are very important characteristics in this system. In general, tight coupling waveguide-loaded cavity is difficult to research by theoretical analysis. Therefore numerical method is applied to analyze tight coupling waveguide-loaded cavity. In most case, some software such as MAFIA is used. In this paper, we manage to use mode-matched method to solve this problem. The model for this system is constructed. A code is developed to simulate this system. The result is coincided with basic physics concept. The reign frequency and loaded Q value are obtained.

## 12.2

### Impulse Radiator Modeling and Experiments

*Morgan, M<sup>1</sup>*

<sup>1</sup>Naval Postgraduate School, USA

Near-fields of impulse-driven antennas located over ground are computed and compared to experiments. Time-domain fields are calculated by first employing stepped-frequency NEC-4 calculations using wire-grid modeling of the antennas over the earth. Near-field frequency-domain data is then extracted from the NEC output file and post-processed using inverse FFT based algorithms programmed in MatLab. Specific impulsive excitation is introduced in post-processing by either circuit modeling (e.g. a Marx bank generator) or by way of measured terminal voltages or currents measured anywhere on the antenna. The procedure employed includes the frequency-dependent effects of impedance mismatch, lossy earth and penetration of impulsive fields into structures.

Comparisons of computations and experimental data will be shown for measurements of near-fields produced by impulsively driven asymmetric horizontal dipoles over ground. Animations of computed fields in the region near to the dipoles will be displayed and discussed.

## 12.4

### Transmission Line Response to a Random External Driving Force

*Primak, S. L<sup>1</sup>; Lo Vetri, J<sup>2</sup>; Roy, J<sup>3</sup>*

<sup>1</sup>The University of Western Ontario, Canada; <sup>2</sup>The University of Manitoba, Canada; <sup>3</sup>Communication Research Centre Canada, Canada

*Introduction.* This paper deals with the numerical simulation of transmission lines under random external electromagnetic excitations. Many practical electromagnetic compatibility problems are too complex to be solved by deterministic methods. It has been suggested recently that an appropriate statistical description would be more helpful and computationally effective. Various statistical models for some external field environments have been suggested in the past (*R. St. John, R. Holland, Proc. ACE, 1994, pp. 554-568*). However, an appropriate mathematical framework for coupling such random fields into lumped and distributed circuits remains an open question and requires further investigation.

*Method.* The first approach is to consider the case of a single two-wire transmission line terminated with linear impedances. A random field is simulated first as an assembly of a number of monochromatic plane waves coming from random directions. The frequency domain formulation is used to model the interaction of these plane waves with the transmission line. The results for several randomly generated instances are accumulated and used to obtain the statistics of the induced near-end and far-end voltages and currents. The dependence of the parameters of these statistical distributions on the length of the transmission line, the number of plane waves per interaction instance and other parameters is investigated. The second approach is to utilize, directly, some statistical models of the electromagnetic field inside an enclosure. Some of the models assume a Chi-square distribution of the field's intensity while more accurate models are based on the family of *K* distributions (*S. Primak, J. LoVetri, N. Simons, J. Roy, and A. Ciccolotta, URSI XXVth General Assembly Abstracts, p. 312, Aug. 13-21, 1999*). The incident random field is generated using a Markov chain approximation and a Stochastic Differential Equations approach. This allows one to reproduce both the distribution of the field values as well as the spatial correlation function. The dependence of the induced voltage on the spatial correlation length of the incident field is also investigated.

*Results.* We have confirmed that if the number of plane waves per interaction instance is relatively large (greater than about 10) and their angle of arrival is close to being uniformly distributed then the induced voltages and currents obey a Gaussian distribution. However, for relatively short transmission lines, these statistics deviate from a Gaussian, especially if a strong spatial correlation is present.

## 12.5

### Analysis of D-Dot EMP Sensors Using Finite Difference Time Domain Method

*Pande, D.C<sup>1</sup>; De, N.C<sup>2</sup>*

<sup>1</sup>LRDE, DRDO Complex, India; <sup>2</sup>Bharat Electronics, India

In measuring the Electromagnetic Pulse (EMP) one has to deal with distributed electromagnetic quantities like electric and magnetic fields, current and charge densities as well as integral quantities such as voltage and currents. In a simpler situation where there is no source currents in and around the sensor and the local medium is well behaved (typically a free space), the D-dot sensors can be used to measure the time derivatives of electric flux density. Basically, a D-dot EMP sensor is an analog passive small antenna, which convert the time derivative of electric flux density to a current at some terminal pair for driving a load impedance.

The Finite Difference Time Domain (FDTD) is one of the efficient numerical techniques for the solution of the time domain electromagnetic problems. The FDTD method shows great promise in its flexibility in handling EMP sensors. The basic advantage of the time domain analysis is that a broad band pulse may be used as the excitation and the frequency domain parameters may be calculated over the entire frequency range of interest by taking discrete Fourier transform of the time domain results.

In the present work FDTD method has been used for the direct time domain analysis of D-dot EMP sensors. The sensors response to double exponential transient and Gaussian pulse are obtained and analyzed. The capacitance and the equivalent area of the sensors are obtained and their variations with the structural dimension of the sensor are determined and compared with that obtained by conventional method. The experimental verification is also done for some of the sensors in the simulated EMP field.

## 13.2

### Development of Component Data to Support System RF Susceptibility Tests

*Latess, J<sup>1</sup>; Gardner, R.L<sup>1</sup>; Stoudt, D.D<sup>1</sup>*

<sup>1</sup>Joint Program Office for Special Technology, USA

The complex systems that make up the infrastructure consist of many component sub-systems. For example, a computer network consists of connected computers located inside a building. Testing of the complete system is most desirable, but is often inconvenient and may not represent all of the system configurations that are of interest. To support extrapolation and understanding it is necessary to test the components of the system under a simulated environment that can, in turn, be related back to the environment experienced in a full system test.

The first step is to characterize the electromagnetic environment in which the computer or other component may be located. This environment is influenced for most cases by commercial buildings of standardized construction. In general, the influence of these structures results in large spatial variations of the field in the vicinity of the test object. Techniques to handle these field variations include statistical electromagnetic analysis although standard test methods do not provide data to quantify the environment in these terms.

Following the environment definition, we can conduct a series of tests in various simulators. Plane wave simulators, like parallel plate devices and GTEM cells, as well as mode-stirred chambers, add information about our understanding of the conditions necessary to make electronic systems fail. Failure thresholds may be expressed in terms of field level, power density, or some other waveform characteristic.

Analysis techniques are also required to extrapolate these results and to help understand the uncertainties in the data. Computers, for example, have so many varieties of subsystems that it is rare to find two identical systems. In this paper, we will describe the current understanding of established test techniques, their shortcomings, and what is needed to provide a more comprehensive analysis of commercial infrastructure susceptibility levels.

## 13.1

### Aspects of HPE Coupling to Systems

*Baum, C.E<sup>1</sup>*

<sup>1</sup>Air Force Research Laboratory DEHP, USA

In this paper a review of coupling of high power electromagnetic (HPE) environments to electronic systems will be provided. New developments in the field will also be presented.

## 13.3

### System Analysis of Potential Illegal RF Weapon System

*Gardner, R.L<sup>1</sup>; Latess, J<sup>1</sup>; Stoudt, D.C<sup>1</sup>*

<sup>1</sup>Joint Program Office for Special Technology, USA

RF weapons are complex assemblies of RF oscillators, pulse forming networks and antennas. These weapons interact with targets along complex paths that are difficult to predict. Complex coupling geometries and varying tactical scenarios lead to varying susceptibility levels that complicate the weapon assessment process. This complex situation requires a combination of empirical and analytical techniques for RF system analysis.

Drawing conclusions from the RF susceptibility data requires careful planning and attention to the requirements of statistical significance. (I. Kohlberg and RL Gardner, EMC Magdeburg, p 37, Oct 99). The chief difficulties in RF susceptibility data analysis are the large number of parameters and the sensitivity of the data to small variations in test conditions. Susceptibility or immunity levels can vary 10 or more orders of magnitude in response to these parameter changes (RL Gardner and CW Jones, SDAN 34, EMP Note Series, 1995). Developing trends in the data therefore requires sample sizes of usually 20 or more examples of the target. On the other hand, large numbers of the test objects are usually not available or are very expensive.

Fortunately, field levels for weapons systems used by criminals and other non-state players are sufficiently low that the weapons rarely cause system damage. Fairly low levels do cause upset (LoVetri, et al, EMC Zurich, p. 39G6, Feb 99). With upset, experiments can be repeated on the same or similar objects. Personal computers are now cheap enough that significant data sets can be developed leaving us with a large amount of parametric data.

This parametric data can be treated using Design of Experiment concepts. In this method only a few (2-3) values of each of the parameters is considered in the experiment planning. This method of experiment planning greatly reduces the total number of tests necessary for statistical significance. In this paper we will describe the methodology used by JPO/STC to study the potential effectiveness of RF weapons.

## 13.4

### Functional Survivability Modeling Tool for Complex Facilities

*Baker, G.H<sup>1</sup>; Mo, C<sup>2</sup>; Calahan, K<sup>3</sup>*

<sup>1</sup>James Madison University, USA; <sup>2</sup>Logicon Advance Technology, USA; <sup>3</sup>Defense Threat Reduction Agency, USA

For critical facilities, survivability and reconstitution in stressful environments generated by electromagnetic transients, sabotage, terrorist activity, military conflict, or Murphy's laws are issues of concern. Critical fixed facilities are likely to be functionally complex and their system-wide failure probabilities, modes, and consequences are often not obvious. To analyze and quantify survivability, existing probabilistic risk assessment tools usually provide a "snapshot" of failure modes at a single point of time for certain initiating conditions. Likewise, elaborate physics models developed to treat weapons effects on structures and individual functional components compute effects at a single time point.

We have developed a tool that improves upon existing computational models by adding the time dimension to the evaluation of functional mission susceptibility to failure of interdependent subsystems of complex facilities. The tool computes the evolution of overall mission failure probability in time by evaluating initial failure probabilities, effects onset times and system repair times for single or combinations of critical facility subsystems. The tool allows the aggregation of scenario and facility functional tree/diagram inputs into an overall system effects evaluation. The model breaks new ground in quantifying and predicting not only initial probability of effect on facility mission execution, but mission outage longevity. Computations invoke a component-up functional fault tree/diagram system analysis to synthesize and quantify overall facility mission survivability. The model is unique in that time evolution of the probability of effects on mission is built-in effectively as a stochastic finite difference equation with initial conditions, deterministic and stochastic, and uses as coded inputs 1) the adverse scenario environmental stresses, 2) the system fault analysis, 3) the individual functional components' damage threshold probability distributions, and 4) the time constants of effects and repairs. The code provides output to users by plotting system mission PE and conditional PE vs. time.

The code is useful for determining the most critical failure points and the most cost-effective protection upgrades. It is a tool well suited for predicting functional impairment due to electromagnetic overstress effects in critical infrastructure systems.

## 14.2

### Primary Forms of Maxwell's Equations in Free Space

*Yaghjian, A.D<sup>1</sup>*

<sup>1</sup>AFRL/ISNH, USA

The traditional form of Maxwell's equations that include electric and magnetic polarization densities ( $\mathbf{P}$  and  $\mathbf{M}$ ) and magnetic charge-current, as well as electric charge-current, is given by

$$\nabla \times \mathbf{E} + \frac{\partial \mathbf{B}}{\partial t} = -\mathbf{J}_m \quad (1), \quad \nabla \cdot \mathbf{B} = \rho_m \quad (2)$$

$$\nabla \times \mathbf{H} - \frac{\partial \mathbf{D}}{\partial t} = \mathbf{J}_e \quad (3), \quad \nabla \cdot \mathbf{D} = \rho_e \quad (4)$$

with the constitutive relations  $\mathbf{D} = \epsilon_0 \mathbf{E} + \mathbf{P}$  and  $\mathbf{B} = \mu_0 (\mathbf{H} + \mathbf{M})$ . The constitutive relations can be used to eliminate  $\mathbf{D}$  or  $\mathbf{E}$  and  $\mathbf{B}$  or  $\mathbf{H}$  from Maxwell's equations in favor of  $\mathbf{P}$  and  $\mathbf{M}$ . Maxwell's equations (1)-(4), which hold in polarized material with the given constitutive relations, can be derived from the free-space Maxwell equations beginning with either bound electric charge-current or bound magnetic charge-current. However, in order to arrive at the same general Maxwell equations (1)-(4) beginning with either bound electric or magnetic charge-current, one must begin with different forms of Maxwell's equations in free space, namely

$$\nabla \times \mathbf{E} + \frac{\partial \mathbf{B}}{\partial t} = 0 \quad (5), \quad \nabla \cdot \mathbf{B} = 0 \quad (6)$$

$$\nabla \times \mathbf{B} - \epsilon_0 \mu_0 \frac{\partial \mathbf{E}}{\partial t} = \mu_0 \mathbf{J}_e \quad (7), \quad \nabla \cdot \mathbf{E} = \rho_e / \epsilon_0 \quad (8)$$

for electric charge-current, and

$$\nabla \times \mathbf{D} + \epsilon_0 \mu_0 \frac{\partial \mathbf{H}}{\partial t} = -\epsilon_0 \mathbf{J}_m \quad (9), \quad \nabla \cdot \mathbf{H} = \rho_m / \mu_0 \quad (10)$$

$$\nabla \times \mathbf{H} - \frac{\partial \mathbf{D}}{\partial t} = 0 \quad (11), \quad \nabla \cdot \mathbf{D} = 0 \quad (12)$$

for magnetic charge-current, provided we retain the usual definitions of  $\mathbf{P}$  and  $\mathbf{M}$  in terms of bound charge and current

$$\mathbf{P}(\mathbf{r}, t) = \lim_{\Delta V \rightarrow 0} \frac{1}{\Delta V} \int_{V_0} \rho_{eb}(\mathbf{r}', t) \mathbf{r}' dV' = - \lim_{\Delta V \rightarrow 0} \frac{\epsilon_0}{2\Delta V} \int_{V_0} \mathbf{r}' \times \mathbf{J}_{mb}(\mathbf{r}', t) dV' \quad (13)$$

$$\mathbf{M}(\mathbf{r}, t) = \lim_{\Delta V \rightarrow 0} \frac{1}{2\Delta V} \int_{V_0} \mathbf{r}' \times \mathbf{J}_{eb}(\mathbf{r}', t) dV' = \lim_{\Delta V \rightarrow 0} \frac{1}{\mu_0 \Delta V} \int_{V_0} \rho_{mb}(\mathbf{r}', t) \mathbf{r}' dV' \quad (14)$$

Therefore, the vectors  $\mathbf{E}$  and  $\mathbf{B}$  are the primary fields in free space produced by electric-charge current, and the vectors  $\mathbf{D}$  and  $\mathbf{H}$  are the primary fields in free space produced by magnetic charge-current. This result and some of its consequences are discussed in the talk.

## 14.1

### Electromagnetic Analysis—from Simple Solutions to Computational Electromagnetics

*Chew, W.C<sup>1</sup>*

<sup>1</sup>University of Illinois Urbana, USA

Despite the century-old advent of Maxwell's theory, electromagnetic analysis is indispensable in many aspects of science and engineering. The primary reason is the pervasiveness of electromagnetic technology in the modern world, e.g., in wireless communication, microchip design, biotechnology, micro-electro-mechanical sensors (MEMS), remote sensing, optoelectronics, etc. The elusiveness of electromagnetic physics and the complexity of the law that governs it have always called for the use of electromagnetic analysis to aid in the understanding and design of systems requiring electromagnetic technology. Electromagnetic analysis is a continuously evolving science up to this day, and recently is an important research topic in computational science.

In the beginning, electromagnetic analysis involved simple shapes, such as spheres, cylinders, planes, half spaces, half-planes. Naturally, the simplicity of the analysis method did not meet engineering and technology demand. In the 1950s, approximate methods were proposed to solve Maxwell's equations and to enlarge the class of solvable problems in order to meet the demand of technology. Examples are high frequency asymptotic methods, and perturbation methods.

To further enhance the versatility of electromagnetic analysis tools, numerical methods were developed in the 1960s with the advent of computer technology. However, these analysis methods consumed exorbitant computer resource, and only small problems can be solved. Nevertheless, numerical methods continuously improve in sophistication in the last three decades in the field of computational electromagnetics.

Recently, fast algorithms have been developed to expedite numerical solutions to Maxwell's equations. These fast algorithms reduce the computational complexity of a dense matrix-vector product from order  $N^2$  to order  $N \log N$  or order  $N$ . Moreover, these methods are matrix free requiring memory proportional to  $N$  instead of  $N^2$ . As a result, problems involving as many as 10 million unknowns can be solved on existing digital computers. It is estimated that solution to such problems would have taken 10 years using classical solution methods and no existing computer has the capability of storing a matrix with 10 million unknowns.

The recent advent in fast algorithms will precipitate a revolution in electromagnetic analysis method, very much in the same manner as fast Fourier transform has done in signal and image processing. Many problems previously thought unsolvable are now solvable on modern day computers, mainly due to the reduced computational complexity and memory requirements of these fast algorithms. This revolution, together with the computer and information technology revolution, will alter the way engineers and scientists use electromagnetic analysis tools.

This talk will review some of the fast solvers from first principles for Maxwell's equations developed at the Center for Computational Electromagnetics at the University of Illinois.

## 15.1

### High Frequency Diffraction by a Rectangular Reactive Cylinder on an Infinite Reactive Plane

*Tayyar, I H<sup>1</sup>; Birbir, F; Büyükkaksoy, A<sup>1</sup>*  
<sup>1</sup>GIT, Gebze Institute of Technology, Turkey

The diffraction of high frequency electromagnetic waves by a rectangular cylinder (thick strip) located on an infinite plane is an important topic in diffraction theory, because it constitutes one of the simplest geometries that display the effects of the multiply diffracted fields between the interacting steps on planar structures.

In this paper, the scattering of a line source field by a rectangular reactive cylinder on an infinite reactive plane with surface reactance  $\eta_1$  is studied (Fig. 1). The lateral wall of the cylinder at  $y = b$ ,  $x \in (-a, a)$  is assumed to be characterized by a constant surface reactance  $\eta_1$  while the surface reactance of the vertical walls at  $x = \pm a$ ,  $y \in (0, b)$  is  $\eta_2$ . The diffraction problem is formulated into a Modified Wiener-Hopf equation of the third kind and then solved approximately. The solution contains two infinite set of constants satisfying two infinite system of linear algebraic equations. Numerical solutions of these systems are obtained for various values of the surface reactance, the width and the height of the cylinder, whereby is studied the effects of these parameters on the diffraction phenomenon.

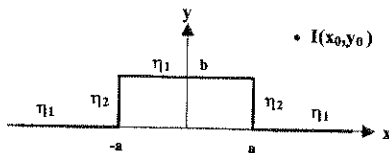


Fig. 1 Geometry of the problem

## 15.3

### Green's Functions for Sheet Currents Placed Over Cylindrical Metal Surface

*Svezhentsev, A Y<sup>1</sup>; Vandenbosch, Guy<sup>1</sup>*  
<sup>1</sup>Katholieke Universiteit Leuven (ESAT-TELEMIC), Belgium

#### INTRODUCTION

In some antenna applications it is preferable to use conformal antennas in which patches are placed on non-planar surfaces, for example, cylindrical ones. To analyse antenna problems for cylindrical structures at least two different approaches can be used. The first one is to obtain the solution in the spectral domain and to perform Inverse Fourier Transform (FT<sup>-1</sup>) in the final stage. Another approach is to deal with Green's functions, which are calculated in the spatial domain. This way has been successfully realised for planar multilayer antennas (Demuyneck F.J., Vandenbosch G.A.E. and Van de Capelle A.R., *IEEE Trans. on Antennas and Propagation*, vol. 46, N 3, March 1998). In this paper this line of strategy will be developed for cylindrical structures.

#### PROBLEM FORMULATION

The problem under investigation is to find the Spatial Green's functions for sheet currents, which are placed over metal cylindrical rod of the circular cross-section. The z-components of the field are derived as a solution of the 2D Spectral Helmholtz equations in two regions. One can find the spectral Green's functions imposing to the boundary conditions at the current interface and at the surface of the cylindrical metal conductor. The electric field components have been written in the in the mixed-potential formulation. The spatial Green's function can be found using inverse FT procedure

$$G(r, \varphi - \varphi', z - z') = FT^{-1} [g(r, h)] = \frac{1}{8\pi i} \sum_{n=-\infty}^{\infty} e^{-i n (\varphi - \varphi')} \int_{h=-\infty}^{\infty} \bar{g}_n(r, h) \cdot e^{-i h (z - z')} dh \quad (1)$$

The direct calculation (1) will fail due to the slow convergence of the spectral Green's function from  $n$  and  $h$ . The way to drastically improve convergence has been realised for the first time in this paper. Special asymptotes were extracted and inverse Fourier transformed in analytical form, which contains all necessary singularities. As a result an extremely efficient algorithm to calculate spatial Green's functions was built. The Green's function dependencies over its parameters are studied in the paper.

## 15.2

### Creeping Discharge Cellular Automaton Model

*Hayakawa, H<sup>1</sup>; Korovkin, N V<sup>1</sup>; Iudin, D I<sup>1</sup>; Selina, E E<sup>2</sup>; Trakhtengerts, V Y<sup>3</sup>*  
<sup>1</sup>The University of Electro-Communications, Japan; <sup>2</sup>Saint Peterburg State Technical University, Russia; <sup>3</sup>Russian Academy of Science, Russia

**Abstract.** An aircraft or a space vehicle traversing opaque clouds or dense air stratus, considerable surface charge is generated on their dielectric surfaces. Aircraft windshields and front heat shield of space vehicles may be regarded as such a kind of dielectric surfaces. The surface charge distribution is highly inhomogeneous and one may observe in that case the creeping discharge appearance. This creeping discharge produces strong electrical noise and disturbance that get into an apparatus through apertures. Our report represents a new approach that allows us to describe creeping discharge intrinsic peculiarities. We develop a fractal model based on a cellular automaton procedure which reproduces dynamics of the surface electrical charges. The surface discharge is considered as a stochastic network growth. The process manifests itself as a self-maintaining chain reaction and may be considered as a self-organised critical phenomenon. Also, we have shown that the model exhibits critical behaviour. We obtain current fluctuations of different scales. These fluctuations yield to power law in compliance with theoretical prediction and experimental data. The model permits to reproduce not only integrated characteristics of the discharge, but also its local properties, that is extremely important in applications. The creeping discharge development is considered under different surface conditions. We obtain universal relations between the channel losses, external current and the discharge zone spatial scale. We also study surface discharge as an extreme case of the creeping discharge when the surface of any dirty, moist dielectric possesses conductive properties and energy is supplied to the channel by leakage currents through the contact surface between the channel plasma and the conductive surface.

We suggest a new method that efficiently reduces the influence of surface discharge.

## 16.1

### Ray Tracing Assessment of Antenna Arrays and Subsurface Propagation for GPR Systems.

*Pennock, S<sup>1</sup>; Redfern, M<sup>1</sup>*  
<sup>1</sup>University of Bath, UK

The design of antenna arrays for Ground Penetrating Radar systems has proven to be as much an art as a science. The assessment of the design of the antenna and the subsurface propagation has been greatly assisted using the well established technique of ray tracing. In this work we extend its use to include a complex arrangement of electromagnetically different objects, such as is typical of the cluttered subsurface environment encountered by a GPR system.

To concentrate the transmitted signal into the ground, it was quickly found to be advantageous to embed the radiating elements in a medium with similar properties to the ground material. In order to minimise radiation to the atmosphere, creating possible EMC complications a conducting back plane was included in the array assembly. Mathematical analysis of such a structure is challenging, and results were not convincing. Simple application of ray tracing techniques at spot frequencies over the operational range of the system provided an invaluable insight into the performance of the entire structure when in close contact with a variety of ground media.

Extensive ray tracing analysis of a variety of different antenna and assembly designs over a variety of ground media enabled an optimised design to be produced. The results of the ray tracing model were compared with field tests on an FMCW ground penetrating radar system.

The paper details the modelling of the designs, and provides a comparison between the simulated performance and that found in practice. Several signal shaping and signal processing systems were also simulated by this process. In this their performance was assessed, and an optimal solution determined.



## 16.2

### Ground Penetrating Radar System for Locating Buried Utilities

*Pennock, S<sup>1</sup>; Redfern, M<sup>1</sup>*  
<sup>1</sup>University of Bath, UK

In this paper the design and operation of a ground penetrating FMCW radar is described. Simulation and example measurements over a test site containing three targets at separations typical of those for real buried utilities are presented. It is seen that the position of the targets is accurately found and that quite closely spaced targets can be distinguished.

The increased use of buried utilities in urban areas has produced a need for mapping tools to accurately locate buried pipes, electricity cables and more recently optical fibre ducting. Damage to these facilities during trenching operations can not only lead to health and safety hazards, but also to prove to be embarrassingly expensive. Ground penetrating radar is one of the few technologies capable of meeting this demand.

The use of pulsed radar is well established using the sub-nanosecond pulses that are required for this short range probing. These systems unfortunately tend to be expensive, whereas FMCW or set-frequency systems can take advantage of the mass availability of microwave/RF devices used in the mobile telephone and communications industries.

For accurate location of buried targets multiple measurement points are needed, often requiring several transmitter and receiver antennas. This presents a signal interpretation problem in being able to distinguish between the desired target response and the direct coupling between antennas. This affects both the design of the antenna array and the signal processing used in the system.

The paper discusses the choice of the operational frequency range. Although high frequencies are preferred to provide higher resolution of the location of an object, lower frequencies are preferred for their lower signal attenuation in the ground medium.

The electronic system is described in the paper including the techniques used to compensate for the non-ideal characteristics of the relatively inexpensive components used. The response from the targets can be further enhanced by suitable matched filtering to suppress random noise, or by clutter filtering to remove particular targets, such as the direct path signal between the transmitter and receiver antenna.

## 17.2

### Imaging of Underground Objects by Using the Short-Term Videopulses

*Vertiy, A<sup>1</sup>; Gavrilov, S<sup>2</sup>; Levitas, B<sup>3</sup>; Voynovskiy, I<sup>1</sup>; Kudelya, A<sup>1</sup>; Stepanuyk, V<sup>1</sup>; Aksoy, S<sup>1</sup>*

<sup>1</sup>Marmara Research Center, Turkey; <sup>2</sup>IRE, National Academy of Sciences of Ukraine, Ukraine; <sup>3</sup>Geozondas, Lithuania

In the given work we present the experimental results of the system designed for obtaining microwave images of the buried objects. It may be done in time domain using scattered fields data. Our experimental system for investigation of scattering in time domain contains a source of pulses (radiation pulse generator with duration of pulses of 30 Ps and amplitude of 25 V); transmitting and receiving antenna and receiving oscilloscope interfaced with the personal computer controlling operational system and signal processing. The operating frequency range of the antenna system is 1.0-18 GHz.

The measurement method for reconstruction algorithm of radioimages in time domain includes the following steps:

- Irradiation of the ground with underground object by electromagnetic pulse at normal incidence;
- Measurement of phase and amplitude of the scattered pulse signal at all frequency points;
- Storage of experimental data in PC data files;
- Calculation of the envelope modulation of a carrier frequency of scattered field.

The GPR images consist of multiple synthesized profiles that were collected as antennas were moved in a plane along the ground. The simple methods of the signal processing are utilized in the image reconstruction. They are the differentiation, the integration, the linear detection and quasi-optimal filtering.

The cross-section images of embedded underground dielectric objects were obtained in the experiments. The experiment was carried out with minelike dielectric objects that are placed in a box filled with sand. The objects had sizes of  $d \cong 1 \div 5\lambda_0$  and heights of  $h \cong 0.5 \div 2\lambda_0$  ( $\lambda_0 = 0.075m$ ).

Used GPR method has been compared with developed pulse time-domain Diffraction tomography method for same objects. In the Diffraction tomography method the image function is the modulus of the normalized polarization current distribution calculated for the subsurface region.

It is shown that results obtained may be applied in practical setups for detection and observation of different undersurface objects.

## 17.1

### Image Reconstruction of the Subsurface Object Cross-Section from the Angle Spectrum of Scattered Field

*Vertiy, A<sup>1</sup>; Gavrilov, S<sup>2</sup>; Voynovskiy, I<sup>1</sup>; Salman, A O<sup>1</sup>*

<sup>1</sup>Marmara Research Center, Turkey; <sup>2</sup>IRE, National Academy of Sciences of Ukraine, Ukraine

It is known that the scattered electromagnetic field may be expanded in terms of plane waves. A nonevanescant part of the plane waves spectrum may be obtained by measuring of the scattered field amplitude and phase at an arbitrary distance from the boundary "air-medium". Evanescent part of plane waves spectrum corresponds to nonhomogeneous plane waves with amplitudes exponentially damping with increase of distance from the interface. Use of these various parts of the scattered field spectrum allows obtaining different images of the object investigated.

In the present work the results of the modeling and experiment in area of the buried objects imaging are given and studied by using the measurement data about the angle spectrum of scattered field and microwave tomography method.

Our experiments were carried out at frequencies from 1.25 to 5GHz. The following steps were taken to obtain the images:

- irradiation of the ground with embedded objects by an electromagnetic wave at normal incidence;
- rotation (scanning along circuit) of the receiving antenna in respect to a boundary "air-medium" normal;
- measurement of phase and amplitude of the total super high frequency scattered signal in dependence on the inclination angle of receiving antenna at all frequency points;
- calculation of the Fourier transform of the scattered field into direct line above the boundary of two media.

In the inverse problem, a complex function of space coordinates representing the normalized polarization currents, have been reconstructed. A modulus of the complex function is the image of the object under investigation. The reconstruction algorithm is based on Fourier inverse formulas. In the experiment, data on back-scattered field at 19 angles in the angle range of  $0-180^\circ$  with a constant angle step were used. As receiving and transmitting antennas, the horn measuring antennas were used. The investigation was carried out using different media (sand, pebble) that are placed in a box with dimensions of  $1.5 \times 1.0m^2$ . Metallic and dielectric objects with dimensions of  $d \cong 1 \div 5\lambda_0$  and heights of  $h \cong 0.5 \div 2\lambda_0$  ( $\lambda_0 = 0.075m$ ) were studied during the experiment.

It is shown that results obtained may be applied in practical tomography setups for detection and observation of different undersurface objects.

## 17.3

### Comparison of Modelled Data with Ultra-wideband Impulse Radar Observations of Canonical Targets Buried in Dry Sand

*Gooding-Williams, G<sup>1</sup>; Cloude, S<sup>2</sup>*

<sup>1</sup>DERA, UK; <sup>2</sup>Applied Electromagnetics, UK

In support of a vehicle mounted forward looking UWB radar sensor for detecting surface laid landmines, measurements are being conducted to investigate the feasibility of detecting shallow buried landmines.

This ultra-wideband impulse radar system is utilises a bistatic TX/RX antenna arrangement transmitting a 120ps risetime impulse by a TEM horn. The bandwidth of which extends approximately from 500MHz to 2.5GHz. Radar backscatter measurements have been performed at incident angles of  $20^\circ$  to  $40^\circ$  to the ground.

Results of initial backscatter experiments conducted in a dry sand medium are compared with the backscatter signals predicted by FDTD modelled data. FDTD modelled data for target backscatter in moist soil conditions are also presented.

## 18.1

### Comparison of Threshold and Destruction Levels at a Generic Electronic Device irradiated with UWB and NNEMP Pulses

*Sonnemann, F<sup>1</sup>; Bohl, J<sup>1</sup>; Ehlen, T<sup>1</sup>*  
<sup>1</sup>Diehl Munitionssysteme GmbH CoKg, Germany

The potential for high-power microwaves (HPM) and ultra wide band (UWB) weapons has increased due to advanced source technology and the increased vulnerability of targets because of widespread use of solid state electronics. HPM weapons are sources with extremely high power RF sinus at some fixed frequency, whereas NNEMP and UWB sources radiate at a much wider band of frequency and thus ensure that some pulse energy is at a frequency to stimulate system resonances that can effectively couple to an electronic system.

Although the pulse energy of a NNEMP is much higher compared to an UWB pulse, the radiated spectrum is limited to the lower frequencies. For smaller systems which may be additional partly shielded (i.e. computers, missiles) an UWB source seems to be more suitable to couple into slots and antenna-like apertures determined by the system.

The paper presents a comparison of threshold and saturation levels of a missile like generic electronic system and the experimental damage results of an unshielded microprocessor board irradiated with NEMP and UWB pulses. The test results are explained in a causal correlation to the specific spectral energy densities (J/m<sup>2</sup>/Hz).

## 18.3

### HPM Threat of Airborne Systems

*Rothenhaeusler, M<sup>1</sup>; Schultz, S<sup>1</sup>; Jaeger, D<sup>1</sup>*  
<sup>1</sup>Daimler Chrysler Aerospace AG, Germany

Until now the risk for airborne systems such as aircrafts, drones and missiles against HPM threats, generated by HPM weapons, cannot be reliably predicted. The way how HPM penetrates into systems is not new, but the available field levels now reached dimensions, which are not covered by any military or civil specification. Hence there is a great demand of investigation.

The German Federal Office of Military Technology and Procurement (BWB) raised a programme in 1994, where DASA-Military Aircraft Division took the part to investigate the vulnerability of airborne systems. Based on the experience of Dasa's EMC Team, skilled in full aircraft HIRF testing and the associated problems of availability of aircraft with the related costs.

Instead of illuminating the whole aircraft system the idea of this approach is, that the path, electromagnetic energy penetrates into a system can be reproduced by simulating all the parts that are needed for full operation of the system and only the direct connected devices and cables for the device under test are built into a special area. This area must have the same dimensions as the original one but is much more easier to handle than the whole aircraft system. This procedure can be compared with an organic transplantation were these requirements have to be fulfilled too. The realisation of this idea is an HPM Experimental Pod which allows to study the penetration path including the operational equipment that may be disturbed. Inside the HPM Experimental Pod an equipment is installed to energise, stimulate and monitor the selected equipment boxes. The devices under test are then transplanted into the Pod and work under comparable conditions as they would do in an operational airborne system. So we fulfil all the required conditions at the equipment box boundaries and are able to investigate the vulnerability in the laboratory with much less restrictions than by using complete airborne systems. With the ability of the HPM Experimental Pod to remove or open specific parts of its structure the attenuation of the skin can be varied from 30 dB to 0 dB. By this way these results can be scaled up or down to different systems of interest, e.g. missiles, drones, if the skin attenuation is known.

First results of the beginning phase have been presented at the EUROEM 1998 in Tel Aviv. Now the main phase with operational equipment was started and the Experimental Pod was illuminated with full levels of several HPM sources. Interesting new results were obtained and with this data a deeper understanding of HPM threats took place. The HPM sources with which we made further investigations, allowed a systematic research on the influence of repetition rate and pulse width on the failure of equipment, at realistic HPM levels. The installed equipment showed already known but also new types of HPM effects. These failures varied from perturbation up to destruction of the devices in the HPM Experimental Pod. By the fact, that we have made researches with different types of HPM sources we are now able to compare the results of them and give an overview of their ability to threat airborne equipment. It is not only the maximum field level that decides whether an equipment is damaged or not but also the other parameters of a HPM source (pulse width...) have a strong influence on the resulting effects.

## 18.2

### UWB and EMP Susceptibility of Modern Electronics

*Nitsch, D<sup>1</sup>; Friedhoff, H<sup>1</sup>; Maack, J<sup>1</sup>; Camp, M<sup>2</sup>*  
<sup>1</sup>Wherwissenschaftliches Inst. f. Schutztechnologien, Germany;  
<sup>2</sup>University of Hannover, Germany

Modern electronic components are of vital importance for the functioning of traffic systems (e.g. airplanes, traffic guidance), security systems and modern communication. An intentional threat to these systems could be of big interest for terrorists and criminal elements. Nowadays, HPM and UWB equipment can be taken off the shelf (fast rise time generators as well as explosively driven systems), and highly sophisticated antennas are available on the public market. Therefore the susceptibility of modern electronic components to HPM threats and pulsed electromagnetic fields, like EMP - and UWB - pulses, is of great interest. The effect of an em-threat on electronics (Welectronic) can be described as a function of the threat spectrum (Spulse), the transferfunctions of the structure (Tstructure) and the PCB (TPCB), and the susceptibility of the electronic components (Fsusceptibility) (comp. equation 1): Welectronic = Welectronic( Spulse Tstructure TPCB Fsusceptibility) (1)

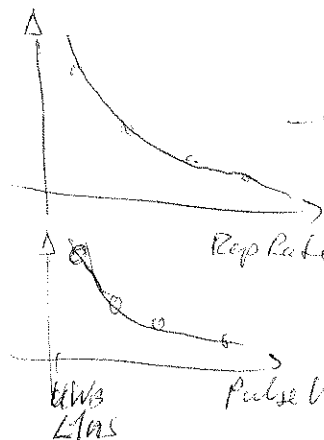
In this paper the coupling mechanism of pulsed electromagnetic (em) fields (EMP, UWB) to printed circuit boards (PCBs), and the susceptibility of microprocessor boards to these fields is investigated. In using these results one covers all aspects of the effect (comp. equation 1) of em fields on modern electronics. PCBs and modern microprocessor boards were exposed to EMP and UWB unipolar fast rise time pulses. Rise times down to 50 ps and field amplitudes up to 100 kV/m can be generated at our laboratory. The first goal was the determination of the energy and peak voltage coupling of em fields to a generic PCB. The coupled energy turned out to be not a function of the entire energy content of the threat pulse but the energy content which was taken of a certain part of the threat pulse spectrum (comp. equation 2):

$$E_{\text{FreqInt}} = (1/2\pi Z) \int_{f_1}^{f_2} \text{Abs}(F(i\omega))^2 d\omega \quad (2) \quad Z = \text{Load Impedance, } f_1 = \text{lower frequency, } f_2 = \text{higher frequency}$$

The second goal of this analysis was to measure the susceptibility of microelectronics to electromagnetic field threat without any external shielding and connected wires. Only direct coupling via the bus- and other board- structures was taken into account. To realize that, we chose industrial mainboards, which represented a complete computer. The tests showed, that the mainboard is much more sensitive against amplitude and rise time of the pulsed electromagnetic field than to the time domain energy content.

← Tests in Schweden und CEG

Suscept - (Failure Field level)



→ find the critical state of system

- 4 levels
- no effect
- Disturbance
- Fatal Disturbance
- Defect

Cond:  $\times \times \times \mu s$  to  $\times \mu s$  pulses | HPM  
 • Fields:  $>> \times \times \text{ kV/m}$   
 • Rep Rate:  $> 1 \text{ kHz}$   
 $\times \times \text{ kV/m}$   
 $> 1 \text{ kHz}$  | UWB

## 18.4

### Radio-Frequency Susceptibility Experiments Using a Model 5317 GTEM Cell

*Coburn, W<sup>1</sup>; Berry, M<sup>1</sup>; Turner, T<sup>1</sup>*  
<sup>1</sup>U.S. Army Research Laboratory, USA

This report describes an experimental method to determine the susceptibility of an electronic system when exposed to a rectangular pulse-modulated rf carrier. Radio frequency (rf) effects experiments were conducted in a model 5317 gigahertz transverse electromagnetic (GTEM!) cell, supplied, installed, and certified by the Electro-Mechanics Company. The GTEM! is a terminated transmission line that provides a test volume over which the field amplitude is approximately uniform. The system under test is not described here, but is configured to represent an operational electronic system. Diagnostics to indicate the system-under-test response to the radiation environment are obtained through a fiber-optic telemetry link. The functional response to a pulse-modulated signal is monitored, and when an adverse response is observed, the threshold susceptibility level is established in terms of the on-target power density. The experiments were designed to characterize the system operational susceptibility as a function of the source modulation parameters and to identify sample-to-sample variations. The results, presented in terms of a normalized power density required to induce an adverse effect, demonstrate consistent trends in the measured susceptibility levels. The system susceptibility depends on the modulation waveform, and the measured data can be used to estimate system vulnerabilities to pulse-modulated signals.

The test samples were in a powered and operational state in the GTEM! cell and exposed to pulse modulated signals with rf carrier frequencies in the range of 1 to 2 GHz. The threshold level for system susceptibility was found to depend on the pulse modulation and the rf carrier frequency. The critical modulation parameter is identified to be the pulse repetition rate to provide the optimum side-frequency components in the transmitted spectrum. To account for the experimental repeatability and uncertain engagement geometries, we include a factor of two margin (i.e., 3 dB) in the susceptibility threshold level. For pulse-modulated signals, we find that this system is susceptible when exposed to sufficient average power density. The results can be used to establish an upper bound on the HPM susceptibility of this electronic system.

GTEM! is a registered trademark of the Electro-Mechanics Company

## 18.5

### Development and Performance of a Transient and RF Hardened Power Cord

*Stewart, R W<sup>1</sup>; Scott, W<sup>2</sup>; Fischer, J<sup>1</sup>; Harlacher, B L<sup>1</sup>*  
<sup>1</sup>Fischer Custom Communications, Inc, USA; <sup>2</sup>Defense Threat Reduction Agency, USA

Military systems are increasingly dependent on COTS. However, the intrinsic electromagnetic protection embedded in COTS is often inadequate for adverse environments. To provide protection against all forms of power line transients, DTRA and FCC have developed a form, fit and function replacement for a standard IEC 320 power cord. This cord, the em pro Cord, protects against EMP, lightning and other severe transients with performance significantly above standard commercial transient suppressors. The cord also provides a degree of protection against radiated transients and suppresses emissions. The em pro Cord is UL certified and designed for high volume production at a cost much less than previous custom hardening retrofits. The paper presents specific performance of the em pro Cord and contrasts that performance with commercial transient suppressors.

*em pro cord*

## 19.1

### Numerical Solution of Frequency Characteristics Based on Analogy between H- and E-Plane Planar Circuit

*Anada, T<sup>1</sup>; Hiraoka, T<sup>1</sup>; Jui-Pang, H<sup>1</sup>*  
<sup>1</sup>Kanagawa University, Japan

**Abstract:** The concept of two-dimensional planar circuits was introduced in 1969 by Okoshi as an approach for analyzing and synthesizing planar stripline-type circuits. The planar circuit thus defined has two possible basic configurations as shown in Fig.1. They are H-plane stripline-type planar circuits having open-boundary condition and only transverse magnetic field is presented. On the other hand, E-plane planar circuit has the same open-boundary condition and is waveguide-type circuits in which only transverse electric field is presented. The numerical analysis of E- and H-plane planar circuits is based on the basic planar circuit equations proposed by the authors. Then, the frequency characteristics of both planar circuits are obtained in principle by solving both planar circuit equations under given boundary and excitation conditions. It is found that both planar circuits have essentially the same planar circuit equations and boundary conditions except for the lateral wavenumber  $\beta(\omega)$ . If the frequency characteristics are obtained by solving planar circuit equations of H-plane stripline-type circuits, the frequency characteristics of E-plane planar circuits can be obtained by means of an analogy with the relation of frequency translation  $\beta(\omega)$  in both circuits and vice versa. In this paper, we will explain through some examples how to calculate the frequency characteristics of both planar circuits as shown in Fig.2. In order to show the validity and usefulness of an analogy existing between E- and H-plane planar circuits, some typical planar circuits are taken up and are calculated based on the Green function expansion method.

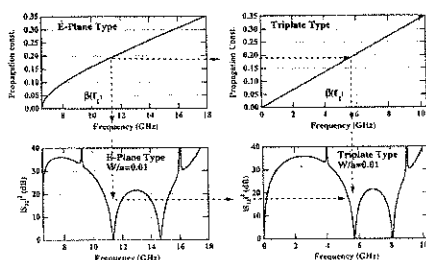
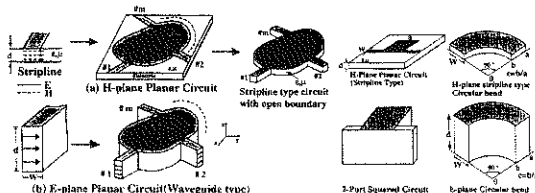


Fig.2 frequency characteristics of E- and H-plane squared planar circuit.

## 19.2

### Formulations using the Finite Integration Technique for Moving Conductor Eddy Current Problems

*Wilke, M<sup>1</sup>; Clemens, M<sup>1</sup>; Weiland, T<sup>1</sup>*

<sup>1</sup>Darmstadt University of Technology, Fachgebiet Theorie Elektromagnetischer Felder, Germany

The Finite Integration Technique (FIT: T. Weiland, "Time domain electromagnetic field computation with finite difference methods", *Int. J. Num. Mod.*, 9:259-319, 1996) is a consistent discretization scheme which maps Maxwell's equations in integral form on a dual grid-doublet and results in a set of sparse matrix equations, the so-called Maxwell-Grid-Equations (MGE).

Based on this conformal discretization technique, time domain formulations for transient magneto-quasistatic problems using a modified vector potential have been introduced. They result in a differential-algebraic double curl equation to be solved by implicit time integration schemes (M. Clemens and T. Weiland, "Transient eddy current calculation with the FI-method", *IEEE Trans. Magn.*, 35:1163-1166, May 1999).

The consideration of eddy currents induced by motional effects requires additional modelling. The paper presents suitable extensions of the formulations for moving conductive media under following assumptions: The motion is unidirectional; the conductor is infinitely long; the cross section as well as the conductivity of the moving body is invariant in the direction of motion; and the motion can be regarded quasistationary with respect to electrodynamics (which is usually the case for technical systems). Under these assumptions, the reference frame for the electromagnetic problem can be chosen arbitrarily via Galilean transformations (S. Kurz, J. Fetzer, G. Lehner, W. M. Rucker, "A novel formulation for 3D eddy current problems with moving bodies using a Lagrangian description and BEM-FEM Coupling, *IEEE Trans. Magn.*, 34:3068-3073, Sept 1998).

In the fixed-coordinate approach the coordinate system is tied to the field excitation. The motional emf experienced by the moving conductors introduces a velocity dependent term in the governing equation of the formulation, which now forms a convection-diffusion problem. Making use of implicit time integration schemes such as Gear's backward differentiation formulae this term leads to an

asymmetric system matrix. This asymmetry requires the usage of more expensive algorithms to solve the arising systems of equations and is known to cause numerical instabilities for high Peclet numbers resulting in oscillating solutions.

On the other hand, the moving-coordinate formulation, i.e., a Lagrangian description uses the rest frame of the moving body, thus avoiding any explicit motion term. Hence, this approach is suited even for high-speed motion calculations.

The time integration with implicit methods involves the repetitive solution of large equation systems. An efficiency improvement for the employed preconditioned conjugate-gradient methods represents a deflation strategy (H. de Gersem, S. Vandewalle, K. Hameyer, "A finite-element/equivalent-circuit two-level method for magnetic field simulations", submitted to *Lecture Notes on Scientific Computing*), whose applicability for the FIT is investigated. An alternative to the cg-methods are algebraic multigrid techniques with their optimal asymptotical complexity. However, the convergence properties of these techniques are only proven for elliptic problems, so their utilization for the degenerate parabolic curlcurl equation is problematic.

As evaluation example a configuration presented by K. Yamazaki ("Generalization of 3D eddy current analysis for moving conductors due to coordinate systems and gauge conditions", *IEEE Trans. Magn.*, 33(2):1259-1262, 1997) is simulated.

More information about the method will be published in the upcoming full paper.

## 19.4

### Coupling of Electromagnetic Pulses between Communication Channels

*Al-Asadi, M<sup>1</sup>; Duffy, A<sup>1</sup>; Hodge, K<sup>2</sup>; Willis, A<sup>2</sup>*

<sup>1</sup>De Montfort University, UK; <sup>2</sup>Brand-Rex Ltd, UK

Data transmission systems are particularly susceptible to the effects of electromagnetic disturbance. While a direct lightning strike, or other similar threat is unlikely, it is more probable that energy will couple from one transmission line to another through near field coupling. The effect of this indirect coupling could be disastrous to any digital equipment affected by such a mechanism. It is important to be able to undertake an analysis of the level of possible threat posed by the routing of the communications transmission lines.

A promising method of performing this threat analysis is presented in this paper. A transmission-line matrix (TLM) model of a communications channel is used to simulate the passage of a pulse. This 'threat' communications line is coupled to a second 'victim' line by treating the first line as an array of antennas. The 'victim' communications channel is similarly modelled using the TLM method.

The benefits of this approach are:

- The simulation is undertaken in the time domain and actual induced pulse shapes can be reproduced exactly. Multiple pulses of varying duration can be modelled in this way.
- The use of TLM allows the electrical parameters, shape and construction of the communications channels, as well as their separation, to be varied arbitrarily with length. Further, the key desired parameters, namely the effective output of the two ends of the victim wire, can be determined as both functions of time and of frequency.

The full paper will discuss the TLM model of the communications channels and describe the antenna approach to studying the coupling. It will present results to illustrate the effect of pulse shape, and duration, and variation of the electrical parameters of the communications channel on the coupling from a 'threat' to a 'victim'.

19.5

### Numerical Analysis of Worst-Case System Coupling Using Reciprocity and Matrix Pencil Procedures

*Elliott, J R<sup>1</sup>; Kawalko, S F<sup>1</sup>; Perala, R A<sup>1</sup>*  
<sup>1</sup>Electro Magnetic Applications Inc, USA

Typically, a system is required to be operational in some electromagnetic environment whose definition grows out of the intended function or mission. Parameters of this external EM environment (e.g. frequency, field strength, polarization, angle of incidence, modulation, and pulse patterns) may all vary simultaneously. As a consequence, the range of systems coupling levels can be rather broad and complete characterization by test/measurement is rarely done because of the equipment and time required. Usually, testing occurs at only a handful of angles of incidence and system configurations and often at only a sparse set of frequencies. It is ideal to have more comprehensive testing to assure that the system can function reliably in its defined EM environment, but it is, at least, desirable to know that the available testing samples the worst-case (strongest coupling) frequencies and geometries..

Even before an actual system exists for testing, it is valuable to have a comprehensive characterization of system coupling. Obvious reasons for this include performance design, susceptibility analysis, and subsystem/component specification. Numerical simulation is the most widely used tool for coupling characterizations at this stage, but traditional methods have difficulties in the levels of effort required; i.e. too many lengthy computer runs. This is especially true when the system has a complex geometry, perhaps with interior cavity resonances, which take a long time to equilibrate electromagnetically.

This paper describes a small study combining two numerical procedures, reciprocity and matrix pencil to efficiently analyze the strengths of coupling to a relatively complex canonical system. By reciprocity, we mean that, instead of illuminating the system externally from a variety of angles with various polarizations, we excite a test EM field at a location inside the system and calculate the field projections at distant points on a dense hemispherical grid.

The inside-to-outside coupling strengths are then transformed to outside-to-inside coupling via reciprocity to find the worst-case angle of incidence. While the calculations are performed using the finite-difference method in the time domain, we are interested in frequency domain results for the problem at hand. In the nearly enclosed space typical of systems of interest, even a short-lived EM driver will cause very long-lived excitations that prevent the application of simple-minded Fourier transforms when computer time is limited. A matrix pencil procedure efficiently characterizes waveforms that die out slowly with a pole-zeros type description. This procedure is applied to the fields at each point on the projection grid to extract results in the frequency domain.

The result is a characterization of the outside-to-inside EM couplings as a function of frequency for all polarizations and angles of incidence. From this information, the worst-case coupling configuration is easily identified for test planning or for construction of coupling/margin envelopes. Example results are presented for a selected canonical system.

## 21.1

### UWB Analysis of EM fields in Complex Laminates: An MRA Homogenization Approach

*Heyman, E<sup>1</sup>; Lomakin, V<sup>1</sup>; Steinberg, B Z<sup>1</sup>*  
<sup>1</sup>Tel Aviv University, Israel

We consider source-excited electromagnetic fields in complex laminates, characterized by multi-scale heterogeneities. Our goal is to derive an effective formulation for the observed field, which smoothes out the micro-scale heterogeneities while retaining their effect on the macro scale observables. This problem is addressed here by utilizing multiresolution analysis (MRA) as systematic homogenization procedure. This method is applied by projecting the heterogeneous electromagnetic field operator onto the resolution spaces, thereby obtaining a systematic hierarchy to deal with multi-scale and across-scales phenomenology. This leads to a new homogenization scheme whereby only the relevant scales are retained.

Having presented this basic scale-based electromagnetic framework, we proceed with the theory applications to ultra wideband (UWB) electromagnetic sources and fields. Through the dependence of the basic homogenization scale on the frequency, we also obtain the frequency dependence of the effective medium formulation that describes the field observables in the most compact fashion, yet reveals a frequency dependence of the effective medium properties, i.e., effective dispersion. Thus the choice of the homogenization scale poses a trade-off between spatial complexity (i.e., heterogeneity) and temporal complexity (i.e., effective dispersion), that depends on the medium properties and on the excitation bandwidth and collimation. As one application of the theory we consider the "effective resonances" of complex laminates which may be used for UWB characterization or identification via the singularity expansion method (SEM).

## 21.2

### Time Domain Exact Solution of Problem of UWB Pulse Diffraction on a Conducting Half-Plane

*Galstjan, E<sup>1</sup>*  
<sup>1</sup>Moscow Radiotechnical Institute of RAS, Russia

The exact solution of the task of diffraction of plane electromagnetic UWB pulse on an ideally conductive half-plane in the time-domain representation has been obtained. For arbitrary polarized pulse of the considered form the exact solution was demonstrated to be expressed through elementary functions of coordinates and time.

## 21.3

### Spherical Wave Expansion of the Time Domain Free-Space Dyadic Green's Function

*Alp Azizoglu, S<sup>1</sup>; Sencer Koç, S<sup>2</sup>; Merih Büyükdura, O<sup>2</sup>*

<sup>1</sup>ASELSAN Electronics Industries Inc, Turkey; <sup>2</sup>Middle East Technical University, Turkey

The importance of expanding Green's functions, particularly free-space Green's functions, in terms of orthogonal wave functions is practically self-evident when frequency domain scattering problems are of interest. With the relatively recent and widespread interest in time domain scattering problems, similar expansions of Green's functions are expected to be useful in the time domain. In this paper, an expression, expanded in terms of orthogonal spherical vector wave functions, for the time domain free-space dyadic Green's function is presented and scattering by a perfectly conducting sphere is studied as an application to check numerically the validity and to demonstrate the utility of this expression.

In the expression derived, in addition to the dependence on  $\theta$ ,  $\theta'$ ,  $\phi$  and  $\phi'$ , the dependence on  $R$  and  $R'$  is also 'separated' in the sense that each term in the expansion appears as a function of  $R$  convolved with a function of  $R'$ . Such a dependence in the Green's function is useful in a scattering formulation as it lets one set up an equation (for instance integral) for some unknown quantities which in turn yield the equivalent sources.  $(R, \theta, \phi)$  are the familiar spherical coordinates of the point of observation and their primed counterparts are those of the source point.

The time domain analysis has become attractive since short pulses and wide bandwidths are being used increasingly in communication and radar systems. The time domain computation scheme is simpler and more efficient when compared to the conventional frequency domain methods in dealing with broadband signals. The spherical wave expansion of the time domain scalar free-space Green's function is presented in (O. M. Büyükdura and S. S. Koç, 'Two alternative expressions for the spherical wave ...', *J. Acoust. Soc. Am.*, vol. 101, no. 2, pp. 87-91, 1997); therein a similar expression to our dyadic Green's function is derived for the scalar Green's function. Some of the work done on the spherical wave expansion for the radiation from time dependent source distributions using multipole expansion of the sources are given in (W. C. Davidson, 'Time-dependent multipole analysis', *J. Phys. A: Math. Nucl. Gen.*, vol. 6, pp. 1635-1646, November 1973), (E. Heyman and A. J. Devaney, 'Time-dependent multipoles and their application for ...', *J. Math. Phys.*, vol. 37, no. 2, pp. 682-692, 1996.) and (A. Shlivinski and E. Heyman, 'Time-Domain Near-Field Analysis of Short-Pulse Antennas - Part I: Spherical Wave (Multipole) Expansion', *IEEE Trans. Antennas Propagat.*, vol. 47, no. 2, pp. 271-279, 1999). In these, the space-time dependence of the source enters via an  $n$ th order linear operator ( $n$  denoting the order of the associated Legendre functions), while in the present work, the same dependence enters via two (superposition (in space) and convolution (in time)) integrals.

## 21.5

### On Superluminal Photonic Tunnelling

*Nimtz, G<sup>1</sup>; Stahlhofen, A A<sup>2</sup>*

<sup>1</sup>Physikalisches Institut, Germany; <sup>2</sup>University of Koblenz, Germany

Photonic tunnelling means the electromagnetic field regime of evanescent modes. The latter are characterized by a purely imaginary wavenumber which results in an exponential decay of the field with distance and the field is spreading out in no time which results in superluminal signal velocities as was demonstrated recently.\* Photonic barriers are presented e.g. by i) Undersized waveguides, ii) by photonic lattices, i.e. by periodic dielectric hetero structures, and iii) by frustrated total internal reflection, for instance realized in the case of a double prism. The theoretical description of the barrier transmission of signal and its energy is understood in the case of the two barriers mentioned first. However, in the case of frustrated total reflection the theoretical and experimental situation is not clear at all. Most of the published data are contradictory. This is amazing, since the double prism represents the classical tunnelling analogy which has been studied now for about 350 years. An important fact for this surprising situation is the Goos-Haenchen shift which takes place in the case of total reflection and its sophisticated mathematical description. We present a critical analysis of old and new experimental and theoretical investigations. In connection with a superluminal signal velocity a signal's definition has to be revisited. A fundamental result of the field quantization is the frequency band limitation of practical, moreover of any physical signal.\* Finally we demonstrate an interesting universal behaviour of the tunnelling process: The reciprocal tunnelling time normalized by Planck's constant is of the order of the frequency of the evanescent mode, respectively the corresponding frequency of a quantum mechanical wave packet. This holds for all potential barriers as well as for any energy of the tunnelling quantum or wave. \* (G.Nimtz, Eur.Phys.J. B7 (1999)523)

## 21.4

### On the Localization of Electromagnetic Energy

*Schantz, H<sup>1</sup>*

<sup>1</sup>Time Domain, USA

This paper explores the interesting question of whether electromagnetic energy can be localized. Three specific areas will be addressed. First, the historical development of the Poynting - Heaviside theory will be traced. Then, the problems and alleged paradoxes of this theory will be examined. Finally, a novel method of tracking electromagnetic energy will be presented and applied to some simple examples.

This paper surveys the history of attempts to localize electromagnetic energy, beginning with the pioneering work of Helmholtz whose action-at-a-distance theory was the earliest attempt to localize electromagnetic energy. Then, attention turns to the way in which Faraday's field concept led Kelvin and Maxwell to postulate that energy is distributed throughout space. Finally, our current understanding of electromagnetic energy transfer as formulated by Poynting and Heaviside will be discussed.

Next, this paper considers various problems and "paradoxes" in the Poynting - Heaviside theory. It is often argued that the Poynting vector is arbitrary to a solenoidal correction, or that it only has meaning when integrated over a closed surface. The presence of closed circulating "loops" of energy is also sometimes taken as evidence that the Poynting vector is not physically meaningful. These claims will be analyzed and discussed. The constraints imposed by conservation of energy and momentum (both angular and linear) will also be considered. Then, experimental limits on deviations from the Poynting-Heaviside theory will be presented.

Finally, the method of "causal surfaces" will be introduced for bounding and tracking regions of electromagnetic energy flow. These are surfaces on which the normal Poynting vector is zero so that there is no energy flow through the surface. This method will be applied to track energy flow around accelerating and decelerating charges, as well as around dipoles.

The challenge of short pulse electromagnetics is to understand the time evolution of a transient electromagnetic system. The physical insight provided by understanding electromagnetic energy transfer can be a valuable means to that end.

## 22.1

### Optimal Measurements

*Cheney, M<sup>1,2</sup>; Isaacson, D<sup>2</sup>; Lassas, M<sup>3</sup>*

<sup>1</sup>Lund Institute of Technology, Sweden; <sup>2</sup>Rensselaer Polytechnic Institute, USA; <sup>3</sup>University of Helsinki, Finland

We consider the problem of obtaining information about an inaccessible half-space from acoustic measurements made in the accessible half-space. If the measurements are of limited precision, some scatterers will be undetectable because their scattered fields are below the precision of the measuring instrument. How can we make optimal measurements? In other words, what incident fields should we apply that will result in the biggest measurements?

There are many ways to formulate this question, depending on the measuring instruments. In this talk we consider a formulation involving wave-splitting in the accessible half-space: what downgoing wave will result in an upgoing wave of greatest total energy?

A closely related question arises in the case when we have a guess about the configuration of the inaccessible half-space. What measurements should we make to determine whether our guess is accurate? In this case we compare the scattered field to the field computed from the guessed configuration. Again we look for the incident field that results in the greatest energy difference.

We show that the optimal incident field can be found by an iterative process involving time reversal "mirrors". For band-limited incident fields and compactly supported scatterers, this iterative process converges to a finite sum of time-harmonic fields. In other words, the optimal incident field is generally time-harmonic. This provides a theoretical foundation for the pulse-broadening observed in certain computations and time-reversal experiments. Moreover, this result suggests that from the point of view of distinguishing the presence of a scatterer, the chirps and pulses that are usually used may not be best.



## 22.2

### Full-Wave Solution of the Propagation of General Shaped Impulses and Wide Band Application in Anisotropic Plasmas

*Ferencz, C S<sup>1</sup>*

<sup>1</sup>*Eötvös University, Hungary*

One of the most interesting wave propagational problems is the investigation of arbitrarily shaped signals, i.e. impulses in different media. The paper deals with propagation of impulses in inhomogeneous magnetoionic media, presenting a new and theoretically general method of the solution of Maxwell's equations and the results of application.

During the solution of Maxwell's equations in this case it is necessary to use functionals modelling the arbitrarily shaped signals and the media. The application of the Laplace-transformation makes manageable the essentially transient character of the signal and the propagational task itself - well known in the electric network analysis. The most important part of the solution uses the Method of Inhomogeneous Basic Modes (MIBM). A great advantage of this method is hidden in the fact, that the "transfer function" of the media - the system-answer given for a Dirac-impulse - can be available, which makes possible to develop a very flexible model for linear propagational problems.

The application of the results (transfer functions and signals generated by different excitations) make the separation of propagational and excitational effects possible. In this paper two important examples will be presented for this separation: demonstration of differences between the transfer functions and the effects of general-shaped excitations; demonstration of differences between the effects of the form of excitation and of the propagational interference.

An important result of extremely wide-band application of impulse propagation in the ELF-VHF band is the consistent explanation of the electron- and ion-whistlers, the TIPP events (Transionospheric Pulse Pairs) and the Faraday rotation using only a single impulse-answer propagating in the Earth's plasmasphere.

## 22.4

### Asymptotic Description of Ultrawideband, Ultrashort Pulsed Electromagnetic Beam Field Propagation in Dispersive, Attenuative Media

*Oughstun, K E<sup>1</sup>*

<sup>1</sup>*University of Vermont, USA*

The asymptotic description of the coupled spatio-temporal evolution of an ultrawideband, ultrashort pulsed electromagnetic beam field that is propagating in a dispersive, attenuative material occupying the half-space  $z \geq 0$  is obtained from the angular spectrum of plane waves representation (K E Oughstun & G C Sherman, *Electromagnetic Pulse Propagation in Causal Dielectrics*, Springer-Verlag, Berlin-Heidelberg, 1994). The analysis begins with the generalized Sherman expansion (G C Sherman, *J Opt Soc Am* 59, 697-711, 1969; K E Oughstun, *J Eur Opt Soc A* 7, 1059-1078, 1998) of that exact integral representation, which provides a spatial series representation of a pulsed, source-free electromagnetic beam field. This spatial series representation explicitly displays the temporal evolution of the pulsed beam wave packet throughout the half-space  $z \geq 0$  through a single contour integral that is of the same form as that obtained in the Fourier-Laplace integral description of a pulsed plane wave field that is propagating in the positive  $z$ -direction in the complex dispersive medium. The spatio-temporal pulsed beam-field evolution is shown to depend upon the transverse spatial position in the propagated field through the spatial derivatives of the initial field boundary values at  $z=0$ . These general results are illustrated through the specific example of a pulsed gaussian beam field that is propagating through a single resonance Lorentz model dielectric. The Sommerfeld and Brillouin precursor fields, which are a characteristic of the dispersive material, cause the ultrashort pulsed beam field to break up into several localized subpulses which travel at their own characteristic velocity through the dispersive material. This asymptotic description has direct application to the design and analysis of ultrawideband radar systems.

## 22.3

### Picosecond Optical Pulses in Kerr-type Planar Waveguides - Catastrophic Self-Focusing, Spatio-Temporal Splitting and Self-Trapped Solutions.

*Pietrzyk, M<sup>1</sup>*

<sup>1</sup>*Warsaw University of Technology, Poland*

Properties of two pulses propagating simultaneously in different dispersion regimes, i.e. anomalous and normal, in a Kerr-type planar waveguide are considered. The propagation is described by two coupled nonlinear Schrödinger equations. The interaction between pulses is assumed to be limited to cross-phase modulation. Four wave mixing describing energy transfer between pulses and the difference of group velocities of the pulses are neglected. The analysis is based on the variational method and numerical simulations.

First we studied the influence of the parameters of the pulse propagating in normal dispersion regime on the threshold of catastrophic self-focusing of the pulse with anomalous dispersion. We observed that catastrophic self-focusing of the pulse propagating in anomalous dispersion regime can be arrested by the pulse propagating in normal dispersion regime when the energy of the later pulse is sufficiently large and the strength of its dispersion belongs to a certain interval of parameters.

We also investigated whether the nonlinear coupling between pulses can cause catastrophic self-focusing of the pulse propagating in normal dispersion regime. The variational method and numerical simulations indicate that when catastrophic self-focusing of the anomalous pulse occurs, the normal pulse can display, depending on the parameters of the system, two different characteristics: (i) both widths of the pulse (the temporal one and the spatial one) initially decrease, reaching a minimum on a certain distance of propagation, and then they start to increase, (ii) the spatial width of the pulse vanishes to zero on a finite distance of propagation whereas the temporal width initially decreases, reaching a minimum on a certain distance of propagation, and then it increases.

Using the numerical simulations we found also that the presence of the pulse propagating in normal dispersion regime can lead to spatio-temporal splitting of the pulse propagating in anomalous dispersion regime (note that splitting of an anomalous pulse does not occur when it propagates as a single pulse).

Finally, we considered the limiting case of vanishing dispersion of the pulse propagating in normal dispersion regime. The main motivation was to study whether such a configuration can lead to a stable, self-trapped propagation of the pulses. The positive answer has been obtained within the variational and the numerical methods. Namely, it was observed that neither spreading nor catastrophic self-focusing can develop and an oscillating, self-trapped solution arises. Numerical results show, in contradiction to the variational ones, that amplitudes of those oscillations decrease with propagation distance and for sufficiently large distances they vanish to zero (such a stabilization is similar to the one which was found earlier in media with saturation-type nonlinearity).

Note in conclusion that the existence of a stable, self-trapped solution could be useful, for example, in the optical switching devices. Besides, the configuration of two simultaneously propagating pulses in a planar waveguide could find applications in optical compression techniques.

## 22.5

### Dispersion Reduction in a Coaxial Transmission Line Bend by a Layered Approximation of a Graded Dielectric Lens

*Bigelow, W. S.<sup>1</sup>; Farr, E. G.<sup>1</sup>*  
<sup>1</sup>Farr Research Inc, USA

When a UWB pulse must traverse a bend in an electrically large transmission line, electrical path length differences from inner to outer bend radii lead to significant dispersion of the transmitted pulse. In high-voltage systems, this phenomenon can severely limit the bandwidth.

Conventional transmission line may be filled with a homogeneous dielectric material, sometimes air, or may be evacuated. Here we consider electrical path length compensation of a coaxial transmission line bend by an inhomogeneous, low-loss dielectric lens. If the index of refraction of the lens is made to vary inversely as the radius of curvature, then the electrical path length through the bend will be independent of the radius, and path length dispersion will be eliminated.

We previously summarized the theory behind this approach to dispersion reduction and presented our hardware implementation of a strip line bend approximately compensated by coarsely graded layers of dielectric materials having various uniform permittivities (W. S. Bigelow, E. G. Farr, *Ultra-Wideband, Short-Pulse Electromagnetics 4*, 213-219, 1999). The layered strip line achieved a 70 picosecond reduction in pulse rise time when compared to an identical air-filled line.

Here, we apply lessons learned in the earlier strip line work to precisely designed square coaxial hardware. We summarize the derivation of a finite element-based impedance model for inhomogeneous bends. We mention our use of a time-domain transmission line method to obtain broadband dielectric property data for candidate lens materials. We also discuss optimization of layered bend designs. Finally, we present the results of comparative measurements and analyses of UWB impulse propagation through homogeneous coaxial transmission lines and through a coaxial bend compensated by layered dielectric materials.

In the future, dielectric compensating lenses may permit even electrically large transmission line bends to be implemented with negligible dispersion. Use of such bends would permit more compact and efficient designs of high-voltage, UWB systems.

## 23.2

### A New Method For Generating Computational Structure Models to Study the Effects of Undesired High-Power Electromagnetic Energy On Complex Systems

*Drozd, A. L.<sup>1</sup>; Carroll, C. E.<sup>1</sup>; Miller, J. R.<sup>1</sup>; Sunderland, K. V.<sup>1</sup>*  
<sup>1</sup>ANDRO Consulting Services, USA

This topic will describe a new method for generating computational structure models to simulate and study the effects of undesired high-power electromagnetic energy on complex systems. This method involves the application of an expert system, knowledge-based pre-processing approach to rapidly create valid computational electromagnetics (CEM) models. The CEM system models may include co-located communications and multi-sensor electronics subsystems as well as incident high power electromagnetic environments or sources. The models are used to analyze monostatic or bistatic scattering cross section, predict electromagnetic interference/compatibility, compute front-door and back-door path coupling, assess the effects of far-field source-to-object scatter and induced surface currents, determine near-field radiation hazards, and analyze antenna jamming. This paper will focus on the capabilities and application of the Intelligent Computational Electromagnetics Expert System (ICEMES) and how it is used as part of an overall CEM modeling, simulation, analysis and prediction procedure to study these concerns. In ICEMES, an expert system is first used to generate the computational model consisting of the geometry superstructure, its co-located electromagnetic radiators, and external sources. The inputs to the process are computer-aided design (CAD) data or available model data (to be validated) for selected CEM codes. Ensemble electromagnetic "state" drivers (frequency, desired accuracy, CEM physics, target analysis code, and other decision criteria) are then assessed to determine how these influence the generation of the final, validated CEM model. Prior treatments of this subject have focused on the general capabilities of the tool and its ongoing development (A. Drozd, et. al., *ACES*, 1133-1140, 1997; A. Drozd, et. al., *SCS*, 471-476, 1998; A. Drozd

T. Blocher, *IEEE EMC*, 1144-1149, 1998). The focus in this paper will be (a) automatically building a model; (b) describing the recent application of additional geometrical and CEM modeling rules that

## 23.1

### EMEC - System EMC Simulator

*Karlsson, T.<sup>1</sup>; Carlsson, J.<sup>2</sup>*

<sup>1</sup>Emicon, Sweden; <sup>2</sup>SP Swedish Testing Research Institute, Sweden

EMEC - System EMC Simulator is a Windows based tool for analysing conducted and radiated disturbances in complex systems. A unique feature is the ability to assess the susceptibility of equipment by comparison with immunity levels deduced from EMC standards. The structure of the simulator more or less forces the user to describe the whole system in a way so it can be analysed by methods involving electromagnetic theory. This capability and the graphical user interface makes it easy to use by skilled engineers as well as EMC laymen.

The simulator computes circuit equivalents at various points in a complex system from conducted as well as radiated disturbances. These equivalents can be compared with circuit equivalents deduced from standardised immunity test methods. This makes it possible to estimate the vulnerability of products complying with a certain EMC standard.

The electromagnetic topology of the system is defined in the graphical user interface, see figure. In this interface an arbitrary system is constructed by adding objects to the drawing area and placing them in accordance with the electromagnetic topology of the system. There are six types of objects: zone, functional unit, transmission line, junction, port, and excitation unit. A zone can either be an outermost zone, representing the environment where the system is placed, or an ordinary zone placed inside another zone. One property of the zone object is the attenuation in the boundary (shielding effectiveness). For the outermost zone an environment including lightning, EMP, radio transmitters etc. can be specified. A functional unit represents anything from a single component to an entire system. Its properties comprise emission as well as susceptibility levels. Conducted emission is defined in ports belonging to the unit as Norton equivalent multi-port circuits. For ports placed on zone boundaries it is possible to define a transfer function representing the port e.g. a filter. Excitation units can represent local or distributed excitation of transmission lines by field or other sources. They can also be used for apertures in volume shields.

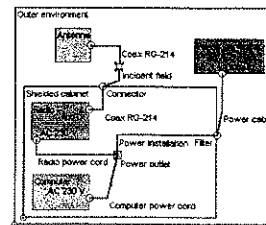


Figure. Simple system given a topological definition in the simulator.

An object is easily defined in the interface and may be saved together with associated properties as a module for later use in another project. Properties, such as emission and susceptibility levels, are set by double-clicking on objects and simply selecting from lists or from files containing e.g. measured data. Certain properties can be computed in the simulator. Per unit-length parameters for multiconductor transmission lines are calculated using a method of moments formulation. For irregular cross sections a finite difference method is used. Routines are available for computing the attenuation in homogeneous and meshed shields, transfer impedance and admittance for homogeneous and braided cable shields and more.

When a simulation is done, data can be processed and presented as graphs. The extensive postprocessing capability includes comparison, convolution, adding, multiplication etc.

The program is developed for the Swedish Defence Materiel Administration (FMV) to be used by technical officers dealing with procurement of military systems and installations.

ensure the creation of valid simulation models; (c) translating models from smooth surfaces to meshes based on the state drivers; and (d) application to high-power electromagnetics. The knowledge base rules verify the validity and completeness of imported CAD and CEM model definitions (geometric reasoning); assure a valid model for changing frequencies or states (CEM reasoning); and suggest smart defaults as well as perform range checking (data inferencing). The expert system provides useful information to the analyst in order to work out a solution when a modeling problem is detected. The modeling and simulation codes supported by ICEMES include GEMACS, NEC-MOM, NEC-BSC, Carlos-3D, Apatch and Xpatch. The output created by ICEMES consists of model data consistent with one of these codes. This paper will illustrate code "crossover" modeling techniques, the ability to transform models from surfaces to meshes as a function of the state parameters, and the influence of high-power electromagnetic environments on the model generation process. Additionally, the paper will highlight the realizable benefits of integrating CEM modeling rules, an expert system, CEM data dictionaries, CAD data translators, data reduction methods, and visualization utilities within the ICEMES framework.

## 23.3

### Extension of the BLT Equation into Time Domain

Baum, C. E.<sup>1</sup>

<sup>1</sup>Air Force Research Laboratory DEHP, USA

For the analysis of multiconductor-transmission-line (MTL) networks there are various forms of the BLT equation that have been introduced. The original form (BLT1) has been formulated in terms of uniform MTLs for the tubes connecting the junction characterized by scattering matrices (C.E. Baum, T.K. Liu, and F.M. Tesche, Interaction Note 350, 1978). This is the basis for the CRIPTE computer code for calculating the electromagnetic response of complex systems (J.P. Parmentier et al., Interaction Note 506, 1993).

The tubes can be shrunk to zero length by modelling them as junctions. This gives another form called the BLT2 equation (C.E. Baum, Proc. 13th Int'l. Zurich Sym. and Technical Exhibition on EMC, pp. 131-136, 1999). In this form, tubes can be replaced by more general structures which are characterized by scattering matrices, as are the original junctions. Yet another form is the NBLT equation which allows the inclusion of NMTLs (nonuniform MTLs) in the tubes with propagation on such tubes representable in terms of product integrals.

This paper develops a form, BLT3, which is appropriate for efficient early-time representation based on a geometric-series expansion of a supernatrix inverse. The delays on the uniform-multiconductor-transmission-line tubes play a key role.

For late-time computations the SEM forms of appropriate BLT equations are more efficient. This leaves some theoretical questions concerning how early in time SEM can be appropriately used. This also involves the entire-function issues.

Perhaps yet more BLT forms will emerge with their own special applications.

## 23.5

### Nonuniform Transmission Lines and a Statistical Analysis of Cable Harness

Steinmetz, T.; Nitsch, J.<sup>1</sup>

<sup>1</sup>Otto-von-Guericke-Universitat Magdeburg, Germany

Modern complex systems like cars or aircraft contain miles of cables. These cables connect various electrical sensors and actuators which work on a low energetic level. Knowledge of the electromagnetic behaviour of such a system already in the design phase would help to ensure the electromagnetic compatibility of the entire system. If the disturbances on the cables are known then the separate circuits of the system could appropriately be hardened.

An effective method to treat such problems is the electromagnetic topology in conjunction with the transmission line theory. However, in real systems the cable geometry often does not meet the basic assumptions of the transmission line theory. In many cases the cables are nonuniform lines.

Therefore a method is presented which allows one to treat nonuniform lines in a network code. This method is based on the product integral which is the solution of a system of ordinary linear differential equations with non-constant coefficients [1]. The use of this product integral permits the calculation of corresponding scattering or propagation parameters for nonuniform tubes and admits to introduce them as n-ports in a network code. These scattering or propagation parameters can be used in the BLT-equation [2] to obtain the solutions for the disturbances on the cables of the entire system, including nonuniform cable sections. This method is applied to some frequently used nonuniform lines, like a wavy shaped line or a twisted wire line. Differences to a uniform tube, resulting from the continuous reflections along the nonuniform tube are pointed out.

For the exact calculation of the corresponding scattering or propagation parameters all geometric data of the cable harness has to be known. This means that at every cross section along the nonuniform line the location of every single conductor must be known. However, in many cases they are unknown along the whole line, only at certain locations (e.g. on the connectors) they are available and well known. This suggests the performance of a statistical analysis of nonuniform tubes. Many calculations of randomly generated tube geometries have to be completed to estimate maximal and minimal bounds for the scattering or propagation parameters. The disturbances on the cables of the system can roughly be estimated with these results. Also a calculation of the statistical distribution of the disturbances on the cables is possible using the resulting scattering or propagation parameters of the randomly generated tubes in the BLT-equation.

The electromagnetic topology together with the transmission line theory is a very powerful tool to calculate disturbances in complex systems [3]. The extension to nonuniform tubes makes it possible to investigate the influence of nonuniformities on the propagation of disturbances in the system. It allows a statistical analysis of a system with almost unknown cable geometry, too. This can identify some critical cables and give an estimate for protection measures.

[1] J.Nitsch, F.Gronwald, *Analytical Solutions in Nonuniform Multiconductor Transmission Line Theory*, IEEE Transaction on EMC, Vol. 41, No. 4, 1999, p. 469-479

[2] C.E.Baum, T.K.Liu, F.M.Tesche, *On the Analysis of General Multiconductor Transmission Line Networks*, Interaction Note 350, November 1978

[3] J.P.Parmentier et al., *ETE III: Application of the Electromagnetic Topology Theory on EMP/AC*, Interaction Note 527, May 1997

## 23.4

### General Transmission-Line Model of Shielded Cables: Application to EM Coupling and EM Emission

Parmentier, J.P.<sup>1</sup>; Issac, F.<sup>1</sup>; Bertuol, S.<sup>1</sup>; Boulay, F.<sup>1</sup>

<sup>1</sup>ONERA, France

#### Objective

To represent EM coupling on shielded cables it is common to introduce the concept of transfer impedance,  $Z_t$ , and transfer admittance,  $Y_t$ . Generally, the derivation of the coupling response of a shielded cable is performed in two steps, solving two problems separately. First, the response of the shield is determined by calculating external currents  $I_{ext}$  and external voltages  $V_{ext}$ . Then, they are used to derive the distributed equivalent voltage generators,  $Z_t I_{ext}$ , and current generators,  $Y_t V_{ext}$ , on the inner wires (E. Vance, *Coupling to Shielded Cables*, Wiley Interscience Publications, 1978). The expression of those generators is fully correct but the decomposition in two independent domains requires an important assumption that may be easily forgotten: the shield must be short-circuited at both ends.

However, in the general case, the connections of the shields at the ends determine the performance of the shielding. Therefore, the knowledge of the equivalent generators is not sufficient and mutual coupling terms between the shields and the inner wires may become more relevant than the transfer parameters through the shields. The objective of the talk is to present a general model of a multishield-multiconductor cable enabling one to account for EM coupling and EM emission at the same time, whatever the connections at the ends of the shields are. Such a model has been already applied at ONERA for a long time (J.P. Parmentier and al.: *An Application of Electromagnetic Topology on the Test-Bed Aircraft, EMP/AC*, Interaction Notes, Note 506, 1993) and is still improved, but up to now, we did not have the opportunity to devote a paper to demonstrate all its advantages.

#### Transmission line model derivation

First, we present the derivation of the model on a simple example: a coaxial cable. We show how to establish the per-unit length impedance and admittance matrices in a multiple reference model. In this case, the transfer impedance and admittance terms appear in extra-diagonal blocks linking the external domain and the internal domain. Then, we transform those matrices in order to consider only one reference as it is usually the case in multiconductor-transmission-line theory. The analysis of the obtained resistance, inductance and capacitance matrices emphasizes the fact that transfer parameters are a significant part of the propagation characteristics of the cable. The generalization of the coaxial cable case to a multishield-multiconductor cable is carried out through the use of transformation matrices that make the derivation of single reference models easier for a computer.

#### Transmission line model derivation

We propose two applications of this model. The first one is an EM coupling model based on the derivation of the equivalent transfer impedance of a triaxial cable (one core, one shield and another shield). The second one describes the EM emission of a coaxial cable for which the connections at the ends vary from short-circuit to open circuit. In both cases, the transmission-line model is compared to measurements (figure 1 and figure 2). The EM coupling and EM emission examples we present here come from results obtained in studies carried out from 1996 to 1999 for CNES-Toulouse and Aérospatiale-Missile-and-Defense.

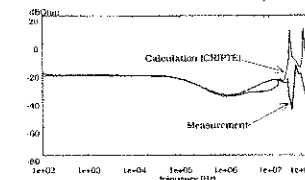


Fig. 1 : measurement and calculation comparison of the equivalent transfer impedance of a triaxial cable

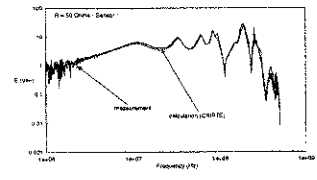


Fig. 2 : electric field generated by a coaxial cable in the vicinity (shield in open circuit at one end)

## 24.1

### Overview of Scattering Processes and Statistical Decision Theory for Detecting Buried Objects

Kohlberg, J.<sup>1</sup>

<sup>1</sup>Kohlberg Associates Inc., USA

The problem of detecting Unexploded Ordnance (UXO) and landmines is of great interest around the world. Although the physical characteristics of UXO and landmines are generally very different, the conceptual basis for initially detecting them, and subsequently identifying them has much in common. The first step in developing robust practical detection and identification methods in both cases is to understand the basic physical models and fundamental mathematical methods that should be used in the detection identification processes. This statement applies even though we may not be able to solve the problem today; it is especially important to go through this process even if for no other reason than to assess the inherent limitations of current Ground Penetrating Radar (GPR) algorithms.

This paper is an overview of the theoretical foundations for detecting and identifying objects that are buried underneath the ground. Its primary purpose is to provide an introduction and roadmap to the other papers presented in this tutorial session. In addition, this paper also renders an evaluation of traditional radar theory as it applies to GPR. This enables us to assess more clearly the conditions under which traditional radar theory can be applied successfully to detect buried objects, and to demonstrate the importance of establishing a rigorous theoretical foundation for detecting objects below the ground.

The issues linked together in the overview include:- computation of electromagnetic signature from a buried object in - uniform ground- application of electromagnetic symmetry in detection - application of singularity expansion in detection- interpretation of electromagnetic signature in weak clutter- interpretation of electromagnetic signature in strong clutter- traditional and novel signal processing techniques- detection algorithm based on likelihood ratio applied in an actual experiment - detection algorithms based on combining different information

## 24.3

### General Decision Models for Electromagnetic Detection of Objects *Boling, R<sup>1</sup>*

<sup>1</sup>*Institute for Defence Analyses, USA*

This paper provides an overview of modern signal detection concepts as applied to the problem of detection and classification of buried man-made objects by reflected or scattered electromagnetic fields.

First a suite of sensors arrayed in time and space to detect reflected EM energy is postulated. The n-dimensional received signal space is described. In addition to considering the detected signals over time as a series of point estimates, the detected signal is characterized as a dynamic surface in n-space, and a rules for interpolation are posed.

Next, some basic pattern recognition techniques are proposed to evaluate this surface in time, leading to a classification of subsets of the received signals as one of m object types, including the "no object" decision. These techniques are based upon classical feature definition and classification schemes. The parameterization of the classification and decision algorithms is discussed, along with automatic training techniques. General analytic tools, such as classical Kalman filtering techniques, are discussed as means to accelerate and enhance dynamic and spatial classification tasks.

## 24.5

### On Discriminating Between Buried Metallic Mines and Metallic Clutter Using Spatial Symmetry and Temporal Exponential Decay Rates

*Riggs, L<sup>1</sup>*

<sup>1</sup>*Auburn University, USA*

We have collected data at the JUXOCO test site located at Fort A. P. Hill, VA with the U. S. Army's standard metal detector the AN/PSS-12. The AN/PSS-12 is a pulse-induction metal detector, and our instrumentation allowed us to collect "raw" data by amplifying and recording the time-domain response immediately following the metal detector's receiver coil. The JUXOCO test site has a large test grid made up of 980 adjacent 1m square test locations (20 adjacent rows and each row has 49 test squares). At the center of each square there is nothing at all (a blank), a mine, or a clutter item (metallic trash). Time domain response data was collected at a number of different positions on an x-y grid centered over each square in the large test grid. This presentation describes the the signal processing algorithms that were used to discriminate among blanks, metallic mines, and metallic clutter.

The baseline receiver operating characteristic (ROC) curve (probability-of-detection versus probability-of-false alarm curve) for the AN/PSS-12 is shown to lie along the chance diagonal indicating that the instrument has no ability to discriminate between mines and clutter when used in its normal mode of operation (i.e. as a metal detector). We discovered that the spatial energy signature for mines is symmetrical, almost without exception, whereas in many instances the metallic clutter did not demonstrate this symmetry. This finding lead us to develop a very simple "symmetry detector" (algorithm) that enjoys a ROC curve well above the chance diagonal. Thus, by taking advantage of spatial information we were able to transform the AN/PSS-12 from a simple metal detector into a mine detector! This paper will describe in greater detail the signal processing techniques that lead to the baseline and improved symmetry ROCs.

As pointed out by Baum (C.E. Baum, Interaction Note 499, November 1993) the low frequency response of highly but not perfectly, conducting bodies is characterized by negative real natural frequencies that correspond to a damped exponential response in time domain. There is a unique correspondence between a metallic object's geometry (shape) and constitutive parameters (conductivity and permittivity) and its poles or time domain decay rates. This unique correspondence affords an opportunity for discrimination among metallic objects based on their negative real natural frequencies - a method referred to as magnetic singularity identification (MSI). We are currently working to use MSI to improve our symmetry ROC, and this presentation will summarize progress on this front.

## 24.4

### Detection and Classification of Targets Embedded in a Random Soil Media

*Carin, L<sup>1</sup>; Dogaru, T<sup>1</sup>*

<sup>1</sup>*Duke University, USA*

In this paper, we consider the case of a deterministic (fixed) target in the presence of a rough surface, the latter being parametrized statistically. This study is motivated by electromagnetic sensing of buried targets (e.g., mines, unexploded-ordnance, etc.). For electromagnetic scattering from the ocean surface, a stochastic surface parametrization is clearly required, since the sea-surface characteristics generally change with time in a seemingly random fashion. However, for the sensing of an underground target, the air-ground interface is fixed (deterministic), calling into question the need for a statistical analysis. However, although a given portion of the air-ground interface is fixed, it will in general be different from that of another (fixed) region of the interface. Thus, while the fields scattered from any particular portion of the rough surface are deterministic, to characterize the fields scattered from a general such surface, the surface (roughness) parameters must be characterized statistically, and therefore so must the associated scattered fields. Consequently, to characterize the fields scattered from such a rough air-ground interface, the surface properties are modeled as a random process, with any particular surface constituting one realization of an ensemble, each of which is parametrized by the same probability density function. In turn, the scattered fields from such a surface are also treated as a random process.

The time-domain field scattered from a rough (random) surface constitutes a random process, which in general is non-white. Therefore, for detecting a target in the vicinity of such a rough surface, optimal detectors (under appropriate conditions) are preceded by a whitening filter, such that the clutter becomes a white (uncorrelated) time sequence. The whitening filter employs the clutter's correlation matrix, which, for wide-sense stationary (WSS) clutter, can be represented in the Fourier domain in terms of the clutter's power spectral density (PSD). As discussed below, in the cases we have examined thus far, the WSS model has been found to be quite accurate, and therefore here we quantify the transient clutter statistics via the PSD.

In this paper we employ a two-dimensional multi-resolution time domain (MRTD) algorithm, to model electromagnetic scattering from a general two-dimensional rough-surface interface. We implement an optimal Bayesian processor, and quantify detector performance via the receiver-operating characteristic (ROC). The principal focus of this paper is consideration of several different rough-surface statistical profiles. In particular, we address sensor performance when the surface is Gaussian, exponential and fractal in nature. In addition to the properties of the interface, we consider variable target and soil properties.

## 25.1

### Live Fire Test and Evaluation and the RF Vulnerability Testing Mission

*O'Bryon, J.F.*

*Operational Test and Evaluation, Office Sec. Defense, USA*

The Office of the Secretary of Defense, Operational Test and Evaluation, Live Fire Test and Evaluation, live fire test and evaluation (LFT&E) program is oriented towards providing a timely and realistic assessment of the survivability (of systems designed to provide user protection) and lethality (of missiles, rockets, and munitions) of a military system as it progresses through its development cycle and prior to full-rate production. The LFT&E requirement was placed in law by the United States (U.S.) Congress in 1986 and now covers air, land, and sea platforms, as well as a variety of weapons from small arms to national missile defense systems. The program is particularly aimed at providing information to decision makers on potential user casualties, survivability, vulnerability, and lethality, taking into equal consideration susceptibility to attack and combat performance of the system. It is also directed towards ensuring that knowledge of user casualties and system vulnerabilities or lethalties are based upon testing of the system against expected threats under realistic combat conditions. LFT&E begins with component testing, followed by subsystem tests, system-level tests, and culminating in full-up system-level tests using complete systems configured for combat. The Live Fire Test and Evaluation Office is currently responsible for the oversight of more than 80 systems with a procurement value in excess of \$500 billion.

LFT&E requires that testing be done not just against current threats, but also against expected threats when the system under development is fielded. Live fire testing initially was focused on conventional, ballistic threats. As the projected threats have changed, so have the test plans to incorporate them. These new threats include radio frequency (RF), low, medium, and high-energy lasers, incendiaries, blast/fuel air explosives, charged particle beams, and high-powered microwaves (HPM). LFT&E is concerned with persistent effects of these non-ballistic threats, i.e., the damage or degradation remains after the target ceases to be engaged by the device.

## 25.4

### Electromagnetic Environments and Consequences on Modern Weapon Systems

*Serafin, D.*

*DGA, France*

Weapon systems are more and more dependent on sophisticated electronics equipments. Functions including surveillance, target acquisition, tracking, targeting, command, control, communications and intelligence, all strongly depending on the use of sophisticated electronic equipments, have been demonstrated indispensable to increase the effectiveness of the armed forces in recent conflicts. Reliance on high technology capabilities will continue to grow.

New weapons and support systems must be capable of operating in the hostile environments such as EMI (electromagnetic interference), EMC (electromagnetic compatibility), lightning, ESD (electrostatic discharge), HIRF (high intensity radiated fields, transmitters, NEMP (nuclear electromagnetic pulse), HPM (high power microwaves) and so-called RF weapons..

During the development phase, it is indispensable to reproduce these electromagnetic environments on the system itself to validate the technical choices, to characterize safety margins and reinforce the confidence. Testing is one of the major issue of the acquisition process with the ultimate goal of reducing program risk and cost.

Large test facilities have been implemented for this purpose. Some examples of the most important test capabilities developed in the DGA will be presented with systems under test.

Recent technological advances make RF devices more feasible to build and use. These enable major adversaries and even small rogue factions to potentially apply asymmetric threats (the spending of small sums of money on terrorist weapons/tactics to attack the high technology, high expensive weapons of our military forces) to exploit a specific area of vulnerability such as communications, information warfare, or other selected areas. The threat of RF devices has matured to the point that it justifies serious characterization and testing. It is necessary to determine the vulnerability and susceptibility of virtually all hardware that is electronics based. Based on the development of foreign sources recently observed this technology is expected to be seen in the field of battle against high-technology assets within the next decade.

The LFT&E program has been testing and evaluating the on-target effects of potential RF devices over the past three years. This endeavor has been a small but pioneering effort. Tests were conducted in 1997 using both conventional HPM and high power transient electromagnetic devices (HPTED). They demonstrated the proof of principle and improved upon the methodology required to perform HPTED survivability testing. A follow-on test was performed during 1998 with an HPTED provided to the Department of Defense by a private company. The contractor was asked to design and build a device characteristic of what a rogue nation or terrorist could fabricate using only "open source" information and commonly available hardware components. A field test of an HPM wideband device against a computer network of 48 personal computers and related technologies took place this past year. Two tests are planned for this year: one on the East Coast, the other on the West Coast of the U.S. They will be outdoor, live-fire, open-air field tests. Both will employ wideband RF devices against military systems and commercial off-the-shelf technology.

## 25.5

### Experimental High Power Microwave Facilities at the US Army Research Laboratory

*Litz, M.; Kehs, R.A.*

*Army Research Laboratory, USA*

The Army Research Lab microwave simulation facilities provide an economical way to explore the effects of high power microwave environments on equipment prior to more expensive experiments in the field.

ARL facilities cover the full range of narrow band from DC to 35 GHz as well as broad variety of ultra wide band capabilities. Three buildings house this effort - a 50' x 30' x 25' high anechoic chamber supported by a full range of sources, a 130' x 90' x 70' wood frame structure for electromagnetic studies, and a series of high average power test beds with an associated 15m x 20m x 5m electromagnetic and gamma radiation shielded test cell.

The associated power conditioning research facilities provide a range of fully regulated and protected power sources up to 1 MW CW and 3 MW for short (~ 60 sec) intervals. Power supplies include variable frequency up to 1800 Hz and inductrols that allow regulated voltage to be stepped to desired levels. These supplies currently support high average MW tube research on Reltrons and broadband klystron amplifiers.

Supporting assets include all the necessary tools needed for a world-class facility. A calibration laboratory is available to support calibrations of crystal detectors, attenuators, filters, and other hardware necessary for accurate measurement of sources and radiated power. Computerized data acquisition systems are available to easily accommodate a variety of experiments. The facility includes automated antenna pedestals for mapping antenna patterns and characterizing their performance.

## 26.1

**Time-Domain Simulation Technique for Antenna Transient Radiation, Reception and Scattering***Borysenko, A<sup>1</sup>*<sup>1</sup>*Principal Engineer of Research Comp. Diascarb, Ukraine*

Current developments in UWB radars and electromagnetic pulse technique based in sufficient degree on time-domain electromagnetic phenomena in antennas and antenna-like structures. In contrast to traditional electromagnetics with sinusoidal or complex amplitude signals a transient electromagnetics should be employed for treating pulse radiation, reception and scattering. Traditionally powerful numerical approaches implemented in frequency-domain (FD) or in time-domain (TD) are considered as principal means available for the transient electromagnetic problems. Generally TD models are more adequate to such electromagnetics events than FD ones due to the fact that principal aspect of transient events involves waveforms transformation with extremely wide frequency spectrum. Moreover the numeric approaches have principal drawback resulted from sufficient programming and computing efforts to solve specific problems. Finally the physical meaning of the most numerical solutions is not evident unfortunately.

In this work a linear antenna is considered analytically and experimentally in TD under pulse excitation for three possible operation modes:

1) radiating or transmitting antenna with excitation by discrete current sources for antenna pulse driving; 2) receiving antenna, which is excited by external transient electromagnetic field and terminated to resistive load where received signal is registered; 3) scatterer (target) that combined consequently both previous cases when this structure is excited firstly by external incident electromagnetic pulse and then it re-radiates electromagnetic signal.

The first mode is under consideration ordinarily as simplest case among others. Of course, all listed above modes may be treated simultaneously by their mathematical models in form of integral or differential equations. The last are solving by finite-difference techniques like FDTD, MoM-MoT etc. Ultimate goal of this study is

obtaining solutions for all three problems by using simple mathematical and numerical technique based on universal math software like Mathcad, Matlab etc. Moreover the developed approach allows understanding main basic regularities of antenna transient behavior. Note that accordingly to the author's own design experience in UWB antennas and radars such problem's treatment is effective and productive one in practice.

The further generalization of considered problems involve complicating of antenna structure and its analysis by vector and tensor algebra relations including effects of mutual coupling, antenna lumped loading, disperse and nonlinear effects in antennas etc. Using the physical-optics technique can treat behavior of transient antennas and targets near or inside media with electrical features quite different from air-filled medium. Results of experimental examinations will present the measured data on transient antennas obtained by using of compact TD antenna testing assembly.

## 26.2

**Collapsible Impulse Radiating Antennas***Bowen, L<sup>1</sup>; Prather, W<sup>2</sup>; Farr, E<sup>1</sup>*<sup>1</sup>*Farr Research Inc., USA; <sup>2</sup>Air Force Research laboratory, USA*

A reflector impulse radiating antenna (IRA) consists of a parabolic reflector with a TEM feed. This antenna has a beamwidth which is too narrow for some applications. To broaden the beam, the Multifunction IRA, or MIRA was introduced in (E. G. Farr, C. E. Baum, and W. D. Prather, Multifunction Impulse Radiating Antennas: Theory and Experiment, Sensor and Simulation Note 413, 1997). The current paper describes the development of collapsible, man-portable IRAs both with and without the multifunction capability. The approach selected by Farr Research utilizes an umbrella like-design, with a reflector sewn from conductive fabric. Three versions of the antenna were constructed. The first antenna did not have multifunction capability and, therefore was described as a Collapsible IRA, or CIRA. The second had expansion seams in the reflector to allow the surface curvature to be adjustable. This antenna was described as a Collapsible MIRA, or CMIRA. The third antenna was an improved design without the multifunction capability. This antenna is called CIRA-2. The parabolic reflectors were 1.22 m (48 in) in diameter with a focal length of 0.488 m ( $F/D = 0.4$ ). The multifunction capability of the CMIRA was achieved by flattening the dish somewhat by opening 4 seams in the reflector surface. For the focused case, these seams are held closed by conductive Velcro. The first two antennas had reflectors and feed arms constructed from conductive rip-stop nylon. The third antenna had a reflector constructed of a conductive mesh fabric to reduce wind resistance. Also, the number of panels in the reflector was reduced from 20 to 12 to reduce the weight and size of the antenna.

The characteristics of the antennas were measured using time domain techniques to obtain the normalized impulse response as described in (E. G. Farr and C. E. Baum, Time Domain Characterization of Antennas with TEM Feeds, Sensor and Simulation Note 426, 1998). The data processing includes conversion to IEEE standard gain in the frequency domain.

This class of antenna is compact, lightweight and man-portable and provides very good RF characteristics. For the CIRA-2, the FWHM of the normalized impulse response is 80 ps. This antenna is usable from around 100 MHz to nearly 10 GHz, based on the IEEE standard gain on boresight. The peak gain is 23 dB at 4 GHz, and it has a gain of greater than 15 dB between 2 and 9 GHz.



## 26.3

### High-Power Ultrawideband Radiation for Radar Application

*Koshelev, V<sup>1</sup>*

<sup>1</sup>Institute of High Current Electronics RAS, Russia

Investigations directed to the creation of gigawatt-power-level ultrawideband (UWB) radiation sources are carried out intensively during last years. This is related to the expansion of possibility to apply UWB radiation not only for investigations of high-power short electromagnetic pulses influence on media and electronic systems but also for detection, recognition, reconstruction of aerospace objects shape, surface and underground sounding. Informational application of high-power ultrawideband radiation is a complex scientific and technological problem and it requires a development of new approaches to a creation of UWB sources and computer models for extraction of information from the electromagnetic pulses reflected by objects and media.

In the paper, a review of the theoretical and experimental investigation results on the generation and radar application of high-power UWB radiation obtained by our research team during several last years is presented. The main results can be formulated as follows: - a new approach to creation of ultrawideband radiators intended to operate in multielement steering antenna systems has been developed; - on the basis of the approach suggested, the radiators having a constant phase center in a wide frequency band, a cardioid pattern of linearly polarized radiation, a high efficiency (up to 90 percent) of bipolar nanosecond electrical pulse transformation into electromagnetic radiation by energy and peak power and presenting a combination of an electrical monopole and magnetic dipole have been created; - different variants of multielement antenna systems have been investigated both theoretically and experimentally, a minimum level of a background radiation is shown to be realized for equiamplitude rectangular arrays; - ultrawideband radiation sources with a 0.1-1 GW peak power and 100 Hz pulse rate have been developed on the basis of singular antennas and arrays; - new approaches to the solving the problem of the object shape reconstruction for the radar with a small angle base have been suggested.

## 26.5

### A New Impedance Matching Part for Microstrip Patch Antenna

*Karakus, C<sup>1</sup>; Akduman, I<sup>2</sup>*

<sup>1</sup>Nortel Networks Netas, Turkey; <sup>2</sup>Istanbul Technical University, Turkey

The microstrip patch antenna printed on a dielectric substrate is a narrow band element. That is mainly due to the limitations imposed by the dielectric substrate. Because of efficiency and cost considerations, the substrate can not be too thick. At the same time the main disadvantages of the microstrip antennas are narrow bandwidth, loss hence somewhat lower gain, poor isolation between the feed and radiating element, difficulty in obtaining the radiating impedance. Dielectric constant of the substrate is also a very important factor for return loss and efficiency. Currently, additional resonators ( slots and parasitic elements ) are used in order to increase the bandwidth of the microstrip element. The aim of this paper is to give a another method to increase the bandwidth and gain of the antenna without using a dielectric substrate. The method is based on the theory of the spiral antennas. It is well known that the spiral antennas in which no dielectricsubstrate is used can radiate broadband and by adjusting the height between the radiating element and the ground plane, the radiation frequency of the antenna can be changed. The reason of having a broadband in spiral antennas is the shape of the impedance matching part ( IMP) . The geometrical structure of matching part has a shape which extends from feeding point to radiating element. By using this idea, we have connected the feeding point and radiating element of the microstrip patch antenna with such an IMP. The height of the IMP has a linear variation while its width varies exponentially. And also, we used air or foam instead of dielectric substrate. Then, it has been proven that the bandwidth and the gain have increased. We have realized a microstrip Antenna having a bandwidth and gain of ( 1.6 GHz, 3GHz) and 10 dBi, respectively. We called this antenna Sloping Microstrip Feeding Patch Antenna ( SMFPA). We have applied for its patent.

## 26.4

### High Power UWB Pulse Radiation Source

*Fanbao, M<sup>1</sup>; Zhoubing, Y<sup>1</sup>; Wei, L<sup>1</sup>; Huilong, Y<sup>1</sup>; Hongge, M<sup>1</sup>; Chuanming, Z<sup>1</sup>; Bonan, D<sup>1</sup>*

<sup>1</sup>Institute of Applied Electronics, China

This paper describes the test of the subnanosecond impulse generation and the TEM horn with lens. The peaking and cutoff gap spark gaps was used to form the sub-ns impulse, 300kV output voltage of impulse generator with about 600ps rise time and 300ps fall time have been achieved by high pressure(60atms) N2 multi-channel ring gap switch, the repetitive rate is 100Hz.

The need for high voltage balun is driven by the fact that many UWB source have a coaxial, or single-ended output, but many antennas, such as TEM horn, require a balanced source. The output structure of our impulse generator is a coaxial transmission line, it does not adapt well to a balanced antennas such as the IRA or A balanced TEM horn. Therefore, to properly radiate the energy from our impulse generator, the balun which is designed and fabricated matches the coaxial feeds to an unbalanced conical transmission line structure, then feeds to the TEM horn. The TEM horn has the dielectric window for high voltage insulation, the match circuit for the low frequency compensation and the lens at the output of the horn for concentration the energy into a narrower beam. A variety of low voltage measurements were performed, including TDR and field measurements. The radiated pulse performance is presented when TEM horn mated to high voltage impulse generator.

## 27.1

### Introduction of Cables into the Combination of MOM and GTD/UTD

*Gonschorek, K.H<sup>1</sup>; von Siemens, C.F<sup>1</sup>*

<sup>1</sup>Technische Universität Dresden, Germany

*Fig. A. Struww*

**Summary:** In the contribution the coupling into shielded cables installed in a complex electromagnetic environment will be treated. The environment consists of electrically small and large bodies. A field radiated by an antenna is producing currents on all metallic bodies, also on the shield of cables. By means of the cable transfer impedance the current on a shield is transferred into interference voltages inside the cable. Considering a linear system also pulse coupling from external sources can be analyzed by the presented procedure.

#### Introduction

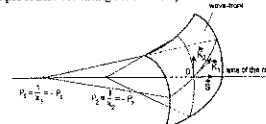
The method of moments (MOM) has proven to be a very useful tool for analyzing electromagnetic interactions in complex environments. The normal procedure within the MOM, the discretization of the metallic bodies into segments for thin wire structures or patches for larger surfaces, limits its use. Not only the size of the so-called system matrix is a boundary, also the matrix becomes more and more ill-conditioned. To overcome this difficulties the geometrical theory of diffraction (GTD) was introduced by Keller in 1962, which was later on extended to the uniform geometrical theory of diffraction (UTD). In this theory the electromagnetic interaction between two points in space is described by a limited number of rays, the higher the frequency the better the results. Combining the MOM and the GTD/UTD allows to treat electromagnetic interaction within complex environments, containing both electrically small and electrically large bodies. The last step to come to the interference voltage at the interface of an device is to consider the cable shields as conducting tubes and transferring the current on a tube into interference voltages by use of the cable transfer impedance.

#### Some aspects of the GTD/UTD

In the geometrical theory of diffraction the field from the source point to the field point is rebuild by a limited number of rays. Normally the following rays are given: direct ray, reflected rays, edge or tip diffracted rays and creeping waves. Knowing the reflection resp. diffraction coefficients the problem cuts down to a more or less geometrical problem. A check can easily be carried out whether all or enough rays are considered by calculating not only the field in a certain field point but also in its near vicinity. From physics it is known that the field cannot change drastically for two field points having a spatial distance of less than  $\lambda/2$ . The GTD/UTD in its basic form is defined for or in rays. In Fig. 1 the general description of such a ray is shown. It can easily be seen that the ray has two main curvatures. To combine GTD/UTD with the method of moments, which is mathematically based on currents, it is necessary to have a suitable transformation from currents to fields. The best seems to be the use of so-called Ekelman-Sources, which are a rebuilding of unsoidal current functions into a series of three point sources.

#### Procedure for combining MOM with GTD/UTD

Having a MOM- and a GTD/UTD-program available the combination is easily realized. The complex environment under investigation is divided into two parts, the MOM-part, containing the electrically small bodies, and the GTD/UTD-part with the electrically large structures. A system matrix for the MOM-part is build up and modified by correction terms coming from diffraction processes at the large bodies. The procedure has been presented several times. By doing this some conditions have to be obeyed, for instance if the MOM-part consists of two spatial regions, which are partly or totally shadowed by the large objects. Also a special procedure is needed if the MOM-bodies are directly connected to the GTD/UTD-structure. In the presentation the modified procedure for filling the MOM-system-matrix will be explained in detail.



#### Procedure to calculate the interference voltage inside a cable

The last step in the whole story is also not difficult to understand. Defining the cable under investigation as a metallic tube, the current on the tube (part of MOM-bodies) can be determined. Using the transfer impedance of the cable and applying transmission line theory for the inner part of the cable allows predicting the interference voltage at the interfaces inside the cable. In the presentation some example will be treated.

## 27.2

### Numerical Accuracy of the Geometrically Extended UTD

Sturm, A<sup>1</sup>; Gonschorek, K H<sup>1</sup>

<sup>1</sup>Technische Universität Dresden, Germany

#### Summary

In its original form the Uniform Geometrical Theory of Diffraction (UTD) is restricted to canonical scattering objects like cylinders, spheres and planes. Some geometrical extensions have been introduced but up to now only bodies, that may be described analytically, were taken into account. The new approach using Parametric Bicubic Splines (PBS) allows to describe objects of more technical relevance with (nearly) arbitrary curved surfaces. For this new class of surfaces which is now accessible the classical algorithm of Ray Tracing is no longer applicable and some new concepts of Ray Tracing had to be developed.

For validation purposes a number of shapes were selected which on one hand were rebuild with PBS and for which on the other exact solutions for diffracted rays exist. The reflection is known for the parabolic and the spherical antennas.

For the analysis of the creeping waves, the geodesics on the scattering surfaces are needed. The geodesics are the solutions of a differential equation. Exact solutions exist for planes, cylinders and spheres. The solution given for all surfaces of revolution is described by an integral. For the torus, which is also a body revolution, also an exact solution exists. Some of these bodies were rebuild with PBS, their geodesics were calculated and compared with the analytical solutions.

Finally the scattered electromagnetic fields of some special arrangements were calculated:

1. The exact solutions of the scattering of electromagnetic fields are only known for a few examples (e.g. the sphere). The comparison of calculated fields with these exact solutions is the first step of validation for the new UTD code.
2. For other bodies only numerical solutions exist. The scattered fields of different sets of canonical bodies were calculated with classical code and then compared with the new geometrically extended UTD code.

It will be shown that describing surfaces with PBS extends the application range of the UTD. Examples of the numerical accuracy will be discussed.

## 27.4

### On the Response of a Simple Electrical Wiring Harness to Fast-Transient EM Field Excitations

Schaefer, W J<sup>1</sup>; Byers Jr, W B<sup>1</sup>; Tigner, J E<sup>1</sup>; Tesche, F M<sup>1</sup>

<sup>1</sup>Science Applications International Corp

Understanding the response of electrical wiring in buildings and other facilities to external electromagnetic (EM) environments is an important issue in quantifying the potential threats posed to electrical systems by nuclear electromagnetic pulse (NEMP), high-power microwave (HPM) or ultra-wideband (UWB) environments. In the past, many EM coupling models involve the use of *common mode assumptions* to provide an indication of the induced currents and voltages on electrical cables. However, for power or communication cables having two or more conductors, the *differential mode response* is frequently required.

Under an IR & D program from SAIC, a combined theoretical and experimental study of the differential mode response of a simple wiring harness was conducted. A simple 1-meter, 2-conductor line having a 2 cm separation and a wire radius of 0.05 cm was illuminated by a normally-incident transient EM plane wave (see Figure 1). This line was terminated in a 1 Ω load at the bottom, was shorted at the top, and had an open circuit (representing a switch) at a position  $x_s$  along one of the conductors.

Using the Numerical Electromagnetics Code (NEC), calculations were performed for the induced cable currents and the open-circuit voltage at the switch location. For these calculations, two different transient waveforms were considered: a fast and a slow waveform arising from the Advanced Research EMP Simulator (ARES) at Kirtland AFB, NM. Figure 2 illustrates a typical ARES test waveform.

A particular response of interest of this circuit is the short-circuit current at the location of the switch. This is important, because if the induced voltage at this point is sufficiently high, arcing can occur and the resulting large current may cause permanent damage to the switching mechanism. One measure of this current stress is the *action integral*, which is the time integral of the square of the current (in  $A^2 \times sec$ ). Using this NEC model, Figure 3 presents this computed action integral for both the slower and faster ARES waveform.

This paper discusses this computational model in more detail, and illustrates some of the measured transient results that were obtained for this wiring harness. Presently, these studies are being extended to faster pulses, such as those produced by an impulse-radiating antenna (IRA), for possible application to HPM effects studies.

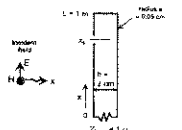


Figure 1. Geometry of the two-wire line illuminated by a transient EM field.

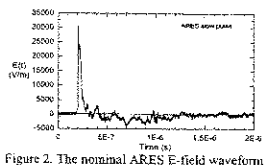


Figure 2. The nominal ARES E-field waveform.

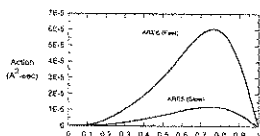


Figure 3. Computed action integrals for the induced current for the ARES environments, as a function of the observation location.

## 27.3

### PROTHEUS - A Simulation Package for HPM/EMC Effects

Bunger, R<sup>1</sup>; Ritter, J<sup>1</sup>; Murso, M<sup>1</sup>; Reiter, J<sup>1</sup>

<sup>1</sup>DaimlerChrysler Aerospace AG, Germany

In future conflict scenarios, High-Power Microwaves (HPM) are an emerging threat to autonomously flying systems such as reconnaissance aircraft and cruise missile. Compared to the nuclear electromagnetic pulse (NEMP), HPM has an increased impact on mission-systems due to the controllability of several parameters such as pulse-envelope, contained frequency spectrum, dwell-times etc.. These parameters can be adjusted to match the vulnerability of mission-critical equipment, e.g. the guidance control unit.

Most of the in-service equipment has no specific protection against HPM, so that it can be expected that besides of the incorporation of HPM hardening measures into new designs, several retrofit-HPM-hardening activities will take place in future. In order to implement an effective HPM-protection, first of all, the HPM-vulnerability of the threatened system has to be assessed. This is a cost-dominating process since many measurements are usually required to evaluate the coupling paths leading to undesired effects.

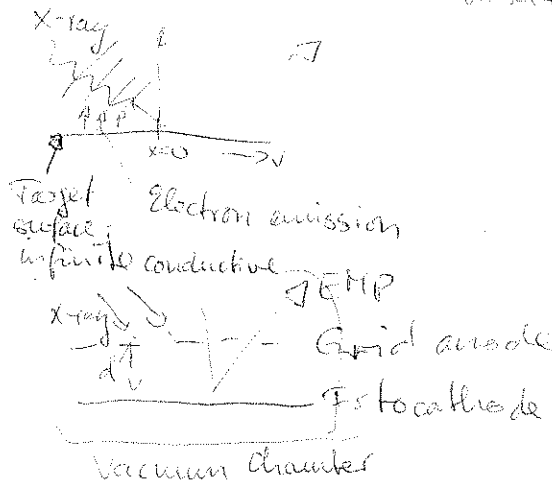
Due to the increasing availability of high performance computers, numerical simulation of the electromagnetic interactions gains importance in this process. Actually, even with increasing computational power at hand, commercially available simulation software does often not allow the simulation of complex problems such as a complete drone mainly made of composite (e.g. radar absorbing) material, at microwave frequencies. Furthermore, many practical relevant cases have to be treated with hybrid methods, which are not commercially available at all.

This situation is the motivation for the initiation of the EM-simulation software system PROTHEUS, which is currently under development at DaimlerChrysler Aerospace, military aircraft business unit. The work is funded by the Federal Office for Defense Technology and Procurement (BWB).

The aim of PROTHEUS is to provide a set of modern, most recently developed simulation tools under a common user interface. The dominating methods are modern integral equation methods for large number of unknowns, such as the Multilevel Fast Multipole Algorithm (MLFMA), Finite Difference (FD) and asymptotic methods. At the symposium, several computational examples will be presented which demonstrate the performance of the methods already implemented.

## 27.5

*Experimental observation of the Cerenkov EMP faster than light macroscopic source in vacuum.* Bessab, A.V.



*Chamber → x-ray → Target Pulse 3x shorter than x-ray*

## 28.1

## Symmetry Analysis of Targets Near an Earth/Air Interface

Baum, C E<sup>1</sup><sup>1</sup>Air Force Research Laboratory DEHP, USA

For the identification of buried targets symmetry plays an important role. In this paper we restrict ourselves to the case of electromagnetic singularity identification (EMSI) for which wavelengths in the external medium (soil) are of the order of the target dimensions. For typical mines and other unexploded ordnance (UXO) this implies 100s of MHz to several GHz for the pulse or set of frequencies used to illuminate the target from some sort of ground-penetrating radar (GPR). In contrast to the low-frequency magnetic-singularity identification (MSI) for which the magnetic-polarizability dyadic and its associated symmetries are important, in the case of EMSI much more geometric detail and associated symmetries are important.

An important result is the vampire signature of zero cross polarization ( $h_v$ ) in the usual  $h, v$  radar coordinates for the backscattered fields from a target with  $O_2 (=C_{\infty a})$  symmetry. Note here that the rotation axis is required to be perpendicular to the surface  $S_g$  of the local earth on which or in which the target resides. Small deviations from this symmetry split the 2-fold modal degeneracy applicable to most of the resonant modes (poles).

Here we consider the cases of  $C_N$  and  $C_{N_a}$  symmetries in the targets of interest, as appropriate to targets in the presence of a layered medium such as near the earth surface. The symmetry of the target appears directly in the symmetry and associated description\* of the eigenmodes. This does not actually give a detailed calculation of the eigenmodes, but decomposes the problem in a way that reduces the computation to a subset of the target geometry. The present approach should be applicable to targets with other symmetries corresponding to the various point symmetry groups (rotations and reflections in three dimensions).

While we have been considering electromagnetic scattering and modes, the same techniques should be applicable in quantum mechanics. The quantum wave function of molecules exhibit the point symmetries of the molecules, and the energy levels are analogous to electromagnetic natural frequencies. Quantum wave functions (Schrödinger eqn.) are scalar rather than vector functions, thereby being simpler in at least one respect.

## 28.4

## Parsimony in Signature-Based Target Identification

Baum, C E<sup>1</sup><sup>1</sup>Air Force Research Laboratory DEHP, USA

In fitting scattering data to target signature in some library, it is useful to have as much constraint on the target-signature parameters as possible so as to make it difficult to fit the data with the signature of the wrong target type. Minimizing the number of variable parameters (and the ranges of their variation) in fitting signatures to the scattering data can be called parsimony. This paper discusses various ways of achieving parsimony.

In signature-based target identification the scattering dyadic of each type of target is characterized by a set of functions based on a particular scattering model (e.g., complex exponentials for the late-time response, or delta, step, ramp, etc., for the early-time response). Each of the functions is characterized by a small number of parameters (e.g., complex natural frequencies  $s_n$ ) including a scaling coefficient (scalar, dyadic) to adjust the amplitude (perhaps including vector orientation). Each of the targets is represented in a target library by an appropriate set of functions with parameter values particular to the individual target types (e.g. a particular type of aircraft such as a 707). The approach is to associate these parameter values with the characteristics of the electromagnetic waves scattered (usually backscattered, but not necessarily so) from the target by some appropriate radar.

One type of parameter (fixed) assumes particular values (scalar, vector, dyadic) for each target type. A second type, which we might call a variable parameter is adjusted as part of the process of fitting the scattering model to the data. Such variable parameters are typically the coefficients of the fitting functions, which adjust the amplitudes (not necessarily scalars) of the fitting functions, to best fit the data. Since we wish to discriminate between various targets we would like it to be difficult to fit the wrong target parameters to the data (including noise). So we would like to reduce the number of variable parameters (and the range of their variation) as much as we can. This is aided by constraining these scaling coefficients (e.g., pole residues) to values appropriate to the target type to the degree practical.

## 28.2

## Buried Object Identification with a New Log-log Singular Value Threshold

Løstamlien, Y<sup>1</sup>; Uguen, B<sup>1</sup>; Corre, Y<sup>1</sup><sup>1</sup>LCSTIIRERINSIA, France

Detection and identification of hidden object by means of a radar system, is an important problem of great interest to many civilian and military agencies, as witnessed by the literature on the topic. The proposed paper will describe an improved method of target detection based on poles extraction. This method is very well suited to the analysis of sets of data produced by ultrawideband radars.

Many targets have a simple geometry and their late time impulse responses are dominated by only a few complex natural resonances (CNR). These CNR's represent an attractive way for target identification.

Modifications of the original Prony's method (R. Prony, "Essai expérimental et analytique, etc.", Paris J. L'École Polytechnique, pp 24-76, 1795) are used to identify target while studying the CNR's. Though most of the existing algorithms suffer from low SNR, spurious poles.

Prony's method assumes that the number of poles is known a priori. However the actual number of significant resonances is usually unknown, depending on the features of the systems. Underestimating model order results in errors and should be avoided. Overestimating model order leads to the generation of both correct and spurious poles. The model order is usually estimated by the dominant eigenvalues or the pole energy. It was also found that the magnitude of the coefficient associated with the poles can be used for the same purpose. Our work optimises of the classical SVD-based Total Least Square Prony Method (R. Carriere and R. L. Moses, "High Resolution radar target modeling using a modified Prony estimator", IEEE Trans Antennas Propagation, vol AP-40, pp 13-18, 1992).

First, we apply our method to a sphere. This canonical object is particularly well suited to validate our algorithm for its poles and their location in z-plane are well known. We improve the method in determining automatically the optimal value of the number of the singular values (SV). We consider the representation in log-log scale of the SV ranked in a decreasing order. We notice that a part of the curve is linear. By calculating the regression line, we are able to determine when the SV does not follow the linear behaviour anymore. We then choose this rank to be the number of SV to be kept. In a second part, we apply this method to the detection and identification of a buried mine illuminated by an ultrawideband pulse. By focusing on the location of the obtained poles in s-plane for various A-scans, when the antennas are moved along a surface line, we are able to detect the presence and location of the searched mine. The GPR measurement is noisy and contaminated by clutter from antenna resonances, surface roughness and soil inhomogeneities, making it especially difficult to extract the CNR's.

The proposed paper will present thoroughly the advantages and the limits of the new method, emphasising its novelty. Many viewgraphs will illustrate the results obtained by our codes and our data analysis. We will discuss those examples with special attention given to mine and unexploded object detection by an ultrawideband radar. Thus we will show how our method based on CNR's extraction can be used to correctly detect, locate and identify targets.

## 29.1

**RF Experimental Facilities at the AFRL Directed Energy Directorate**  
*Harrison, Michael<sup>1</sup>*  
<sup>1</sup>AFRL/DEHE, USA

Abstract not available

## 29.2

**Joint US Army-Navy Development of the Transverse Electromagnetic/Mode-Stir (TEMMS) Facility**  
*Frazier, S<sup>1</sup>; Meadows, E<sup>2</sup>*  
<sup>1</sup>US Navy, Naval Air Warfare Cnt Aircraft Div, USA; <sup>2</sup>Aegis Technology Group, Inc, USA

The Army and Navy are jointly sponsoring a large Transverse Electromagnetic/Mode-Stir (TEMMS) Chamber as part of the United States Department of Defense (DOD) Central Test and Evaluation Improvement Program. The TEMMS facility will effectively address key electromagnetic environmental effects (E3), RF Weapons and electronic warfare (EW) RDTE issues. The TEMMS will provide uniform illumination of full-scale aircraft/systems by using mode-tuned and/or mode-stirred techniques. TEMMS technology is unique, and will provide DOD with a capability to test to high power levels while minimizing test setup time and rotation of the test aircraft or illumination source. This will benefit the DOD in several ways: reduced test cost, increased personnel safety, significantly less hazards to other equipment/aircraft, less aircraft test time, more thorough tests, more realistic tests, reduced manpower, flexible test scheduling, secure tests, all weather test capability, reduced training for facility operators, and high quality tests.

The Naval Air Warfare Center Aircraft Division (NAWCAD), Patuxent River, MD, a DOD Major Range and Test Facility Base has been proposed as the new TEMMS location. Most Army and Navy aviation E3 RDTE is routinely conducted at Patuxent River. NAWCAD has DOD's largest, most modern, and diverse RF RDTE infrastructure. The NAWCAD has seamlessly integrated E3, EW, and electromagnetic technologies. The large in-place E3 and EW RDTE simulation, stimulation, measurement, modeling and analysis capabilities will reduce TEMMS long-term investment requirements, while increasing effectiveness. All TEMMS related facilities are co-located within the same complex. Other large-system test structures already located in the area where TEMMS will be constructed include: a small-aircraft Anechoic Chamber, a large shielded hangar, an outdoor test area, and a new large-aircraft Anechoic Chamber. All these capabilities are integrated into an Installed Systems Test Facility, incorporating a Manned Flight Simulator; numerous weapon systems and electronics laboratories; and a DOD high power computing center for high level modeling and simulation. By being located at NAWCAD, TEMMS will benefit from the considerable leverage afforded by this unique, large-scale RF and Military RDTE technology base.

The TEMMS would provide a large 127'x 113'x 50' shielded chamber and supporting equipment to illuminate full scale weapon systems such as tanks, vehicles, C4I elements, helicopters, and aircraft up to the size of a Navy P-3 aircraft. This capability can support special access classified projects up to the Top Secret security level. The controlled electromagnetic environment is provided over the frequency range of 10 kHz to 40 GHz. The average electromagnetic field levels will range from 10V/m to 400 V/m with peak field to 80,000 V/m. Interfaces to data acquisition and data processing, man-in-the-loop test/simulation capabilities, and databases will be available. Also, an interface with MIL-STD-1553 MUX Bus for the control of aircraft/weapon systems will be used to simulate mission profiles and to exercise specific systems. This shielded volume will also be used as a TEM cell to test to high powers at the lower end of the frequency range. The TEMMS facility will provide the three services, DOD agencies, other Government Agencies, and industry with a one-of-a-kind test capability. Such a facility would complement present high power test capabilities and support a wide range of weapon systems and variety of RF RDTE technologies.

## 29.3

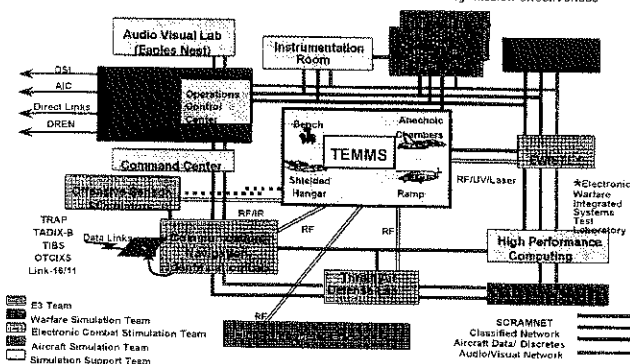
**Electromagnetic Environmental Effects RDTE in a Large-Scale Installed System Test Facility**

*Frazier, S<sup>1</sup>*  
<sup>1</sup>US Navy, Naval Air Warfare Cnt Aircraft Div, USA

The United States Department of Defense (DOD) has developed a number of Electromagnetic Environmental Effects (E<sup>3</sup>) and Electronic Warfare (EW) simulators and Research, Development, Test, and Evaluation (RDTE) facilities within the Major Range and Test Facility Base (MRTFB) infrastructure. This paper discusses performing E3 RDTE using a Large-scale Installed System Test Facility (ISTF) capable of providing closed-loop and distributed simulation environments.

The ISTF has proven to significantly speed the acquisition process while reducing acquisition costs. One of the largest ISTF's is the Air Combat Environment Test & Evaluation Facility (ACETEF), located aboard the Naval Air Warfare Center Aircraft Division (NAWCAD), Patuxent River, MD, a DOD MRTFB. With a very large E3 and EW T&E customer base, ACETEF has amassed the world's largest collection of E3 emitters, and an extensive EW assessment suite. This capability makes ACETEF ideally suited to simulate and assess system performance in complex theatre-wide scenarios. A functional block diagram of the ACETEF is shown below. Specific test areas for ACETEF include a small anechoic chamber, a large shielded hangar, and an outdoor test pad which support E<sup>3</sup> and EW RDTE, and a new, larger anechoic chamber that can accommodate aircraft up to the size of a Boeing 707. This capability allows flexible, secure RDTE, incorporating full mission and flight simulation and integration. An interface with MIL-STD-1553 MUX Bus for the control of aircraft/weapon systems will be used to simulate mission profiles and to exercise specific systems. Test point and test volume instrumentation and data processing is available. To simulate complex mission profiles and to fully exercise specific systems, a Manned Flight Simulator and a DOD high power computing center provide realistic high level modeling and simulation data.

ACETEF's existing E3 and EW infrastructure allow the system under test to interface with distributed systems while immersed in a dense, realistic, real-time RF environment. System performance can be assessed in a secure environment, and the system can even participate in real time external activities and exercises. The large, in-place E3 and EW RDTE simulation, stimulation, measurement, modeling and analysis capabilities reduce E3 uncertainties, while increasing mission effectiveness.



## 29.4

### US Office of the Secretary of Defense, Operational Test and Evaluation, Live Fire Test: Broad Agency Announcement - Vulnerability Assessment of Radio Frequency

Frazier, S<sup>1</sup>; O'Byron, J<sup>2</sup>; Carter, D<sup>3</sup>; Heard, J<sup>4</sup>; Harrison, M<sup>4</sup>; Dickson, D<sup>5</sup>; Henderson, M<sup>1</sup>; Grothus, M<sup>5</sup>  
<sup>1</sup>Naval Air Warfare Center, USA; <sup>2</sup>Director, Live Fire Test, USA; <sup>3</sup>Live Fire Test, USA; <sup>4</sup>Air Force Research Laboratory, USA; <sup>5</sup>Southwest Research Institute, USA

The Office of the Secretary of Defense, Operational Test and Evaluation, Live Fire Test and Evaluation (OSD/OTE/LFTE) is concerned by the potential adverse threat posed to current and future United States (U.S.) weapons and supporting defense systems by emerging, non-traditional threats such as those posed by low, medium, and high energy lasers and by weapons capable of generating a high-power electromagnetic pulse. These weapons might be used by an adversary to exploit a specific area of vulnerability, such as communications, information warfare, or other selected areas, to attack U.S. forces more effectively and efficiently, and thereby achieve an asymmetric advantage.

In support of the LFTE Charter, a Broad Agency Announcement (BAA) has been created and executed to assess the vulnerability and susceptibility of specific Military, Commercial Off-The-Shelf (COTS), and Non-Developmental Items (NDI) against Ultra-wideband RF Threats similar to those available to terrorists and/or Rogue Nations. The BAA testing will be focused on two test teams: An East Coast operation headed by the Air Force Research Laboratory, and located at Eglin AFB FL; and a West Coast operation located at China Lake, CA and headed by the Naval Air Warfare Center. Central program management will remain under the control of a LFTE led Steering Committee which will be responsible for overall program coordination, pre test analysis and data analysis.

The BAA test approach relies on realistic Operational Test Evaluation concepts and processes. The test matrix of threat, victim and interaction will be realistic in consideration to operationally relevant scenarios. No attempt will be made to determine RF-effects/upset

thresholds above expected operationally significant levels. Test planning will include pre-test predictions. Where test schedule and tempo permits test object RF measurements will be obtained to assist in understanding the coupling/upset mechanisms involved as well as isolating/mitigating failure/upset modes. Throughout all testing, a thorough mapping and characterization of the incident RF fields at the test object will be recorded to establish performance thresholds and allow accurate reporting and analysis.

The RF devices selected to be threats, are unclassified laboratory sources, representing a wide variety of UWB waveform characteristics, including varying pulse shapes, intensities and burst characteristics. Where practicable, a variety of characteristic waveforms will be generated for each test series to better characterize system effects.

The target systems selected for testing include a representative cross-section of military, COTS and NDI equipment. Systems will range from small, stand-alone electronic devices such as laptop computers, and handheld communications, to complex, integrated weapons systems such as state-of-the-art aircraft and helicopters.

The specific RF effects test results on individual test objects will be controlled by one or more guidelines/organizations, and may be restricted or classified. Although much of the data obtained through this program may be unavailable to the public, it will be available to the decision makers for risk assessments, and to assist in protecting US systems against future threats

## 29.5

### Closed-Loop Facility For the Investigation of High Power Radio Frequency Effects on Dynamic Systems.

Andreadis, T<sup>1</sup>; Wieting, T<sup>1</sup>  
<sup>1</sup>US Naval Research Laboratory, USA

The full response of a dynamical system to high-power radiofrequency (HPRF) radiation can only be obtained in a closed-loop experiment. Static testing is an important part in the investigation of such effects because it provides a relatively inexpensive way to investigate quickly an extensive parameter space. However, static testing ignores the contribution of the dynamics and at some point it is important to make use of a closed loop facility. In this paper we describe a closed-loop system that we have designed and constructed at the Naval Research Laboratory for the investigation of effects on missiles by high-power radio-frequency waveforms. One of our primary requirements was to be able to test full missile systems. This constraint drove us to a novel design in which the missile body stays still and the HPRF and target antennas move during the engagement scenario. This approach eliminated the need to orient heavy missiles rapidly and to employ expensive metal tables that could interfere with the experimental results. Control of the system is provided through two Pentium computers with Windows NT operating systems. Graphical display of the missile flight is obtained through a linked Silicon Graphics computer. Views from both the target and from the missile may be selected so that the engagement may be observed in real time. Instrumentation to adjust RF intensities is controlled through GPIB interfaces and is managed using a Visual C++ program. A software autopilot model that is linked to the seeker hardware is used to provide the response of the missile.

## 30.1

### Wideband Radiation Patterns using a Koch Monopole

Litz, M<sup>1</sup>; Fazi, C<sup>1</sup>  
<sup>1</sup>Army Research Laboratory, USA

Wideband Antennas are required for the development of impulse communications, and impulse radars. Efficient use of spread-spectrum techniques and frequency hopping radios make use of broadband antennas. Multi-use antennas that enable minimization of antenna volume are of great interest for space saving reasons. Many command centers include large antenna farms that must be installed to accommodate the wide variety of narrowband communications networked to inform the commanders. For all these reasons, compact wideband antennas would be a valuable tool in the arsenal of network and communication developers. Wideband antennas on wide-area-network impulse links are already available in the commercial marketplace. The type of system considered includes the fast impulse switches radiating sub-nanosecond rf pulses, time-gated receivers taking advantage of the filtering available in time-gating for gain and sensitivity.

The US Army Research Laboratory (ARL) is exploring technologies in each of these areas in order to minimize antenna size, develop conformal EM radiating systems that can withstand the environments of future tactical battlefield. In particular, fractal antennas represent a compact, lightweight, broadband, agile structure for radiating a large set of frequencies from a single antenna. Experimental and numerical results of five iterations Koch curve wire antennas, and Koch curve printed-circuit-board antennas are compared. Radiation pattern measured in a 50' anechoic chamber in the frequency range of 50 MHz to 10.05 GHz compare are compared to NEC simulations of the same structures. NEC (Method-of-Moment) computed input impedance is also compared to measured input impedance from the S11 S-parameter.

Frequency response and gain of the antenna increases with complexity of the antenna structure. Beyond iteration three of the Koch curve, little is gained. Results of numerical modelling and experiments show good agreement.

## 30.2

### Broadband Operation of Tapered Inset Dielectric Guide and Bowtie Slot Antennas

*Hannigan, AB<sup>1</sup>; Pennock, SR<sup>1</sup>; Shepherd, PR<sup>1</sup>*  
<sup>1</sup>University of Bath, UK

In this paper, two promising broadband radiating structures are evaluated. The inset dielectric guide tapered slot antenna (IDG-TSA) and the bowtie slot antenna are simple, rugged, lightweight structures which perform well over a broad band, offering moderate gain and low levels of cross-polarisation as well as being easy to integrate with planar circuitry.

The IDG-TSA is a travelling wave structure consisting of a tapered dielectric-filled slot cut into a ground plane. The width and orientation of the main radiated beam is determined by the slot and ground plane geometry. Previously, the structure has been fed using rectangular waveguide. In this contribution it will be shown how microstrip and stripline feeds can be used to extend the useable bandwidth of the antenna as well as allowing much easier integration with planar circuitry. Measurements will be presented demonstrating an operating bandwidth of more than 3:1 using these feeds, with cross-polarised radiation being generally more than 20dB lower than co-polarised levels.

The bowtie slot antenna is a planar version of the wideband bifurcated antenna. The structure under consideration here consists of a bowtie etched into a metallised substrate, fed by a microstrip line printed on the reverse side of the board, terminated in a radial stub. Measurements of this structure are depicted in Fig. 1, showing good operation over a broad frequency band. However, operation of the antenna is possibly restricted by high levels of cross-polarisation, between 8 and 9GHz in this example. Work is continuing to establish the full useable bandwidth of this structure.

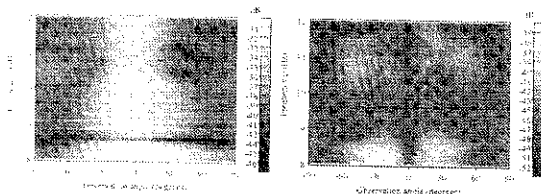


Figure 1: Bowtie slot antenna radiation pattern in decibels as a function of frequency and elevation angle: (a) co-, and (b) cross-polarised radiation.

## 30.4

### Accurate Simulation of Multi-beam Antennas Based on a Luneburg Lens.

*Daniel, J-P<sup>1</sup>; Vinogradov, S<sup>2</sup>*  
<sup>1</sup>Université de Rennes 1, France; <sup>2</sup>Dundee University, UK

In recent years, multi-beam antennas (MBA), based on the Luneburg lens, are of great interest because of their good performance in a wide frequency range. Most theoretical analyses of such MBA are studies of mono-beam antennas. The information so obtained is generalised to the MBA by simple "mechanical" composition of secondary beams, which are characteristic of the mono-beam antennas.

In contrast to this simplified concept, the present investigation includes all possible aspects of theoretical analysis, only with the exception of shadowing effects of secondary beams by the actual feed system. Basically, we use the Mie series approach. A variant of MBA used in practice was taken as the object of simulation, the hemisphere lying on reflecting (metallic) background. The feed system is simulated by a set of so-called Complex Huygens Sources (CHS). It permits primary Gaussian beams of specified beamwidth. The method applied here has no restrictions on the electrical size of MBA, number of layers of Luneburg lens, losses in dielectrics, or possible air gaps between interfaces (arising from displacement of the polarised feed system). Simulation of the feed system is made possible by a consideration of regularly and "irregularly" located CHS. Some of these results are verified by experiments, in which we use open waveguides as feeds.

## 30.3

### Focal Region Studies for Some Focusing Systems

*Vinogradov, S<sup>1</sup>; Smith, P<sup>1</sup>*  
<sup>1</sup>University of Dundee, UK

Although simple in a geometrical sense, focusing systems such as the spherical dish and the dielectric sphere demonstrate how exact knowledge about the details of the electromagnetic field distribution in a focal region makes it possible to design reflector antennas with a performance essentially better than that obtained from designs with generic high frequency methods (GTD etc.).

In the case of the reflecting spherical dish, we use both point and line sources located in the focal region to predict the distribution of electromagnetic field, for the receiving region. The same procedure was applied for "well-known" dielectric sphere. The proper location of complex point sources, producing the Gaussian beams near the dielectric sphere, leads to a surprisingly excellent performance of the dielectric sphere, as a simple antenna device with high value of directivity, and low level of the side lobes (less than -20 dB).

A more striking example is the metallo-dielectric focusing structure. It consists of a partially screened dielectric sphere. With an appropriate choice of parameters this system provides a better performance than either the spherical dish or the dielectric sphere, taken individually.

## 30.5

### Fragmented Aperture Antennas Designed for Pulse Radiation

*Maloney, J<sup>1</sup>; Kesler, M<sup>1</sup>; Smith, G<sup>2</sup>*  
<sup>1</sup>Georgia Tech Research Institute, USA; <sup>2</sup>Georgia Institute of Technology

Over the last few years, we have been exploring how to best configure an aperture of given size so as to obtain a specified level of performance, for example, the highest gain (including mismatch) over a specified bandwidth. The approach we have adopted led to a class of radiators we call Fragmented Aperture Antennas. This type of antenna is a patchwork of discrete conducting and dielectric units distributed over the specified aperture. The arrangement of the units is determined using an efficient, multistage procedure that incorporates the genetic algorithm for the optimization and the finite-difference time-domain method for the electromagnetic computation.

In practice, we have designed and built fragmented aperture antennas with a single feed point that achieve a gain in the broadside direction comparable to that from a sheet of uniform current of the same size. The gain of these fragmented aperture antennas can approach that of the sheet of uniform current over frequency bandwidths greater than 8:1. The design procedure has also been used to produce fragmented aperture antennas with beams in directions other than broadside.

Our initial investigations of the fragmented aperture antenna were concerned with obtaining high amplitude (gain) for the radiated field, and the phase of the radiated field was not a parameter directly involved in the optimization. However, a step in the optimization procedure inherently produces designs with nearly linear phase for the field in the desired direction. Hence, these fragmented aperture antennas are suitable for radiating pulses.

In this paper, we will present results for several fragmented aperture antennas that were designed to radiate ultrawideband, short pulse waveforms, discuss the details of the optimization procedure, and show comparisons of measured and predicted antenna performance.



## 30.6

### A Unified Kinematic Theory of Transient Array

*Shlivinski, A<sup>1</sup>*

<sup>1</sup>Tel Aviv University, Israel

We present a unified framework for the kinematic analysis of transient arrays, i.e., arrays driven by pulsed waveforms and controlled by the time shifts between the array elements. The properties of the radiated field depend on the waveform parameters: the center frequency  $f_0$ ; the fractional bandwidth of the waveforms  $B/f_0$ ; the pulse repetition rate  $f_p$ ; the interelement spacing  $d$  and the total number of elements  $N$ . Following a previous work (A. Shlivinski, E. Heyman & R. Kastner, IEEE Trans. Antennas Propagat., AP-45, 1140-1149, 1997) we present here a unified parameterization for the kinematic properties that covers the entire parameter range, from the conventional monochromatic dense array to the ultra wideband sparse array. The radiation pattern consists of an interlace of grids of lobes, generated by different mechanisms: In addition to the *side-lobes* and the *grating-lobes* grids, which are mainly monochromatic phase-interference phenomena extended to the wideband regime, we also identify a grid of *cross-pulse-lobes* which is an intrinsic wideband phenomenon. The total lobe structure represents an interplay of all three phenomena that depends on the ratio between the parameters mentioned above.

Having established a unified representation we then focus on the ultra wideband regime where the lobe structure is dominated by the cross-pulse-lobes that are mainly controlled by the pulse repetition rate  $f_p$ , the  $d$  and the total number of elements  $N$ . It is shown that under certain conditions one may design a sparse array (with interelement spacing much larger than the wavelength for all frequencies in the band) which basically does not suffer from these lobes. These results are demonstrated both theoretically and numerically in the  $L_2$  and  $L_\infty$  detector (norm) spaces.

## 31.1

### TODREAM - A Topological EMC Performance Analysis Tool

*Carter, N<sup>1</sup>; Robinson, J<sup>2</sup>*

<sup>1</sup>DERA, UK; <sup>2</sup>SARS Inc, USA

Over the past year SARA Inc have been developing in conjunction with DERA under MOD funding, an analysis tool which can be used throughout the life of a project to monitor its EM Hardness performance. The tool consists of a graphical front end coupled to a EM database developed by SARA to DERA requirements. This database is capable of handling all EMC data; both immunity and emission and coupling data, and has an extensive signal processing capability.

The graphical front end enables the data which is fed into the database during the life of the programme to be assigned to the various topological areas of the asset being developed using a Windows explorer type interface. Algorithms within the software compare the data input highlighting problem areas in the asset or areas where data is missing. In the early stages of an asset development programme the only data available will be legacy data from previous similar programmes and modelling predictions. These can be fed into TODREAM to enable a better method of determining the stress levels that will be imposed at equipment or module level enabling a more reliable method of tailoring the equipment qualification test specification levels. As the programme progresses, actual coupling/immunity data will be fed into TODREAM enabling problem areas to be highlighted and additional hardening requirements to be determined.

The first version of TODREAM will be completed by April 2000.

## 31.2

### Electromagnetic Coupling of High Power Microwave (HPM) into Unmanned Aerial Vehicle

*Hastedt, R<sup>1</sup>; Grünfeld, M<sup>1</sup>*

<sup>1</sup>STN Atlas Elektronik GmbH, Germany

The recent HPM-Technology is a significant threat also for airborne systems, therefore it's necessary to get information about the HPM compatibility or vulnerability. Particularly the characteristics of small air vehicle configurations combined with high integration scale have main influence to the protection against HPM.

Taking the HPM into consideration the behaviour of generic and operative airborne systems has to be analyzed with different investigations.

STN ATLAS Elektronik performs several studies with a HPM-TESTDRONE, made by STN ATLAS Elektronik.

The version of the HPM-TESTDRONE is based on the design and process technology of an operative Drone.

The characteristics of the HPM-TESTDRONE are:

- Stealth technology, metallic and shielded electronic cover and cables and
- electronic sub-equipment (Flight Control and Navigation System).

Each characteristic has to be investigated with special procedures taking into consideration the HPM-threat.

The transfer function of stealth and metallic structures were analyzed on the basis of following measurements:

- Radar Cross Section and Scattering Center Analysis; Surface Current and
- Shielding Analysis (reflected and absorbed).

The electronic system of the HPM-TESTDRONE will be examined by measurements and theoretical studies.

The theoretical studies (system analysis) cover the actions:

- Semiconductor list; determination of interference and destruction energy;

determination of critical paths, description of coupling characteristics and

analog simulation.

The information of the system analysis leads to the measurement concept with the parts:

Description of signals which have to be examined; description of the test area and test procedure.

The HPM-test of electronic equipment will be performed together with the EMC-department of the WTD81 in Germany.

The variable parameters of the tests are:

Orientation of the HPM-TESTDRONE in the HPM field; HPM power density and modulation.

The results of the different investigations will offer information on: Future HPM protection as a part of the common protection; using impuls measurement procedures as susceptibility measurement method for electronic systems; effective parameter of HPM sources; application of introduced and future Drones as carrier systems for HPM payloads as well as for detection and suppression of high radiation sources.

## 31.3

**Mono-Pulse and Repetitive Pulse HIRF-HPM Interaction with Small Systems***Lövstrad, K.G.**<sup>1</sup>Defence Materiel Administration, Sweden*

For analysis and testing of the effects of HIRF and HPM-exposure it is necessary to characterise the radiation by several parameters. Not only the frequency, intensity and pulse energy, but also the pulse repetition pattern is of importance for a good understanding of HIRF and HPM-effects and for susceptibility test planning.

An analysis method has been developed where coupling of mono-pulses and various forms of pulse repetition patterns are considered. The geometrical model includes the radiation geometry and direction, intensity and radiation aspect angle at a fast moving disturbance victim. The coupling into system skins often shows a great variability depending on the aspect angle of the exposure. The system response shows a similar great variability depending of the phase in a functional cycle when a pulsed exposure occurs and of the character and persistence of a disturbance sequence. By determination of the incident coupling over 360 deg. aspect angle it is possible to make a statistical estimate of the internal EM environment for a defined dynamic situation with static or fast moving HIRF or HPM-sources and victims.

An exposure/coupling model can determine the statistical behaviour of the exposure-coupling function. The model can e.g. be used to determine the required number of test variations for specified test accuracy. The model may also illustrate the observations of low risk for a disturbance at a single fly-by near a radar. The threat from various types of HPM-weapons can be compared by use of data of measured coupling features of a certain object.

Numerical methods can be used at the equipment bay and PCB levels for estimation of the functional upset. Such estimates of internal disturbance fields are of statistical nature and render probability functions. The accuracy of such an estimate is poor but it can be used for comparisons between various exposure cases.

The exposure model has been used for fly-by situations for various radar sources. Radar frequency, PFR, pulse length, antenna pattern and antenna sweep rate have been included in the calculations as well as the statistics of fly-by patterns of aircraft with statistical variations of their flight path and velocity. Calculations with the Monte Carlo method render good exposure statistics that differ between counter rotation and with rotation fly-by of a sweeping radar antenna.

Statistical skin transfer function results from missile tests have been used for estimation of the internal disturbance fields. The results from varying exposures to HPM-weapons are compared with emphasis on the importance of the pulse repetition parameter.

Vulnerability tests of electronic systems with repetitive fields of varying PRF and persistence are discussed in view of electronic functional features that may influence the susceptibility to repetitive disturbances.

## 31.4

**Two Level, In-Band/Out-of-Band Modelling RF Interference Effects in Integrated Circuits and Electronic Systems***Whyman, N.L.<sup>1</sup>; Dawson, J.P.<sup>2</sup>**<sup>1</sup>DERA Farnborough, UK; <sup>2</sup>University of York, UK*

In this paper we present a behavioural model that combines high frequency and low frequency subcircuits to predict the effect of Radio Frequency Interference (RFI) on linear integrated circuits. The model is constructed from detailed measurements and manufacturers data, and can be used to determine the upset mechanism in analogue systems subjected to RFI. The HF subcircuit is characterised by *s*-parameters measured using an IC test jig and can be modelled directly in the frequency domain by a circuit simulator program such as Pspice. This will define the pin input impedance and pin-to-pin coupling of each device. This data can be used to define the transfer function of a recursive digital filter to enable the synthesis of a lumped model to define the devices characteristics to time domain waveforms using HPEM and UWB signals. The voltages generated in the LF subsystem are derived from measurements carried out by injecting RF into each IC device pin terminals to determine a set of polynomial functions of frequency and incident power. The results of measurements and simulation of circuits containing one and two op-amps including different configurations of amplifier, using coupling via multiple pins, are used to demonstrate the principle of the model. The approach presented allows the possibility of predicting the propagation of RF and the effect of EM interference in electronic systems in a single simulation.

References James J. Whalen, "Predicting RFI Effects in Semiconductor Devices at Frequencies above 100MHz" IEEE Transactions on Electromagnetic Compatibility, Vol. EMC-21, No.4, pp. 281-282, November 1979.

## 31.5

**Galvanic Corrosion of RF Gasket Materials and the Effects on Meeting EMC Requirements Over Time***Fenical, G<sup>1</sup>*<sup>1</sup>*Instrument Specialties Co., Inc, USA***INTRODUCTION**

The European EMC Directive essential requirements must be met for the intended life of a product. Not only is this important from a regulatory point of view but from a quality or customer satisfaction point of view as well.

Many factors can affect the EMC performance of electrical and electronic apparatus. One factor is the shielding effectiveness of the enclosure that houses the apparatus. Many times various types of RF shielding gaskets are employed to increase the shielding effectiveness of the enclosure to values that are acceptable. The shielded enclosure is effective for both radiated emissions and radiated immunity. The enclosure also plays an important role in ESD, EFT, Surge, and Conducted RF because it can assist in shielding the internal or sensitive components from the radiated portion of the conducted interference signal.

The shielding effectiveness of any enclosure, large or small, is affected over time. A major consideration is the proper choice of materials for the enclosure and RF gaskets to minimize the effects of time on these materials due to galvanic corrosion. Many time devices meet their requirements by only a few dB. Degradation of the shielding effectiveness of the enclosure by small amounts can put the device out of compliance. Other considerations such as operating environment, shipping, and storage must be considered as well.

**EFFECTS OF CORROSION ON EMI GASKET PERFORMANCE**

Radio Frequency (RF) joints lose shielding effectiveness over time due to corrosion. Conditions affecting this degradation include the corrosiveness of the environment, materials used for the joint, size and type of RF gasket, measurement frequency, and a variety of

other factors. Corrosion buildup in the RF joint slowly forces the joint apart. As the joint opens, the shielding effectiveness degrades. The rate of degradation is directly related to the speed at which corrosion deposits are formed. Some environments, such as moist salt air, form corrosion deposits at very high rates, while dry environments produce very slow rates.

The materials present in the RF joint also affect the rate of corrosion buildup. In general, the greater the galvanic difference between metals making up the joint, the faster the corrosion rate. Galvanic compatibility is a simple but crude guide to corrosion rates. Many other factors also influence the corrosion rate.

The test frequency is important in determining the degradation of RF shielding due to corrosion. The type of corrosive deposits formed can, in special cases, increase shielding effectiveness at different frequencies. This can be due to whisker growth, or simply that the corrosion deposits are conductive at radio frequencies. For this reason, D.C. measurements are generally a poor guide to RF shielding effectiveness, especially at frequencies greater than 10 MHz.

## 32.1

**Nearby Lightning-induced Electromagnetic Stresses on Structures at Launch Sites***Chai, J C<sup>1</sup>; Monos, S<sup>1</sup>; Britting, A O<sup>1</sup>*<sup>1</sup>*The Aerospace Corporation, USA*

Lightning has been a major recurring concern for space launch operations at Cape Canaveral Air Station (CCAS) in Florida, USA. In order to protect launch vehicle (LV) and space vehicle (SV) systems against the electromagnetic (EM) effects induced by frequent nearby lightning events and to guide launch processing operations, the knowledge about the EM environment generated by nearby lightning and the corresponding EM responses of major structures at launch sites is highly desirable.

In attending to this need, analyses were performed to characterize the EM environment for the Space Launch Complex (SLCs) at CCAS and major structures' responses ("stresses" in terms of electromagnetic quantities) to this EM environment. Using structures at CCAS/SLC17 and a typical 30kA nearby lightning strike 1-kilometer away as an example, this paper describes the analytical tools and models used in the study, summarizes the analytical results, and concludes with a brief discussion.

Because of the broad frequency spectrum of the lightning-induced EM effects and complex launch site configurations, a method-of-moments computer code is employed for the analysis. The E- and H-fields induced on the surfaces of selected structures/objects are obtained, which can then be used to guide the sizing and placement of the measurement sensors and protection devices. In assessing the lightning-induced EM effects on the LV/SV system during launch processing, it is emphasized that the severity of the lightning threat must be considered together with the probability of such an event occurring (J C Chai, S Monos J L Montegut, Zurich EMC Symposium, 607-612, 1999). For a cost-effective risk reduction and management, well-planned and well-conducted tests and measurements on the system responses are needed for the validation and verification. As an important step in this direction, an on-line lightning monitoring system (P R Sechi, R Adamo J C Chai, ICLSE, 103-111, 1999) is being implemented at CCAS. It is shown that an on-line lightning monitoring system with a correlated retest algorithm is one of the best ways to assess the lightning-induced threat, to lead lightning protection activities, and to guide launch operations through major lightning storms.

## 32.3

**Nuclear Electromagnetic Disturbance Modelling***Hayakawa, M<sup>1</sup>; Korovkin, N V<sup>1</sup>; Selina, E E<sup>2</sup>; Iudin, D I<sup>1</sup>; Kotchetov, S V<sup>2</sup>*<sup>1</sup>*The University of Electro-Communications, Japan;* <sup>2</sup>*Saint Peterburg State Technical University, Russia*

**Abstract.** The report deals with electromagnetic pulses produced by high-altitude nuclear explosion in any electric device. The electric system is represented as a conglomeration of transmission lines with non-linear connecting elements and non-linear circuit. We suggested a new method that efficiently analyses dynamical processes in systems of such kind. The method is based on using discrete macro-models of lines and loads. Some theorems have been proved, which make the process of calculation of the discrete macro-models equivalent parameters and voltage and current distribution along the line much faster as compared to the solution of this problem by common integration of the system of differential equations. In the large number of applications these characteristics can be determined only experimentally and have not smooth and monotone properties. For example, the frequency characteristics of the equivalent parameters of electrical machines windings (high-frequency processes consideration) have a complicated multi-extreme nature. Therefore there is a problem of a construction of mathematical models of devices, which equivalent parameters depend on frequency, for using in the time domain. A method permitting to use the models, described by the frequency responses, in the time domain is offered. Other methods of solving such problems do not permit to take simultaneously into account both experimental frequency responses and non-linear elements. The estimation of an error of the offered methods is presented. An application of the method is illustrated by the examples. The transient in the distributed system with taking into account the process of electromagnetic energy radiation is investigated.

## 32.4

### Architecture and Simulated Performance of a Pseudo-Plane Wave Generator

*Timmons, M<sup>1</sup>; Courtney, C<sup>2</sup>; Voss, D<sup>2</sup>*

<sup>1</sup>412 TW/EWWA, USAF, USA; <sup>2</sup>Voss Scientific, USA

Planewave stimulus and measured response of integrated aircraft electronic systems are critical components of aircraft test and certification programs. To conduct such a test, a planewave environment in the volume occupied by the system under test (SUT) is typically required. Unfortunately, for large SUTs (aircraft) the ability to generate a planewave over its volume is limited, to a large extent, by the test frequency and size of the test facility. Traditionally, to improve the quality of the incident field, the SUT is located at a position far from transmitting antenna (far field), but the size of the test facility limits the available separation distance and for frequencies below 1 GHz this separation is unachievable in indoor facilities. For accurate RCS measurements the entire SUT must be illuminated by a planewave. But for electronic systems that are coupled to the exterior environment via distributed apertures, is a planewave over the entire asset required? Instead of demanding that a planewave environment exist over a volume, we suggest that to measure electronic systems' response, it is only necessary to create an incident field that is planewave in nature only over local points and volumes on the SUT. In practice, the test engineer would identify the locations on an asset where the apertures of interest are located. A Pseudo-Planewave Generator (PWG) would then produce a field distribution where the incident field has planewave-like qualities only over these locations. The field is free to assume any value in other areas of the test volume. By relaxing the requirement on the EM field over the entire test volume, we have greatly reduced the complexity of the problem. The new problem is more tractable, and potentially has an engineering solution. Such a PWG system could be comprised of a set (three or four) of transmitting stations, each an array of broadband elements with individual amplitude and phase control. These stations could then be distributed about the test facility. The excitation of each element (phase and amplitude) is determined using a Genetic Algorithm. The exact aperture location(s) on the asset, and the direction and polarization of the desired

planewave are input to the GA by the user. The GA then searches the near-infinite number of possible excitation vectors for a near-optimal solution, one that produces a "best-fit" field distribution with "local" planewave behavior over the SUT's apertures. This presentation will begin with a brief description of the problem. Next, our approach will be presented, and a description of the system architecture (hardware and software) will be given. An explanation of the application and use of a genetic algorithm (GA) will be presented, and will include a description of the GA process and definition of the GA "fitness" criteria used to evaluate the quality of the electromagnetic field associated with a particular excitation vector. Finally, simulated results for several cases will be presented.

## 32.5

### Fast-Running Computer Models for the Calculation of Source Region EMP Environments and Coupling

*Gilbert, J<sup>1</sup>; Madrid, M<sup>1</sup>*

<sup>1</sup>Metatech Corporation, USA

The detonation of nuclear weapons near the surface of the earth produces strong horizontal electric fields at the air-ground interface which may drive large currents on horizontal overhead or buried lines. At early times the air conductivity is an important factor in determining the currents; at later times, the currents depend more strongly on the ground conductivity and the connection between the fireball and the line. This paper describes the technical aspects of a pair of user-friendly computer codes developed for the Deutsche Wehrwissenschaftliches Institut fuer Schutztechnologien (German Defense Science Institute for Protective Technologies) for the rapid calculation of early and late time currents on extended conductors.

The early time environment and coupling code uses a local plane-wave, retarded-time approximation where the early time flux of gamma rays and the current on the line are assumed to be only functions of retarded time and only vary spatially through this dependence. This is justified because the air and ground conductivities limit the propagation of electromagnetic radiation. The electromagnetic fields in the air and ground are solved using a one dimensional implicit technique with prescribed sources, and the line current is solved using the telegrapher's equations in retarded time.

The late time environment and coupling code uses a two step procedure where the electric and magnetic fields in the air are calculated first assuming that the ground is perfectly conducting. This defines the magnetic fields at the air-ground interface, which are then used as a boundary condition to determine the horizontal electric fields at the air-ground interface. The currents on extended conductors are then solved using the telegrapher's equations in the usual technique.

The pair of codes runs on personal computers using the Win 95/98 or NT family of operating systems, and require only a few seconds per calculation.

## 32.6

### Leader-Pulse Step-Formation Process

*Baum, C E<sup>1</sup>*

<sup>1</sup>Air Force Research Laboratory DEHP, USA

In natural lightning and triggered lightning there are fast impulsive events often called steps that are a fundamental part of the discharge process. These include the stepped leader, both downward propagating (usually negative) from the cloud and upward propagating (usually positive) from the ground including field-enhancement devices such as a small rocket and wires to initiate the streamer. These leaders often have a stepping behavior, during which the propagation speeds are larger than the average speed of leader propagation. This paper expands on the previously developed corona model for a nonlinear transmission line to include both forward and backward propagating current pulses during the leader pulse. Based on measured electromagnetic data the ratio of leader-tip speed during the leader pulse to the average speed is estimated. This is combined with reported optically measured average speeds to estimate the leader-tip speed which is observed to be consistent with the model. It would be useful to have more and better such data. The time resolution of the electromagnetic waveforms can be improved using transient-waveform digitizers currently available. Perhaps this can be combined with appropriate optical data, with a similarly high (10 ns) resolution.

One needs to recognize that the numbers developed herein are order-of-magnitude estimates based on an approximate model of the currents and speeds in the leader pulse based on the corona nonlinear-transmission-line model. Fundamental to these estimates is the ratio of leader-tip speed during the fast step to the speed averaged over many steps. This ratio estimate would be decreased if there were significant but slow leader-tip advance between the leader pulses. Note this and other assumption used in constructing the model. This is tempered by the constraint of  $c$  on the various speeds and reasonable values of  $I$  during the pulses.

## 33.1

### Space Weather Chain from Sun to Earth's Surface

*Jansen, F'*

*'Astrophysical Institute Potsdam, Germany*

The chain of Space Weather effects from Sun to Earth's surface and the contribution of galactic cosmic rays to Space Weather will be sketched. By means of examples we will show the enormous influence of Space Weather to different technical systems as spacecrafts, aircrafts, railways or to power systems, pipelines and others. However: all the aspects of the entire Space Weather chain were not studied for events on-line. Therefore a prototyping activity of monitoring of Space Weather events from the Sun lift-off to Earth surface is necessary. A consortium, which has the task to connect different Space Weather recording stations - natural as well as technical - for the prototyping activity will be described.

## 33.2

### Coupling Between the Magnetosphere and Ionosphere

*Lemaire, J'*

*'Institut d'Aronomie Spatiale, Belgium*

The magnetosphere is a reservoir of electrons and ions (mainly protons) trapped in the geomagnetic field. Their energies ranges from less than 0.1 eV up to 500 MeV. The particles of lowest energies (up to 20 eV) form the ionosphere, polar wind and the plasmasphere; those with energies up to 100 keV constitute the Ring Current, while the most energetic ones up to several hundred MeV form what is call the Radiation Belts; particles of intermediate energies fill in the other regions of the magnetosphere: e.g. the plasmatrough, auroral regions, polar caps and plasmashet. The spectrum of these different populations of trapped particles have been measured for over four decades using in-situ satellites. The variability of these spectra as a function of solar activity and geomagnetic activity has been extensively studied. As a consequence of the coupling between the magnetosphere and the ionosphere the temporal variations of the fluxes of magnetospheric particles influence the distribution of the ionospheric plasma density and temperature. It is these effects that will be presented and discussed in this talk.

## 33.3

### Particle Fluxes in the Earth's Radiation Belts during Geomagnetic Storms

*Heynderickx, D'*

*'BIRA, Belgium*

Dramatic changes in the Earth's radiation belt population during magnetic storms have been observed since the early 1960's. It is well established that the radiation belts are not a static environment, but are strongly variable on different time scales, ranging from one hour or less to periods of the order of the solar cycle. Most of the variations are driven by conditions on the Sun, which interact with the trapped populations in a number of ways.

The trapped proton population mainly reacts to changes in the neutral atmosphere density distribution, but also undergoes abrupt enhancements that can take months to disappear again. Similarly, the outer electron belt undergoes violent perturbations with orders of magnitude changes in particle fluxes and acceleration and transport of particles into the inner regions of the magnetosphere. In addition, changes on the solar cycle time scale and seasonal effects are now firmly established.

The changes in the radiation belt population during geomagnetic storms will be illustrated by means of spacecraft observations for a selected case study and by a computer simulation of the environment with the Salammb code.

The changes in the near Earth proton and electron fluxes can pose considerable hazards to spacecraft systems and crew members. Increased fluxes of energetic electrons are responsible for deep dielectric charging which is known to have caused several spacecraft failures. The creation of secondary trapped proton belts during strong injection events results in elevated ionising and non-ionising dose rates and increases in proton induced single event upset rates. These effects will be illustrated for typical orbits by applying standard radiation effect models and tools.

## 33.4

### On the Use of Geomagnetic Indices to Monitor Geomagnetic Storms

*Menvielle, M'*

*'Université Paris Sud, France*

Geomagnetic indices constitute homogeneous data series aiming at describing the magnetic activity or some of its components. The great diversity of magnetospheric and ionospheric phenomena results in a great complexity in the transient variations of the Earth magnetic field, and different indices have then been designed: aa, am and Kp (magnetic activity at a planetary scale), Dst (magnetic signature of the magnetospheric equatorial ring current), and AE (auroral electrojet activity). The data series are homogeneous since 1868 for aa, 1932 for Kp, 1957 for Dst and 1959 for am. As a result of their unique temporal and spatial coverage, these remarkable data series are basic data in activities dealing with 'Space weather' and effects of geomagnetic storms on technological systems.

Geomagnetic indices are based on the analysis of magnetograms recorded at networks of permanent magnetic observatories. Provisional values are computed using the data circulated by the observatories within a delay of a few weeks. They aim at providing estimates of the definitive values of the indices. The possibility of dissemination of data through electronic network opened a new era. The I.S.G.I. Publication Office (for K-derived planetary indices) and the WDC-C2 for Geomagnetism (for Dst and AE indices) started routinely preparing and circulating quick-look values of geomagnetic indices within delays of the order of a few days. The present status of geomagnetic indices dissemination and availability is presented. The processes of derivation of the geomagnetic indices can be described in terms of four components: - the quantity to be measured, or estimated, which can be either the range of variation or the derivation from a base value, - the time interval over which it is measured, - the location of the station, or network of station, - the method of derivation. This description is used to discuss the use of geomagnetic indices in monitoring the intensity of geomagnetic activity, with particular emphasis to hazards on technological systems.

## 33.5

### The Hazards of Cosmic Radiation to Air crew

*Hunter, R<sup>1</sup>*

<sup>1</sup>Civil Aviation Authority, UK

**Objective:** To discuss the problem of cosmic radiation in air crew (pilots, flight engineers and cabin crew) and identify protective measures.

Air crew are occupationally exposed to cosmic radiation. Cosmic radiation is a complex mixed field radiation of solar and galactic origin. Solar modulation should, on average, reduce radiation exposures at aircraft cruising altitudes during the forthcoming solar maximal period. However, for brief periods, following significant solar particle events, the exposures may substantially increase. Air crew have the highest occupational radiation exposure in the UK. Doses to air crew are greatest at increasing altitude and latitude. The projected growth of commercial air traffic and the trend towards flights being of longer durations at higher altitudes is discussed. In-flight radiation monitoring studies and studies of patterns of disease and death in air crew are described. In the case of receiving an average annual air crew occupational exposure of 3mSv over a working lifetime, the probability of attributable death is approximately 0.25%. By 13 May 2000 the implementation of the Euratom Directive will require a system of radiation protection for Air crew. The estimation of doses using computer programs and other methods of compliance with the Directive are described.

**Conclusions:** Air crew are unlikely to exceed annual occupational exposure limits. The future development of a space weather forecasting and alerting service, integrated with flight operations, may represent a better system of radiation protection than currently proposed techniques.

## 34.2

### Optical Polarimetry for Target Detection in Cluttered Environments

*Lewis, Gareth D<sup>1</sup>; Jordan, David L<sup>1</sup>*

<sup>1</sup>DERA, UK

The passive remote sensing of man-made objects using electro-optical imaging sensors are often limited not by fundamental signal to noise considerations but by scene clutter. An optical method of discriminating man-made objects from the natural background is to use the polarised content of the image. In this paper the polarization signatures of man-made objects in the both visible (0.4-0.7mm) and thermal infrared wavebands (3-5mm and 8-12mm) are considered. In the thermal wavebands man-made objects tend to exhibit significant levels of partial linear polarization whilst the natural background does not. Whilst in the visible waveband the sky and vegetation can be significantly polarized although man-made objects show greater polarization levels under a number of environmental conditions. Thus rotating a polarizer in these wavebands, the object modulates like a Belisha beacon effect. If the object fills a few image pixels then simple processing will allow the polarization state to be determined. Results showing the variation of polarization in the 8-12mm infrared waveband for different materials of varying surface textures are presented. In addition polarimetric images will be shown for visible and infrared wavebands.

## 34.1

### A Review of Polarisation Effects in Wave Scattering

*Boerner, W<sup>1</sup>; Cloude, S<sup>2</sup>*

<sup>1</sup>University of Chicago, USA; <sup>2</sup>Applied Electromagnetics, UK

There is currently widespread interest in the use of electromagnetic sensors for the detection of surface and buried targets. An important feature of electromagnetic radiation is its state of polarisation and a whole range of classification algorithms have been suggested based on the transformation of polarisation by the object. This paper seeks to review the state of progress in this subject and to provide a unified approach to the different algorithms published in the literature.

The classical method to formulate passive radiometric sensing is the Stokes vector and associated Mueller matrix. The latter has been used largely in a projective form to establish a limited set of transformations, e.g. from natural unpolarised incident light into polarised reflectance. However recent developments in active sensor technology have enabled full population of the scattering matrix and hence have lead to increased possibilities for target classification based on full matrix analyses.

In particular the depolarising capability of a target has been defined in a basis invariant manner by using a mapping from the Mueller matrix into a 4x4 Hermitian coherency matrix. The eigenvalues of this matrix relate to the inherent depolarisation properties of the target through the scattering entropy and scattering anisotropy. This has lead to a fuller understanding of the depolarisation effects of foliage and ground clutter in radar and rough surfaces in optics.

Here we review these developments and use them to assess current and future possibilities for discrimination of targets based on complex amplitude ratios, channel coherence and eigenvalue decompositions.

We provide a summary of Radar, Optical and IR system capabilities and a review of current sensor performance.

## 34.3

### Unipolarized Currents for Antenna Polarization Control

*Baum, C E<sup>1</sup>*

<sup>1</sup>Air Force Research Laboratory DEHP, USA

For certain types of radars, specifically polarimetric SAR (synthetic aperture radar), control of the polarization of the incident wave on the target and the polarization of the receive antennas is important. This relates to certain signatures in the target scattering which can be used for target identification.

Symmetry is an important concept in controlling antenna patterns, including polarization. This can be thought of as complementary to the symmetry in the target which strongly influences the scattering pattern, including polarization. The antenna symmetry can be used for polarization control, but with limitations depending on the relative orientations of the antenna and target (assumed in the antenna's far field).

In the present paper we consider another technique for antenna polarization control: the restriction of the antenna currents to flow only parallel/antiparallel to a given frequency/time-independent direction designated  $\vec{1}_a$ . This gives a particular real frequency/time-independent polarization at each point in the far field. However, this polarization in general differs from point to point. Taking two choices for  $\vec{1}_a$  (conveniently orthogonal) for two such antennas gives two independent polarizations at each point in the far field which can be used to mathematically construct the usual h,v radar polarizations and scattering dyadic for the transmit/receive properties of the two antennas. Furthermore, by use of two orthogonal symmetry planes for the two antennas (with currents on thin wires) the two antennas can be made mutually noninteracting so as not to disturb each other's pattern/polarization. Making the antennas electrically small further simplifies the analysis by making the pattern simply that of an electric dipole.

Within these constraints there is still much flexibility in designing arrays of parallel thin wires. Furthermore, such wires can be symmetrically impedance loaded for various reasons, including a desire to make them electrically small so as to simplify the analysis in terms of a unipolarized electric-dipole moment.



## 34.4

### Multi-Channel Impulse Radiating Antennas with Polarization Diversity

*Farr, E<sup>1</sup>; Bowen, L<sup>1</sup>; Baum, C<sup>2</sup>; Prather, W<sup>2</sup>*

<sup>1</sup>Farr Research Inc, USA; <sup>2</sup>Air Force Research Laboratory, USA

We describe here a new class of antenna that may be useful in locating mines based on symmetry considerations. We introduce here the tri-IRA and quad-IRA, which are derived from earlier versions of Impulse Radiating Antennas. In these new designs, the aperture is divided into three or four sections, in order to provide at least two receive channels and at least one transmit channel, all within a very compact structure. The two receive channels allow one to receive two orthogonal polarizations. This configuration will be useful when searching for mines using the so-called "vampire" radar signature, which is a characteristic of certain manmade objects in certain symmetry configurations. Such objects cannot scatter any cross-polarized field, whereas natural objects scatter a stronger cross-polarized field component. In this note, we analyze the radiated fields of the tri-IRA and quad-IRA. We optimize the feed impedance, and we build a model tri-IRA. This model is tested in various configurations, and compared to theory.

In a previous note (C. E. Baum, Interaction Note 523, 1996), it is shown that a rotationally symmetry mine, sitting parallel to an air/soil interface, can scatter only co-polarized fields, and not cross-polarized fields. If we wish to use this effect to discriminate between mines and clutter, we will require an antenna that provides at least two of the four polarizations in the scattering dyadic.

We calculate here the radiated field on boresight by converting the aperture integral into a contour integral. Results are shown for the tri-IRA, consisting of three sections, and for the quad-IRA, consisting of four sections. We also calculate various figures of merit, so one can determine the optimal impedance.

In order to test our theory, we designed, built, and tested a tri-IRA with a 91.4-cm diameter, a focal length of  $F = 34$  cm, and an F/D ratio of 0.37. Testing included TDRs and antenna patterns in the principal planes. Our measured results for the aperture height is 84% of the theoretical results. We also tested the antenna in radar mode.

We found considerable late-time noise in the receive channel, due to crosstalk and mismatched impedances. We suggest various methods for reducing this crosstalk in future designs.

## 35.1

### New Design for a Regulated High Current Transfer in a Lightning Simulator

*Brasile, J.P<sup>1</sup>; Moncho, S<sup>1</sup>; Jousse, D<sup>1</sup>; Venet, D<sup>1</sup>*

<sup>1</sup>Thomson Shorts Systemes, France

Lightning simulator requires the generation of regulated current up to 800 A for "C" wave modelling.

Former designs used a bank of lead batteries with a poor safety standard since very high energy remains stored even when the system is not operating. Use of power supplies is costly since they are designed for continuous operation and they necessitate a few megawatt electrical power connection.

The Thomson Shorts Systemes development of a low cost, compact generator consists of a capacitor bank storage and a servo controlled mechanically adjustable resistor.

The capacitor bank consists of eight discharge capacitors switched by an IGBT switch.

The voltage decrease on the load during the discharge of the capacitor is compensated by decreasing the value of the resistance in series.

This is automatically done during the pulse by a servo-controlled electrical jack associated with a ceramic disk resistor assembly. Constant current injection on a resistive constant load requires a constant speed of the jack movement. The system can be used on various load values and to various currents by adjusting the initial position of the resistor.

The charge transfer can be precisely controlled by an appropriate voltage setting and by a dump switch to terminate the pulse. The characteristics of the pulse are the following:

Regulated current :	200 A to 800 A,
Pulse duration:	2s to .5s,
Total charge transfer:	400 C
Peak power :	1.6 MW

Scaling to higher current and power is straightforward.

## 34.5

### Model Problems of Pulse Sensing

*Velychko, L<sup>1</sup>; Perov, A<sup>1</sup>; Sirenko, Y<sup>1</sup>; Yaldiz, E<sup>2</sup>*

<sup>1</sup>Institute of Radiophysics and Electronics, Ukraine; <sup>2</sup>Gebze Institute of Technology, Turkey

The radio-locating means for determination of layered media parameters and visualization of objects or voids hidden in them have gained wide-spread acceptance in various fields, namely, civil engineering, geodesy, use of hydraulic-engineering structures and oil-pipe-lines, etc. The solution of the engineering problems arising therewith requires the development of essentially new approaches. Traditional theoretical and experimental methods have made possible only the first generation of radars with both small signal penetration depth and incomplete retrieval of useful information from remote sensing data. Quite reasonable hopes for improvement of the situation are widely associated with the construction of radars in nonsinusoidal waves. A central theoretical problem here lies in correct interpretation of the results of the measurements, and it cannot be solved without development of adequate mathematical models (and algorithms) describing the transient processes in the part of space under research.

The model problems of pulse sensing are the initial boundary value problems in infinite domains with locally-inhomogeneous compact scattering objects. The key to the effective solution of them is in a proper truncation of the computational domain in finite-difference methods, i.e. in a restriction of such kind that, on the one hand, reduces the essentially open problem to the closed one and, on the other hand, does not reflect on accuracy and reliability of the numerical data obtained. Our paper is just devoted to the analysis of this key problem of the mathematical simulation in the interests of pulse sensing. In the first section, the problem on scattering of nonsinusoidal waves by a perfectly conducting compact object imbedded in a locally-inhomogeneous half-space with a locally-irregular boundary is considered. The second section is devoted to the extension of the results to other situations peculiar for pulse sensing: a locally-inhomogeneous compact object and a stratified dielectric structure in a field of nonsinusoidal waves and a pattern-forming structure with both a wide range of potentialities for optimization of the radiation field and pulse excitation from the aperture of a semi-infinite regular waveguide. All model problems are two-dimensional and scalar ones (we consider the E-polarization of electromagnetic field), and yet the results can be generalized and modified as applied to solution of three-dimensional scalar (acoustic) and vector (electromagnetic) problems. In the third section of the paper, an example of correct incorporation of exact conditions on virtual boundaries into a standard computational scheme of the finite-difference method is given, the results of the numerical experiments focused on testing and approbation of the constructed algorithms are presented.

The theoretical and methodological foundations for the approach being developed here are laid in papers of Y. K. Sirenko, A. O. Perov, and N. P. Yashina, which are devoted to the origination of new rigorous and efficient techniques for the analysis of electromagnetic field transients in open periodic resonators (gratings) and waveguide resonators (inhomogeneities of regular waveguides). We follow these papers, extending the results obtained there to another class of topical problems of electromagnetic theory that are of practical significance.

## 35.2

### 2 MJ Modular Capacitor Bank for Electrothermal-Chemical (ETC) Application

*Brasile, J P<sup>1</sup>; Moncho, S<sup>1</sup>; Venet, D<sup>1</sup>*  
<sup>1</sup>Thomson Shorts Systemes, France

ETC application requires, especially during the experimental phase, a capacitor bank able to deliver various pulse waveforms on the load.

Thomson Shorts Systemes is developing a new modular capacitor bank system, consisting of 20 modules, to achieve this goal.

Each module is composed of a 500 F capacitor, a crowbar and forward diode packs for protection, a dump and an inductance for pulse shaping. Modelling showed that a 20 kV charging voltage was necessary for achieving the specified requirements due to the 50 meters distance between the capacitor bank and the load.

The system is integrated into a shelter on a trailer so as to be fully autonomous.

The command and control is fully isolated from the capacitor bank through fibre optic and pneumatic links.

Each module can be switched to the load at any voltage up to 20 kV, with a timing accuracy of one microsecond.

This permits a large variety of pulse waveforms on the load since the modules can be fired either synchronously (to achieve maximum peak power) or sequentially (to tailor for example a long pulse, at constant current).

The bank can deliver up to 500 kA on the load and is fully protected to operate on a short circuit.

These performances are achieved with the use of a specifically designed sealed vacuum switch. The vacuum switch is able to operate at up to 250 kA with an energy transfer of 1 MJ, for single shot application. The interest of using a vacuum switch in this design is the very wide operating range which can be achieved while avoiding pressure or gap control as in a spark gap.

## 35.4

### Sub-nanosecond Gas Breakdown Phenomena in the Voltage Regime Below 15 kV

*Krompholz, H<sup>1</sup>; Hatfield, L<sup>1</sup>; Short, B<sup>1</sup>; Kristiansen, M<sup>1</sup>*  
<sup>1</sup>Texas Tech University, USA

Fast gaseous breakdown is of interest for both UWB/short pulse electromagnetics, and for plasma limiters to protect devices from high power microwave radiation. A quantitative investigation of fast breakdown phenomena, especially for relatively low voltages and for special geometries, does not exist to the authors' knowledge. With fast high voltage pulsers, covering the parameter range of voltage amplitude 1.7 to 7.5 kV, risetime 400 ps to 1 ns, pulse duration 1 to 20 ns, breakdown in gases is studied in a point-plane geometry. The setup consists of a pulser, 50-Ohm transmission line, axial needle-plane gap with outer conductor, and 50-Ohm load line. The needle consists of tungsten and has a radius of curvature below 0.5 mm. The constant system impedance of 50 Ohm (except in the vicinity of the gap) and special transmission-line-type current sensors enables sub-nanosecond current and voltage measurements with a dynamic range covering several orders of magnitude. Digitizing oscilloscopes with sampling rates of 5 ps and 50 ps are used, with analog risetimes of 80 and 240 ps. In addition, the luminosity is measured with a sensitivity of about  $10^4$  V/W and a risetime of 800 ps. For pulse amplitudes of 1.7 kV (which are doubled at the open gap before breakdown), and long pulse duration, and a gap distance of 1 mm, delay times between start of the pulse and start of a measurable current flow (amplitude > several milliamperes) have a minimum of about 8 ns. Here the pressure dependence of this delay time was measured, in 10 to 600 torr argon, and this minimum is observed at 50 torr. Voltages of 7.5 kV produce breakdowns with a delay of about 1 ns. Statistical delays could not be found in both cases, with the tip positively pulsed. Further breakdown data (dependence on gap width, needle radius of curvature, ambient pressure, gas type, polarity) will be presented, and possible mechanisms for breakdown in this regime will be discussed.

This work is supported by the US Army Space and Missile Defense Command.

## 35.3

### Compact HPM and UWB Sources using Explosives - The Potential of Future non-lethal Warhead Systems

*Ehlen, T<sup>1</sup>; Bohl, J<sup>1</sup>; Sonnemann, F<sup>1</sup>*  
<sup>1</sup>Diehl Munitionssysteme GmbH CoKG, Germany

The consideration of semiconductor destruction levels at irradiation exposure and RF-power levels for effective electronic distortion in combination with output-power and energy of HPM and UWB sources give a first overview of the achievable source-sink distances (SSD).

In contrast to stationary sources non stationary system enable to enlarge the effective distance. To deliver the primary electrical system energy explosively driven HPM and UWB source concepts are considered with regard to conversion efficiency, performance, weight, volume and directivity.

The energy density (J/m<sup>2</sup>) of the radiating field necessary for a burn out in specific irradiated electronic systems is extremely lower for an UWB-pulse than for a HPM-pulse. Given a fixed amount of primary source-energy UWB-sources will reach a longer SSD than HPM-sources.

The pulse length dependent break-through-fieldstrength in air and in the sources itself limit the maximum source output power at UWB and therefore limit the absolute SSD for a given irradiated device. To overcome this limit in UWB a pulselength reduction has to take place - in HPM a pulselength extension.

A comparison of usable devices and typical arrangements are presented as well as potential targets at the battlefield and the scenario to create burn-out and interference. The conclusion derive the potential carrier platform from the advantage of an electromagnetic field as a non lethal weapon with its specific illumination area and hit accuracy.

## 35.5

### High-Power, High-PRF Subnanosecond Modulator Based on a Nanosecond All-Solid-State Driver and a Gas Gap Pulse Sharper

*Yalandin, M I<sup>1</sup>; Lyubutin, S K<sup>1</sup>; Oulmascoulov, M R<sup>1</sup>; Rukin, S N<sup>1</sup>; Shpak, V G<sup>1</sup>; Shunailov, S A<sup>1</sup>; Slovikovskiy, B G<sup>1</sup>*  
<sup>1</sup>Institute of Electrophysics, RAS, Russia

Further improvement and commercialization of high-power ultrawideband electromagnetic pulse generators and wideband subnanosecond coherent microwave oscillators call for modulators providing both high pulse power and high pulse repetition rate. This paper presents the results of tests of a new subnanosecond modulator which combines for the first time a solid-state nanosecond driver based on an inductive energy store with a semiconductor opening switch and a pulse sharper based on ultrahigh-pressure gas gaps.

The SM-3NS nanosecond driver is a system consisting of several energy compression stages (intermediate capacitive energy stores), a pulse transformer, and saturable magnetic switches. The output stage includes an inductive energy store and a high-current semiconductor opening switch. As this switch operates, a voltage of 400 kV with a pulse duration of 6 ns is generated at the open output of the driver. The driver provides a packet operation of the modulator with a pulse repetition rate of up to 2 kHz.

In producing pulses of nanosecond duration, this driver is used to charge a short pulse-forming line (PFL) with a wave resistance of 50 Ohm and a capacitance of ~20 pF. The highest voltage achievable across the PFL is ~300kV. Constructionally, the pulse-forming line is combined with a unit consisting of a sharper and a chopper both operating at an ultrahigh-pressure (up to 100 atm). A short (leading edge of 300 ps; width of 0.5-1 ns) pulse is formed by successive sharpening and chopping. Served as the load of the pulse former was a 50-Ohm long coaxial line imitating the input feeder of a TEM horn or the transmission line used to connect an electron diode.

The modulator was tested for operation at pulse repetition rates of up to 100 and 2000 Hz with nitrogen and hydrogen used, respectively, as the working gas for the spark gaps. Forced circulation of the working gas was not used. Comparative data are given for hydrogen and nitrogen on the decrease in breakdown voltage with increasing pulse repetition rate, the stability of the breakdown voltage, and the time delay of the breakdown of the chopping gas gap relative to that of the sharpening gas gap.

*Pulse sharper 100 ns + SOS: Solid state opening*

## 36.1

### Fast Method for Calculation of Mutual Coupling in Planar Microwave Circuits on General Multilayer Substrates

*Van Thielen, B<sup>1</sup>; Vanderbosch, G<sup>1</sup>*  
<sup>1</sup>Katholieke Universiteit, Belgium

A fast method for the calculation of mutual coupling in planar circuits in a general multilayer substrate is described in this paper.

A circuit consists of the following three classes of building blocks:

- 1) Transmission lines: Any kind of transmission line (microstrip, stripline, ...).
- 2) Discontinuities (components): These can be semiconductors, passive components and metal discontinuities that are much smaller than a wavelength
- 3) Meshed structures: Metal structures comparable to or bigger than a wavelength

Using appropriate approximations and rigorous Green's functions (for a random multilayer substrate) software modules are constructed that can calculate the couplings between these three classes.

The module for the calculation of mutual coupling between transmission lines is developed starting from the general method of moments that can handle random shapes. Only first order coupling is taken into account: the radiation effect of the induced currents is neglected. The calculations are speeded up for the specific case of coupling between lines. This is accomplished by assuming that all lines are terminated in their characteristic impedance and using the travelling current waves on these matched lines. The current on the source line is assumed to be a travelling wave. The current on the observation line can then be calculated by convolving the incident field on this line with its "impulse response". The impulse response is the current on an infinitely long line when a spatial dirac impulse is applied in the middle. This results in a much faster method because no matrix inversion has to be performed and no deembedding step is needed (All lines are terminated in their  $Z_c$  so  $v^- = Z_c \cdot i$  at the ports).

For the calculation of mutual coupling between discontinuities, the discontinuities must be small compared to the wavelength and compared to the distance between them. For most circuits these assumptions are valid. Under these circumstances the component's (discontinuity) radiation behaviour can be accurately modelled by using adequately placed dipoles. This method uses far less unknowns than the method of moments. If the distances between the components become smaller or the components become bigger then the accuracy can be improved by using more dipoles. The position of the dipoles is determined by an optimisation procedure that matches the combined radiation pattern of the dipoles to that of the component. Each port of the component will generate a different radiation pattern and need a different set of dipole positions. The outgoing transmission line waves on the component for a unity incident electric field are calculated or measured and the dipole model is calibrated to give the same output. Meshed surfaces are solved with the method of moments.

The new method is considerably faster and needs far less memory than the method of moments, which is normally used when mutual coupling in a circuit is calculated. Therefore it can be used for large circuits which could never be calculated using the method of moments.

Simple circuits are calculated, proving the validity of the method.

## 36.2

### Investigation of Protection Measures against Very Steep Transients using Spice-Simulations

*Weber, T<sup>1</sup>; ter Haseborg, J L<sup>1</sup>*  
<sup>1</sup>TU-Hamburg-Harburg, Germany

There are requirements to protect sensitive electronic equipment against induced steep transients in transmission lines, e. g. traces on printed circuit boards. This may be realized by nonlinear protection circuits consisting of different stages with fast electronic components. For rise times of the transients to be suppressed smaller than 1 ns the solution of this problem is complex. Very short transients represent a threat for various sensitive electronic equipment. This becomes even more important since UWB-pulses can be created using less technical and financial capability than performing high altitude nuclear explosions (HEMP). With pulse durations (at half amplitude) smaller than 10 ns and rise-times (10% - 90%) of 1 ns and shorter, UWB-pulses cover a broad frequency spectrum. The UWB-pulse has a comparatively small energy content regarding a wide frequency spectrum, considering the higher frequencies these pulses contain significant energy. This complicates the protection. With reasonable values for an UWB-pulse of e.g. 20 kV/m at a distance of about 100 meter and an overall attenuation of about -40 dB for a system (e.g. an airplane) induced voltages in transmission lines of about 100 V are realistic. Considering the development in electronics resulting in dimension reduced designs with decreasing operating voltages this is a serious threat, which not only causes temporary disturbances or upsets, but frequently also destroys devices or electronic components. Therefore protective measures have to be considered. Protection against transients is possible using nonlinear protection circuits. In their combination nonlinear elements like spark gaps, thyristors and metal oxide varistors as well as suppressor- or Z-diodes offer an effective protection of sensitive electronic device inputs. With the design of nonlinear protection circuits comes the basic problem of uniting competitive demands, which are reliable protection, low attenuation of the source signal, impedance matching for signal frequencies, low nonlinear distortions of the source signal and non-electrical criteria (e.g. costs, weight, dimensions). The design by trial and error is unsatisfactory and it is worthwhile developing alternative

procedures. One approach to design and analyse nonlinear protection circuits for several applications is the SPICE-based procedure. The simulation of nonlinear protection circuits implies the modeling of the nonlinear components, which are not included in standard SPICE-libraries. Therefore models have been developed, which consider voltage/current-characteristics as well as frequency dependent parameters. Especially the energy absorption is an essential parameter determining the failure levels not only of the electronics to be protected, but also of the nonlinear protection elements. There has been a good agreement between measured and simulated data. The feasibility of this approach has been demonstrated for pulses in the micro-second-range, further investigation results in the nano-second-range will be presented and discussed.

## 36.3

### EM Hardness Protection Margin Probability Bounds at Different Field Levels

Mo. C<sup>1</sup>; Scott, W<sup>2</sup>

<sup>1</sup>Logicon Advanced Technology; <sup>2</sup>Defense Threat Reduction Agency, USA

Consider a given hardening technology that hardens electronics systems to provide a safety margin against an EM (electromagnetic) field of  $E_0$  kV/m with a protection probability  $p_0$ . I.e., the margin affords a probability of survival  $p(E_0) = \Pr\{T > S(E_0)\} = p_0$ . Here  $T$  is the strength threshold and  $S(E_0)$  is the  $E_0$  induced electric stress at a hardening protected system-interface where they encounter. Then, what is the protection probability  $p(E)$  against a stronger EM field  $E$ , say  $D$  ( $>0$ ) dB higher than  $E_0$ ?

Assume **linear** EM coupling to the common interface and applicability of the amplitude norm to system survival, for a class of waveforms and systems. Then at stronger field  $E$  the given hardness margin's protection probability  $p(E)$  is of course  $\leq p_0$ . The extent the protection is reduced depends on how "tight" the hardening technology had been achieved in the original protection margin in the first place. This tightness is usually quantified by a *variation* uncertainty measure, the standard deviation  $s_{T,S(E_0)}$ , abbreviated as  $s$ , of the technology's hardening strengths relative to the coupled stresses on points at the selected interface. A larger  $s$  means a more loosely controlled and inaccurately implemented hardening technology. As such, *qualitatively*, the sensitivity of protection effectiveness to EM field obviously depends on  $s$ . E.g., if the original  $p_0$  probability protection margin against field  $E_0$  was achieved quite loosely, then many units of the system exposed to  $E_0$  or many different-configuration incident on a system at  $E_0$ , must have been well over-protected. Thus, increasing the field a little makes practically no difference to the margin of protection. In the other extreme case, if the original protection  $p_0$  was achieved by a fine tuned hardening technology that accurately but barely protects a fraction  $p_0$  just up to the field level  $E_0$ , then no protection is offered to all of them at any  $E_0 + D$ .

Quantitatively, a known distribution of  $T-S(E_0)$  immediately computes the corresponding  $p(E)$ . E.g., in the case of normal distribution,  $p(E) = F(F^{-1}(p_0) - D/s)$ , a function of how many  $s$  the  $E$  lies above  $E_0$ . Here,  $F(\cdot)$  is cumulative distribution function of the standardized normal and  $F^{-1}(\cdot)$  is its inverse. If, say,  $p_0=99\%$  margin protection at  $E_0$  and  $s.d. s=4$ dB; then increasing the EM field to twice,  $D=6$ dB, results in a margin protection  $p(E) = F(F^{-1}(0.99) - 6/4) = 80\%$ .

When the distribution is *not known*, often the case in practice, we can bound the  $p(E)$  by *distribution-free bounds* with a minimum necessary information. *This note presents* the most general simple bounds based on  $p_0, s, m_{T-S(E_0)}$ , the mean of hardened strength above  $E_0$  coupled stress. One useful numerical observation is when the known information approximates, and is plausible to, either cases, the normal distribution has its  $p(E)$  near middle region allowed by the general distribution-free bounds.

## 36.4

### A Band-Rejection Filter Using Ground Through Hole-Ring Resonators

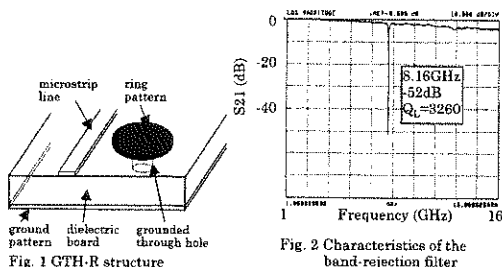
Kawasaki, F<sup>1</sup>; Ishida, H<sup>1</sup>; Kawakami, Y<sup>1</sup>

<sup>1</sup>Advanced Space Communications Res. Lab, Japan

Recently, operation frequencies of wireless communications equipment have increased higher and higher. For example, the IMT2000 system operates at 2GHz, and wireless LANs, in the 5GHz band. A band-rejection filter is necessary to eliminate the transmit signal from the receive signal in wireless communications equipment. A microwave band-rejection filter consists of resonators and a transmission line. We have investigated a novel band-rejection filter using Ground Through Hole-Ring (GTH-R) resonators, for the purpose of designing the microwave equipment over 2GHz.

The resonator is constructed with a ring pattern and a grounded through hole as shown in Fig. 1. Parasitic capacitance is both between the ring pattern and the ground pattern, and between the ring pattern and the microstrip line. The through hole acts as inductor. These capacitance and inductance form a resonator. And the band-rejection filter consists of microstrip line and some GTH-R resonators located on the side of the microstrip.

We measured many filters with different size of inner and outer ring radius. It is clarified as follows. We can design the filter, which resonates at an arbitrary frequency between four to ten GHz. High loaded Q of more than three thousands can be easily achieved as shown in Figure 2. A dual band-rejection filter was composed using the two GTH-R resonator groups with different ring radius. And the filter is easy to manufacture and set in a housing, because the rear side of the dielectric board is covered with ground plane all over.



## 36.5

### The Finite Element Method Modelling of Grounding Electrodes Transient Behaviour

Lucić, R<sup>1</sup>; Cizmic, J<sup>1</sup>; Kurtović, M<sup>1</sup>

<sup>1</sup>University of Split, Croatia

The paper presents the use of the finite element method when modelling a transient ground impedance. The use of the finite element method for electromagnetic transients simulation on single transmission line has been presented in (R. Lucić, V. Jović & M. Kurtović, EMC York 99, IEE Conference Publication No. 464, 41-46, 1999). This paper presents the results of the finite element method (FEM) investigations to evaluate the transient (impulse) impedance of horizontal buried grounding electrodes. The validity of the results have been verified with analytical solution obtained by use of the Laplace double transformation method (R. Velasquez & D. Mukhedkar, IEEE, Vol. PAS-103, No. 6, 1314-1322, June 1984).

FEM solution in time domain has been obtained from the first order system of differential equations of telegraphy. Using weighted residual method and linear combination of linear interpolation functions which represent current and voltage on finite element, system of ordinary differential equations for finite element has been obtained. Time integration has been performed by explicit/implicit mixed procedure ( $\theta$ -method) and local system of algebraic equations has been obtained. The union of all local systems of algebraic equations, obtained by the use of continuity equation for each node, gives a global system of equations. Solution of global system equations gives voltage distribution along buried conductor for each time step. Once known voltage at nodes determinates current on elements by the use of local system of equations. Knowing voltage and current, transient impedance can be obtained as the ratio of the potential at the current injection point to the current injected. Figure 2 shows some results of impulse impedance obtained by the use of FEM.

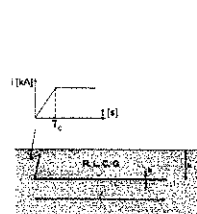


Figure 1. Current applied at the beginning of horizontal grounding electrode

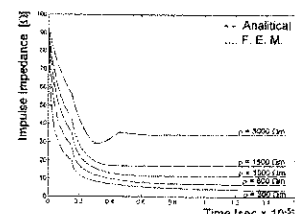


Figure 2. Impulse grounding impedance for electrode as shown on Figure 1.

## 37.1

### Scattering of Electromagnetic Waves by an Inhomogeneous Impedance Plane Beyond a Layered Media

Akduman, I<sup>1</sup>; Yapar, A<sup>1</sup>  
<sup>1</sup>Istanbul Technical University, Turkey

The scattering of electromagnetic waves from inhomogeneous boundaries has been one of the interesting research topics in the past four decades. In some special cases, i.e.: for two or three-part plane boundaries the problem has been solved through asymptotic techniques. But for more general cases, there is no analytical solution to this kind of problems. The main objective of this paper is to solve the scattering problem by an inhomogeneous impedance boundary beyond a layered media. In the problem which constitutes the subject of this work, a layered half-space is bounded by an impedance plane whose surface impedance varies in one direction and the impedance surface is illuminated from the upper part of the layered half-space by a monochromatic line source.

The problem is first reduced to the solution of two functional equations by the use of Fourier transformation and its convolution properties. The first equation is solved by iterative techniques to obtain the spectral coefficient which is required in the second equation. Then the second equation is reduced first to the solution of a system of algebraic equations and then solved numerically, which gives us the scattered field. With the method developed here one can obtain the near and far field expressions of the scattered field.

In order to see the applicability and the accuracy of the theory developed here it has been applied to some examples whose analytic solutions are given in the open literature. At the same time those problems is solved through the method of moments. The comparison of the results obtained through the method given here to those calculated by other techniques shows that the method is effective and yields very accurate results.

## 37.3

### On the Effects of Uncertainties of the earth Electrical Parameters on Fast-Transient Responses of Electrical Systems

Tesche, F M<sup>1</sup>; Kálin, A<sup>2</sup>  
<sup>1</sup>Electromagnetics Consultant, USA; <sup>2</sup>NEMP Laboratory, Switzerland

Electromagnetic coupling and interaction models used for estimating the effects of nuclear electromagnetic pulse (NEMP), high-power microwave (HPM) or ultra-wideband (UWB) environments frequently have a need to include the effects of a lossy earth. Early investigators of the earth's electrical conductivity  $\sigma$  and permittivity  $\epsilon$  have provided both measured data and curve-fit representations for these parameters. In some cases, attempts are made to insure that causality is enforced in a curve-fit solution, or that the measured data is filtered using a causal Hilbert filter.

In developing an alternative curve-fit solution to the Scott data, Messier ["The Propagation of an Electromagnetic Impulse Through Soil: Influence of Frequency Dependent Parameters, MRC-N-415, Mission Research Corp., Santa Barbara, CA, Feb. 1980] discovered that an empirical model for fitting the parameters for  $\epsilon_{eff}$  and  $\sigma_{eff}$  given by the expressions

$$\epsilon_{eff}(\omega) = \epsilon_s + \frac{\sqrt{2\sigma_s \epsilon_s}}{\omega} \quad \text{and} \quad \sigma_{eff}(\omega) = \sigma_s + \sqrt{2\sigma_s \epsilon_s} \omega$$

can be rather accurate. Moreover, these expressions can be shown to provide causal results for computed responses, and hence, they obey the Kramer-Kronig relationships. This model for the lossy earth depends only on two parameters: the high frequency dielectric constant  $\epsilon_{\infty}$ , and on the DC conductivity  $\sigma_0$  (together, of course, with the frequency.) It should be noted that these model parameters could depend on the water content of the soil as given by Scott's data.

Given a particular methodology for representing the frequency-dependent earth parameters for a wide-band electromagnetic (EM) calculation, it is apparent that there can be large uncertainties in the final values of  $\sigma$  and  $\epsilon$ . For example, many models require a knowledge of the ground water content, the value of which is uncertain. These uncertainties in the electrical parameters, in turn, lead to uncertainties in the final solution of the EM field interaction with a structure or target.

The purpose of this paper, therefore, is to provide an indication of the variations in the response of an EM coupling calculation that could arise due to uncertainties in earth parameters. After a brief review of past work by investigators into ways of representing the earth parameters (Scott, Eberic, Longmire, Wail, Messier), a simple above-ground transmission line problem is considered. The line has a length  $l = 5$  m and is at a height of  $h = 0.8$  m over a lossy earth. The first earth model is a constant parameter one with  $\epsilon_0 = 7.09$  and  $\sigma = 8.0 \times 10^{-3}$  (S/m). The second is the frequency dependent model proposed by Messier, with parameters  $\epsilon_{\infty} = 7.09$  and  $\sigma_0 = 8.0 \times 10^{-3}$  (S/m). A short-pulse EM environment, which is representative of a UWB signal, excites the line. Using standard transmission line analysis techniques, the sensitivity of the induced current on the line is studied as a function of variations in the earth parameters. Figure 1 illustrates the behavior of the induced current on the line for one particular angle of incidence ( $\psi = 45^\circ$ ) and load resistances ( $R_L = 20 \Omega$ ). Further details will be provided in the presentation.

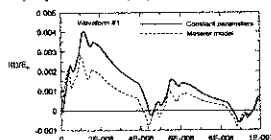


Figure 1. Plot of the induced current on a 5-meter line by an incident transient plane wave.

Work sponsored by the Swiss Defense Procurement Agency under Contract 151-186.

## 37.2

### Transient Electromagnetic Field of a Vertical Magnetic Dipole on a Two-Layer Conducting Earth

Seida, O A<sup>1</sup>; Bishay, S T<sup>2</sup>; Sami, G M<sup>1</sup>  
<sup>1</sup>Tanta University, Egypt; <sup>2</sup>Ain Shams University, Egypt

The frequency domain full wave solution for fields of a small horizontal loop, i.e. a vertical magnetic dipole, on a two-layer conducting earth's model, including the waveguide modes propagating within the earth, have been derived in an analytical form. A special attention is paid to the solution of the eigenvalue equation of the problem, where the displacement currents in the two layer ground regions are accounted for. The transient fields are expressed using Laplace transforms of the derived full wave time-harmonic solutions which leads to the fields in the frequency-domain. The frequency-domain solution is obtained as a summation of waveguide modes plus contributions from branch cuts in the complex plane of the longitudinal wave-number. The magnitude of the frequency rate of change of the vertical magnetic field due to a rectangular pulse is computed for different cases. The numerical values for the branch-cut contribution, the waveguide mode contribution as well as the overall frequency were plotted for different frequencies.

Having determined the location of the poles in the complex  $s$ -plane, the guided modes may be calculated as residues and compared with the total field. The poles are located between the branch points  $l = -ig0$  and  $l = -ig2$ . The normalized vertical magnetic field of the dipole is drawn versus the normalized frequencies, and it is found that increasing the frequency increases the waveguide mode contribution up to a certain limit, after which this contribution starts to diminish again.

The evaluation of these frequency-domain fields numerically with different frequency-dependent  $s$  and  $l$  is a diagnostic feature of the subsurface contaminants and hazardous fluid materials.

## 37.4

### A Novel Methodology for the Development of Closed-Form Electromagnetic Green's Functions in Layered Media

Cangellaris, A C<sup>1</sup>; Okhmatovskiy, V<sup>1</sup>  
<sup>1</sup>University of Illinois at Urbana-Champaign, USA

A novel methodology is presented for the development of closed-form expressions for spatial electromagnetic Green's functions in layered media. Availability and expedient numerical calculation of such Green's functions is highly desired for the modeling of electromagnetic field interactions in a variety of applications such as scattering by targets in the vicinity of a layered earth, radiation coupling to wire structures in the vicinity of layered earth, radiation coupling to interconnections in multi-layered printed circuit boards, design of integrated, planar microwave circuits and antenna arrays. A variety of methodologies have been proposed over the years for the efficient calculation of the Sommerfeld-type integrals associated with such Green's functions. Among the most popular methods, the so-called discrete complex image method (DCIM) (D. G. Fang et al, *Inst. Elect. Eng. Proc.*, vol. 135, pt. H, 297-303, Oct. 1998) appears to offer the flexibility needed for handling an arbitrary number of layers. DCIM and its variants are based on the approximation of the kernel in the Sommerfeld integrals by a sum of complex exponentials. Such an approximation is effected using, for example, the generalized pencil-of-function method (T. K. Sarkar and O. Pereira, *IEEE Antennas & Propagation Magazine*, vol. 37, 48-55, Feb. 1995). However, for this method to work effectively and accurately, the quasi-static contributions and the surface wave contributions need be extracted first from the spectral kernel.

The proposed new method does not rely on the approximation of the integral kernels by complex exponentials. In fact, the analytic form of the spectral Green's function is not needed. Thus, the extraction of the quasi-static terms and the surface wave contributions are avoided. Instead, a discrete approximation of the governing differential equation in the spectral domain is used as the vehicle for the development of a rational function approximation of the spectral form of the Green's function at all planes at which it is required. A closed-form expression of the spatial Green's function in the form of a finite sum of Hankel and modified Hankel functions of zero order is then obtained in a straightforward manner from the Hankel transform of the pole-residue representation of the aforementioned rational function approximation of the spectral Green's function. The proposed methodology is straightforward, computationally efficient, and very accurate. In order to demonstrate the validity and accuracy of the proposed method, results from its application to the calculation of electromagnetic fields due to both vertical and horizontal electric dipoles in layered media will be presented and compared with those obtained through direct integration of the Sommerfeld integrals.

## 37.5

### Time-Domain Study of Transient Fields for a Thin Circular Loop Antenna

*Bishay, S.T<sup>1</sup>; Sami, G.M<sup>1</sup>*

<sup>1</sup>*Ain Shams University, Egypt*

The transient fields, in the time-domain, of a thin circular loop antenna on a two-layer conducting earth's model are expressed in analytical form. In these expressions, the displacement currents both in the two ground layers and in the air region are taken into consideration. The closed-form expressions of the time-domain are obtained as the inverse Laplace transform of the derived full wave time-harmonic solution. These time-domain solutions are obtained as a summation of waveguide modes plus contributions from branch cuts in the complex plane of the longitudinal wave-number. Numerical examples are given to indicate the important features in the waveforms of the surface fields due to step and pulsed current excitation. These features provide means of detecting the earth's stratification, measuring the overburden height and determining the ratio of the conductivities of the layers.

## 38.1

### The Impact of Geomagnetic Storms on Electric Power Systems

*Kappenman, J<sup>1</sup>*

<sup>1</sup>*Metatech, USA*

Geomagnetic disturbances (i.e. space storms) can impact the operational reliability of transmission systems. Solar Cycle 22 (the most recent solar cycle extending from 1986-1996) demonstrated to the power industry the need to take into consideration the potential impacts of geomagnetic storms. Experience gained from the unprecedented scale of these recent storm events provides compelling evidence of a general increase in electric power system susceptibility. Important infrastructure advances have recently been put in place that provide solar wind data. This new data source along with numeric model advances allows the capability for predictive forecasts of severe storm conditions, which can be used by impacted power system operators to better prepare for and manage storm impacts.

## 38.2

### Strategy for Managing the Impact of Geomagnetically Induced Currents on the NGC Transmission System.

*Erinmez, A<sup>1</sup>*

<sup>1</sup>*National Grid Company Plc., UK*

The National Grid Company plc is the owner and operator of one of the world's largest privatised high voltage electric power transmission systems in England and Wales at 400 and 275kV. As the sole holder of the transmission licence in England and Wales it is responsible for developing an efficient and co-ordinated transmission system, operating interconnections, dispatching generation and procuring ancillary services ensuring the security of the system.

The transmission systems in mainland UK have experienced significant effects during geomagnetic storm events especially during cycles 21 and 22. These effects encompassed generator reactive power output swings, voltage dips, negative sequence alarms and attributable transformer failures. In response to these manifestations the transmission operators installed GIC monitoring and operational procedures based on global impact predictions. These measures were either only useful for forensic purposes or gave many false alarms.

Since the cycle 22 solar peak activity the UK transmission system has developed to become more meshed, heavily loaded and dependent on the availability of reactive compensation equipment for voltage control.

Since 1997 NGC has carried out GIC impact risk assessment and examined the available options for managing this risk. It concluded that an effective strategy was an operational strategy based upon managing system security and voltage. This required the availability of a local GIC forecast, GIC monitoring, a review of transmission equipment capabilities to withstand GIC conditions and operational procedures to manage the risk.

As a result NGC proceeded with the procurement of the Spacecast/Powercast forecasting and EPRI Sunburst 2000 based monitoring systems in mid 1998. These systems have been commissioned in time for solar storm cycle 23 peak activity expected to stretch to 2003.

This presentation will describe the above efforts in detail together with the risk management processes put in place.

## 38.3

### Geomagnetically Induced Currents in the Finnish High-Voltage Power System and in the Finnish Natural Gas Pipeline

*Pirjola, R<sup>1</sup>; Viljanen, A<sup>1</sup>; Pulkkinen, A<sup>1</sup>*

<sup>1</sup>*Finnish Meteorological Institute, Finland*

Space weather refers to conditions in the Earth's near-space associated with particles and electromagnetic fields which may influence the operation of space-borne and ground-based technological systems. While affected by the Sun, space weather phenomena statistically follow the eleven-year sunspot cycle. At the Earth's surface a space weather event manifests itself as a geomagnetic storm accompanied by a geoelectric field that drives "geomagnetically induced currents" (GIC) in technological systems, like electric power transmission grids, pipelines, phone cables and railway systems. In power grids, saturation of transformers may occur, which can have several harmful consequences and even result in a black-out of the whole system and in permanent damage of transformers. In pipelines, GIC may cause trouble associated with corrosion and its control. So far, Finland has not suffered from GIC problems but, due to the location at auroral latitudes, GIC are a potential risk in the country. Consequently, the phenomenon has been and is studied as a collaboration between the Finnish Meteorological Institute and the Fingrid power and Gasum pipeline companies. An active GIC research was started in Finland already at the end of the 1970's, so it already contains two sunspot cycles. In a study finished in spring 2000, we estimate the occurrence of GIC in the Finnish 400 kV and 220 kV power systems using theoretical model calculations of the geoelectric field and measured geomagnetic and GIC data. A special attention is paid to the possibility of large GIC at several transformers simultaneously since such a situation is critical regarding reactive power consumption in the system. In another study carried out in 1998 to 1999, we derived statistical probabilities of the expectable GIC and pipe-to-soil voltages in the Finnish natural gas pipeline. As expected by the theory, the largest voltages tend to occur at the ends of the pipeline making these sites risky regarding corrosion problems while sites in the middle of the pipeline do not usually suffer from large voltages.



## 38.4

### Monitoring Geomagnetically Induced Currents in the Scottish Power Grid

Clark, T<sup>1</sup>; Cumming, T<sup>2</sup>; Nicol, D<sup>2</sup>; Thomson, A<sup>1</sup>

<sup>1</sup>British Geological Survey, UK; <sup>2</sup>Scottish Power UK plc, UK

In the last two decades a number of large geomagnetic storms have been correlated with geomagnetically induced current (GIC) effects, for example, reports of gas alarms and raised harmonic content, in power transformers in the UK. With the observation of a rise in geomagnetic activity in the current solar cycle towards a peak expected in 2000 to 2003, ScottishPower plc has installed GIC monitoring equipment on three large supergrid autotransformers at three locations on their part of the British Grid System covering central and southern Scotland. The locations are at East and West Coastal sites where the effects are expected to be strongest and a central location where measurements were previously taken in 1989.

The equipment consists of a Hall Effect probe that measures the quasi DC current flowing in the neutral earth connection of the transformer, the currents flowing in the high and low voltage windings and the 400kV system voltage. A Hydran Dissolved Gas Analyser measures the amount of dissolved gases in the transformer oil which are generated as a result of discharge activity within the transformer. Both the quasi DC measurements and the dissolved gas data is available on-line at the Control Centre, while high speed recording (kHz) of the load currents, voltages, DC current and harmonics can be replayed to show the effect of GIC currents. In addition to monitoring GICs in the grid, ScottishPower is collaborating with the British Geological Survey (BGS) to monitor magnetic storms in the UK. BGS operates three geomagnetic observatories at Hartland, in the south of England, at Eskdalemuir, in the south of Scotland, and at Lerwick, in Shetland. An assessment is given here of the degree of correlation between measured currents at the ScottishPower sites and the field variations measured at the BGS observatories. A simple measure of the power in the geomagnetic field variation, namely the hourly standard deviation (HSD) in the North and Easterly components of the geomagnetic field vector, is also discussed as a useful proxy for increased GIC levels. An hourly index of variation is

an appropriate time scale for monitoring typical geomagnetic substorms. BGS has developed a robust system for communicating the HSD data for the UK at 10 minutes past the hour, every hour, to ScottishPower for routine monitoring of geomagnetic activity levels within the grid control room.

A further service provided by BGS is the provision of daily forecasts of the global level of geomagnetic activity covering the 1-3 day ahead time interval as part of the data required by ScottishPower for planning of work schedules. These forecasts are based on an ongoing assessment of the available solar, interplanetary and magnetospheric activity data, as well as the outputs from linear and non-linear predictors of geomagnetic indices. A discussion of the accuracy of these forecasts is presented.

The objective of these arrangements is to enable ScottishPower to warn system users of possible disturbances and to run the Grid System in a manner which will minimise the effects of these disturbances on the Grid System. After the event system effects can be correlated with GICs, which should also allow improvements to the forecasting and monitoring service.

## 38.5

### GIC Observations in the Norwegian Power Grid

Sæthre, E<sup>1</sup>; Ohnstad, T M<sup>1</sup>

<sup>1</sup>Statnett SF, Norway

The paper presents results of observations and measurements of GIC in the Norwegian Power Grid during February 1999 – February 2000. The work is motivated by the coming Solar Cycle 23.

The Norwegian Transmission network consists of 420kV (1645 km) and 300kV (3800 km) solid earthed system and 132kV (2635 km) of resonant earthed neutral system. The long transmission lines runs both West – East and North – South.

Statnett need to know the size of the GIC's and the influence to the Power Grid. The neutral current to earth in some of the 420 kV transformers are measured. In addition the phase currents and voltages at 420 kV are measured. Equipment used consists of a transient recorder and a Power Quality instrument. The neutral current is measured through a resistive shunt. Sampling rate of 1kHz.

GIC's are measured during the storms of 18.02.99, 01.03.99, 10.03.99, 17.04.99, 22.10.99 and 28.10.99. The figures A and B shows an example of a measured neutral current to earth on a grounded 420/300 kV, 1000 MVA transformer under the storm 01.03.99.

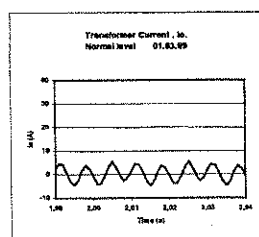


Fig.A : "Normal" current

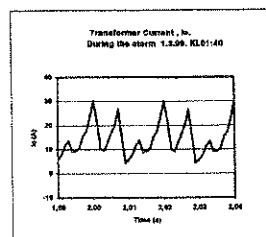


Fig.B : Current with GIC

Figure A shows the "normal" neutral current to earth, in a situation without GIC. It's a small 3<sup>rd</sup> harmonic current with no DC component. Figure B shows the transformer neutral current during the storm. The current now have a DC component of 15 A and a AC component with peak value up to 30 A and a large 5<sup>th</sup> harmonic component. Simultaneous voltage measurements shows a considerable harmonic distortion mainly due to a 5<sup>th</sup> harmonic component of 2%. During the storms the SVC's and filters on HVDC stations have been activated to prevent the voltage drop.

## 39.1

### Polarimetric Radar Interferometry: A New Sensor for Vehicle Based Mine Detection

Cloude, S<sup>1</sup>; Thornhill, C<sup>2</sup>

<sup>1</sup>Applied Electromagnetics, UK; <sup>2</sup>DERA, UK

In this paper we introduce a new type of radar sensor for vehicle based forward looking buried target detection. In this situation surface clutter is a serious problem and a key challenge is to obtain sub-clutter visibility through matched filtering. The two key features which distinguish a buried from a surface target are a slight shift of scattering phase centre and differences in the polarimetric scattering characteristics due to surface coupling. This effect is especially important for dielectric objects, where internal waves undergo internal reflection and show distinctive polarisation dependency.

The matched filter for these two features is a polarimetric interferometer (S R Cloude, K P Papathanassiou, IEEE Transactions on Geoscience and Remote Sensing, Vol 36, No. 5, pp 1551-1565, September 1998). This type of sensor deploys separated antenna arrays to achieve interferometric sensitivity to the shift in phase centres and employs a scattering matrix measurement at each array to permit polarisation filtering to suppress surface clutter. Polarimetric Interferometry is an optimum fusion of these two principles to achieve target detection in poor S/C environments.

We first summarise the main principles behind this technique then demonstrate its potential by using numerical simulations based on a finite difference time domain (FDTD) code. We then present initial experimental data as collected by DERA Malvern using their vehicle based ultra wide band (UWB) impulse radar system, developed as part of the MINDER Applied Research program. We show that the temporal stability of this system is very good and permits broad band phase processing to achieve the interferometric processing required.

## 39.2

### Polarimetric SAR Imaging of Buried Landmines

*Carin, L<sup>1</sup>; Baum, C<sup>2</sup>*

<sup>1</sup>Duke University, USA; <sup>2</sup>Air Force Research Laboratory, USA

Over the last several decades ground-penetrating radar (GPR) has been an important tool for buried-target detection and identification. In most GPR systems the antenna is placed on or near the ground, such that the buried target is generally in the near zone of the often complicated antenna pattern. Since the fields incident on the target are usually not polarized simply (especially as the target-sensor orientation varies), polarimetric processing is difficult. Alternatively, there has been recent interest in synthetic aperture radar (SAR) for buried-mine detection. Such systems offer the advantage of significant stand-off distance; moreover, since the targets are in the far zone of the source, relatively simple antenna designs can realize linearly polarized incident fields.

Given that a SAR system affords the potential for polarimetric detection of buried mines, in this paper we explore this issue by considering a special but important class of land mines. In particular, we assume that the mine and the background media can be modeled as a body of revolution (BOR). A special case of such is a BOR mine buried in a half space, with the BOR axis perpendicular to the air-ground interface. In this paper we demonstrate that the backscattered fields from such a target have zero cross polarization, and therefore this signal can in principle be used for discrimination. Moreover, we investigate the effect of the target tilt on both the co- and cross-polarized scattered fields. It is demonstrated that even a slight tilt can dramatically affect the co-polarized fields, while the cross-polarized fields remain small for modest tilts (they are zero for no tilt). However, by considering a non-BOR target (a buried cube), it is shown that, for relatively small targets, the cross-polarized fields are generally significantly smaller than their co-polarized counterparts. This undermines the utility of cross-polarization as a feature. In particular, for small targets like mines, the cross-polarized response is relatively small, even when the target is not a BOR.

## 39.4

### Ultra-Wideband Polarimetric Borehole Radar

*Sato, M<sup>1</sup>*

<sup>1</sup>Center for Northeast Asian Studies, Japan

Borehole radar is a new technology for subsurface sensing. It is used for water permeable subsurface fracture detection, geological survey and mineral exploration. Due to the high attenuation of the geological material, the radars are normally operated under 100MHz and its radar resolution is not enough in many applications. The diameter of borehole is often less than 10cm, and the restriction to antenna configuration is strict. The authors have introduced a polarimetric approach to borehole radar and showed its ability of characterizing fractures.

Borehole radar is one form of ground penetrating radar (GPR), and is ultra wide-band radar. In addition, we need a flexibility of the radar system in this study, because we have to test various kinds of antennas to control the polarization status, which have different frequency characteristics. We selected stepped frequency radar system for this purpose.

We have developed a polarimetric borehole radar system using the stepped frequency radar system due to its advantages over impulse radar systems (Miwa et al., IEEE Trans. GRS, 828-837, 1999). The radar system is composed from a vector network analyzer, an analog optical signal link with a 100m optical fiber cable and a downhole radar sonde. All the downhole equipments are powered by battery, so they are electrically isolated from a cable suspending the downhole sonde. This configuration enables an ideal radiation pattern of antennas. The frequency bandwidth of the developed analog optical link is 0.1-500MHz with a dynamic range over 70dB. The down hole R/O (RF signal to Optical signal) converters are installed in a cylindrical casing with a diameter of 20mm, which is easy to assemble inside antennas.

By using this radar system, we have conducted full-polarimetric borehole radar measurements for subsurface fracture characterization. Polarimetric signature is a common technique to

## 39.3

### Modelling of the Air-ground Interface for UWB Radar Applications

*Lostanlen, Y<sup>1</sup>; Uguen, B<sup>1</sup>; Griffiths, H<sup>2</sup>; Chassay, G<sup>1</sup>*

<sup>1</sup>IRER, France; <sup>2</sup>UCL, UK

The proposed paper will describe an analysis of the backscattering from the air-soil interface for ultrawideband (UWB) radar systems and hence, a means of modelling clutter in UWB radar systems. Understanding the phenomenology of electromagnetic interactions between very short pulses and the complex dielectric ground surface should provide an important input to the design of UWB radar systems, leading to improved clutter cancellation and detection performance. Among the existing electromagnetic analysis methods, the Time-Domain method seemed to be the best suited for UWB signals. Yet there has been very little work done on time-domain operation (although time-domain algorithms have been recently presented) or on dielectric interface response in the time domain.

In this paper we focus on the surface clutter, defined as the unwanted backscattering from the interaction of the ultra-short pulse and the air-ground interface (including the vegetation layer). Experiments have shown that this first electromagnetic interaction of the waves with objects yields a coherent clutter of high intensity (Van Kempen L. et al, Digital Signal/image Processing for mine Detection. Part 1: Airborne Approach, Mine '99, Firenze, Italy, 1999). This type of clutter strongly depends on the local roughness of the surface at high frequencies and more on the ground dielectric properties at low frequencies. We propose an electromagnetic analysis of this clutter by two methods: FDTD and Physical Optics. The first approach is a Finite difference Time Domain (FDTD) aimed at understanding the clutter degrading effects from Ultrawideband (UWB) experiments. This method is very well suited for a fine characterisation of objects embedded in a dielectric medium, but not very practical for a full characterisation of the clutter which takes into account the effects of the antenna and of the entire interface. Thus, we propose a technique based on physical optics in harmonic domain. The time domain is then obtained through a Discrete Fourier Transform of a frequency signal with a forced Hermitian Symmetry in order to obtain a real time response. One should notice that, with this last method, we do not try to get the exact response from the volume but our aim is to describe the interface return in time domain. We have presented in a previous paper the modifications that we brought to the classical algorithm (Lostanlen Y. et al., "Characterisation of clutter for ultrawideband radar", Proc. IEE Radar 99).

We use in our second approach an integral formulation which is not exactly the Helmholtz integral as in (J.A Ogilvy, "Theory of wave scattering from random rough surfaces", Adam Hilger, Bristol, 1991) but a physical optics integral which explicitly uses the electric and magnetic current density over the interface. The densities are derived from the incident field (depending on antenna features) and reflection coefficients. This gives an integral expression which is numerically evaluated.

The proposed paper will describe thoroughly the advantages and the limits of each method, emphasising their novelty and their complementarity. Some results obtained by our code will be presented and discussed with special attention given to those taking into account a genuine UWB antenna pattern that we have included in our simulations to draw a comparison of these results with real measurements.

represent the characteristics of scatterer, however it is not stable in the filed data. The ratio of energy in co- and cross-polarization reflection corresponded to other geological information of the fractures.

The radar system we have developed can be assembled to different bistatic radar configurations. We have tested surface GPR and vertical radar profiling (VRP), where antennas are set on the ground surface and in a borehole. The flexibility of the system is a great advantage in most practical field measurement.

## 39.5

**Buried Mine Detection by Polarimetric Radar Interferometry**Sagues, L<sup>1</sup>; Manuel, J<sup>2</sup>; Fortuny, J<sup>2</sup>; Fabregas, X<sup>1</sup><sup>1</sup>*Teoría del Senyal i comunicacions, Spain;* <sup>2</sup>*DFISTAS, Spain;*<sup>3</sup>*Technologies for Detection and Positioning, Italy*

During the last years, Ground-Based SAR systems have been used for different subsurface imaging applications, such as buried mine detection. It has been proved that metallic conducting mines can be detected by using an ultra-wide-band SAR system. However, buried plastic mines are near-invisible to the radar and can not be easily detected due to the weak target-background contrast and the low backscattering behaviour of the mine compared to the strong surface clutter (L. Carin, N. Geng, M. McClure, J. Sichina, L. Nguyen, "Ultra-Wide-Band Synthetic Aperture Radar for Mine-Field Detection", IEEE Antennas and Propagation Magazine, vol. 41, no. 1, pp. 18-33, February 1999).

Polarimetric SAR Interferometry is a new technique that can be used to distinguish two scatterers in height, even if one scatterer is much weaker than the other. Interferometry uses relative phase information from two SAR images to estimate the height of scattering phase centres, whereas polarimetry can distinguish between scattering behaviours. Therefore, polarimetry and Interferometry can be combined together in order to extract the height of independent scattering mechanisms that can be present in the same resolution cell. The selection of the scattering mechanisms can be based on selecting those polarization states that maximize the interferometric coherence. As a result of this process, the interferometric phase associated to these independent scattering mechanisms presents a maximum quality and the accuracy of their height estimation is very high (S.R. Cloude, K.P. Papathanassiou, "Polarimetric SAR Interferometry", IEEE Transactions on Geoscience and Remote Sensing, vol. 36, no. 5, pp. 1551-1565, September 1998).

Several multifrequency experiments were undertaken in the anechoic chamber of the European Microwave Signature Laboratory (EMSL) at JRC (Ispra) in order to test the application of this new technique to buried mine detection. Four plastic mines and a metallic cylinder

were buried below a thick layer of gravel surface. Fully coherent polarimetric data were collected at L, S, C, X band for different baselines. The experimental results show that the plastic mines can not be distinguished by using only the SAR images. However, after applying the proposed polarimetric and interferometric technique, it is possible to separate the scattering mechanism that is associated to the gravel from that corresponding to the mine, and estimate their relative height. Nevertheless, there are some zones where the false-alarm rate is too high and, therefore, some additional information should be used to reduce it. Moreover, it has also been noticed that the probability of detection has a strong dependency on the frequency range.

## 40.1

**Upgrading of the Efficiency of Small-Sized Subnanosecond Modulators**Yalandin, M I<sup>1</sup>; Oulmascoulov, M R<sup>1</sup>; Shpak, V G<sup>1</sup>; Shunailov, S A<sup>1</sup><sup>1</sup>*Institute of Electrophysics, RAS, Russia*

Compact modulators of the RADAN type have found application in high-power ultrawideband electromagnetic pulse generators and in subnanosecond coherent microwave pulse generators. The RADAN devices producing unipolar pulses of amplitude up to 150 kV and duration shorter than 1 ns are based on a circuit where the starting pulse generated by a nanosecond driver is peaked and then chopped with high-pressure gas gaps. With this method of formation of subnanosecond pulses, the output pulse amplitude is always less than that of the starting pulse, i.e., the system efficiency is low. This paper considers two methods for upgrading the efficiency of small-sized subnanosecond pulse generators: by increasing the output power of the modulator and by transforming the shape of its output pulse thereby improving the match with a shock-excited antenna.

1. Additional compression of the energy of the nanosecond driver pulse through resonance C-L-C recharging of a capacitive energy store (short pulse-forming line, SPFL) has been investigated as a means to upgrade the efficiency of an ultrawideband electromagnetic pulse generator. With this way of recharging, the voltage is doubled if the charged capacitance is low compared to the capacitance of the preceding stage. In our case, this conditions was not fulfilled. Another feature of the investigated scheme was that the charging of the SPFL occurred in the traveling wave mode within a time comparable with the risetime of the nanosecond driver pulse. Analytical calculations, a numerical simulation, and an experimental verification have shown that the generator output power can be increased by a factor of 1.8.

2. The efficiency of an ultrawideband electromagnetic pulse generator can be increased by using bipolar pulses. The spectral function of such a pulse tends to zero at low frequencies, and this is favorable to the matching of the generator with a shock-excited antenna system. This paper presents the results of experiments on

the formation of bipolar subnanosecond pulses with the use of two independent untriggered gas gaps and a converter incorporating a short pulse-forming line. The converter operates in the required way if the gas gaps operate simultaneously. Experimentally, it has been demonstrated that a 100-200-ps relative jitter of their operation can be achieved. This is sufficient to form bipolar pulses of duration 0.5-1 ns

## 40.2

### High Voltage and Nanosecond and Picosecond Small Size Generators

*Efanov, V<sup>1</sup>; Kriklenko, A<sup>1</sup>; Yarin, P<sup>1</sup>*  
<sup>1</sup>FID Technology Corp, Russia

It is developed the series of pulsers with amplitude 1-30kV. The voltage pulses can have rise time 1-2ns or 50-200ps. Pulse width can vary from 100ps to tens and hundreds nanoseconds. Pulse repetition rate can reach several tens kilohertz. The pulsers have small dimensions which are from several cubic centimeters to several cubic decimeters depending no the pulser type.

The voltage pulses have very high stability. Jitter is not larger than 10-20ps. Voltage pulses can have very small level of pre- and postpulses, not higher than several percentages.

As the major switches in the pulser there are used opening DRD switches and superpowerful picosecond closing FID switches.

## 40.3

### Characteristics of Trap-Filled GaAs Photoconductive Switches used in High Gain Pulsed Power Applications

*Islam, N E<sup>1</sup>; Schamiloglu, E<sup>1</sup>; Loubriel, G M<sup>2</sup>; Zutavern, F J<sup>2</sup>; Mar, A<sup>2</sup>*  
<sup>1</sup>University of New Mexico, USA; <sup>2</sup>Sandia National Laboratories, USA

Optically triggered, high gain GaAs photoconductive semiconductor switches (PCSS) used in pulsed power applications have been studied to characterize the effects of high concentration of deep level traps and trap sites introduced through radiation damage on the current transport mechanism. These high resistivity switches can be fabricated through many different processing techniques that involve a number of compensation processes. The devices studied were fabricated from GaAs that was grown through the Vertical Gradient and Freeze (VGF) process. The contacts were 1 mm apart. Another set of switches had diffused n<sup>+</sup> and p<sup>+</sup> layer underneath and beyond the contact length with separation between the layers of about 0.8 mm. The devices were 2.5 mm wide and had a depth of 630 μm. Experiments were performed at Sandia National Laboratories, while the simulation studies were carried out at the University of New Mexico using the SILVACO semiconductor simulation code. The GaAs PCSS used in the simulation was generated through an interface with the BLAZE module which simulates III-V semiconductor devices. The simulated I-V characteristics matched the experimental results. Our study shows that the characteristics of the PCSS, such as breakdown voltage, rise time, and turn-on delay can be affected by the impurity concentration, specifically at the deep level and through damage mechanisms such as neutron irradiation. Results indicate that the conduction mechanism is dominated by the high concentration (> 10<sup>16</sup>/cm<sup>3</sup>) of EL2 deep donor and that the breakdown characteristics improved when the device is subjected to a 1x10<sup>14</sup> (/cm<sup>2</sup>-sec) neutron flux. Simulations also elucidate the role of defect levels created as a result of neutron damage and its dominant role in the transport mechanism and breakdown characteristics during current injections through the devices.

## 40.4

### Project of Semiconductor High-Power High-Repetition Rate Compact Current/UWB Pulse Generator

*Galstjan, E<sup>1</sup>; Kazanskyi, L<sup>1</sup>*  
<sup>1</sup>Moscow Radiotechnical Institute of RAS, Russia

New concept of a compact high-current repetitive device is now under consideration in the Moscow Radiotechnical Institute in collaboration with the Pulse Technology Group of the Ioffe Physical-Technical Institute. It shall be based on using of new semiconductor switches and principally have ability of a very high repetitive rate, up to a few MHz. In the case of success, this kind of device could be a good very compact electron beam source not only for a lot of HPMW devices. Besides, the same device can be used as a new generator of high-power broadband EM pulses and as a source of X-rays.

## 41.1

### An Optical Approach to Determine the Statistical Features of the Field Distribution in Modes Stirred Reverberation Chamber

*Baranowski, S<sup>1</sup>; Kone, L<sup>1</sup>; Demoulin, B<sup>1</sup>*  
<sup>1</sup>Universite des Sciences et Technologies de Lille, France

Mode stirred reverberation chambers are suitable tools for electromagnetic compatibility measurements, especially to carry out immunity tests and radiated field measurements. Theoretical simulation of the field distribution inside these oversized cavities are today considered, in order to improve the mode stirred methods and to characterize the electromagnetic coupling phenomena introduced by the devices under test.

At high frequencies range, we can consider that the sizes of the reverberation chamber are large compared to the wavelength. In these conditions an optical approach may be used to predict the field distribution in the room. Then, the electromagnetic field at any point within the cavity may be considered as the sum of the incident wave merging from the source antenna and the multiple reflections occurring on the walls of the room. Paths and amplitude of the reflected waves are equivalent to the radiation of N shifted images of the antenna source weighted by the reflection parameters of the walls.

Due to the high conductivity of the walls, the reflection parameters are closed to one, then a too large number of images is required to reach a numerical convergence.

However, the model aimed in this paper being not to find exactly the field amplitude in the room, but rather to test the efficiency of the modes stirred methods, the proposed simulation will consist in using the statistical feature of the field distribution.

According to many authors, the field distribution provided by a perfect modes stirred method is governed by the well known chi two law (absolute amplitude of the field); a similar law is also observed for a lot of receiving points randomly spaced in the room and for short variations of the carrier frequency of the source. Consequently, the number N of images, required by the computation, are determined when the cumulative distribution function of the field amplitude becomes stationary. The use of this criteria may reduce seriously the consuming time of the computation. Details about this method will be given and illustrations proposed on few selected examples where agreement or failure with the chi two law occur.

## 41.2

### Influence of Variations in the Spectral Transfer Function to Time Domain Measurements

Garbe, H<sup>1</sup>

<sup>1</sup>University of Hannover, Germany

Generating electromagnetic fields as very fast rising (transients or ultra wide band signals) it is often seen, that the measured field pulse is different to the output signal of the generator. Within this presentation reasons are discussed. Therefore the behaviour of the test facility will be described in frequency and time domain. The main goal is to show the links between them.

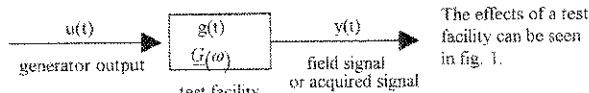


Figure 1: General signal transformation

is given by  $y(t) = \int_0^{\infty} u(t-\tau)g(\tau)d\tau = g(t)*u(t)$  or in the frequency domain as

$Y(\omega) = U(\omega) \cdot G(\omega)$ . The functions  $g(t)$  or  $G(\omega)$  may stand for the behaviour of an amplifier, a test site or a sensor system. The ideal transfer function  $G(\omega)$  should be  $|G(\omega)| = 1$  and  $\arg(G(\omega)) = \omega \cdot T_0$  for the whole frequency range.

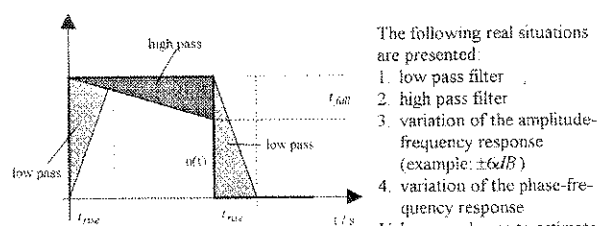


Fig. 2: Principle effects or frequency limitations to a rectangular pulse

The following real situations are presented:

1. low pass filter
2. high pass filter
3. variation of the amplitude-frequency response (example:  $\pm 6\text{dB}$ )
4. variation of the phase-frequency response

Values are shown to estimate the time domain behaviour from given frequency data.

$t_{rise}$  or  $t_{fall}$  in figure can be approximated by the equation  $t_{rise} = \frac{\pi}{f_0}$ . A variation of less than 2 dB in amplitude or 20° in phase results in a variation of 10% for the pulse. The analytical justification will be presented.

## 41.5

### Time-Domain Coupling Responses for Crossing Transmission Lines

Kami, Yoshio<sup>1</sup>

<sup>1</sup>The University of Electro-Communications, Japan

**Introduction** A model of two transmission lines of different height crossing each other is seen in various line systems such as communication lines, power lines, multilayer printed circuit boards, etc. In digital circuit boards, crosstalk is a serious topic according as working voltage becomes low. Coupling or crosstalk between two transmission lines of finite length crossing at right angles is investigated in time domain. The time-domain coupling voltages are measured under some conditions and then the coupling mechanism are studied from the experimental results.

**Models and Experimental Results** We consider a system of two transmission lines crossing each other at right angles; two thin wire lines are set at different heights above a ground plane of aluminum. Two lines are assumed to be inherently of transverse electromagnetic (TEM) mode. The coupling of non-parallel transmission lines has been studied on a basis of circuit concept [1]. There are essentially two coupling mechanism, i.e., electric- and magnetic-field couplings caused by TEM fields and those by currents on risers supporting the wire line of finite-length transmission line.

In our model, the magnetic-field component of TEM mode do not link the other line since the transmission lines are set at right angles. The electric-field interaction still remains though. In frequency domain, induced voltages are mainly caused by the magnetic field at a relative low frequency region. On the contrary, the electric-field contribution gradually becomes more major according as frequency increases. This means that the electric field component may work seriously for our model. To discuss the coupling mechanism in time domain, one transmission line (exciter line) is fed by a step-voltage source of rise time of about 45 pico seconds. Terminal voltage responses of the other transmission line (acceptor line) are measured with a digitizing oscilloscope of 12 GHz bandwidth and 50-ohm internal load. To observe the waveform corresponding to the step voltage used here, its frequency-domain components should be taken

## 41.4

### FDTD Computation Modeling for Electromagnetic Fields due to Electrostatic Discharge between Charged Metals

Fujiwara, O<sup>1</sup>

<sup>1</sup>Nagoya Institute of Technology, Japan

#### Introduction

The electromagnetic fields due to electrostatic discharge (ESD) between charged metals have wide-band frequency spectra up to the microwave region, which often give a fatal shock to high-tech information devices. Such electromagnetic interference is known to be significantly affected by the metals, whereas the effect is not being well understood. In this paper, a FDTD (finite-difference time-domain) modeling was investigated to compute the ESD fields in conjunction with a spark current and a spark voltage both theoretically derived from the Rompe-Weizel spark-resistance formula. The effect of the metal on the ESD fields was numerically examined with respect to their size. Comparison was made between the FDTD computation and the analysis based on the previously proposed dipole model. A simple experiment by the spark between metal balls was also conducted to validate the computation modeling.

#### Computation Modeling and Results

We considered a spark model between two spherical metals being spaced at a gap. The FDTD method was used to compute the electromagnetic fields due to the spark between the metal spheres. Three types of gap excitation were investigated to differentiate the ESD fields for the FDTD computation algorithm. The excitation sources were a spark current or a spark voltage that was obtained in a closed form from the Rompe-Weizel formula for a spark resistance, and the resultant electromagnetic fields around the spark channel. The computation results showed that the metal spheres enhance the ESD field level according to their size. In order to confirm the finding, we calculated the field level from an ESD source model based on the previously proposed dipole model, which consists of numberless pairs of image dipoles that give the equipotential condition on the spherical metal surface. Also for the experimental validation, we measured with a shielded loop probe connected to a wide-band digital oscilloscope the magnetic field waveform due to the spark between metal balls having several sizes.

#### Conclusion

To compute the ESD fields due to the charged metals, we have shown a FDTD computation modeling combined with the Rompe-Weizel formula for the spark resistance. The validity for the computational modeling has been confirmed by wide-band measurement of the magnetic field waveform due to a spark between metal balls.

into account up to 7 GHz, of which condition is enough for the oscilloscope. The rise time of 45 pico seconds also corresponds to the distance resolution of about 14 mm. To study the roll of the risers in time domain, the voltages are also measured under various conditions. The results show that the risers seem receiving antennas for the acceptor line and transmitter antennas for the exciter line, equivalently.

**Conclusion** The time-domain responses of the transmission lines crossing over at right angles are studied experimentally. The coupling mechanism can be interpreted through the experimental results for various terminal conditions.

**References**[1] Y. Kami and W. Liu, Proc. IEEE Intn. Symp. EMC., Aug. 1998.

## 42.1

### Forecasting Magnetic Storms and Substorms with Artificial Neural Networks

*Gleisner, H'*

*<sup>1</sup>Lund University, Sweden*

Since 1998, the solar wind is continuously monitored by the space probe ACE located 1.5 million kilometers upstream in the solar wind. The data received from ACE give us an early warning of arriving solar-wind disturbances up to an hour ahead. With solar-wind data continuously available in real time, short-term forecasting of geomagnetic activity has become a reality and the last few years have witnessed a rapid development of new forecast methods. The special requirements of real-time operation - rapid processing and ability to handle lossy, real-world data - have focused much interest on artificial neural networks (ANN).

This paper describes the present status of short-term geomagnetic activity forecasting using ANNs that operate on a stream of real-time solar-wind data. It is shown that the onset and development of magnetic storms can be accurately predicted. The most important source of geomagnetic disturbances at mid-latitudes can thus be forecasted an hour ahead, and under certain circumstances several hours ahead. The magnetic storm is always accompanied by a sequence of magnetic substorms that constitute the dominating source of magnetic disturbances at higher latitudes, and that are a major cause of induced currents in the ground and in technological systems. It is shown that substorms can be predicted, but that all substorm features are not equally well predicted. Differences between predictions and observations are discussed for the most important features of magnetic storms and substorms, and the fundamental role played by the temporal resolution is pointed out. Aspects of ANN architecture, data preconditioning, and network training and evaluation are discussed. A distinction is made between forecasts of geomagnetic indices that describe the global level of geomagnetic disturbance, and forecasts of geographically local geomagnetic variations. Finally, the use of solar observations to make longer-term - three days ahead and 27 days ahead - forecasts is briefly outlined.

## 42.3

### Modelling Geomagnetically Induced Electric Fields Across the UK

*Beamish, D'*

*<sup>1</sup>British Geological Survey, UK*

Calculations performed to assess geomagnetically induced currents (GIC) in power grids and pipelines typically require estimates of the surface electric field (E). A geomagnetic variation field of given frequency is taken as an external source and Maxwell's equations are used to calculate the E-field distribution within an appropriate, but finite, volume of the Earth. To perform the calculation, the resistivity distribution within the same volume must be estimated. Such earth science information provides the link between solar-terrestrial phenomena and technological systems.

In terms of GIC amplitudes, the highest source frequencies pose the greatest risk. Variation periods of 10 and 30 minutes are considered here. The periods used define the electrical scale lengths for both the earth science and electromagnetic problems. The vertical scale sensitivity of the E-field response extends to depths in excess of 100 km. The British Isles have a distinct resistivity structure and are surrounded by shelf-seas. The development of a 'national-scale' resistivity model is a non-trivial exercise and simplification is required. For the UK problem, the resistivity model was specified over an area of 1100 x 1200 km using six major tectonic terranes both onshore and offshore. Three vertical zones, each 10 km thick, were used to define crustal material. At depths between 30 and 1000 km it is more appropriate, due to lack of information, to adopt a regionally representative 1D model.

3D finite-difference EM modelling (restricted to plane-wave sources) has been used to estimate surface electric fields across the UK resistivity model. No single set of cell constructions can accommodate both skin-depth and scale requirements for the model without become unwieldy. A 20 x 20 km lateral grid model was developed for the initial evaluations described here. The shelf-seas had to be assigned a resistivity of 4 ohm.m (c.f. 0.25 ohm.m) due to algorithm restrictions.

## 42.2

### The Enhancement Near Oceanic Boundaries of Electric Fields from Geomagnetic Disturbances

*Gilbert, J'*

*<sup>1</sup>Metatech Corporation, USA*

The presence of oceans can substantially modify the horizontal electric fields associated with geomagnetic disturbances. The horizontal electric field is, of course, lowered at the surface of the ocean, but the component of this field perpendicular to the interface can be substantially enhanced on the landward side. This enhancement occurs for situations where the electromagnetic skin depth in the ground is much deeper than the ocean depth - on the ocean side, much of the horizontal conduction current flows in the ocean where the electrical conductivity is many orders of magnitude greater than in the ground. Near the boundary this current redistributes itself, flowing down to depths on the order of a skin depth in the ground. In this region the electric field on the landward side is enhanced.

This paper discusses this enhancement using analytic and numerical solutions of an integral equation for the horizontal electric field for different ocean depth profiles. The kernel of the integral equation is a modified Bessel function and singular, but the singularity is integrable and well suited for numerical solution. The integral of the electric field along a line running from the far to the landward side terminating at the edge of the ocean has a surprisingly simple limiting form for cases of interest - the increase in voltage (above that which would be calculated for a uniform ground) has the same time history as the geomagnetic field perturbation. This contrasts with the horizontal electric field far from the edge of the ocean whose time history is the half-derivative of the geomagnetic field.

The 3D modelling results indicate the extent to which 1D resistivity models for the UK problem are unrealistic. When lateral resistivity gradients are considered, excess currents are generated which provide a redistribution of the amplitude and phase of the surface electric fields. The coastal seawater resistivity contrast is particularly significant to the UK problem. Onshore enhancements by factors of between 2 and 4 in the induced electric field are a pervasive feature.

## 42.4

**The Evaluation of Ground Conductivity Profiles for the Purpose of Calculating Ground Induced Currents from Geomagnetic Storms**  
*Radasky, W<sup>1</sup>; Smith, K<sup>1</sup>; Kappenman, J<sup>1</sup>*  
<sup>1</sup>Metatech Corporation, USA

The process of computing the quasi-dc currents induced in long power or other types of conductors is a complicated one. The physics begins with the charged particles generated by the sun and intercepted by the Earth. During a geomagnetic storm, currents will be induced in the Earth's ionosphere, which in turn create the magnetic fields of interest to Earth-bound systems. These magnetic field fluctuations induce electric fields in the Earth which couple through grounded portions of long-line systems. It is well understood that the magnitudes of these electric fields are strongly dependent on the conductivity of the crust and mantle below.

This paper will examine the interaction between different types of storm-produced magnetic field waveforms with the types of ground conductivity profiles that have been established through independent means. Waveform features such as rise time and pulse width are examined to illustrate their importance relative to different types of ground conductivity profiles known throughout the world.

Another factor to be examined in this paper is the role of the type of analysis performed and the time resolution available for measured and forecasted magnetic field waveforms. This aspect is important since the "exact" solution of the coupling problem can be fairly complex, but in many cases, less precise methods may provide a sufficient accuracy considering the uncertainties present in other parts of the problem. While this point will be presented from an analysis point of view, examples are shown which demonstrate the validity of the basic analysis methods with regard to measured data.

## 43.2

**Electromagnetics of Transients in Dispersive Media-Exactly Solvable Time Domain Model**  
*Shvartsburg, A B<sup>1</sup>*  
<sup>1</sup>Russian Academy of Sciences, Russia

The first exactly solvable models of interactions of ultrashort single-cycle pulses, containing only one or few oscillations of EM field, with conductors, dielectrics and transmission lines are presented. These models are based on new exact analytical solutions of Maxwell equations for dispersive media, obtained directly in the time domain, beyond of the scope of Fourier transforms and without the traditional presentation of solutions in terms of products of time- and coordinate- dependent factors (non-separable solutions) (A.B. Shvartsburg, "Impulse Time Domain Electromagnetics of Continuous Media", Birkhauser, Boston, 1999). Generation of different transient orthonormal waveforms due to scattering of the fixed waveform on the target, buried inside the conducting medium (transient "ringing"), is considered subject to the pulse shape, it's characteristic time and EM field relaxation time of the medium.

The physical fundamentals and mathematical basis of the following problems are considered:

1. Using of orthonormal basis, built from the linear combinations of Laguerre functions, for flexible presentation of non-sinusoidal waveforms, irradiated by wideband source.
2. Dynamics of non-stationary unharmonic EM fields in dielectrics and conductors, visualized by means of non-separable time domain solutions of Maxwell equations.
3. Shape- and polarization-dependent instantaneous reflection of single-cycle pulses from dielectrics and conductors (time domain generalization of Fresnel formulae).
4. Transient "ringing" of inhomogeneous dielectrics.
5. Shock excitement of transmission lines (TL) and non-stationary propagation of single-cycle waveforms along TL.

Applications of these results to the problems of underground communication, buried targets identification and optimized regimes of impulse energy transfer through continuous media are considered.

## 43.1

**The Signal Processing of the UWB on the Radio Fuze**  
*Huang, J S<sup>1</sup>; Lui, F<sup>1</sup>; Deng, Q<sup>1</sup>*  
<sup>1</sup>Beijing Research Inst. of Special Elect. Tech, China

### Abstracts

Many experimental investigations for the effects of different power UWB electromagnetic pulse with the duration of several ns and the band from several hundred megahertz to near thousand megahertz on the radio fuze are carried out in order to determine the threshold of trig power density. The signal of UWB electromagnetic fields on the radio fuze is recorded by high sample oscilloscope. The time domain signals and the frequency domain signals such as the frequency spectrums and the power spectrums are processed by a computer software. The results show that the amplitude  $V_{20}$  of the signal is very large and the threshold power density to trig the fuze is  $42.4 \text{ kW/m}^2$ . Fig. 1 and Fig. 2. are the typical results.

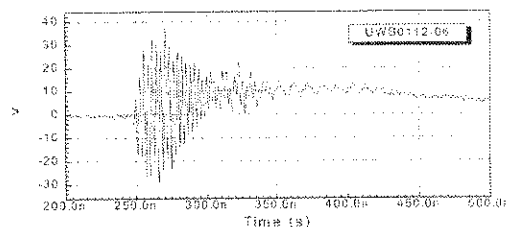


Fig. 1 The waveform of the high frequency of fuze when radiated by UWB

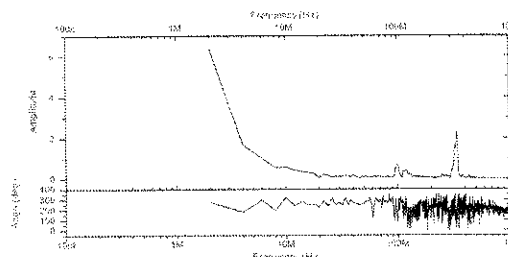


Fig. 2 The spectrum of the high frequency of fuze when radiated by UWB



## 43.3

### Simulation of the Transient Response of Objects Buried in Dispersive Media

González García, S<sup>1</sup>; Hernández-López, M A<sup>2</sup>; Bretones, A R<sup>1</sup>; Martín, R G<sup>1</sup>

<sup>1</sup>Universidad de Granada, Spain; <sup>2</sup>Universidad de Salamanca, Spain

The study of the response of dispersive media excited by a transient electromagnetic signal is of interest in areas such as the simulation of Ground Penetrating Radar, the stimulation of biological tissues and the analysis of broadband communications.

In this paper the hybrid technique combining Finite Difference Time Domain (FDTD) and the method of moments in time domain (MoMTD), described in [1], has been extended to study the transient response of objects buried in dispersive layered media.

The hybrid FDTD-MoMTD method allows the simulation of inhomogeneous problems excited by complex sources, such as wire antennas, which are not easily dealt with alone by FDTD. The fields created by these sources are computed with more suitable methods, such as the MoMTD, and coupled to the FDTD algorithm, which can properly simulate the inhomogeneous part of the problem. This coupling is carried out obtaining the magnetic and electric equivalent sources from the tangential components of the electric and magnetic fields on the surfaces of a Huygens box, which in turn are used as current sources in the FDTD algorithm.

The FDTD code here employed uses a graded mesh non-uniform algorithm to deal with the first order dispersive (Debye) characteristic of the ground, through the convolution method described in [2]. The behaviour of different absorbing boundary conditions has been investigated.

To this end, an ideal hertzian dipole, placed in a homogeneous media above a dispersive ground, has been chosen as the excitation source. This allows us to place the equivalent currents on the Huygens surface straightforwardly in the FDTD zone, using the known closed-form expression of the fields created by the dipole, without any further computation.

Numerical experiments have been carried out, comparing the results when the electromagnetic characteristics of buried objects, and those of the ground that contains them, are varied.

[1] A. Rubio Bretones, R. Mittra and R. Gómez Martín, "A Hybrid Technique Combining the Method of Moments in the Time Domain and FDTD," *IEEE Microwave and Guided Wave Letters*; vol. 8, no. 8, August 1998, pp.281-283. [2] K. S. Kunz and R. J. Luebbers, "The Finite Difference Time Domain Method for Electromagnetics," Boca Raton, FL, CRC Press., 1993.

## 43.4

### Electromagnetic Transient Modelling using Dynamic Adaptive Frequency Sampling

McCowen, A<sup>1</sup>; Tham, C Y<sup>1</sup>; Towers, M S<sup>1</sup>; Poljak, D<sup>2</sup>

<sup>1</sup>University of Wales Swansea, UK; <sup>2</sup>University of Split, Croatia

Transient modelling via the frequency domain is invariably implemented by the FFT technique. It has been demonstrated that this technique when used on a highly resonant structure failed to give correct result (Tesche *et al.*, *EMC Analysis Methods & Computational Models*, Wiley & Sons, 342 - 345, 1997). Even with a less resonant structure the technique relies on empirical insight to select a suitable frequency sampling interval  $\Delta f$  to yield successful result (Tijhuis *et al.*, *IEEE Trans. Antennas Propagat.*, 1132 - 1146, Oct. 1992). Another disadvantage of the technique is the necessity to set the time step  $\Delta t$  several times smaller than what the sampling theorem dictates (*ibid.*) thus increasing computational demand.

In this paper a new systematic and objective technique is proposed. First the paper identifies the problem highlighted by Tesche as due to insufficient resolution of the frequency samples. The main difficulty in frequency domain modelling of highly resonant structure is to characterise its spectrum accurately by selecting suitable values for the frequency resolution and the number of samples. This requires insight of the structure's behaviour which are not available at the beginning. Moreover a high Q spectrum requires high resolution samples which if taken at uniformly spaced intervals as required by the conventional FFT technique is computationally expensive.

Using a resonant structure example of a dipole and a parasitic wire over a ground plane, a dynamic adaptive sampling algorithm is formulated and used on frequency domain data generated as solution to the EFIE via the method of moments. The algorithm takes samples of the spectrum at non-uniformly spaced intervals according to the requirement at different points. The algorithm is based on the method of adaptive integration for unknown functions. However, unlike the standard method the criterion for convergence limit uses the difference of two successively computed integration values express as a ratio of the last. Numerical experiment is carried out to find the optimum value for the criterion. This optimum criterion can be applied universally and does not require further experiment for other similar structures. A modified inverse DFT formula with the numerical accuracy of trapezoidal rule integration is used to process the data. The formula takes into account the different weighting of the samples and uses a new way to calculate the associated phase displacements. This new technique substantially improves the computational efficiency of frequency domain transient analysis. The number of frequency samples required to obtain accurate result can be reduced to less than 10% of that for the conventional FFT technique. For the example considered it is estimated that the new technique requires only about 26 minutes of computer time compares to over 5 hours required by the FFT technique.

## 43.5

### The Time Domain Numerical Calculation of an Integro-Differential Volterra Equation for Ultrashort Electromagnetic Pulse Propagation in Layered Media

Sherbatko, I<sup>1</sup>; Iezekiel, S<sup>1</sup>; Nerukh, A<sup>2</sup>

<sup>1</sup>The University of Leeds, UK; <sup>2</sup>Kharkov Techn. Univ of Radio Electronics, Ukraine

Problems for spatial-time-varying parameters are of interest for the purpose of investigation of an electromagnetic wave and pulse propagation as in the ionosphere, for remote sensing of transient objects by ultrashort electromagnetic pulses, as well as for optical signal processing and terahertz intravision. The necessity of considering such problems stems from the investigation of ultrafast electromagnetic transients in a complex media. An evolutionary algorithm for the direct numerical calculation of EM wave and ultrashort pulse propagation in dielectric and semiconductor layered medium is presented.

The continuous and pulsed EM field evolution is described by the time domain two-dimension integro-differential Volterra equation of the second kind, that corresponds to the integral Maxwell equation in time-domain. The exact analytical solutions of such equations can be derived by resolvent method only for a few special cases. The numerical algorithm is more general and based on the marching scheme in time and space. Proposed numerical scheme of this equation does not impose restrictions on the signal shape and duration as well as on time behaviour of medium parameters. It is shown, that improving of the integration procedure by implementing of subgrid into scheme leads to increasing of stability and precision of the previously developed algorithm.

The numerical calculations have been justified by known exact analytical solutions for the case of normal propagation in layered media. The influence of spatial distribution of permittivity and conductivity as well as relation between pulse width and depth of layer on stability and precision of the proposed scheme are discussed.

## 44.1

### Electromagnetic Noise Emission of Industrial Pulse Power Equipment for Material Treatment

Wollenberg, Ing G<sup>1</sup>; Luhn, F<sup>1</sup>; Zange, R<sup>1</sup>; Scheibe, H P<sup>1</sup>; Schätzing, W<sup>1</sup>  
<sup>1</sup>Otto von Guericke University Magdeburg, Germany

In the industrial field pulse power equipment is used for a wide range of applications, as there are electromagnetic workpiece deformation (magnetic forming), material disintegration by impulsive sound, or test purposes. In view of EMC those processes are characterized by a strong emission of transient electromagnetic noise, which may arise as a single event or as events with a very low repetition rate.

Here the electromagnetic emission of industrial pulse power equipment will be discussed by means of magnetic forming. Figure 1 shows the equivalent circuit diagram of the equipment. For processing a conductive workpiece is inserted into the coil arrangement, and the high voltage capacitor is discharged over a spark gap and the coil. The workpiece is deformed by the Lorentz forces resulting from the induced eddy currents. The resonant circuit formed by the capacitor and the coil leads to a damped middle-frequency oscillation of the process current.

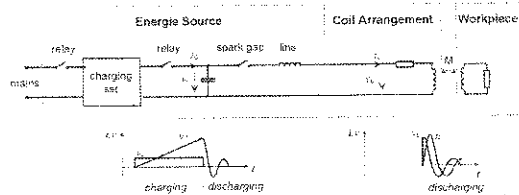
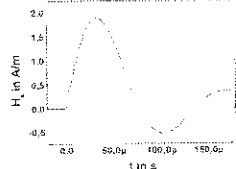


Figure 1: Equivalent circuit diagram of an arrangement for magnetic forming.

During the discharge phase the process current yields a strong middle-frequency magnetic field in the vicinity of the coil (figure 2). Additionally the ignition of the spark gap causes a transient broadband field. The disturbance voltage at the mains connection is predominantly generated by the relay control.



The phenomena will be discussed by means of measurement results.

Figure 2: Magnetic field strength in a distance of 3m from the coil.

## 44.2

### 100kV Picosecond All Solid State Generator

Efanov, V<sup>1</sup>; Kriklenko, A<sup>1</sup>; Yarin, P<sup>1</sup>  
<sup>1</sup>FID Technology Corp, Russia

It is developed a pulser with a maximal amplitude 100kV. Rise time is about 200ps, pulse width at half maximum is 1ns. Maximal pulse repetition rate is 1kHz. Power supply 220/110V AC. The dimensions are 300x300x180mm.

The pulser is implemented with a use of super powerful nanosecond opening switches - Drift Recovery Diodes (DRD) and super powerful picosecond closing switches - Fast Ionization Devices (FID). Voltage pulses are very stable. Jitter is not larger than 20ps. The pulser is capable to operate with load 50 Ohm. The pulser has an internal triggering and also can operate with an external triggering.

## 44.3

### Ferro-Electric

#### A Test Chamber for a Ferrite-Triggered Gas Switch

Farr, E<sup>1</sup>; Elizondo, J<sup>2</sup>; Lehr, P<sup>2</sup>; Baum, C<sup>2</sup>  
<sup>1</sup>Farr Research Inc, USA; <sup>2</sup>Electromagnetic Technologies Corp., USA; <sup>3</sup>Air Force Research Laboratory, USA

We consider here a test chamber for determining the output of a gas switch. This test chamber is being used to experiment with a new switch called the ferratron, which provides a high-voltage output at low jitter and fast repetition rate (L. H. Bowen, et al, Switching Note 29, 1999).

The test chamber is designed to launch a fast-risetime wave into an electrically large coaxial structure. The transition from gas to oil is accomplished with a polyethylene lens with one surface being a hyperbola of revolution. Since the output coax is electrically large, optical methods are required in order to maintain a planar phase front.

We will also review some of the early results of the ferratron that have been demonstrated to date. The ferratron is a novel application of ferroelectric ceramics combined with a gas flow scheme that provides reliable triggering at high repetition rates. The design can be interpreted as an active trigatron-like switch, where the ferroelectric ceramic behaves as an electron/corona source and the trigger configuration is that of a simple trigatron, with the advantage that the trigger voltages are not as high as the gap voltage.

The trigger system is integrated into a fast gas flow switch chamber design. The switch chamber is tailored to reduce field stresses and to provide a low inductance current path with a very compact geometry. The high gas flow allows the replacement of the gas in the discharge region on a time scale necessary to sustain the required repetition rate (100 Hz to 1 kHz).

The ferratron has been successfully operated during preliminary tests using nitrogen at low pressure. The jitter was found to be less than 70ps at a rep rate of 1 Hz. The rise time was on the order of 500ps. Higher rep rates, faster rise times, and higher voltages will be attained as testing and development continue.

→ Ferratron

- Polar material (ceramic), example LTZ  
 - Potentially flipped with applic. of trigger voltage (slow voltage)

Trigatron - Ferratron Mode tested

↓  
 less jitter

## 44.4

*www.dvtechs.com*

### Compact, Solid State Pulse Modulators High Power Microwave Applications

Gaudreau, Marcel P. J<sup>1</sup>; Casey, Jeffrey<sup>1</sup>; Mulvaney, J. Michael<sup>1</sup>; Kempkes, Michael A<sup>1</sup>

<sup>1</sup>Diversified Technologies Inc, USA

Diversified Technologies, Inc. (DTI) has developed and patented a line of versatile, high voltage, high power solid state modulators which have the potential to significantly increase the performance and efficiency of commercial accelerator systems. DTI has developed and demonstrated a new approach to solid state switching, which provides orders of magnitude improvements over current modulator designs, at high efficiency. DTI's solid state modulators utilize a patented approach to combining low voltage elements, such as IGBT and FETs, to reach voltages of 5 to 200 kV, and peak currents from 30 A to 5000 A. DTI's modular approach to manufacturing of these systems allows construction of modulators which ideally meet the requirements of a wide range of commercial accelerators, at cost levels which are competitive with conventional modulator designs.

DTI's modulators are capable of driving a wide range of microwave sources, including magnetrons, klystrons, and TWTs. A 70 MW (peak) modulator, capable of operating at up to 140 kV, 500 A, has recently been commissioned at CPI in Palo Alto, CA. CPI is using this modulator specifically to condition and test many of the RF sources used high power microwave systems. This unit is based on the same core technology used throughout DTI's line of solid state, pulsed power systems. DTI has also built a high efficiency radar modulator for the U.S. Navy which has been demonstrated at 400 kHz.

DTI's solid state modulators, alone or in combination with pulse transformers, completely eliminate the need for thyatrons, PFNs, or switch tubes in HPEM systems - significantly enhancing the overall reliability and stability of these systems. Solid state modulators provide previously unattainable flexibility in pulsewidth and pulse repetition frequency - opening completely new regimes of accelerator performance. Due to their submicrosecond switch times, DTI has demonstrated that crowbar systems for microwave tube

protection are unnecessary in combination with these solid state modulators.

DTI's ongoing RD efforts are focused on three primary areas: increasing peak power, increasing both speed, and cost reduction. These efforts, funded by the U.S. Department of Energy, Department of Defense, and DTI's commercial partners, are opening new regimes of HPEM performance to the advantages of solid state technology. These RD efforts include development of very high voltage (200 - 500 kV) solid state hard switches at high power (250 MW peak), and development of very fast (500 kHz - MHz) pulsed power systems with switching times in the 10's of nanoseconds.

In this paper, DTI will describe the basic modulator design, and present performance results from both systems currently in operation and our RD efforts addressing voltage, peak power, pulse frequency, pulse stability, and efficiency of solid state modulators for HPEM systems.

*10-500ns risetime, 22kV, 80A(?)*

*fails short (like diode)*

$$\frac{dI}{dt} \approx \frac{100 \text{ A}}{50 \text{ ns}} = 2 \text{ kA}/\mu\text{s}$$

*2-3000 \$/kV, fastest IGBT ~ 10ns*

## 45.1

*WSA*

### A Waveguide-Slotted-Array Antenna for HPM Transmission

Coburn, W<sup>1</sup>; Litz, M<sup>1</sup>; Miletta, J<sup>1</sup>; Tesny, N<sup>1</sup>

<sup>1</sup>U.S. Army Research Laboratory, USA - Directed Energy Division

Directive antennas are required for the development of high-power microwave (HPM) transmission systems for mobile applications. The type of system considered includes a single HPM source with waveguide output, the antenna and the control/support equipment integrated onto a ground-mobile platform. The Army Research Laboratory (ARL) is exploring technologies in each of these areas in order to investigate HPM concepts for future Army applications. In particular, the relativistic klystron (or "Reltron") microwave tube represents a compact, lightweight, frequency-tunable HPM source. A parabolic reflector with a custom-designed horn-feed is one antenna option that allows direct connection to the HPM source waveguide output. A concept demonstration system, implemented on a ground-mobile vehicle, includes a cylindrical waveguide slip-joint to allow mechanical rotation in azimuth (AZ) and flexible rectangular waveguide ("flex-guide") for limited elevation (EL) control.

Because of size considerations, an alternative approach to reflector antennas is desired, so waveguide-slotted-array (WSA) antennas have been investigated. Large arrays of identical row waveguide are attractive to minimize cost and complexity in the antenna design, fabrication, and assembly. The evaluation process selected the longitudinal (shunt) slot, resonant array with Chebyshev (cosine-squared, "on-a-pedestal") taper to meet the operational requirements. The WSA design is modular (with four symmetric modules) for ease of fabrication and to maximize transportability and reparability. A rectangular waveguide corporate feed network is used to minimize the antenna subsystem volume (i.e., depth). The Reltron is integrated into the WSA feed structure so that the HPM source and antenna can be mounted on a gimbal base for mechanical pointing.

The WSA modules and corporate feed are fabricated out of WR-284 (S-band) copper waveguide with brass endcaps and 80-mil wall

thickness to a tolerance of  $\pm 5$  mils. The array design, fabrication, assembly, and testing are discussed. Preliminary test data for a single module and the four-module WSA are presented. Analytical results for an idealized array are in qualitative agreement with the measured data. The WSA has the expected performance of a broadside array, except resonance is shifted from the design frequency believed to be due to perturbation of the slot conductance associated with the waveguide finite wall thickness. The radiation pattern is somewhat more complex than predicted and includes scattering effects from the array edges. The results indicate that the WSA design should include tunable elements to empirically optimize the performance of the as-fabricated array.

*S-Band WR-284*

*a magic-tee to split power*

## 46.1

### Progress in Ultrawideband Short Range Radar Detection of Buried Mines

*Daniels, D<sup>1</sup>; Phillipakis, M<sup>1</sup>; Martel, C<sup>1</sup>*  
<sup>1</sup>ERA Technology, UK

The paper will describe recent work that has been carried on the radar detection of buried mines. Three areas of work have been addressed,

1) Optimisation of loaded quasi-TEM horn antennas. This work has concentrated on the modelling and characterisation of a novel TEM horn composed of a set of radiating loaded fingers. The design has resulted in a very lightweight structure with low timesidelobes. Both the results of the modelled characterisation and the prototype antennas will be presented

2) Investigation of the parameters of sparse arrays and their effect on system performance. Earlier work has shown that for antennas spaced up to 150mm from the ground surface the spatial density of the measurements is a important factor in image quality. The practical issues associated with closely spaced antennas elements has a direct relationship to both image quality and probability of detection for a given size of mine. The paper will discuss this issue and present the results from recent measurements

3) Methods of signal processing and data fusion. Very often the performance of particular radar systems is significantly affected by the type of signal processing as much as by the basic sensor. The paper will consider methods of processing radar data using a basic spatial gradient operator.

## 46.3

### Cost-efficient Surface Penetrating Radar Device for Humanitarian Demining

*Ratcliffe, J A<sup>1</sup>; Sachs, J<sup>2</sup>; Peyerl, P<sup>3</sup>; Cloude, S<sup>4</sup>; Crisp, G N<sup>5</sup>; Sahli, H<sup>5</sup>; De Pasquale, G<sup>6</sup>*  
<sup>1</sup>DERA, UK; <sup>2</sup>TUI, Germany; <sup>3</sup>MEODAT, Germany; <sup>4</sup>AEL, UK; <sup>5</sup>VUB, Belgium; <sup>6</sup>IDS, Italy

A consortium of European companies and universities are collaborating on an EC supported project to develop a novel hand-held SPR device which is able to detect Anti-Personnel Landmines (APLs).

The sensor utilises a new Ultra-Wideband (UWB) radar principle based on Maximal Length Binary Sequence (MLBS) techniques, already successfully tested in acoustic wide band devices. A 6 element multi-static linear antenna array has been designed to fully exploit the radar technology. The array consists of unique planar bow-tie elements with distributed resistive loading. The data processing techniques investigated include the study of inverse problems, adapted to extract features of the reflecting targets, and to eliminate non-target related influences such as antenna and soil characteristics. Pseudo-tomographic methods extract measurements of the size and shape of the reflectors. This information is combined in a robust target classification algorithm. Acoustic impulse time-of-flight techniques are being used to register the movement of the antenna array in the X-Y plane.

In this paper we present an overview of the key principles and techniques which are being exploited in the development of the device.

## 46.2

### Multi-Channel GPRS for Mine Detection and Range Clearance

*Chignell, R<sup>1</sup>; Dabis, H<sup>1</sup>; Frost, N<sup>1</sup>; Stephen, W<sup>1</sup>*  
<sup>1</sup>Emrad Limited, UK

Pressure from the Ottawa process to ensure that the world is cleared of mines, and in the Western World for the clearance of disused military ranges presents a major technological challenge. The challenge is to detect, localise, and clear these dangerous objects, which are distributed over large tracts of land, with the detection rate and confidence that allows children back into the area to play.

Pushed GPR systems have demonstrated the ability to find these objects in small areas, but major improvements in system productivity and detection reliability are essential if the potential impact of this technology is to be fully realised.

This paper presents two multi-channel technology demonstrator systems that point the way forward. Both systems are designed to be vehicle mounted. The first is specifically designed to detect plastic anti-personnel mines buried at up to a maximum of 0.3m. The second system is derived from the requirement to find pipes and cables in the street typically at a depth of around 1m. Many shells are pipe like and the requirement for UXO detection is in many senses similar. The paper will concentrate upon the first system because it is the most extensive array and includes significant real-time processing, while the second demonstrator shows how the approach may be implemented for deeper searches.

The first demonstrator is from the "MINEREC" project and is based upon a sixteen channel antenna array. The array with spatial and polarisation diversity provides four semi-independent searches of a swathe 0.75m wide in a single pass. The demonstrator is regarded as a sub-array of a full sixty four element system that would provide a search width of 3m.

The system has been designed with a view to ultimately achieving an operational speed of 15 kph, but as at this time this speed can not be demonstrated, lower performance components have been specified in some areas. A real-time mapping capability has been developed that allows targets to be located.

## 46.4

### Advanced Hand Held Mine Detector and Mine Detection Neutralisation and Route Marking System Overview.

*Gardiner, P<sup>1</sup>; Burch, J<sup>1</sup>; Allsopp, D<sup>1</sup>*  
<sup>1</sup>Defence Evaluation Research Agency, UK

This paper will present an overview of the UK MOD Applied Research Program For Land Mine Detection. The Defence Evaluation and Research Agency carries out and manages the whole of the UK MODs Counter Minewarfare Applied Research program both within its own laboratories and in partnership with industrial and academic research organisations. This paper will address two specific Counter Minewarfare programs, the Advanced Hand Held Mine Detector which started in April 1995 and the Mine Detection Neutralisation and Route Marking System which started in April 1997.

The paper will first address program matters like the operational requirement for the AHHMD and MINDER systems, the DERA capability and programme management before proceeding to an overview of the technologies under research. The technology overview will consider the physics of each of the sensors and their combination into co-operative multi sensor systems.

The paper will conclude with a review of the achievements to date and the future programme.

KEY WORDS: Mine Detection Technologies, MINDER, AHHMD, Applied Research for Defence.

## 46.5

### Vehicle Mounted Forward Looking Mine Detection

*Amazeen, C<sup>1</sup>; Kositsky, Joe<sup>2</sup>*

<sup>1</sup>U.S. Army Cecom NVEDS, USA; <sup>2</sup>SRI International, USA

In 1998 the U.S. Army initiated a research program to investigate, develop, and field test competing forward looking mine detection technologies and signal processing techniques applicable to the detection of on-route surface and buried antitank mines. Forward looking detection distances would be up to 20 meters in front of the host vehicle. Technical goals are to achieve a probability of detection of greater than 0.90 per square meter and a false alarm rate of less than 0.02 per square meter at forward looking distances. Currently, the vehicular mounted mine detection advanced technology demonstration program has provided significant progress for downward looking mine detection. However, the missions proceed at a relatively slow rate of advance (up to 5 kph). The forward looking sensor suite, with associated detection algorithms, is expected to significantly improve the rate of advance.

The approach is to develop a vehicular mounted multisensor suite and detection algorithms. This multisensor system will combine active and passive sensors to detect likely targets with probable mine-like features and alert the operator to their presence and to their location in front of the host vehicle.

Sensor technologies currently being investigated include forward looking ground penetrating radar, passive staring infrared, passive millimeter wave radar, and acoustic laser Doppler vibrometer techniques.

This paper will discuss the forward looking mine detection program, technologies currently being pursued, and will provide some data from recent experimentation.

## 47.2

### Picosecond Pulse Generators for UWB Radars

*Andrews, J R<sup>1</sup>*

<sup>1</sup>Picosecond Pulse Labs, USA

**ABSTRACT:** This paper discusses some PSPL pulse generators that have been used successfully by researchers to build picosecond resolution Ultra-WideBand (UWB) radars. The paper to be presented will present a selection of various available ps waveforms, including step functions, impulses, monocycles and RF pulses. Their corresponding spectrums will also be presented. The fastest pulser generates a -9V step pulse waveform with a 15 ps falltime, Fig. 1. When step waveforms are driven into an antenna which acts as a differentiator (dV/dt), then the resultant radiated electro-magnetic field waveform is an impulse. An impulse transmitter waveform is also popular, in which case the differentiated radiated EM field waveform is a monocycle. The simple addition of a PSPL Impulse Forming Network (IFN) on the output of the Fig. 1 pulser results in a -3V, 22 ps wide impulse, Fig. 2. If two IFNs are connected in cascade, the second derivative function results and the original step waveform is converted into a monocycle pulse. These generators along with their IFNs have been used by many time domain antenna designers on their time domain antenna ranges to evaluate their antenna performances. When building an actual UWB radar, system designers oftentimes need more peak power than is available from PSPL pulse generators. This can be accomplished by using a PSPL pulse generator as an "exciter" to drive a high powered amplifier. Fig. 3 shows such an example. The -3V, 22 ps impulse, Fig. 2, was used as the exciter to drive a 10 watt, 7-18 GHz, TWT amplifier. The resulting output was a 30 watt peak, 12 GHz, 2 1/2 cycle RF pulse. An advantage of this method of generating a very short RF pulse is the resultant RF pulse is phase coherent.

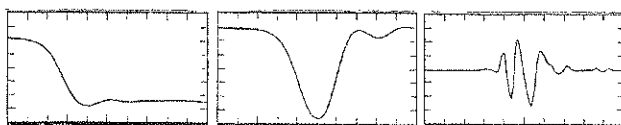


Fig. 1 -9V, 15ps Step  
2 V/div & 10 ps/div

Fig. 2 -3V, 22ps Impulse  
0.5 V/div & 10 ps/div

Fig. 3 30W, 12GHz Pulse  
15 V/div & 100 ps/div

## 47.1

### A Time Domain Antenna Range - Sensors, Calibration, and Signal Processing

*Farr, E<sup>1</sup>; Bowen, L<sup>1</sup>*

<sup>1</sup>Farr Research Inc, USA

We provide here a summary of the time domain antenna range that is owned by Farr Research. Included are the sensors, the calibration procedure, and the signal processing.

The sensors used at our range are the commercially available calibrated TEM sensors manufactured by Farr Research. These devices provide an impulse response that is very close to a pure impulse, with Full Width Half Max as fast as 30 ps. Because these devices replicate the incoming signal, they have much improved sensitivity over the B-dot or D-dot sensors that are commonly used. This is important, because pulsers with adequate risetime have quite low output voltage.

The calibration procedure involves using two identical TEM sensors, and deconvolving the system response, including the response of the cables, pulser, and digitizer. The deconvolution procedure is discussed in detail, including a low-pass filter for reducing noise and an adaptive filter for avoiding division by zero in the frequency domain calibration waveform. Finally, we point out the importance of phase unwrapping when taking the square root of a function in the frequency domain.

Determination of the characteristics of the antenna under test (AUT) is now straightforward. One of the two identical sensors is replaced by the antenna under test (AUT). A normalized impulse response is determined by deconvolving the combined sensor and system response. This normalized impulse response can then be converted to gain and effective aperture in the frequency domain. Preliminary measurements have demonstrated a nice correlation between our time domain technique and other measurements made in the frequency domain.

Future enhancements to the facility may include an azimuth / elevation positioner with computer control, and real-time calculation of the impulse response and gain.

*1/4 of price freq. domain*

## 47.3

### Influence of the Precursor Fields on Ultrashort Pulse Measurements

*Oughstun, K E<sup>1</sup>; Xiao, H<sup>2</sup>*

<sup>1</sup>University of Vermont, USA; <sup>2</sup>JDS Uniphase, USA

A useful experimental measure of the fundamental characteristics of ultrashort pulse evolution is provided by interferometric autocorrelation techniques (D J Bradley & G H C New, Proc. IEEE 62, 313-345, 1974). Optical pulse widths as short as 5 femtoseconds have been measured using this technique (A Baltuska, Z Wei, M S Pshenichnikov, & D A Wiersma, Opt. Lett. 22, 102-104, 1997). The interpretation of these measurements has been almost exclusively based upon the well-known group velocity description of dispersive pulse propagation phenomena. Unfortunately, this approximate description breaks down in either the ultrashort pulse or ultrawideband signal regimes (H Xiao & K E Oughstun, J Opt Soc Am B 16, 1773-1785, 1999) and so cannot be used to accurately interpret these experimental results. In particular, the group velocity description is incapable of providing an accurate description of the precursor fields that are a characteristic of the dispersive medium and are responsible for pulse distortion. A more accurate experimental measure of the fundamental characteristics of an ultrashort pulse is provided by frequency-resolved optical gating (FROG) techniques (R Trebino, K W DeLong, D N Fittinghoff, J W Sweetser, M A Krumbügel, & B A Richman, Rev. Sci. Instrum. 68, 3277-3295, 1997). Pulse widths down to a few femtoseconds have been measured with this technique. The interpretation of these results has also been framed within the group velocity approximation. This paper presents the manner in which the precursor fields that are characteristic of a double resonance Lorentz model dielectric influence both the interferometric autocorrelation function and the frequency-resolved optical gating (FROG) trace of an ultrashort pulse as it propagates through the linear dispersive medium. Comparison of exacting numerical results with results obtained using the group velocity description shows the profound effect produced by the precursor fields as the propagation distance increases above the penetration depth at the carrier frequency of the input pulse. It is hoped that these results will stimulate careful experimental studies of this important physical phenomenon that has heretofore been widely ignored.

## 47.4

### Compact Sensors for Time-Domain Measurements

*Tyo, S<sup>1</sup>; Buchenauer, J<sup>2</sup>*

<sup>1</sup>US Naval Postgraduate School, USA; <sup>2</sup>Los Alamos National Labs NIS - 9, USA

High-quality measurements of ultra-wideband (UWB) electromagnetic fields are difficult to make because of the limited bandwidth of sensors, transmission channels, and measurement devices. Numerous techniques have been developed to deconvolve the response of the measurement system in order to accurately reconstruct the incident signal. A number of sensors have been introduced that utilize loaded and unloaded monopole and TEM horn antennas in order to achieve a flat impulse response over a reasonable frequency range. In contrast to frequency-domain processing, where temporal signals are converted to the Fourier domain for deconvolution before being converted back to the time domain for presentation, true-time-domain processing involves no Fourier processing. In this paper techniques are presented that have been designed to be used strictly in the time domain, and the benefits and limitations are discussed.

A transient antenna prototyping facility has been developed for time-domain characterization of wideband antennas. The range consists of a large ground plane, a moncone transmitting antenna, low-voltage transient step generators, and digital sampling oscilloscopes. The range is designed for a 4-ns clear time, and all components are optimized for a 50-ps risetime. Prospective antennas are prototyped on this range (either scaled down for large radiating systems or scaled up for small sensors), and the results of modifications can be seen in real-time. In addition to the main range (a 13-m x 6-m rectangular ground plane), there is a TEM test cell for testing smaller geometries.

In addition to the measurement facility, a number of true-time-domain probes have been developed. These probes are designed to have well-behaved responses in the early time, with little regard to their performance after some clear time. These probes are all motivated by the receiving response of the unloaded TEM horn, and involve addition of transmission-line extensions to the TEM horn to

delay the TEM horn falloff on receive. Extensions can be forward, to the sides, or even wrap around, and they serve as a means for charge to propagate before returning to the feed point, and the clear time of the sensor is related to the electrical length of these extensions. We are investigating the use of dielectrics to slow down the propagating current wave, thereby extending the electrical length of the sensor without changing the physical size.

In this talk, experimental and modeled results will be presented. These probes will be modeled using the finite-difference/time-domain method, and experimental measurements will be collected on the antenna range. Finally, the time-domain signal processing strategies that have been developed for this facility will be discussed.

## 47.5

### Antenna Characteristics Measurements using Ultrawideband Signals

*Milyaev, P<sup>1</sup>*

<sup>1</sup>Science Production Enterprise SPECTR, Russia

Antenna measurement complexes, that use ultrawideband (UWB) pulse signals, possess the following advantages as compared with the traditional narrow band systems:

1. measurements can be made quickly thanks to the wide frequency band (practically from approximately 10 MHz to 40 GHz), it allows to measure antenna characteristics for all the frequencies at the same time without readjustment of transmitting and receiving parts of the system;
2. it is not necessary to use any additional equipment to measure phase antenna pattern;
3. it is unnecessary to use expensive anechoic chambers due to the possibility to separate useful signal and surface harmful reflections;
4. in collimator measurement complexes - it is possible to separate in time useful signal and direct signal of feeding antenna, as well as useful signal and mirror edge diffraction signal;
5. it is possible to select reflections, introduced by the feeder.

UWB pulse signals are used to measure antenna characteristics with the help of the most well known methods of far and near field.

The present measurement complex uses probing pulses with the width of about 25 ps at half an amplitude, which allows to provide working frequency band of 0,06 - 40 GHz.

It is possible to measure the following antenna characteristics: magnitude antenna pattern, phase antenna pattern, antenna phase centre position, complex antenna gain (with the help of reference antenna and 3 antennas methods), antenna polarisation characteristics (axial ratio of polarisation ellipse and polarisation ellipse slope).

As a conclusion we would like to say that in the recent years considerable results have been achieved both in the sphere of building equipment for UWB measurement complexes (first of all - generators of picoseconds width pulses and wide band sampling receivers), and in development of algorithmic software for antenna measurement complexes. Experience received while measuring antennas' characteristics with the help of UWB signals allows us to say that this way of development of antenna measurement technique has big perspectives, as it helps to achieve better precision, fastness and dynamic range of measurements at the less expensive cost of the measurement complex.

## 49.1

### Solving Electromagnetic Field Equations with a Varying Physical Parameter.

*Tijhuis, A<sup>1</sup>; Zwamborn, P<sup>2</sup>*

<sup>1</sup>Eindhoven University of Technology, Netherlands; <sup>2</sup>TNO Physics and Electronics Laboratory, Netherlands

In this paper, we consider the determination of electromagnetic fields for a (large) number of values of a physical parameter. We restrict ourselves to the case where the discretized fields are the solution of a linear system of equations. We apply an iterative procedure based on the minimization of an integrated squared error, and start this procedure from an initial estimate that is a linear combination of the last few "final" results. When the coefficients in this extrapolation are determined by minimizing the integrated squared error for the actual value of the parameter, the built-in orthogonality in this type of scheme ensures that only a few iteration steps are required to obtain the solution.

Examples of physical parameters for which this idea has been applied thus far are:

- Frequency: as in conventional time-marching solutions, a fixed space discretization is introduced. However, the subsequent time discretization is replaced by a temporal Laplace or Fourier transformation. The result is a system of linear equations of a fixed dimension, which must be solved for increasing frequency. The time signals are then obtained by a straightforward FFT operation.
- Angle of incidence: in EMC applications, it may be necessary to obtain the electromagnetic plane-wave response of an object for a large number of directions of incidence. Now, the operator products required for the initial guess are already available from carrying out the iterative procedure at "previous" angles.
- Source position: in conventional iterative techniques for solving multi-dimensional inverse-scattering problems, it is necessary in each step to compute the result of a point- or line-source

excitation for a varying position of the source. This can be achieved in the same manner as the variation in angle of incidence.

- Contrast and search direction: in the inverse-scattering problems mentioned above, it may be preferable to determine the initial estimate for the unknown field quantity for the same source position with a gradually varying configuration. In linearized techniques, we use the field in the previous configuration; in nonlinear techniques, the procedure has been successfully combined with a line search in a standard optimization algorithm.
- Shape: in the design of integrated antennas or microstrip circuits, it may be necessary to "tune" the dimensions of one or more elements of the structure. Although this can also be carried out with the aid of a sensitivity analysis, a fast computation for a varying characteristic size may be easier to implement. A similar situation arises when the shape of a scattering object changes gradually in time.

## 49.2

### Correlation of Antenna Measurements Using the Oversampled Gabor Transform

*Fourestié, B<sup>1</sup>; Altman, Z<sup>1</sup>*

<sup>1</sup>France Télécom R&D, France

Very recently Gabor analysis aroused considerable interest in its new oversampled formulation. The Oversampled Gabor Transform (OGT) has been successfully applied to the representation of plane aperture radiation and to scattering analysis. The purpose of this paper is put forward the OGT to analyze antenna measurements in amplitude and phase. The measured signal is decomposed on the time-frequency plane and the provided resolution allows one to identify and separate the propagating wave constituents of the signal. The proposed technique has been compared to a short time Fourier analysis, namely, the Windowed Short Time Fourier Transform (WSTFT), and to a super resolution technique, the Matrix Pencil (MP) method. The comparison has been carried out for two types of canonical signals, i.e. sinusoids with frequencies very close to each other, and contiguous chirp signals. It is shown that the OGT can provide a better resolution than the WSTFT, and that the problem of mathematical artifacts which may appear in the MP method, and may prevent physical identification, is avoided. Consider measurements performed in a semi-anechoic chamber using log-periodic antennas in the frequency range of 100-1,000 MHz. By applying the OGT to the measurement results, we show that the component reflected on the ground can be systematically identified and removed to retrieve the measurements performed in a fully anechoic chamber in the frequency range of 350-1,000 MHz. The reconstructed signal and the signal measured in a fully anechoic chamber agree to less than 1.3 dB with an average of 0.44 dB, and a standard deviation of 0.33 dB. The proposed method can be used to correlate measurements in different test sites.



## 49.3

### On a Rational Model Interpolation Technique of Ultra-Wideband Signals

*Younan, N<sup>1</sup>; Taylor, C<sup>1</sup>; Gu, J<sup>1</sup>*

<sup>1</sup>Mississippi State University, USA

Applications of ultra-wideband pulsed RF energy are increasing. These applications range from the treatment of cancer and other maladies to non-destructive testing, remote sensing, and ultra-wideband weapons. Monitoring the time history and the energy spectrum of ultra-wideband pulses pushes the state of the art in electronic instrumentation. This paper examines how limited data can be used to infer data outside the range of the instrumentation.

Generally, discrete-time or discrete-frequency data are obtained via uniform sampling. In some cases, this may not be practical. For instance, logarithmic spacing is often used to limit the samples to a practical number in frequency domain data, collected for frequencies over several decades. Moreover, for high frequency measurements, gaps in the frequency domain data occur as a result of skipping certain frequency bands. Accordingly, interpolation is used to characterize the frequency domain response.

Interpolation techniques require a data model to restore the unknown data samples. Often, the model is quite simple. Consequently, interpolation is related to function approximation. In general, interpolation schemes presume some degree of smoothness for the function to be interpolated. However, this may not be valid for noisy data. Moreover, if the interpolating function is fitted to the known data points with additive noise, significant interpolation error may occur.

Various interpolation schemes have been used to restore unknown data samples. However, most of them have been performed on time-series data. Techniques for interpolating complex frequency data have received little attention. Traditional techniques, such as linear, cubic spline, and Lagrange interpolation, have been shown to be data dependent and are generally not satisfactory. They become highly unstable for data corrupted with noise.

A regressive rational function interpolation for noisy data is presented. This technique incorporates the use of the singular value decomposition method and a statistical measure of goodness-of-fit to obtain the best estimate of the model coefficients. Additional features include a self-tuning ability to obtain an optimum model order and noise reduction. Compared to traditional interpolation techniques, this method is shown to be more robust. Results are obtained for noisy data with low signal-to-noise ratios to ascertain the validity of the technique.

## 50.1

### Ferroelectric Loaded Waveguide for Traveling-Wave Antenna Applications

*Coburn, W<sup>1</sup>; Wasyliwskyj, W<sup>2</sup>*

<sup>1</sup>U.S. Army Research Laboratory, USA; <sup>2</sup>George Washington University, USA

The design and development of customized rectangular waveguide to control the guide propagation constant is of interest for traveling-wave antenna applications. In particular, a means to extend the frequency scan range of such antennas over a narrow (i.e., <10%) source frequency bandwidth is desired. Here we consider radiating slots in perturbed waveguide structures, such as the tapered slot in the narrow wall of rectangular waveguide. Dielectric loading can be used to control the guide propagation constant, hence the beam position as a function of the source frequency. Dielectric materials have been developed with novel properties, including the ability to control the material permittivity,  $\epsilon_r$ , with an applied static electric field. A ferroelectric ceramic composite, barium, strontium, titanium/magnesium oxide (BST/MgO), has this property, with a low loss tangent ( $\sim 10^{-3}$ ) and tailored  $\epsilon_r$  ranging from about 80 to 5000. Such BST/MgO composites have variable  $\epsilon_r$  over a relatively wide range, decreasing in proportion to an applied voltage (PARATEK Microwave, Inc., Aberdeen, MD).

A frequency-scanning antenna constructed of dielectric-loaded waveguide could be supplemented with electronic controls by incorporating this type of ferroelectric. The dielectric permittivity could be adjusted by an applied voltage (which could be synchronized to the source modulation) to steer the beam to a desired position for subsequent frequency scanning. A rectangular waveguide partially loaded with a voltage-controlled dielectric provides additional electronic control, but is problematic for developing suitable control circuits. The double-ridged waveguide is a better choice, since electrodes can be integrated into the dielectric center septum. Feed-through wires and control circuits can be designed for applying a high-voltage control signal. At fixed frequency, the beam could be positioned or scanned by varying this applied voltage. Typical analytical results for slotted waveguide traveling-wave

antennas are shown for rectangular and ridged waveguide. Although this approach would complicate the control system design of a phased-array antenna, it would not significantly increase the on-board power ( $\sim 1$ -W) requirements for these low-current control systems (J.B.L. Rao, D. P. Patel, and V. Krichevsky, "Voltage-Controlled Ferroelectric Lens Phased Arrays," IEEE Trans. Antennas Propagat., Vol. AP47, pp. 458-468, Mar. 1999). A slotted, dual-ridged waveguide, traveling-wave antenna design that uses currently available ferroelectric composite materials is presented. The analytical results and applications to slotted-waveguide-antenna array design are discussed.

## 50.2

### Compact HPM Antenna Design At L-Band

Miletta, J R<sup>1</sup>

<sup>1</sup>U.S. Army Research Laboratory, USA

Size and weight are key constraints in the design and development of any tactical ground vehicle weapon system. These constraints severely limit HPM applications at L-Band. There are many technical issues in weaponizing an HPM system, ranging from prime power to source development and integration. This paper will address the design of the antenna system. An approach to minimizing the size and weight, while maintaining gain and side-lobe attributes will be addressed.

ARL has a number of ongoing small exploratory efforts internally and through contract to develop compact antennas at L-Band. The target specifications that we are trying to meet or beat are:

Weight:	<250kg
Cross-sectional Area:	<7 square meters deployed
Largest side dimension:	<1.2m deployed
Gain:	>30dB
Frequency:	L-band (1.3 GHz)
Bandwidth:	>10%
Power:	>100MW Pulse
Width:	>5 microseconds
Pulse rep-rate:	>100 Hertz

Where the goal is to develop a complete integrated system on one or more standard tactical vehicles.

Antenna gain is directly related to the effective antenna area. Compact antenna design is directed at increasing the effective area while constraining the physical area (and volume). This paper will address the use of dielectrics in the design of aperture arrays to achieve the above goals. Both the development of low VSWR transformers, which match the source to the antenna, and the antenna to air radiation interface will be addressed. Graded and shaped dielectrics incorporated into standard waveguide and antenna designs to affect appropriate matching will be discussed.

## 50.4

### Cross-Field Characterization of Dipole Radiation in Fresnel Zone

Badic, M<sup>1</sup>; Marinescu, M J<sup>1</sup>

<sup>1</sup>Research Institute for Electrical Engineering-ICPE, Romania

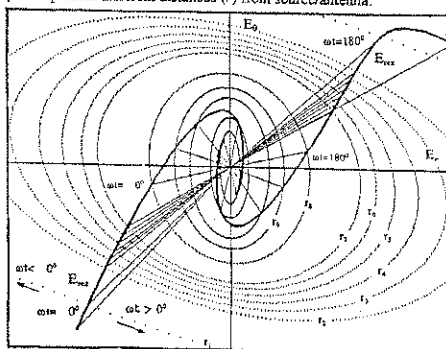
The paper deals with vectorial characterization of  $\vec{E}$  and  $\vec{H}$  fields in Fresnel zone of a short dipole antenna. As known, in the Fresnel zone, electric and magnetic fields may be related as in standing waves, so that they may result in a reactive energy flow coming back to the source. It may occur the situation when  $\vec{E}$  resultant vector may be placed in a plane parallel with the travelling direction. This cross-field phenomenon is characteristic to wave guides, reflexion and Fresnel zone of radiating systems.

In order to characterize the cross-field phenomenon authors consider the equations of short dipole antenna:

$$H_{\theta} = \frac{1}{Z_0} K \sin \theta \left[ \left( \frac{\lambda}{2\pi r} \right)^2 \cos \psi + \frac{\lambda}{2\pi r} \sin \psi \right]; \quad E_{\theta} = 2K \cos \theta \left[ \left( \frac{\lambda}{2\pi r} \right)^2 \sin \psi + \left( \frac{\lambda}{2\pi r} \right) \cos \psi \right]$$

$$E_{\phi} = K \sin \theta \left[ - \left( \frac{\lambda}{2\pi r} \right)^2 \sin \psi + \left( \frac{\lambda}{2\pi r} \right) \cos \psi + \frac{\lambda}{2\pi r} \sin \psi \right]$$

having  $\psi = \alpha r - \beta r$ , with a view to emphasize the spacial variations versus  $r$  and  $\theta$  (the directivity characteristic) as well as the temporal variation. These equations are mathematically processed and certain conditions are considered ( $\beta=1 \Rightarrow 2\pi=\lambda \Rightarrow f=47.7 \text{ MHz}$ ;  $\alpha t=0 \Rightarrow \psi=\pi$ ), but all of these don't alter the radiation phenomenon. Resultant field  $E_{\text{rez}}$  of components  $E_{\theta}$  and  $E_{\phi}$  is calculated. According to the mathematical demonstration, authors present 2D and 3D diagrams which fully characterize vectors  $\vec{E}$  and  $\vec{H}$  in the Fresnel zone of the short dipole antenna. In the figure below is presented an example for the locus of  $\vec{E}$  when  $\theta=50^\circ$ ,  $\alpha t=180^\circ$  and  $\alpha t=0^\circ$ , ellipses represent different distances ( $r$ ) from source/antenna.



The paper also presents the way to measure vectors  $\vec{E}$  and  $\vec{H}$  in the Fresnel zone of a short dipole antenna.

## 50.3

### The Offset Dipole: An Alternative to a Hertzian Broadband Element

Litz, M<sup>1</sup>

<sup>1</sup>Army Research Laboratory, USA

Several Wideband antennas have been developed that are designed to maintain signal pulse shape fidelity. These antennas are often large horn designs that occupy a volume difficult to integrate into an existing platform. While there is little chance of eliminating the need for large antenna area, planar arrays offer more options to minimize the volume and offer higher gain through conformal arrays. This investigation supports the requirements of the future battlefield; development of wideband antennas for use both communications and radar applications.

The use of offset feed is common in reflector antennas to reduce aperture blockage and provide greater installation flexibility. Planar arrays move one step further towards volume reduction by reducing the reflector to planar geometry. This investigation is motivated by the goals of reducing the volume required for a parabolic reflector and increasing the gain bandwidth product of a dipole arrays. The offset fed dipole offers broadband radiation patterns and a higher gain bandwidth product than that found in a center-fed dipole.

The results of measured data taken in a 50' anechoic chamber and computations using NEC Method-of-Moments code are compared for both principle-plane radiation patterns and input impedance. The results of both techniques compare well. The data show that at 45 degrees off boresight the E-plane gain-bandwidth product appears largest. By moving the feedpoint of the typical centerfed dipole 80% towards the end of the dipole arm, the gain-bandwidth product is maximized. Agile antenna arrays are considered. Offset-fed dipoles may be combined into arrays offering the advantages of planar antenna technology, providing a space-saving alternative to parabolic reflectors.

## 50.5

### Parallel Charging of Marx Generators for High Pulse Repetition Rate Operation

Lehr, J<sup>1</sup>; Baum, CE<sup>1</sup>

<sup>1</sup>Air Force Research Laboratory, USA

Marx generators are commonly used components of many high voltage systems but are generally limited to single pulse or low pulse repetition operation. For high pulse repetition rate applications, transformers are a proven technology. However, as desired voltages approach 1 MV, it becomes more difficult to use pulse transformers in high pulse repetition rate operation. Marx generators are interesting as a voltage amplification component in the generation of high power, ultra-wideband radiation. However, for a Marx circuit to be seriously considered in an ultra-wideband radiating system, high pulse repetition rate operation must be demonstrated. Towards this goal, a circuit scheme for the parallel charging of a Marx generator has been developed.

In general, the charge and discharge circuits of the Marx generator can be considered only loosely coupled. Initial efforts focus on the charging circuit. For Marx generators to operate with a high pulse-repetition frequency, one needs to minimize the time required to charge the capacitors, while not significantly loading the Marx during erection and discharge. Typical design of the charging circuit involves a series string of resistors, or even a series string of inductors, running along the capacitor stack. In this paper we consider parallel charging with inductors and resistors in which the charging elements (and series combinations) are all connected in parallel to the power supplies (two for differential charging).

## 51.1

### Results of Testing the University of Mississippi's Acoustic/Laser Doppler Vibrometer Mine Detection Apparatus at Fort A.P. Hill, March 1999

*Rosen, E<sup>1</sup>; Sherbondy, K<sup>2</sup>; Sabatier, J<sup>3</sup>*

<sup>1</sup>Institute for Defense Analyses, USA; <sup>2</sup>US Army CECOM, USA;

<sup>3</sup>National Center for Physical Acoustics, USA

In March of 1999, the University of Mississippi brought their acoustic/laser-doppler-vibrometer (LDV) mine detection apparatus to Fort A. P. Hill in Virginia for the purpose of collecting data over a variety of mines and to participate in a blind test. In the blind test, the mine detection apparatus was brought to several 1-meter by 1-meter locations in the anti-tank (AT) test lanes and University of Mississippi personnel were to determine if a mine was buried in the area of interrogation. These 1-meter by 1-meter areas included a mix of mines, blank spots, and clutter spots as determined from prior tests. The data collected over each of these spots was visualized in real-time and a mine/no mine decision was made. The resultant probability of detection (Pd) was 95% with a false alarm rate (FAR) of 0.03 m-2.

We present, in this paper, a description of the test and a detailed analysis of the data collected by the University of Mississippi in the mine lanes at A.P. Hill. With knowledge of the baseline, we compute target and clutter statistics including signal to noise ratios for various categories of mine types and mine depths. Detection trends as a function of frequency are examined, and subtraction of the incident sound field is investigated. Applying image-processing techniques to the data, features such as size and shape are extracted, and the resultant feature level target and clutter histograms are used to generate receiver-operator characteristic (ROC) curves. The expected performance with and without features is compared to the demonstrated performance.

## 51.3

### Landmine Detection System with NMR Gradiometer

*Cattin, V<sup>1</sup>; Lger, J M<sup>1</sup>; Ittel, J M<sup>1</sup>; Bruschini, C<sup>2</sup>*

<sup>1</sup>LETI (CEA - Technologie Avances) DSYS CSME, France; <sup>2</sup>EPFL-LAMI VUB-ETRO-IRIS, Switzerland

During the last 5-10 years, landmine problems became increasingly urgent. Since detection and clearance are very often carried out using manual methods, new systems are being studied to provide safer and more powerful detection and localisation functions. In this context, we have implemented a mine detection system based on high resolution scalar magnetic sensors.

Passive magnetic sensors detect the presence of ferromagnetic material. They measure both the remanent magnetization and the magnetization induced by the earth magnetic field in such materials. Most land mines contain enough metal to be detected by this method even if their metallic pieces are often very small (<1g). We propose to use a Leti NMR scalar magnetic sensor (Abraham-Overhauser effect). Such a sensor measures the module of the ambient field, or the projection of the magnetic response of the mine on the earth field direction. Its main advantages compared to other magnetic sensors are higher resolution (pT/rac(Hz)), especially in the DC band, its robustness and insensitivity to movements. The high-resolution demonstration system we set up consists of a vertical gradiometer composed of two NMR sensors. The first sensor is moved along a profile at about 10 cm from the ground and measures the magnetic mine effect. The other is about 1.5 m above the ground and is used as a reference to measure the ambient electromagnetic noise perturbations, both industrial and geological, which may screen the target response.

## 51.2

### Time-Domain Electromagnetic Identification (TEMID) Sensor System

*Nelson, C<sup>1</sup>; Smith, D<sup>1</sup>; Sherbondy, K<sup>2</sup>; Huynh, J<sup>2</sup>*

<sup>1</sup>Johns Hopkins University Applied Physics Labs, USA; <sup>2</sup>U.S. Army, USA

The TEMID sensor system is an advanced prototype electromagnetic induction (EMI) landmine sensor system developed by The Johns Hopkins University Applied Physics Laboratory (JHU/APL) in conjunction with the U.S. Army CECOM Night Vision Electronic Sensors Directorate (NVESD). The self-contained, portable, prototype TEMID sensor system has demonstrated the capabilities to detect, identify and discriminate from metal clutter high and medium content metal landmines, as well as plastic cased landmines with metal parts. Compared to conventional EMI metal detectors, the TEMID sensor's discrimination feature results in a lower false alarm rate from metal clutter. The TEMID sensor system operates on the principle of eddy current time decay. A pulsed magnetic field excites eddy currents in a target. The time decay of the target's eddy currents is a function of the target's mechanical, electrical and magnetic properties. A target's identity can be determined by comparing accurately measured time decay characteristics of the target with a time decay characteristics of known mines.

This paper will describe the sensor and present data from recent field trials at the Ft. Belvoir mine lanes and Ft. A. P. Hill (JUXOCO) test site.

## 51.4

### Microbial Mine Detection System (MMDS)

*Fliermans, C B<sup>1</sup>*

<sup>1</sup>Westinghouse Savannah River Co LLC, USA

The 1998, U.S. State Department publication, Hidden Killers, contains an estimate that there are approximately 60-70 million uncleared land mines in 70 countries. The International Red Cross continues to estimate that land mines claim some 26,000 civilian victims annually. Aside from the carnage, the presence of land mines can reduce to to abject poverty the economy of poorer nations through the loss of arable land resources and livestock. Land mine detection and removal is a slow, deliberate process that requires painstaking attention to detail. In order to improve detection rates, a radically different approach is required.

During the past two years, scientists at the Savannah River Technology Center (SRTC), a Department of Energy, applied RD laboratory located at the Savannah River Site (SRS) near Aiken, South Carolina, have been developing a safe, reliable method for detecting land mines. This method employs naturally occurring, bioluminescent microorganisms as the primary biosensor detector.

SRTC research has demonstrated that certain naturally occurring bacteria possess an affinity for the off-gasses of nitrogen containing explosive materials. SRTC scientists have conducted their research using a cross section of carefully selected and screened soil samples. The samples were collected at abandoned TNT manufacturing sites and various test minefields located in the USA, as well as at actual live minefields in Mozambique. The findings demonstrated that certain bacteria were stimulated by trinitrotoluene (TNT) and dinitrotoluene (DNT) as the sole nitrogen source. These results confirm that selected, naturally occurring microorganisms will respond to off-gasses produced by conventional explosives by bioluminescing in the immediate vicinity of existing land mines.

The next phase of research is to down select those microorganisms that provide maximum response. Field deployment methodologies could be by hand held and vehicular mounted devices, as well as remote or manned air platforms. Naturally based Microbial Mine Detection Systems (MMDS) are a renewable resource, easy to prepare, inexpensive to maintain under field conditions, and provide a high probability response recognition technology.

## 51.5

### Mineseeker

*Bishop, PK<sup>1</sup>; Parkes, D<sup>1</sup>; Crisp G<sup>1</sup>; Thornhill C<sup>1</sup>; Christoforato S<sup>1</sup>*  
<sup>1</sup>DERA, UK

A unique joint venture between DERA (Defence Evaluation & Research Agency) and Sir Richard Branson's The Lightship Group (TLG), plans to exploit the best in military radar technology and airship design in locating deadly mined areas around the world.

According to the UN, there are at least 60 – 70 million landmines left in the world and some 25,000 people are maimed or killed annually (70 people daily). The Landmine Monitor also estimates that there are currently more than 250 million antipersonnel mines stored in the arsenals of at least 104 countries. UN records some 900,000 square kilometres lost to mined areas which is the equivalent to a useable space the size of France and Germany combined. With figures like these, the Mineseeker collaboration will represent a significant advance in the humanitarian de-mining effort. This airborne radar system will be able to accurately and quickly direct costly resources - saving money, time and lives.

Currently, mined areas are identified in the first instance through post-conflict intelligence gathering from local hearsay and information given by the ex-warring factions. Inaccurate information leads to some 80% of areas being mis-diagnosed so that mined areas remain unreliably mapped, or worse, unidentified - risking lives and rendering potentially life sustaining farming land unusable. It is expected that the Mineseeker™ system will be able to uniquely map mined areas quickly and safely, covering ground at a rate equivalent to more than 100 square metres per second - which is many thousands of times faster than the average rate for a manual search.

The first trials of the airship-borne radar system called Mineseeker™ took place in mid-January at a DERA site in Worcestershire, where TLG's A60+ Airship was fitted out with an innovative prototype radar system built by DERA. Early results are extremely promising with the system performing at least as well as previous ground based trials.

The January trial was essentially the culmination of a feasibility study into the operation of a prototype Ultra-Wide Band Synthetic Aperture Radar (UWB SAR) from an airship for the detection of mined areas in a humanitarian role. Targets imaged by the experimental radar system were surface laid metal and plastic mines and mine-like targets of varying sizes. The smallest of these targets were only 10cm in diameter and entirely plastic which represents a significant advance over conventional airborne radar systems.

The next phase of the development is to optimise the radar to meet the specific requirements of mined area detection in a humanitarian role. The science and technology involved is widely recognised as frontier breaking and particularly challenging. This is an ambitious programme but the resulting system will have unique capabilities and contribute a significant advance in ridding the world of these deadly legacies.

## 52.1

### The Possibility of Submillimeter Waves Generation in the Semiconductor Structures by a Flow of Electrons

*Yakovenko, V<sup>1</sup>*

<sup>1</sup>Institute of Radiophysics and Electronics, Ukraine

Instability of surface oscillations in an inhomogeneous semiconductor plasma is theoretically investigated as a result of their interaction with a flow of charged particles crossing the boundary. It is well known that the charged particle radiates an electromagnetic field when it crosses the interface of media of different electromagnetic properties. The electromagnetic field connected with particle depends not only on the radiator properties but also on the properties of medium. Therefore at the interface the reconstruction of the field takes place and the part of this field breaks away from the particle. Then a free field arises. This field can be an eigen oscillation of the system. The kinetic energy of the particles can be transformed into energy of oscillations of system. Under conditions of reverse connection, the opposite process also exists. It is clear that generation of the eigen oscillations can arise if the first process prevails over the second one. Such a situation can be realized in the case when the temperature of the particles in the flow is smaller than a quantum of the electromagnetic field energy. Since the process of mutual transformation of energy of the waves and the particles takes place at the two-media interface, it is more advisable to investigate the interaction of particles and surface oscillations (the surface plasmons). The hamiltonian of this interaction has been found and the increment has been determined in the submillimeter wave range.

## 52.2

### A Repetitive X-Band Relativistic Backward-Wave Oscillator

*Chen, C<sup>1</sup>; Liu, G<sup>1</sup>; Song, Z<sup>1</sup>; Fan, J<sup>1</sup>*

<sup>1</sup>Northwest Institute of Nuclear Technology, China

A repetitive X-band relativistic backward-wave oscillator is introduced in this paper. This device consists of a high power relativistic BWO, special electron collector and a superconducting magnet system. Both BWO and electron collector are designed based on numerical simulation using KARAT code. The end reflection is optimized to increase microwave power by attaching a piece of cylindrical transmission waveguide to the end of slow wave structure. Numerical simulation proves that microwave power and transform efficiency can be increased by 28 percent and 6.8 percent respectively through end reflection optimization. The electron collector is designed and used to collect electron beams in order to prevent ionization and breakdown near electron bump which is responsible for microwave decreasing at repetitive operation of BWO. In experiments, an accelerator SINUS-881 is used to drive the repetitive device. 100 Hz repetitive relativistic beams of 5.4 kA and pulse voltage of 610 kV are generated by SINUS-881, then guided through the corrugated waveguide by axial magnetic field of 3.0 Tesla produced by superconducting coils and bump into electron collector. This BWO produces a microwave pulsed power of 1.1 GW at 100 Hz repetitive rate, frequency of 9.38 GHz, pulse duration of 23 ns and transforming efficiency of 33 percent.

## 52.3

### Broadband, High-Gain, Gyro-Traveling Wave Amplifier with a Helically Corrugated Waveguide

*Cross, A.W<sup>1</sup>; Bratman, V.L<sup>2</sup>; Denisov, G.G<sup>2</sup>; He, W<sup>1</sup>; Phelps, A.D.R<sup>1</sup>; Ronald, K<sup>1</sup>; Young, A.R<sup>1</sup>; Samsonov, S.V<sup>2</sup>; Whyte, C.G<sup>1</sup>*

<sup>1</sup>University of Strathclyde, UK; <sup>2</sup>Russian Academy of Sciences, Russia

The first bandwidth measurements of a novel type of gyrotron amplifier will be presented. The coupling between the second harmonic cyclotron mode of a gyrating electron beam and the radiation field occurred in the region of near infinite phase velocity over a broad bandwidth by using a cylindrical waveguide with a helical corrugation on its internal surface [1], [2]. The experiment used an axis encircling electron beam with an energy of 185keV, current 20A and duration of 120ns moving in a guiding magnetic field of 0.21T as the gain medium of the amplifier. A broadband, conventional Helix-TWT amplifier in conjunction with a solid state oscillator provided an input signal. In this configuration the amplifier achieved a saturated maximum output power of 1.1MW with a gain of 37dB, corresponding to an efficiency of 29%. The instantaneous bandwidth of the saturated gain extended from 8.4 to 10.4GHz (taking the -3dB points), a 21% relative bandwidth. Linear regime gain of 47dB was recorded. The observations are in good agreement with predictions of the theory. These results have important implications for existing amplifier applications (e.g. RADAR, Telecommunications).

The work was supported by the United Kingdom DERA, Gycom Ltd., Nizhny Novgorod, Russia and the Russian Foundation for Basic Research under Grant 98-02-17208.

#### References

- [1] G.G. Denisov, V.L. Bratman, A.D.R. Phelps, and S.V. Samsonov, IEEE Trans. Plasma Sci. **26**, 508-517 (1998).
- [2] G.G. Denisov, V.L. Bratman, A.W. Cross, W. He, A.D.R. Phelps, K. Ronald, S.V. Samsonov and C.G. Whyte, Phys. Rev. Lett. **81**, 5680-5683, (1998).

## 52.5

### The Interaction of Symmetric and Asymmetric Modes with Free Electrons

*Banna, S<sup>1</sup>; Schachter, L<sup>1</sup>; Schieber, D<sup>1</sup>*

<sup>1</sup>Dept. of Electrical Engineering - Technion, Israel

In high-power and high-efficiency traveling-wave amplifiers the electron beam is assumed to interact with the lowest symmetric TM mode. Efficiencies as high as 70% and even higher may be achieved in coupled cavity traveling-wave structures, driven by a relativistic, bunched beam, when high order modes do not play a significant role. However, asymmetry may occur either due to the input or output arm, due to uneven azimuthal electron distribution or due to beam misalignment; as a result asymmetric modes may develop. In such a case, a longitudinally modulated beam may interact with one of the asymmetric modes. The main problem with these modes is their ability to deflect the beam to the wall. Since pulse shortening was observed experimentally, this study investigates the impact of asymmetric modes on the interaction process in a traveling-wave amplifier.

A 3D model has been developed in order to investigate the coupling of the lowest symmetric and asymmetric modes in a high-power (>50MW), high-efficiency traveling-wave amplifier. It was shown that in a uniform structure and for an initially non-bunched beam, the interaction efficiency of the asymmetric mode may be much higher than that of the symmetric mode. It is also shown that the coupling between these two modes is determined by a single parameter that depends on the beam characteristics, its value varying between zero when no coupling exists and unity in case of maximum coupling. For a beam that is uniform at the input end this parameter depends linearly on the guiding magnetic field. In case of a bunched beam it decreases linearly with increase of the phase-spread of the bunch. Due to the interaction, the radius of the beam increases linearly with the power associated with the asymmetric mode at the input end; it increases more rapidly in the case of an initially uniform beam when compared to the increase of a pre-bunched beam. As the existence of an asymmetric mode is therefore impairing the performance of the amplifier, a way to suppress the asymmetric mode is described and analyzed. In conclusion, the design of a traveling-wave amplifier has to take into consideration the effect of the asymmetric modes that may interact with the beam.

## 52.4

### Relativistic X-band Plasma Maser with 7-fold Frequency Tuning at 50-MW Power Level.

*Strelkov, P<sup>1</sup>; Ulyanov, D<sup>1</sup>*

<sup>1</sup>General Physics Institute, Russia

Powerful microwave devices based on exciting of plasma eigenmodes by relativistic electron beam differ principally from their vacuum analogues. Presence of plasma allows to overcome the restriction imposed by electron beam space charge on the total current, as well as the problem of HPM pulse shortening. Plasma permits to change microwave radiation frequency in a broad band and to place the device on the desired frequency in a very short time interval.

The report describes new achievements in our studies of relativistic Cherenkov plasma masers (CPM) [O.T.Loza, A.G.Shkvarunets, P.S.Strelkov. Experimental Plasma Relativistic Microwave Electronics. IEEE Trans. on plasma science, Special Issue on high power microwave generation, June 1998, Vol 26,

3, pp. 615-627.]. A new CPM has been designed where the axially symmetric eigenmode of plasma waveguide with the lowest radial index was excited. For the first time the 7-fold frequency tuning, from 4 GHz to 28 GHz, was obtained at almost constant 50-MW power level. The frequency tuning was carried out due to the variation of only one parameter, namely, plasma density. Experimental dependence of radiated frequency on plasma density coincides with the results of numerical calculations. Remote control over plasma density permitted to reset the device to a new radiation frequency during 30 microseconds.

The experiments were conducted at an accelerator operated in the single-shot regime with the following parameters of relativistic electron beam: 500 keV, 2 kA, 35 ns. The microwave radiation bandwidth was 15-25% at 28 GHz and 40-60% at 9 GHz. The spectra measurements were fulfilled using the design of: [I.L.Bogdankevich, Y.Caillez, A.G.Shkvarunets, et al. Calorimeter-spectrometer for single pulses of relativistic high-current microwave oscillators. Proc. of Int. Symp. EUROEM'98].

## 53.1

### Ultra-Wideband (UWB) Radio-Frequency (RF) Bioeffects Research at DERA Porton Down

*Holden, S<sup>1</sup>; Inns, RH<sup>1</sup>; Lindsay, CD<sup>1</sup>; Tattersall, JH<sup>1</sup>; Rice, P<sup>1</sup>; Hambrook, JL<sup>1</sup>*

<sup>1</sup>DERA, UK

The Biomedical Sciences group of the Chemical and Biological Defence (CBD) sector, DERA Porton Down, undertakes fundamental and applied research on the biological effects of RF radiation. The main area of investigation is into the effects of ultra wide-band (UWB) radiofrequency radiation on human and animal cell cultures, using a variety of biochemical and morphological parameters. The present issue arises because current guidelines controlling exposure of personnel to radiofrequency fields are not specifically relevant to situations where subjects may be exposed to UWB pulses. In addition, there is an increasing awareness that cellular effects below the thermal threshold may be induced by pulses of low mean power, with effects being found in windows of a particular frequency. A programme of research is being undertaken at DERA Porton down to establish whether personnel may be at risk from exposure to radiofrequency radiation of low mean power both pulsed and continuous wave. The main areas of research are:

- Physical and computer based dosimetry modelling;
  - Physical models using dosimetry phantoms filled with tissue simulants (CW);
  - Computer based models using computational electromagnetic methods such as FDTD, TLM and Quasi-optical methods (CW and UWB).
- In vivo animal studies;
  - Rat behavioural work (CW).
  - Chronic exposure of Rabbits to UWB.
- In vitro human and animal tissue studies;
  - Human and animal cell cultures exposed to UWB.
  - Rat hippocampal brain slice exposed to CW (microwave).

This paper will describe details of the work programme and provide examples of the findings to date.

## 53.2

**Clinical Cosmobiology: Some Differences in Correlation Between Monthly Cardiovascular and Suicidal Deaths Number and Space Proton Flux of Two Energy Levels >60 MeV Versus > 90 MeV.**

*Stoupel, E G<sup>1</sup>; Israaelevich, P<sup>2</sup>; Gabbay, U<sup>3</sup>; Abramson, E<sup>2</sup>; Petruskiene, J<sup>4</sup>; Kalediene, R<sup>4</sup>; Domarkiene, S<sup>4</sup>; Sulkes, J<sup>4</sup>*  
<sup>1</sup>Rabin Medical Center, Israel; <sup>2</sup>Tel Aviv University, Israel; <sup>3</sup>Israel; <sup>4</sup>Kaunas Medical University, Lithuania

In our previous studies (1995-1997), we described some significant links between the monthly number of deaths due to cardiovascular disease and suicide and space proton flux >90 MeV. The purposes of the present study were to compare the relationship of some solar and geomagnetic parameters with space proton fluxes of >60, and those of >90MeV; to examine the monthly correlation of those two proton groups with the monthly death distribution in two countries, Israel and Lithuania. The physical data were obtained from the National Geophysical Data Center and the SESC in Boulder, CO., the NSSDC in Goddard Space Flight Center, USA and the Izmiran Institute of the Academy of Sciences in Russia. Pearson correlation coefficients and their probabilities were compared for 56-180 consecutive months. **Results:** 1) Proton flux of >60 MeV significantly correlated with three of the four studied monthly geomagnetic activity indices (Ap., Am., Dst), but not with such solar activity markers as sunspot number and solar flux (2800 MGH, 10.6 cm). 2) There was no significant relationship between proton flux of >60 MeV and monthly number of deaths from cardiovascular diseases and suicide, in contrast to the results for >90 MeV. 3) In the data available during the 36 months (1986-1988), there was no correlation between monthly levels of >60 to >90 MeV. **In conclusion,** monthly space proton flux of >60 MeV is not significantly correlated with the monthly death distribution from cardiovascular disease and suicide and some solar activity indices, like proton flux of >90MeV. It is possible that the 60-90 MeV fraction in the >60 MeV proton flux "blunts" the cosmobiological relationship between proton flux of >90 MeV and monthly death number.

## 53.4

**New Method of EHF-therapy at Treatment of Endogene Mental Diseases**

*Vadim, D<sup>1</sup>; Bacherikov, A<sup>2</sup>*  
<sup>1</sup>Usikov Institute for Radiophysics Electronics, Ukraine; <sup>2</sup>of Clinical Experimental Neurology Psychiatry, Ukraine

The method of treatment of endogenic psychoses is offered by use of EHF-therapy. The method consists in action by low intensive microwave radiation on the cooled areas of a body of the man. Frequency of electromagnetic radiation (30 - 60 GHz), temperature of a skin in a band of action (+5 - +20C) and the bands of action are selected individually because of subjective response. The treatment 30 patients were carried out. In all cases the positive effect was marked.

In a basis of the physical concept of influence of EHF-radiowaves the supposition about their information action on organism of person is put. According to this concept, the related cells exchange an information by means of electromagnetic waves of EHF range. The functional violations, which arise in organism of person, reduce to decrease of a common emitted potency and shift of emitted frequencies from eigenfrequency of organism or organ, that in turn reduces in violation of information connections between cells and, as a corollary, to the further development of pathological process. To prevent this process it is possible by action onto biologically active zones (biologically active dots, zones of Zaharina-Geda) by the electromagnetic radiation. The effectiveness of EHF-therapy (to the present time) was shown at treatment of diseases of gastrointestinal tract, cardiovascular systems, nervous and dermal disease etc.

It is established that the effect of EHF-therapy largely depends on a water condition in tissue, its structural organization and percentage of free and connected phases. As the specified physicochemical (electrophysiological) properties of water are defined in temperature, it is natural to assume, that the effect of action EHF also will depend that of temperature of a surface layer of a skin in zone of action.

We have tested a new method of treatment with the help of EHF-therapy. Essence of the method is what the action of low-intensity electromagnetic radiation is produced on cooled (up to temperature + 5 + 20) areas of the skin. The cooling was reached by ventilation of zone of action by a cooled air. The EHF influence was carried out on the developed technique on

## 53.3

**Comparison Between SAR Distributions Inside Lossy Dielectric Material Radiated by a Straight Dipole and a Helical Antenna**

*Russo, P<sup>1</sup>; De Leo, R<sup>1</sup>; Cerri, G<sup>1</sup>; Chiarandini, S<sup>1</sup>*  
<sup>1</sup>Universita di Ancona, Italy

In the present contribution we show the results obtained evaluating the SAR distribution inside a dielectric cube, placed in the near field of a straight dipole and a normal mode helical antenna of dimensions typical of the commonly used radiating structures in cellular phones, at the operating frequency of 1710 MHz. At first we analysed a straight dipole of length 8.77 cm and wire radius 0.625 mm, with a 1 Volt feeding voltage. The antenna radiates at distance of 1.75 cm from a dielectric cube. We compare the results of the dipole with a helical antenna in the normal mode of radiation of these characteristics: number of turns 8, helical diameter 5 mm, pitch angle 4.55°, helical step 1.25mm, wire radius 0.098 mm, with a 1 Volt feeding voltage. An hybrid Method MoMTD/FDTD was applied to solve the electromagnetic problem: in particular the radiating antennas are studied by MoM and the field inside a complex penetrable object is evaluated by FDTD. The spatial distribution of the computed current along the antenna wire exhibits the typical behaviour of a  $l/2$  straight dipole antenna. The input impedance found for the antenna in the presence of the cube was  $Z=56.2 + j 99.5$  W. The current behaviour for the normal mode helix is similar to the previous, according to the similarity in the radiation pattern that characterise these two structures. The main differences are located in the feeding region, where the structure presents an abrupt change in the curvature due to the wire connecting the helix and the voltage generator placed along the antenna axis. The input impedance found for the antenna in the presence of the cube was  $Z=9.5 + j 119.42$  W. Concerning the SAR distributions inside the cube we can observe that, as expected, for the case of the helix it is concentrated in a region smaller than that of the straight dipole case. This depends on the geometry of the two antennas: in particular, even if the wire length of the helix is longer than the one of the dipole, the whole structure is more compact so that the field source is concentrated in a smaller volume. Moreover, for the helix structure the field penetration is confined in a more superficial layer: in our opinion this is due to the different field distribution in the near field region. In particular the dipole radiation can be considered as the superposition of fields radiated by elementary vertical dipoles. On the other hand the helix radiation can be considered mainly as superposition of elementary horizontal loops because the adopted pitch angle is very small, so that the two structures have different near field distributions. Also the polarisation of the two antennas is different: linear for the dipole, elliptic for the helix (Axial Ratio AR=1.77). The maximum value of SAR (normalised to 1W of radiated power) we found inside the cube for dipole antenna is  $SAR_{maxA} = 13.38$  W/Kg. For the helix we found  $SAR_{maxB} = 6.58$  W/Kg that is lower of that obtained for the straight dipole.

biologically active dots and zones of Zaharina -Geda. Such approach allows to use individual singularities of the patients organism more completely, to increase effectiveness of a mode of EHF-therapy and as a corollary to decrease period of treatment.

The treatment with application of a new method of EHF-therapy was conducted to 30 patients (females, of 25 to 40) with manic-depressive psychosis in a condition of depression. Depression at the patients in basic was determined following axial syndromes: suppressed mood, intellectual inhibition, psychomotor inhibition, bradyllalia. At all patients the expressed alarm and anguish was marked that also was accompanied by physical burdensome sensations and the feeling of gravity in epigastric area or in the field of heart. Suicidal ideas at 18 of 30 patients were marked that testified to extreme painful of depression.

After a course of EHF-therapy in all cases the positive effect is marked, and at 22 patients the treatment was carried out without additional application of antidepressants. The study of parameters of a condition of vegetative nervous system (VNS) has shown that positive therapeutic effect of EHF-action was implemented through normalization of adaptation process.

## 53.5

### Experimental and Theoretical Investigations of "Foot Current" in a Human Body Exposed to an Electric Field

Gryz, K<sup>1</sup>; Karpowicz, J<sup>1</sup>

<sup>1</sup>Central Institute for Labour Protection, Poland

**Key words:** electric field, induced current, exposure evaluation, numerical calculations, foot current measurements.

Routine evaluation of human exposure to electric fields is based on electric field strength measurements. This kind of evaluation does not consider the fact that penetration of the energy of an external electric field into the human body (i.e. a health hazard) greatly depends on such factors as location of the body axis in relation to electric field power lines, the shape and size of the body, conductivity of the ground, insulation of the shoes, electrical interaction between human and the field source.

Because of that, a more precise analysis of the health hazard aims at determining the value of the electric current which flows through the body into the ground because of the activity of the external electric field (the so-called "foot current"). This is especially important in relation to exposure to very strong electric fields occurring, for example, at workstands of dielectric welding, physiotherapeutic short-wave diathermy, broadcasting devices.

The investigations concerned radio-frequency electric fields. The value of the currents flowing through the exposed person will be calculated from the analytical model (Korniewicz's equation - H.R. Korniewicz, IEEE Trans. EMC, 296-299, 1995) and by numerical calculation of the body model (Finite Element Method).

Experimental investigations were done in real conditions of occupational exposure at high frequency electric field sources for exposed persons and commercially available human equivalent antenna.

Measurement results compared with model calculations will be presented and discussed.

The results of a "foot current" investigation in field conditions in a vertically polarised electric field of 220 kHz, in a laboratory field of 1.8 MHz and a non-vertical field of typical industrial sources will be presented. These results indicate, for example, that "foot current" for a person wearing shoes with a thick sole increases by about 20% when the person raises his/her arms.

This investigation has been carried out to obtain suitable calculation and measurement models, which would allow evaluating human exposure in a strong electric field without exposing humans.

## 54.4

### Optimal Feeds for 4-Arm Impulse Radiating Antennas

Tyo, S<sup>1</sup>

<sup>1</sup>US Naval Postgraduate School, USA

One of the most common type of impulse radiating antennas (IRAs) in use today is the 4-arm, crossed, coplanar fed reflector IRA (Giri and Baum, UWB, SP Electromagnetics 3, Baum, et al., Eds., pp. 65-72). Previously, the feed configuration of such antennas have been optimized by considering the power normalized gain  $G_p$  and voltage normalized gain  $G_v$  defined by Farr and Baum (Sensor and Simulation Note 354, January 1993), both of these metrics have units of length and can be used to compare the performance of antennas under constant input power and voltage conditions, respectively. Buchenauer, et al., (Sensor and Simulation Note 421, November 1997) introduced a concept of prompt aperture efficiency that is related to power normalized gain. This metric is dimensionless, and allows for the comparison of classes of IRAs regardless of physical size.

In this paper, the aperture efficiency is used to optimize the feed arm configuration of 4-arm IRAs. Traditionally, such IRAs have been fed by perpendicularly crossed feed arms that can be analytically treated. The current configurations allow for an arbitrary angle between the planes containing the feed arms. Such geometries have not been solved in closed form, but by using the finite element method, the TEM mode distribution can be determined and the various antenna parameters computed.

The following results are provided by the analysis. First, the aperture efficiency can be increased from ~25% for the 200W, perpendicularly crossed feed structure to ~35% for the optimum case where the feed arms make an angle of 70° with respect to the horizontal symmetry plane. Second, a unique optimum feed arm angle exists for any specified input impedance. These results allow the performance of UWB systems to be significantly improved by modifying the antenna without affecting the other components of the source.

## 54.3

### Admittance of Bent TEM Waveguides in a CID Medium

Baum, C.E<sup>1</sup>

<sup>1</sup>Air Force Research Laboratory DEHP, USA

Various solutions have been developed for the propagation of TEM waves in an inhomogeneous dielectric medium with permittivity  $\epsilon$  proportional to  $\Psi^2$  in a cylindrical  $(\Psi, \phi, z)$  coordinate system with propagation in the  $\phi$  direction. Experimental work is underway to approximately synthesize such a medium with guiding conductors to form a TEM-transmission-line bend. There are also cases of TEM waves propagating in other directions in such a medium. The general procedures are differential-geometric lens synthesis as discussed in C.E. Baum and A.P. Stonc. *Transient Lens synthesis: Differential Geometry in Electromagnetic Theory*. Taylor & Francis, 1991. This medium then has very special properties. So let us give it a name: cylindrically-inhomogeneous dielectric or CID for short.

This paper considers the effect on the characteristic admittance of bending a TEM waveguide with the uniform dielectric medium replaced by a CID medium which preserves the TEM character of the propagation. First some general properties of guides with certain symmetries in their cross sections are considered, showing a second order correction in terms of bend curvature. Canonical H-plane and E-plane bends are solved in closed form. The case of a bent circular coax is solved up through second order in curvature. The H-plane and coax bends show an increase of the characteristic admittance over that of the straight waveguide with  $\epsilon$  taken as  $\epsilon_m$ , the permittivity in the center of the bent guide. However, the two-conductor version of the E-plane bend shows no change in the characteristic admittance with bending; the three-conductor version shows some increase with bending.

## 54.5

### Transient Fields of Offset-fed Paraboloid

Skulkin, S<sup>1</sup>; Turchin, V<sup>2</sup>

<sup>1</sup>Radiophysical Research Institute, Russia; <sup>2</sup>Institute of Applied Physics, Russia

#### Introduction

Transient fields radiated from aperture antennas was usually calculated for simple planar apertures or prime-focus reflector antenna [C.E. Baum et. al, Review of Radio Science 1996-1999, 403-439, 1999]. However last decades of 20th century introduced a lot of improvements in the design of reflector antennas. For some practical application it is interesting to consider transient fields radiated from other reflector antennas geometries. This paper describes transient fields radiated from offset-fed parabolic reflector antenna taking into account the polarization effect.

#### The techniques

For transient field calculation we use the technique described in [S. P. Skulkin, V. I. Turchin, in book *Ultra-Wideband, Short-Pulse Electromagnetics*, Plenum Press, 81-87, 1996]. The technique is based on the assumption that short pulse is radiated by a small feed that attaches to a shaped reflector surface. We also assume that antenna size is much more than maximal wavelength respective to the minimal frequency of the pulse spectrum. In this case the reflector surface current can be calculated only by the use of the feed magnetic field. The strict formulas were obtained for field in the half-space before the antenna.

#### Results and Conclusions

We show results obtained for orthogonal components of electric field radiated from off-set paraboloid and discuss the properties of this field. We also compare calculation results obtained for offset-fed reflector symmetrical parabolic reflector, circular and rectangular plane apertures. We illustrate that the structure of the spatial-temporal field distribution is quit complex, especially in the near-field region. We show and discuss the difference between transient fields of different aperture antennas. We discuss the problem of diffraction at the edge of the reflector and show the influence of edge-diffraction currents to transient fields.



## 55.1

### Generalized TM and TE Modes in Transient Lens Design

*Stone, A<sup>1</sup>; Baum, C E<sup>2</sup>*

<sup>1</sup>University of New Mexico, USA; <sup>2</sup>Air Force Research Laboratory, USA

In the design of waveguide transitions, we desire to transmit a TEM wave, ideally with no reflection or distortion, from one transmission line to another. Such waveguide transition regions are usually referred to as EM lenses, or more specifically, transient lenses. This goal is accomplished by specifying the lens geometry and constitutive parameters (i.e., the shape and medium of the EM lens). The physical properties of these lenses, given by the permeability and permittivity, may be a function of position, but we assume that these properties are frequency independent. The conductivity of the medium is taken to be zero, and cross sectional dimensions are large compared to the wavelengths at the high frequencies of interest, in contrast to a lens such as the Luneburg lens or Maxwell fish eye, both of which are based on a geometric optics approximation.

Exact solutions to lens design problems have been obtained by the method of differential geometric scaling. The basic idea in the scaling method is the creation of a class of electromagnetic problems, each with a complicated geometry and medium, which are equivalent under the scaling to an electromagnetic problem with a simple geometry and medium. Solutions to Maxwell's equations can then be used to specify various types of lenses.

Recent results concerning generalized inhomogeneous TEM plane waves have been useful in determining acceptable orthogonal curvilinear coordinate systems that imply lens designs. In general, we seek conditions on the media parameters which, in the formal parameters in  $(u_1, u_2, u_3)$  orthogonal curvilinear coordinates, will allow certain modes (TEM, TM, or TE) to exist. Specifically, in this paper, we consider the case of a TM wave propagating in the  $u_3$  direction and look for conditions on the media parameters that lead to solutions of the formal Maxwell equations. Differential geometric scaling will then lead to specific lens designs. In the E-mode case, the media constraints are similar, but more restrictive, than those obtained in the limiting case of a TEM mode. The analysis in the case of H-modes is, of course, dual to that of the case of E-modes.

## 55.3

### Spatial-temporal Solitons in a Planar Microwave Guide

*Arnold, JM<sup>1</sup>*

<sup>1</sup>University of Glasgow, UK

Temporal and spatial solitons are now well-established phenomena in the field of guided-wave nonlinear optics. Temporal solitons, in which dispersion balances nonlinear pulse narrowing, are well known in optical fibres, and recent intensive projects have investigated their potential for high-bandwidth transoceanic communications using picosecond pulses. Spatial solitons, in which in-plane diffraction is balanced by nonlinear self-focussing in a planar waveguide, have been less widely investigated, but nevertheless form an experimentally proven method of promoting self-trapping and self-steering waveguide channels in a nonlinear medium under CW conditions. The combination of temporal and spatial soliton formation (spatial-temporal solitons) would have far-reaching consequences for the realisation of all-optical digital switching, but practical demonstrations have proved elusive because of the high optical intensities required.

Temporal solitons in the microwave domain have been studied experimentally in only a few isolated cases. Microwave solitons have been demonstrated in transmission lines loaded with Schottky barriers, and in magnetostatic waves in thin magnetic films. Microwave transmission line solitons derive from fundamental mathematical properties of the Korteweg-de Vries or Boussinesq equations. There are no experimental demonstrations of microwave spatial solitons.

In this paper it is shown theoretically that baseband microwave spatial-temporal solitons can be realised in a planar geometry consisting of a simple parallel-plate waveguide loaded with MOS capacitors to provide the required nonlinearity. This geometry gives rise, in the paraxial approximation, to the Kadomtsev-Petviashvili equation, which is a completely integrable nonlinear PDE having exact spatial-temporal soliton solutions (J. M. Arnold, *Optical and Quantum Electronics*, Special issue: Spatial solitons, 30, 631-647, 1998.) Some implications for the engineering of such solitons will be examined, including practical schemes for realising self-switching of two solitons on ultra-fast (picosecond) time-scales.

## 55.2

### Electromagnetic Wave Scattering by Smooth Imperfectly Conductive Cylindrical Obstacle

*Tuchkin, Y<sup>1</sup>*

<sup>1</sup>IRE NANU, Ukraine

New strong in mathematical sense and numerically efficient method for investigation of two-dimensional boundary value problem of electromagnetic wave diffraction by infinite and homogeneous in longitudinal direction imperfectly conductive cylinder of arbitrary smooth cross section is suggested. The imperfect conductivity is modelled by the boundary condition of the third kind, for example, by Leontovich condition with impedance, which is supposed to be an arbitrary smooth function of points of the obstacle cross section contour.

The method of investigation is based on generalisation of Analytical Regularisation Method, which is developed in our previous papers. As a result of analytical regularisation procedure constructed, the boundary value problem under consideration is equivalently reduced to a few different equations of the second kind in space of square summable sequences.

A few qualitatively different cases are considered. The simplest one corresponds to regular perturbation of Neumann boundary value problem. Much more interesting and hard case is singular perturbation of Dirichlet boundary value problem, when there is arbitrary small (tending to zero) coefficient before normal derivative in the boundary condition. It corresponds to E-polarised wave diffraction by well-conductive obstacle. In that case we managed to reduce the main singular part of corresponding integral-differential equation to singularly perturbed ordinary differential equation of the second order: with small coefficient before the senior - the second derivative. After that, utilisation of well known for such equations technique enables us to construct the relevant analytical regularisation procedure for the boundary value problem of the third kind under consideration. Moreover, the corresponding perturbation theory power series with small parameter coming from impedance boundary condition is constructed.

In very many practical and engineering applications the correction given by the first term of this series is sufficient for necessary estimation with good accuracy the ohmic losses of well-conductive obstacle by means of the solution of diffraction problem for perfectly conductive obstacle of the same shape. The last problem is much simpler and efficiently solvable numerically in comparison with the original one.

## 55.4

### A Set of Exact Explicit Solutions in Time Domain For UWB Electromagnetic Signals in Waveguides

*Tretyakov, O'*

*<sup>1</sup>Kharkov National University, Ukraine*

In this presentation, two subjects are submitted. The first one is summary of a new Evolutionary Approach for Electromagnetics (EAE) in Time Domain (TD). EAE has been developed as a TD alternative to the classical Method of Complex Amplitudes oriented exclusively on the Frequency Domain. Our approach covers study of steady state and transient, linear and nonlinear electromagnetic phenomena from a uniform methodological position in TD directly. Development of EAE we start with separation of a linear self-adjoint operator from general Maxwell's operator. The latter is nonlinear in the general case due to the constitutive relations involved. The operator separated consists of a matrix differential procedure with respect to two coordinates orthogonal to waveguide axis, and the algebraic operations from the boundary conditions at the perfectly conducting waveguide surface. The self-adjoint operator has an eigenvector set which originates a basis in a Hilbert space of vector functions of the transverse coordinates. Electromagnetic field sought is presented as the eigenvector series. That corresponds physically to the field decompositions in terms of the natural waveguide modes. Coefficients (depending on the longitudinal coordinate  $z$  and time  $t$ ) at these series are equivalent physically to the modal amplitudes. Projecting of input Maxwell's equations onto the same basis elements supplies a system of partial differential equations with respect to those amplitudes. These equations may be linear or nonlinear as the constitutive relations for electromagnetic field in a possible medium filling the waveguide dictate it. In fact, these differential equations are evolutionary. Jointly with appropriate initial conditions for the modal amplitudes, they originate well-studied Cauchy problem for partial differential equations.

The second topic is presentation of a variety of new exact analytical solutions in TD for electromagnetic signals in a waveguide of arbitrary cross section. That gives an impression about a scope of EAE. In the case of a hollow waveguide, analysis of the evolutionary equations

for the modal amplitudes is converted to study of standard unidirectional Klein-Gordon equation with  $z$  and  $t$  variables. Twelve exact explicit solutions have been found, and ten among those are new for electromagnetic field waveguide theory. They correspond physically to UWB signals. In the case of a waveguide filled with a medium with permittivity and permeability depending on  $z$  and  $t$ , a new generalized form of unidirectional Klein-Gordon equation has been obtained, and another twelve new exact analytical solutions have been found. The problem of waveguide excitation by some TD signal is also considered. In particular, a very simple analytical solution has been obtained when excitation of a waveguide is arisen by a UWB signal like Heavyside step function of time.

## 55.5

### Wave Diffraction by Chiral Media Gratings: Analytical Regularization Approach

*Poyedinchuk, A E'; Khizhnyak, A N'*

*<sup>1</sup>Usikov's Institute of Radiophysics Electronics, Ukraine*

Artificial media, which display chiral properties in the microwave range, have been constructed comparatively not long ago. Creation of wave absorbing surfacing and their applications as components of microwave range technique are apparently the most perspective spheres of usage. In connection with aforesaid the necessity of developing the theory of wave diffraction by the open structures with artificial chiral media is arises.

We elaborated the method to solve the problems of diffraction of harmonic waves by the plane perfectly conducting strip gratings, which are disposed on the boundary between chiral layers. The main idea of the method is the following: original problem is reduced to the system of dual summity equations of the I kind for Fourier coefficients which define the electromagnetic field in the chiral media. The regularizing operator in exclusive form has been constructed for these equations. The operator constructing procedure is based on analytical solving of vector Riemann-Hilbert problem for two analytical functions. In the issue the original problem has been reduced to an infinite system of linear algebraic equations of the II kind. Numerical algorithms to solve the matrix equations have been developed. Some numerical experiments to investigate the scattered fields that are formed by grating and layers have been provided.

It is shown that under the condition of normal ( $k$  is perpendicular to the plane of layers) incidence of linearly polarized wave the reflected field is elliptically polarized. It is established that the scattered field amplitude strongly depends on the resonance phenomena and redistribution energy processes when the propagating harmonics quantity essentially differs in different chiral layers.

## 56.1

### Observations Concerning UXO Removal Efforts on the Former Fort Ord

*Maruyama, X K'*

*<sup>1</sup>Institute for Joint Warfare Analysis, USA*

The former Fort Ord is a Base Realignment and Closure (BRAC) site comprising approximately forty square miles in Monterey County, California, located 120 miles south of San Francisco. Initially, it was thought that this former Army base would very rapidly become an integral part of the economic infrastructure of this area. A new campus for California State University was created almost immediately after the base closure and local governmental and non-governmental agencies quickly laid claims to properties on the former Fort Ord. The U.S. Army and its representative agencies have been attempting to proceed to clean-up the site, but have encountered many obstacles in their efforts. Very few of the obstacles are strictly technical in nature. Competing political, economic, environmental and sociological interests impose most of the challenges. As a resident of Monterey, I have observed the developments at Fort Ord and, since the local community is effectively a "small town", many of the parties involved can be personally known through other social and economic interactions. Most "textbook" presentations of the clean-up process present the impression that there are coherent entities, the military, the local political jurisdiction, and citizen groups lumped together as "stakeholders", participating as parties to the clean-up effort. The realities concerning Fort Ord clean-up are much more complex. The Army must contend with the interests of well over a dozen governmental entities each with their spheres of influence and taxing authority. The public interest groups form fluid coalitions and rivaling factions depending upon the issues at stake. Clean-up priorities are set politically and can change fairly rapidly leaving the clean-up agents without the ability to address problems in a coherent and timely manner. Certain groups desire rapid economic development, whereas others would rather see no development. Vegetation clearance to expose unexploded ordnance must contend with requirements to preserve various native animal and plant species of concern and to minimize human exposure to smoke produced by fires. Pressures to avoid litigation have led to decisions making later reactions more complex.

In this presentation, examples of clean-up topics, which contain competing and sometimes emotional issues, will be enumerated.

## 56.3

### Range Delineation Techniques used in the Panamanian Jungle

*Thomsen, K<sup>1</sup>; Dauchy, J W<sup>1</sup>; Valder, K<sup>1</sup>*

<sup>1</sup>Tetra Tech EM Inc., USA

The Empire, Balboa West, and Pina Ranges located, in the Panama Canal Zone, were transferred to the Panamanians at the beginning of this year. In preparation for this transfer, several investigations were focused on the range impact zones and on buffer areas having unknown ordnance density, to refine the boundaries that were previously defined during a 1995 effort. The 1995 effort resulted in a mapping of range firing fans and impact zones based on information collected during an archive search.

The boundary analysis of the range impact zones was conducted by instituting surface and subsurface investigations at portions of the ranges. Data collected during these investigations were consolidated and evaluated to confirm the unexploded ordnance (UXO) density boundaries identified during the 1995 study or to identify and recommend new boundaries. This paper describes the techniques used to collect the data.

To assess site investigation parameters, including target accuracy and precision, several controlled data points were established, and the investigation subcontractor conducted blind surveys of the areas containing the control points. In addition, a number of investigator target declarations were excavated to assess the investigator's ability to discriminate between subsurface UXO and other anomalies.

Range data were collected by cutting transects through the jungle and surface-clearing transects as they were being cut. Transects were then surveyed for UXO and UXO-related material using best available technology. Traditional survey techniques were used to identify exact locations of transects and recognized anomalies. Logistics problems encountered in preparation of conducting the field work, the difficulty of conducting UXO surveys in the Panamanian jungle, and boundary analysis results are also discussed.

## 56.5

### Ultra-Wideband Synthetic Aperture Radar for Detection of Unexploded Ordnance: Modeling and Measurements

*Carin, L<sup>1</sup>; Sullivan, A<sup>2</sup>; Dong, Y<sup>1</sup>*

<sup>1</sup>Duke University, USA; <sup>2</sup>Army Research Laboratory, USA

Although radar-based subsurface sensing is an old technology, until recently there has been very little rigorous modeling done to characterize the target response as a function of frequency, polarization, incidence angle, target geometry and soil type. In previous work, we initially restricted ourselves to those targets that had body-of-revolution (BoR) symmetry, thereby significantly reducing the computational complexity of the problem. For unexploded ordnance (UXO) targets, whose shape and orientation in the soil may be completely arbitrary, the BoR analysis is inappropriate. In the work presented here, we therefore consider a MoM analysis for arbitrary perfectly conducting targets in a layered medium, with the lossy, dispersive layers representing the typical layered character of many soils. In addition to the aforementioned MoM model, we have developed fast multipole method (FMM) and multi-level fast multipole algorithm (MLFMA) models for electrically large conducting targets above or embedded within a lossy half space. The FMM and MLFMA schemes are particularly important at higher frequencies, for which the MoM is computationally less efficient.

Synthetic aperture radar images from actual UXO are presented for data collected with the US Army Research Laboratory BoomSAR, a fully polarimetric experimental radar system, characterized by four TEM antennas placed atop a 40 m boom lift. The measurements have been performed in Yuma, AZ and at Eglin Air Force Base in northern Florida (both in the United States). The BoomSAR operates directly in the time domain, covering an instantaneous bandwidth of 50-1200 MHz. Several comparisons are made between measured and computed SAR images, the latter simulated via the MoM forward solver.

## 56.4

### Detection of Buried Ordnance Using 3D EM Rendering

*Hjelmstad, J<sup>1</sup>*

<sup>1</sup>Norwegian University of Science Technology, Norway

Ground penetration radars generally suffer from pure image fidelity and high false alarm rates. The current contribution suggests an iterative processing method based on data from ultra-wide bandwidth, such as the the RadioSTAR, the polarimetric phased array synthetic aperture radar being developed at the author's laboratory. The processing technique is based on the existence of a plurality of image generation processes, each with specific capabilities in terms of resolution in space and wavenumber, coverage, speckle noise content and other parameters. This plurality of 3D images is combined in an adaptive process to yield a situation awareness representation which is robust in terms of imaging and classifying targets. This process mimics the operation of the human eye which through various sensor mechanisms and image formation processes aided with a priori knowledge stored in the brain gives the brain a detailed awareness representation.

The contribution gives a heuristic introduction to the theory and architecture of 3D EM rendering and presents the suggested implementation in the RadioSTAR programme.

## 57.1

### Broadband High Power Free Electron Maser Amplifier Experiments

*Whyte, C<sup>1</sup>; Jaroszynski, D A<sup>1</sup>; Cross, A W<sup>1</sup>; He, W<sup>1</sup>; Ronald, K<sup>1</sup>; Young, A<sup>1</sup>; Phelps, A D R<sup>1</sup>*

<sup>1</sup>University of Strathclyde, UK

We present results from a reversed guide magnetic field Raman Free Electron Maser (FEM) amplifier experiment at Strathclyde University. The FEM has been designed to achieve maximum power over the largest possible instantaneous bandwidth. The amplifier tuneability has been further extended by adjustment of beam voltage.

A 1kW TWT has been used as the input source for broadband measurements. Results show instantaneous -3dB bandwidth of 30% for a fixed cathode voltage and magnetic field values. The device can be tuned over a range of 70% of the centre frequency by adjusting the cathode voltage. Amplifier saturated gain of 30dB has been measured, giving a peak output power of over 0.5MW. Higher gain can be achieved at lower input power levels.

Two 25kW magnetrons were employed in measurements of the saturated output power at discrete frequencies. The maximum output power achieved to date at a single frequency was 2MW with 23dB gain at an efficiency of over 10%.

A single stage depressed collector for DC operation has been designed. Operation with a depressed collector will considerably increase the overall efficiency of the FEM amplifier and establish the device as practical high power device.

An experiment using a 50A beam from a thermionic cathode electron gun designed at Strathclyde is currently in progress. This will theoretically allow DC operation of the FEM using a DC undulator magnet.

British Crown Copyright 2000. Published with the permission of the Defence Evaluation and Research Agency on behalf of the Controller of HMSO.

## 57.2

### Effective Coupling of "CARM" and "Gyrotron" Modes on a Phase-Synchronized Electron Beam

*Savilov, A<sup>1</sup>; Bratman, V<sup>1</sup>; Samsonov, S<sup>1</sup>; Phelps, A<sup>2</sup>*

<sup>1</sup>Russian Academy of Sciences, Russia; <sup>2</sup>University of Strathclyde, UK

There are two main ways for the frequency enhancement in Cyclotron Resonance Masers (CRMs). The first one is achieving a large Doppler up-conversion of the electron cyclotron frequency in the Cyclotron Autoresonance Maser (CARM), which is based on excitation of a traveling RF wave propagating along the operating magnetic field with a phase velocity close to the speed of light. The second way is the operation at high cyclotron harmonics in the relativistic gyrotron (a type of CRM based on excitation of a near-cutoff wave). According to the theory, the important advantage of the CARM can be a high electronic efficiency. However, most CARM experiments demonstrate relatively low efficiencies. This is caused, in particular, by a strong sensitivity of the CARM to the spread in electron velocity, as well as by problems in the formation of high-quality beams of relativistic electrons oscillating in magnetic field. As for the high-harmonic relativistic gyrotron, its efficiency decreases with the increase of the harmonic number. However, its advantage is a stable and selective excitation of a near-cutoff mode in a simple cavity.

In this work, we propose a device which could combine the advantages of the CARM and the relativistic gyrotron. Its principle is based on the fact that a beam of phase-synchronized cyclotron oscillators can provide an effective interaction between two modes excited at the same frequency. Namely, we consider the "CARM" TE<sub>1,1</sub> and "gyrotron" TE<sub>2,1</sub> modes of a cylindrical cavity, which are excited by an axis-encircling electron beam at the fundamental and second cyclotron harmonics respectively. In such an oscillator, both modes are excited simultaneously in a single cavity, being a piece of cylindrical waveguide with cut-off narrowings at the input and output. Such a simple cavity is closed for the near-cut-off "gyrotron" mode. Correspondingly, the quality of this mode is very high and defined basically by ohmic losses in the cavity walls. At the same time, the slight output narrowing practically does not reflect the

traveling "CARM" mode. Therefore, this cavity provides an effective and selective feedback for the "gyrotron" mode only. The operating "CARM" mode is excited due to the proper electron bunching caused by the "gyrotron" mode and provides a high electronic efficiency. The output radiation is formed by the "CARM" mode only; the power of the "gyrotron" mode is dissipated in the cavity walls. Along with simplicity of the microwave system, this scheme solves the problem of the mode control, which is very important for CARMs. The stable generation of the "gyrotron" mode can fix the frequency of the operating "CARM" mode.

## 57.3

### High-current Magnetized REB Generated by a Field-emission Cathode, with the Geometry and Angular Spectrum Invariable during Microsecond Intervals.

*Loza, O. I<sup>1</sup>; Ivanov, I. E<sup>1</sup>*

<sup>1</sup>General Physics Institute, Russia

Our previous studies allowed to generate a high-current relativistic electron beam (REB) with stabilized shape: see [O.I.Loza, P.S.Strelkov, "Generation of an annular REB of microsecond pulse duration and stabilized transverse dimensions in a diode with a field-emission cathode". Proc. of 12-th Int. Conference on High Power Particle Beams, Haifa, Israel, June 7 - 12, v.1, p.357-360, 1998]. The investigation was carried out using an annular REB with electron energy 500 keV, total current 2 kA, radius 2 cm, thickness ~ 3 mm during 1-ms pulse. The beam was generated on the field-emission cathode in the magnetically-insulated diode. The beam propagated in homogeneous magnetic field 1 T.

For the REB with the geometry invariable during microsecond time intervals, time- and spatially-resolving study of the REB phase portrait is of interest, namely, the investigation of electron velocities. This study is feasible due to the proposed method of measurement of the beam electrons distribution over pitch-angles (the angles between electrons velocities and the guiding magnetic field). The method admits application in case of strong magnetic field and allows to distinguish small pitch-angles (e.g., to measure a distribution from 0 to 20 degrees with the accuracy ~ 1 degree). Besides, the method is suitable for use with microsecond REBs, because it allows to significantly diminish the influence of parasitic plasma (creating on the monitor diaphragm) on the measurement results.

The practical result of the research is the following. The designed electron gun is able to generate a high-current REB from a field-emission cathode, and in the course of its propagation in a strong magnetic field this beam preserves both its annular shape and, according to the tentative results (autumn, 1999), small pitch-angles of electron trajectories during a microsecond. Such an electron beam may be used in high-power microwave devices of microsecond pulse duration, and the electron beam properties can not be the reason for the known effect of "high-power microwave pulse shortening".

## 58.2

### Wide-band Evaluation of the Influence of Power Frequency Magnetic Fields of Transformer Stations

*Karpowicz, J<sup>1</sup>; Gryz, K<sup>1</sup>*

<sup>1</sup>Central Institute for Labour Protection, Poland

**Key words:** environment protection, magnetic field 50 Hz, transformer stations

Transformer stations are located in many buildings (in Poland: 160 kVA to 1000 kVA, 15/0.4 kV, 50 Hz). Supply bus-bars and cables of low voltage are the main source of power frequency magnetic fields around those installations.

The influence of magnetic fields on the environment is evaluated according to permissible exposure values established by regulations: wide-band frequency dependent (like IRPA's formula for threshold value -  $\frac{500 \mu T}{f \text{ Hz}}$ ) or

selective (for power frequency). In Poland, for frequencies from 1 Hz to 1 kHz, there is an established permissible level of a magnetic field for the frequency of 50 Hz only. It is 100  $\mu T$ , the same value as in IRPA's formula. IRPA's formula indicates that evaluation of magnetic fields should include higher harmonics of power frequency, too.

Results of measurements of the spectrum of the magnetic field surrounding transformer stations and the r.m.s. value of the field, done by the authors of this paper in a few hundred cases will be presented. Spectral measurements are done with a special calibrating antenna and a real time spectrum analyser. There are magnetic fields of up to 25  $\mu T$  (r.m.s. value) in rooms next to transformer cells. Inside the transformer stations, near the supply bus-bars and cables, magnetic fields can exceed 500  $\mu T$ . The spectrum of the magnetic field surrounding transformer stations contains uneven harmonics. In many cases the 3rd harmonic can reach 30 %. The harmonics higher than the 15th are below 1 %.

Magnetic fields present in rooms next to transformer stations, when evaluated only on the basis of selective criteria for 50 Hz, can be considered an insignificant hazard. In most cases, they are at least 50 times lower than the permissible level.

It will be demonstrated that proper evaluation on the basis of selective measurements and the criteria for 50 Hz (independently of the field spectrum) can be done for weak magnetic fields (up to 10  $\mu T$ ) only. For stronger fields, the spectrum of frequency should be regarded indispensable because permissible levels change inversely proportionally to the harmonics number. Evaluation including harmonics can be 3-4 times more restrictive than for 50 Hz only. This result is determined by harmonics up to the 13th.

The results can be significant in epidemiological studies connected with exposure to power frequency magnetic fields and for establishing a proper measuring method and evaluations for environmental monitoring.

## 58.3

### Studies of the Biological Effects of Ultrawide Band Emissions

*Merritt, James H<sup>1</sup>; Beason, Charles<sup>1</sup>; Murphy, Michael R<sup>1</sup>*

<sup>1</sup>United States Air Force Laboratory, USA

Ultrawide band (UWB) radiation has the potential for many applications including radar, communication systems, and electronic warfare. UWB pulses are characterized by picosecond rise times and a few nanosecond pulse widths, with peak E fields of up to hundreds of kilovolts/meter. Safety guidelines for personnel protection from radio frequency radiation are based upon thermal considerations, but concerns have been raised that the transient UWB pulses might induce bioeffects, perhaps harmful ones, that would not induce thermal heating. Because of these concerns, the Air Force Research Laboratory has undertaken a series of studies related to the effects of exposure to UWB on test animals. These wide-ranging studies examined a variety of biological endpoints, from behavior to effects upon the fetus to cardiovascular studies. In addition to studies carried out at our laboratory, colleagues in the U. S. Army Medical Research Detachment's Microwave Bioeffects Branch, also located at Brooks Air Force Base, have carried out other studies of UWB bioeffects. Animal species tested include the rat and the rhesus monkey. A number of UWB sources have been used in these investigations including the Hindenberg-2, Bournlea, Kentech, and a source built by Sandia Corp. Peak E fields ranged up to 250 kV/m for the Hindenberg-2. A long-term study, consisting of weekly exposure over a 16-week period, with follow-up over 18 months, has been completed. This study used a mouse mammary tumor animal model and was designed to determine the possibility of long-term exposure on the potential for the promotion of cancer. No effect of these exposures was noted on carcinogenesis. Other studies showed no effects on behavior as a result of exposure. Studies on neonates, exposed in utero, showed an increase in ultrasonic vocalizations. Studies of blood pressure in rats exposed to peak E fields of 100kV/m revealed a hypotensive effect. For the most part the bioeffects revealed in these studies suggest none to few potential health consequences from exposure to UWB, even at levels far in excess of those humans are likely to encounter. Follow-up studies on cardiovascular effects of exposure are planned.

## 59.2

### A New Broad Band 2D Antenna for Ultra-Wide-Band Applications

*Imbs, Y<sup>1</sup>; Andrieu, J<sup>1</sup>; Beillard, B<sup>1</sup>; Gallais, F<sup>1</sup>; Mallepeyre, V<sup>1</sup>; Jecko, B<sup>1</sup>; Le Goff, M<sup>2</sup>*

<sup>1</sup>Université de Limoges, France; <sup>2</sup>CELAR (DGA), France

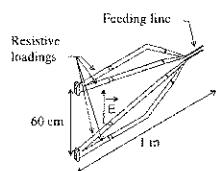
A new wide band antenna radiating short pulses has been designed by the IRCOM for mine detection. The complete system has been developed by the CELAR and is presented in a separate paper.

The theoretical study of the antenna is carried out using a space-time integral equation. This rigorous method uses analysis of the currents induced by the pulse generator on the wire antenna. The electric and magnetic fields are deduced from the knowledge of the currents on the wire structure.

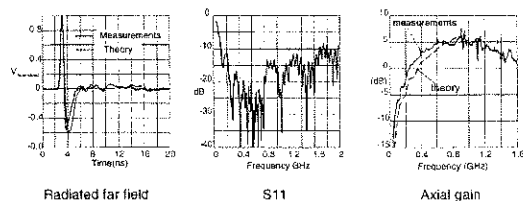
To improve the short pulse radiation, resistive loadings are used along the arms of the antenna. The non-reflecting principle permits also a better input matching.

The essential electromagnetic characteristics are:

- A low pulse distortion (<1.4 for a 150 ps rise time and 700 ps duration generator pulse)
- A wide band matching (-10 dB from 100 MHz to 1.7 GHz)
- A gain reaching 5 dB at 800 MHz.



These measurements have been obtained with the help of a 50Ω to 200Ω balun manufactured by the Europulse Company (Lot, France).



The radiation presents side lobes in the E-plane (antenna plane) at 8 dB below the main lobe level (at 500 MHz). The rear radiation is 15 dB below the axial level. The cross polarisation is very low due to the symmetry of the structure.

In conclusion, the 2D structure permits interesting radiation results for a very small volume, so that it can be used for the constitution of a 1 or 2-D array to improve gain and directivity.

## 59.1

### Design, Fabrication and Testing of a Reflector Type of an Impulse Radiating Antenna

*Nitsch, D<sup>1</sup>; Karathaeuser, H G<sup>1</sup>; Giri, D<sup>2</sup>*

<sup>1</sup>Germany; <sup>2</sup>USA

Abstract not available

## 59.3

### Time Domain Array Design

*Schantz, H<sup>1</sup>*

<sup>1</sup>Time Domain, USA

A short pulse ultra-wideband system imposes different constraints on array design than the usual continuous wave narrow band system. The goals of this paper are threefold: to explore these differences, to show how to model a short pulse array, and to discuss how best to graphically describe the performance of an ultra-wideband antenna system. First, this paper will discuss the differences between narrow band and wide band array design. The implications of wide band/short pulse systems to such array properties as grating lobes will be considered.

Second, this paper will discuss how to model short pulse arrays under the assumption that there is no mutual coupling between elements. As an example, the behavior of a particular end fire array will be calculated and compared to experimental measurements.

Finally, traditional narrow band depictions of antenna performance are ill-adapted for ultra-wideband radiators. Several alternate methods will be presented, including portrayal of the angular dependence of peak instantaneous power, the angular dependence of average power, and the angular dependence of the time domain pulse waveform.

## 60.5

**Transient excitation of a layered dielectric medium by a pulsed electric dipole: spectral representation.**

*Tijhuis, A<sup>1</sup>; Bretones, AR<sup>2</sup>*

<sup>1</sup>Eindhoven University of Technology, Netherlands; <sup>2</sup>Universidad de Granada, Spain

In two companion papers, we consider the transient excitation by a pulsed vertical or horizontal dipole of a continuously layered, lossy dielectric slab embedded in between two dielectric half-spaces. The focus of our work is on developing a highly efficient numerical implementation. In particular, this concerns the inverse spatial Fourier transformation in the Sommerfeld-Weyl representation of the fields and the evaluation of the spectral constituents. The basic idea is that, under realistic restrictions on the transient behavior of the impressed current or incident field, all spatial approximations may be chosen independently of the frequency.

In this paper, we consider the spectral representation. The key idea is to normalize the spatial wavenumber with respect to frequency. Compared with the Cagniard-De Hoop method, our approach is different in the sense that we keep the frequency real, and allow the time variable to become complex. In this respect, our work also resembles the spectral theory of transients. In the normalized wavenumber plane, the spectral constituent has two types of singularities. In the first place, there are two branch cuts, associated with the choice of the "physical" root in the attenuation coefficients for the external medium. Second, we need to consider the occurrence of so-called guide-wave poles. For a lossless configuration, such poles only occur on a finite interval on the real axis. For a lossy slab, the poles occur in the first quadrant of the plane, and approach the same interval in the large-frequency limit. Problems occur in the determination of the spectral constituents in that interval, since the spectral wave equation has homogeneous solutions.

We restrict the temporal Fourier inversion to nonnegative frequencies by expressing the time-domain signal as the real part of a dual analytic signal. Reversing the order of the temporal and spatial Fourier inversions then leads to the so-called time-domain Weyl

representation for the reflected field. In this representation, the accumulated guided-wave poles give rise to an additional branch cut. The representation thus obtained is used to derive a suitable combination of Gaussian quadrature rules for the evaluation of the spectral integral. Compared with an evaluation by FFT operations, this has the advantage that the number of values for which the spectral constituents must be computed is reduced considerably.

## 61.1

**Electromagnetic Technology Developments for the Detection of UXO in North America**

*Bowers, J.R<sup>1</sup>*

<sup>1</sup>UBX International Inc, USA

The use of electromagnetic (EM) techniques in combination with digital mapping is one of the most common methods of locating unexploded ordnance (UXO) in North America. Currently, there are several different EM devices commonly in use to locate ordnance. These include both frequency domain EM that is primarily used to locate pits and trenches and time domain EM that is used to locate individual UXO items. Different manufacturers are developing monostatic broadband EM sensors and multiple time gate EM sensors to better discriminate different types of UXO from metallic scrap that is found on ordnance ranges and other areas containing UXO. Additionally, the use of differential GPS, and other location systems as well as the use of digital mapping techniques has greatly increased the likelihood of detecting UXO from the days of "Mag and flag". This combined with GIS software has put more control into the hands of the project managers running UXO projects as well as increasing the overall effectiveness of the UXO surveys. This paper examines ongoing EM sensor development for the location of UXO in North America as well as associated digital mapping activities.

## 61.3

**Evaluation of Potentials and Efficiency of Ultrawideband Radars for Remote Probing (GPR and/or FOLPEN) with use of Short Pulses at High Repetition Frequencies**

*Kardo-Sysoev, A<sup>1</sup>; Astanin, L<sup>2</sup>*

<sup>1</sup>Ioofe Physico-Technical Institute, Russia; <sup>2</sup>Pulse Systems Group, Russia

Usually, ultrawideband (UWB) long range radars exploit nano and picosecond pulses of peak power 1-10 MW and low pulse repetition frequency (PRF) less than 1 kHz. Such signals are easy to be processed at the receiving end (received signal represents a pulse response of the target) but they cause a lot of such problems, as to prevent breakdowns of feeders and antenna as well as to prevent interference with surrounding electronic equipment.

In recent years, small power UWB short pulse signals at high PRF > 10 MHz have been used in communication systems. The most promising coding for this application is time-position coding.

Such signals are very promising, as well, for long range UWB radars: FOLPENS and GPRs. But the absence of pulse sources with needed powers, PRF and very high time stability constrained development of such radars.

The current work is dedicated to evaluation of the potential of such signals for GPRs and FOLPEN UWB radars, based on the last achievements in the art of all solid state short pulse high PRF generation.

It was shown that very high energy potentials may be realized in this case, providing lower interferences with other electronic equipment. Far lower peak powers lead to simplification of a transmitter and antenna design, as well as improvement of ecology environment. The use of time-position coding and antennae aperture synthesis are considered. Active antenna array with developed synchronized set of pulsers provides needed antenna power and pattern.

## 61.4

### Relationship of Probability of Detection (Pd) Critical Radius Factor (Rcrit) to Background Clutter and Environmental Factors

*Dauchy, Joseph W<sup>1</sup>; Thomsen, Kurt O<sup>1</sup>*

<sup>1</sup>Tetra Tech EM Inc., USA

Over the last 10 years there has been a strong push to advance the "state-of-the-art" of geophysical sensor equipment used for the detection of subsurface unexploded ordnance. Along with this proliferation of equipment there is a need to evaluate effectiveness and provide a metric for improved performance. The preferred performance metric for the detection of unexploded ordnance has been probability of detection (Pd). The basis for this metric is determining how accurately emplaced targets can be located. Assuming that no system would detect the exact location of a target item, some margin of error must be factored into any analysis of Pd. The factor used in most equations used to calculate Pd is Rcrit, or the critical radius around which a target would be scored as identified by the geophysical sensor.

There should be a relationship between the magnitude of Rcrit and the environmental factors of the site. This relationship may vary based on geologic conditions, soil moisture, atmospheric conditions, and any other conditions that may interfere as noise or background clutter to the positioning equipment.

This study looks at geophysical sensor field data from 5 sites. The distance between the center of a emplaced target item, and the nearest sensor anomaly is compared for target sets of greater than 25 items. Assuming that at an infinite distance Pd would be 100% and at 0, Pd would be 0%. Pd calculated for a progression of Rcrit radii is plotted as a function of those radii. A breakpoint, or the Rcrit radius at which the slope of this line approaches 1, should be Rcrit associated with background clutter and noise.

The results of this study from 5 sites are presented in this paper.

## 62.1

### Overview of Chaos and Applications

*Carroll, TL<sup>1</sup>*

<sup>1</sup>US Naval Research Laboratory, USA

While the study of nonlinear dynamics and chaos was originally the province of mathematicians only, in recent years it has appeared that chaos may have significant applications in technology. I will give a brief description of chaos, as well as some of the methods for analyzing chaos, and discuss some of the fields where applications are being studied.

## 61.5

### Flexible Configuration of Technologies for Geophysical Mapping of UXO; New Levels of Efficiency, Productivity, and Effectiveness

*Foley, J<sup>1</sup>*

<sup>1</sup>Sanford Cohen Associates (SCA), USA

The diversity of UXO site conditions around the world and the wide range in the type and spatial distribution of buried UXO make geophysical mapping a complicated task. UXO mapping operations range from 20-mm rounds on the surface to large bombs tens of meters in depth. Furthermore, site conditions range from flat and open facilities, to swampy lowlands and wooded hillsides. As such, the use of geophysical mapping technologies for site characterization must be flexible to safely handle all conditions. This paper deals with a new approach of flexibility and customization of field equipment to characterize the broad spectrum of UXO contaminated sites. No longer limited to "golf course" conditions, digital mapping technologies can be deployed within a wide array of site conditions where UXO are located. Field data acquisition technology is based on a GPS-integrated, man-portable cart system augmented with backpack configurations. This technology has been field proven with magnetometers, gradiometers, time-domain and frequency-domain electromagnetic sensors. Cart-based systems generate essentially noise-free data, as the deployment systems are constructed completely of composite materials. In the magnetometer mode, the system has been proven to routinely collect 40-60 acres per day. More importantly, the system design allows productivity to be scaled to virtually any practical level using commercial off-the-shelf (COTS) sensors and navigation components. Automated UXO target analysis is integrated within a comprehensive geographical information system (GIS) and automatically processes data from any field sensor. These cart-based technologies are designed to keep EOD-qualified personnel as an integral component of the process as operators of the equipment; keeping the people best qualified to work safely on UXO sites directly involved in the work.

## 62.2

### Optimal Input Signals for Driving Nonlinear Electronic Systems into Chaos

*Booker, S<sup>1</sup>; Smith, P<sup>1</sup>; Brennan, P<sup>2</sup>; Bullock, R<sup>2</sup>*

<sup>1</sup>University of Dundee, UK; <sup>2</sup>University College London, UK

Nonlinear feedback loops have found a wide variety of applications in modern electronic systems. In many cases these circuits are vulnerable to chaos if driven by an appropriate input signal. Furthermore, since nonlinear circuits cannot be characterised simply by their spectral response, the onset of chaos is extremely waveform dependent. The question then arises: which input signal is the most effective at driving the circuit into chaos?

It has been shown recently (S M Booker, *Nonlinearity* 13, 145-163, 2000) that an answer can be found to this fundamental question for one particular class of electronic systems. This class comprises those nonlinear electronic systems whose dynamical equation resembles a perturbed Hamiltonian system, when excited by a periodic input signal. In fact, this is a very broad class of electronic systems and includes many practical circuits. For this class of electronic systems a pair of optimal input signals may be determined. These allow the onset of homoclinic chaos in the dynamics of the circuit with the smallest possible amplitude, or power, for which homoclinic chaos can be found. These optimal input signals allow in-band disruption of the nonlinear electronic systems concerned.

We briefly review how these optimal input signals are determined. A particular example is then given, in order to illustrate how the method works in practice. We consider a phased-lock loop (PLL) used as an FM demodulator and derive the modulation waveforms of smallest amplitude and power with which to induce homoclinic chaos in the circuit. Numerical and experimental results are given to illustrate the effectiveness of our method.

Acknowledgement: This work was supported by DERA, Fort Halstead, England.



## 62.3

### In-band Chaos in Commercial Electronic Systems

*Booker, S<sup>1</sup>; Smith, P<sup>1</sup>; Brennan, P<sup>2</sup>; Bullock, R<sup>2</sup>*

<sup>1</sup>University of Dundee, UK; <sup>2</sup>University College London, UK

In this paper we describe a method for inducing chaos in a standard, commercially available electronic sub-system using an in-band signal. In particular, we show how, with relatively little knowledge of the commercial circuit design, an in-band signal can be determined which will disrupt the operation of the circuit and drive it into chaos.

The problem which we consider is the disruption of an INMARSAT standard-A terminal, by driving it into homoclinic chaos. This device, which employs a PLL FM discriminator, is designed to accommodate a 3 kHz modulation bandwidth with 12 kHz of peak FM deviation. In order to model this commercial system a PLL test circuit was designed with an identical specification. This circuit provides a test problem with which analysis and numerical modelling can be compared, the INMARSAT terminal design being, in essence, a 'black box'.

The PLL FM discriminator test circuit can be modelled as a nonlinear feedback loop whose dynamical equation resembles a perturbed Hamiltonian system, when modulated by a periodic input signal. For such an electronic system it is possible to determine an input signal of smallest amplitude (or bandwidth, in this context) which will allow the onset of homoclinic chaos in the circuit (S M Booker, *Nonlinearity* 13, 145-163, 2000). A numerical and experimental investigation of the test circuit is presented which validates the effectiveness of the optimal signal. A comparison with other 'reference' input signals is also presented. Agreement between the analytical predictions, numerical simulations and experimental measurements is excellent in each case.

Measurements were then performed with the INMARSAT standard-A terminal and the optimal input signal was again shown to be superior to the other reference signals, for disrupting the FM demodulation capability of the INMARSAT terminal. Agreement between the experimental behaviour of the INMARSAT terminal and the predicted response of test circuit was excellent. The implications for disruption at relatively low RF power of similar systems will be considered.

Acknowledgement: This work was supported by DERA, England.

## 62.5

### Chaotic Instabilities in Nonlinear Electro-optic RF Experiments

*Wu, D-H<sup>1</sup>; Andreadis, T D<sup>1</sup>; Wieting, T J<sup>1</sup>; Libelo, L F<sup>2</sup>*

<sup>1</sup>US Naval Research Laboratory, USA; <sup>2</sup>SFA Inc, USA

In nonlinear dynamics it is well known that a system containing a feedback loop and a nonlinear medium can undergo transitions from a stationary state to a periodic state, as well as to a nonperiodic state, with the variation in value of a system parameter. This general behavior can be studied using the Ikeda map, which is derived from the coupling between the amplitude and phase of the input and feedback (i.e. output) signals. The phase shift and the enhanced amplitude of the feedback signal, due to the presence of the nonlinear medium, can result in unstable intermittent bursting of the output signal. Some experimental and theoretical studies have indicated that such chaotic behavior appears to be generic for circuits that contain a feedback loop and a nonlinear medium.

For some time now we have been investigating electro-optic (EO) sensors and their use in nonperturbing measurements of the electromagnetic field. The output signals generated by these sensors have sometimes exhibited unstable "noisy" behavior, reminiscent of a transition to a nonperiodic state. Our experiments and analysis, which were carried out on LiNbO<sub>3</sub> single crystals, suggest that intermittent bursting can in fact occur not only in feedback-loop circuits but also in linear circuits. While there is no obvious feedback-loop circuit involved in our experiments, very strong temporal instabilities appeared in the EO output, which were measured using a method similar to transmission ellipsometry with an approximate 300-micron diameter, He-Ne laser beam. Analysis suggests that the temporal instability is identical to the intermittent bursting pattern, which can be obtained from the Ikeda map with appropriate parameter values. The chaotic intermittent bursting in our experiments is due to the strong nonlinearity and intrinsic bistability of the LiNbO<sub>3</sub> single crystals. Detailed experimental results and analysis will be discussed.

## 62.4

### Chaos in Circuits at Microwave Frequencies

*Wallace, C<sup>1</sup>*

<sup>1</sup>TRW, USA

The basic nonlinear element we are concerned with in any RF effects program is the semiconductor p/n junction. Associated with it are resistances, inductance, self-capacitance, external capacitance, and parasitic reactance associated with other elements of the circuit or device of which it is a part. Physical insight comes from understanding effective junction current and voltage behavior and the self-consistent change in boundary conditions associated with the externally imposed RF interaction. Any given semiconductor junction (with reasonable minority carrier lifetime) and its associated parasitic reactance can be considered as a damped nonlinear oscillator that is driven by the time dependent externally imposed RF interaction. The present work applies Hublers principle of the dynamical key to the problem of RF interaction with nonlinear semiconductor oscillators. Results highlight the fact that since the transient response of a nonlinear damped semiconductor oscillator is aperiodic the optimal forcing function that minimizes the action of the external RF drive is chaotic as well. Moreover, the minimal action requirement is shown to also apply to periodic pulsed RF drive signals. Subsequently, the following interesting results are also discussed:

61623; Experimental observation that chaotic behavior will persist over good variations in external RF drive frequency relative to the zero voltage resonant frequency [factor of three for a basic semiconductor nonlinear oscillator circuit and better than an order of magnitude for a nonlinear feedback circuit].

- Good agreement between experiment, theory, and computer simulation for period doubling transitions to chaos in the oscillator circuit - and this for significantly higher frequencies than previously reported in the literature.
- Observation that one can obtain chaotic behavior for transition capacitance and minority carrier lifetime values that are relevant to large numbers of devices.
- Simulations demonstrate several mechanisms to lower the voltage threshold at which chaotic behavior occurs, which highlight the fact that the basic mechanism driving the instability persists at extremely low voltages. The chaotic response is not connected with junction turn-on or rectification but corresponds to the nonlinear boundary condition imposed by the different capacitance functions in the forward and reverse bias directions.

Finally, recent work by Wuensche, along with Sawhill and Kauffman, on chaos in random boolean networks and logic networks suggests that the order-chaos boundary and damage spread rates can be understood by a suitable generalization of the nonlinear variational principle discussed earlier. The implications for a statistical treatment of real world information technology architectures (tree structures, rings, etc.) undergoing external RF stimulus are also described.

## 63.1

### Contribution of Earthing Conductors to Current Reduction Factor of Three-Core Cable Line

Zelić, I<sup>1</sup>; Sarajcević, P<sup>2</sup>; Vučak, S<sup>3</sup>

<sup>1</sup>Hrvatska el Ektroprivreda d.d., Croatia; <sup>2</sup>University of Split, Croatia; <sup>3</sup>Croatian National Electricity, Croatia

#### ABSTRACT

Earthing conductors are often laid together with cables in the same cable trench. Cable sheets and earthing conductors represent a system of passive conductors. They are mostly connected to the earthing grid of incidental substations so making a common earthing system. In case of phase-to-ground short circuit, fault currents in the earthing system as well as through the ground occur. These currents are a consequence of both electromagnetic coupling and potential of earthing grid. Currents caused by electromagnetic coupling in the system of passive conductors may be represented by an adequate current reduction factor. This reduction factor has an important role at solving numerous tasks from the EMC area.

This paper shows calculation of the current reduction factor of a three-core cable line and arbitrary number of earthing conductors laid in a common cable trench. Adequate mathematical model is presented. A quasi-steady-state treatment is used because it deals with sinus alternate values. Geophysical features of the cable route are taken into account. An appropriate equation system in a matrix form is derived, by which current and voltage state in the system of passive conductors is described. By solving this equation system the following final expression is obtained:

$$\bar{k} = \sum_{i=1}^n \sum_{j=1}^n \bar{y}_{ij} \cdot \bar{z}_{jp}$$

where:

- $\bar{k}$  - total current reduction factor of three-core cables and earthing conductors
- $n$  - number of all passive conductors
- $\bar{y}_{ij}$  - element in  $i$ -th row and  $j$ -th column of the matrix  $[\bar{Y}] = [\bar{Z}]^{-1}$ ;  $[\bar{Z}]$  is a matrix of self and mutual impedances of passive conductors with earth return
- $\bar{z}_{jp}$  - mutual impedance between  $j$ -th passive conductor and three-core cable phases with earth return

As a calculation example a three-core cable line of 35 kV rated voltage has been chosen. Contribution of earthing conductors to the cable line current reduction factor has been analyzed. For that purpose different possibilities of laying of earthing conductors have been studied. At that number of earthing conductors and their electromagnetic characteristics have been changed. Geophysical features of the cable route have been changed, too.

## 63.3

### Modal Parameters and Design Characteristics of an Antiwaveguide Packaging for Millimeter and Microwave Circuits

Kohlberg, J<sup>1</sup>; Lahart, M J<sup>2</sup>; Fazi, C<sup>2</sup>

<sup>1</sup>Kohlberg Associates Inc., USA; <sup>2</sup>Army Research Laboratory, USA

For many types of millimeter and microwave circuits, packaging can adversely impact performance if the circuit is operating above the package's cutoff frequency. This can occur if a circuit and its enclosing structure are coupled. If a circuit element is an oscillator, the coupling can change its resonant frequency and its Q. Similarly, a low noise, high-gain amplifier may become destabilized by positive rf feedback caused by an improperly designed metallic package. The same package may affect the performance of a microstrip patch filter and other types of microwave circuits.

A structure that minimizes coupling to a circuit is a cavity that radiates away any rf energy produced by sources inside it. Such a structure, which is functionally the opposite of a waveguide

We analyze characteristics of the modes of an antiwaveguide housing in an approximate manner by performing calculations on a slab antiwaveguide. The spacing between dielectric materials that enclose an air or vacuum volume is computed as a function of the propagation constant and the frequency of the radiation. Cut off frequencies are determined, and magnitudes of the electric fields are calculated inside and outside the enclosed volume. The effects of permeability not equal to unity in the dielectric material are also studied.

We compare the behavior of a slab antiwaveguide to cylindrical and rectangular enclosing structures. Cylindrical structures have hybrid modes, with axial components of both electric and magnetic fields, rather than the transverse electric and transverse magnetic modes of slab waveguides. Rectangular housing structures, which are best for millimeter-wave technology, have discontinuities at the corners that can radiate energy.

We compare analysis and measurements to select suitable materials that have ideal rf suppression properties while maintaining the good rigid structural and thermal properties demanded in military and avionics systems.

## 63.2

### High Frequency Electromagnetic Field Coupling to Uniform and Nonuniform Lines: An Asymptotic Approach

Tkachenko, S<sup>2</sup>; Rachidi, F<sup>1</sup>; Ianoz, M<sup>1</sup>; Martynov, L<sup>3</sup>; Vodopianov, G<sup>2</sup>

<sup>1</sup>Power Systems Laboratory, Switzerland; <sup>2</sup>Radio Research Development Institute, Russia; <sup>3</sup>Ministry of Telecom. of the Russian Federat., Russia

The necessity to analyze the interaction of high-frequency electromagnetic field with transmission lines arises in many problems of electromagnetic compatibility. To solve such problem, the transmission line (TL) approximation is not applicable for the general case of a finite line [1]. Additionally, the presence of nonuniformities, such as line bends, makes the use of the TL approximation more questionable. Therefore, the solution of the problem is found in general by solving numerically the Pocklington's equation.

We propose in this study an asymptotic approach which is based on the fact that in the regions of the wire sufficiently far from nonuniformities (such as terminal loads, line bends, etc.), the influence of the currents in these parts is negligible [2]. Using this approach, it is possible to express analytically the induced current along the asymptotic region of the line as the sum of three terms: a forced-response wave which corresponds to the solution of nonhomogeneous Pocklington's equation for the case of an infinitely long wire, and, two positive and negative traveling waves (with unknown coefficients) corresponding to the solution of the homogeneous Pocklington's equation.

To determine these unknown coefficients, two methods are proposed. The first one is based on the numerical solution of the Pocklington's equation for two similar line configurations, but with significantly shorter length. This method is, therefore, particularly efficient when considering the electromagnetic field coupling to very long lines.

In the second method, analytical expressions are derived for the reflection and transmission coefficients associated with the line nonuniformity (line bend). The method is based on an iterative approach in which the zeroth iteration term is given by the TL solution [3]. The obtained analytical expressions make it possible to consider also nonuniform exciting fields.

- [1] F.Tesche, M.Ianoz, T.Karlson "EMC analysis method and computational models", Wiley, 1997.
- [2] S.Tkachenko, F.Rachidi, M.Ianoz, L. Martynov, "An Asymptotic Approach for the Calculation of Electromagnetic Field Coupling to Long Terminated Lines," Rome Int. Symposium on EMC, EMC'98 ROMA, September 14-18, 1998.
- [3] S.Tkatchenko, F.Rachidi, M.Ianoz, "Electromagnetic Field Coupling to a Line of Finite Length : Theory and a Fast Iterative Solutions in Frequency and Time domains," IEEE EMC, vol. 37, No. 4, pp. 509-518, November 1995.

## 63.4

### Symmetric Renormalization of the Nonuniform Multiconductor-Transmission-Line Equations with a Single Modal Speed for Analytically Solvable Sections

Baum, C E<sup>1</sup>

<sup>1</sup>Air Force Research Laboratory DEHP, USA

A nonuniform multiconductor transmission line (NMTL) can have its propagation represented (and computed numerically) by a product integral corresponding to dot multiplication of the product integrals for a set of uniform sections. For a smoother transition from one section to the next (continuous characteristic-impedance matrix) one can interpolate the characteristic-impedance matrix for each section from its end-point values. The procedure discussed in this paper concerns the case of all modal speeds the same (such as the case of perfect conductors with a uniform dielectric medium). The interpolation is accomplished in a way that preserves the symmetry of the characteristic-impedance matrix (and hence reciprocity) throughout each section.

For the case that all the modal speeds on an NMTL are the same we now have a way to approximately calculate its response based on an interpolation scheme for the geometric-factor matrix (or equivalently, characteristic-impedance matrix) in individual sections of the line. This makes a smoother transition in going from one section to the next, the discontinuity being in the slope (first derivative) at the section boundaries. Compared to another scheme (C.E. Baum, J.B. Nitsch, and R.J. Sturm, Interaction Note 516, 1996) this also maintains a symmetric characteristic-impedance matrix in the interpolation throughout each section. A previous paper (C.E. Baum, *Int'l. J. Numerical Modelling: Electronic Networks, Devices, and Fields*, pp. 175-188, 1988) has considered the high-frequency, or early-time propagation on such NMTLs. The present paper extends this to all frequencies within the transmission-line approximation.

While the present development has been in the context of an approximation, this need not be the only case of interest. Since the characteristic-impedance matrix is now symmetric everywhere along the NMTL, thereby satisfying reciprocity, we can use this to *define* NMTL examples for which the solution is *exact* (within the transmission-line assumption). These can in turn be constructed, thereby giving a *synthesis* procedure for NMTLs for special application.

## 64.1

### UWB SAR Antennas: The IRA, the Pulse Radiating Antenna Element (PRAE), and the Balanced Dipole Antenna (BDA)

Farr, E<sup>1</sup>; Salo, G<sup>2</sup>; Baum, C<sup>3</sup>; Prather, W<sup>3</sup>; Bowen, L<sup>1</sup>

<sup>1</sup>Farr Research Inc, USA; <sup>2</sup>Mission Research Corporation, USA; <sup>3</sup>Air Force Research Laboratory, USA

We consider here the applicability of three Ultra-Wideband antennas for SAR applications, the Impulse Radiating Antenna (IRA), the Pulse Radiating Antenna Element (PRAE), and the Balanced Dipole Antenna (BDA). We have designed, built, and tested two 18-inch diameter antennas, a reflector Impulse Radiating Antenna (IRA), and a Pulse Radiating Antenna Element (PRAE). We provide extensive measurements of the two antennas, made both in the time domain range of Farr Research, and at the frequency domain range of Mission Research.

We introduce here the PRAE, which is a reflector IRA in which the paraboloidal reflector has been replaced by a flat plate. This substitution is made in order to broaden the antenna pattern of the IRA, which is well known to be quite narrow. Certain SAR applications require a broader antenna pattern, so it was thought that the PRAE would be an interesting alternative to explore.

We tested the antennas at two different facilities, the time domain outdoor antenna range of Farr Research, and the frequency domain anechoic chamber of Mission Research Corporation (MRC) in Dayton. This allowed us to compare a set of results from each of the two measurement techniques. We can report here a very nice correlation between the time and frequency domain techniques.

We also introduce here a new design for a sensor related to the Balanced Transmission-line Wave (BTW) sensor with enhanced sensitivity. The new device is called a Balanced-Dipole Antenna (BDA), because it maintains a balance between the electric and magnetic dipoles. Like the BTW, the BDA has a direction pattern with a cardioid shape. By exchanging the load and excitation port with a switch, the BDA can look either left or right. The characteristics of the BDA are calculated using a Method of Moments solution to a static Poisson's equation. Design guidelines are provided to give optimal impedance match for a single-ended version of the sensor against an infinite ground plane, in order to provide a 50 ohm match at late times.

## 63.5

### Issues in Distributed Modelling Package Design

Sasse, H<sup>1</sup>; Duffy, A<sup>1</sup>

<sup>1</sup>de Montfort University, UK

In the field of electromagnetic compatibility, it is often desirable to investigate the performance of systems through numerical modelling. The reasons for this include the difficulty of direct measurements on practical configurations and the intractability of analytical approaches. Further, the cost of such tests and the inherent time delays associated with them may be prohibitive.

The users' requirements of constantly increasing accuracy and reduced run times can not be fully met by simply increasing the clock speed of the single processor systems. This implies that approaches involving parallel processing are desirable. Although there is a market for high powered parallel computers (e.g. the supercomputers used for weather forecasting), these are prohibitively expensive for most applications. However, most organisations already possess many computers networked together. The computing power of these networked machines can be utilised to produce a parallel computer of significantly greater power than a single machine. In most cases, these computers are under-used outside normal business hours, providing many organisations with a numerical modelling resource capable of simulating systems with greater complexity and with a shorter duration.

The Transmission-Line Matrix (TLM) method is used in this paper to illustrate some of the issues in designing and implementing such a system. The key issues are: \* Reliability. The system should not fail if one of the computers fails. The modelling package should be sufficiently robust to recover efficiently from such events; even if the 'controller' fails. \* Network performance. The modelling package should be able to communicate and partition work with computers of varying performance and over sub-networks of varying performance so as to minimise run-time. \* Time varying configuration. The number of computers available may vary according to working patterns associated with the different machines on the network. The modelling package should be able to identify when computers are available and incorporate them into the parallel computer.

## 65.1

### Electromagnetic Low Frequency Scattering by 3D Objects in a Stratified Conducting Seawater Environment

*Mattsson, J<sup>1</sup>*

<sup>1</sup>Defence Research Establishment FOA, Sweden

In this paper electromagnetic low frequency scattering by 3D objects, embedded in a stratified conducting seawater environment, is numerically modelled. The scattering object is partly or completely buried within the seabed. The typical size of the object is in the order of one meter and the incident fields illuminating it are electromagnetic pulses with frequency contents of  $0 < f < 100$  kHz. The application in mind is detection and classification of barrels with hazardous and toxic materials, ammunition wastes, mines etc. buried in the sea bottom sediment. The active electromagnetic source is a submerged finite electric current line placed just a few meters above the seabed. The total field response is then calculated one meter right below this current line, i.e. a mono-static transmitter/receiver configuration is used.

The mathematical solution to the problem is derived in the frequency domain and the resulting electromagnetic scattering response in the time domain is obtained by Fourier synthesis. A solution for the object scattered fields is formulated by using a boundary integral equation (BIE) method where the scattered fields are expressed as integral representations over the surface of the scattering object. Hence, the dyadic Greens functions in these representations satisfy the boundary conditions for the stratified environment. Using a Hertz potential formulation and adaptive numerical integration of the resulting Sommerfeld integrals, (L. Abrahamsson and B. L. Andersson, technical report FOA-R—97-00586-409-SE, ISSN 1104-9154, Oct. 1997), solves the incident fields. The total fields are then the sums of the scattered fields and the incident fields. See e.g. (K. A. Michalski and J. R. Mosig, IEEE Transactions on antennas and propagation, vol. 45, no. 3, p. 508-519, March 1997) and (J. Mattsson, Proceedings of 2nd international conference on marine electromagnetics, Marelec 99, Brest, July 1999) for a thorough description of this BIE formulation.

The integral equations for the unknown tangential field components on the scattering surface are solved by using a global Galerkins method with spherical harmonics as basis and projection functions. The numerical quadratures for the surface integrals are adjusted to taking care of the discontinuities in the integrands when the scattering surface intersects the interface between the seabed and the seawater. The resulting linear system of equations for the unknown expansion coefficients is solved by an iterative method enhanced by pre-conditioning.

Numerical examples are given for a super-ellipsoidally-shaped object in a horizontally stratified geometry. The current-pulses in the transmitting antenna are Ricker-like and the computed scattering responses are compared with those obtained by using a dipole approximation technique.

## 65.2

### Landmine Detection by Nuclear Quadrupole Resonance.

*Matthews, R<sup>1</sup>; Barrall, G<sup>1</sup>; Hibbs, A<sup>2</sup>*

<sup>1</sup>Quantum Magnetics, USA; <sup>2</sup>Information Systems Laboratories Inc, USA

Many high explosive compounds such as TNT and RDX exhibit radio frequency emissions at characteristic frequencies when excited by a properly designed electromagnetic induction (EMI) system. This response is known as nuclear quadrupole resonance (NQR). NQR is ideally suited for discrimination of buried landmines from clutter because it is a unique property of the explosive itself and usually does not exist in either natural or man made clutter. As a result, there are fewer opportunities for false alarms due to clutter. This differs from other sensor modalities which detect attributes that may be characteristic of clutter as well as landmines. For example, EMI sensors may be subject to false alarms due to man made clutter since they detect the presence of metal. Similarly, ground penetrating radar (GPR) systems may be subject to false alarms due to both natural and man made clutter since they detect discontinuities in the electrical properties of the interrogated medium.

Under DARPA sponsorship, Quantum Magnetics is developing a nuclear quadrupole resonance (NQR) based landmine detection system. The current system uses <sup>14</sup>N NQR to detect both RDX and TNT based non-metallic landmines. NQR combines the compound specific detection capability offered by chemical detection techniques with the spatial localization capability and convenience of an induction coil metal detector. In the 20 years since NQR was first applied to mine detection in the U.S., there has been tremendous improvement in the NQR detection sensitivity due to significant progress in hardware design and pulse sequence development. In recent field trials at various military bases, Quantum Magnetics successfully demonstrated the detection capability of a mobile, unshielded system. We will review the progress made by Quantum Magnetics in this area over the last two years, including an overview of the technique, a description of the system hardware, methods for coping with radio frequency interference, and a summary of the results from recent field trials.

## 65.3

### HPM/IR Detection of Land Mines: Measurement and Modeling of Surrogate Mines

Seregelyi, J.S<sup>1</sup>; Kashyap, S<sup>1</sup>; Louie, A<sup>1</sup>; Khanna, S.M<sup>1</sup>  
<sup>1</sup>Defense Research Establishment Ottawa (DREO), Canada

A new hybrid remote-sensing method using high-power microwave (HPM) illumination and passive infrared (IR) detection is being developed at the Defence Research Establishment Ottawa (DREO). In order to support this effort, the scattering of electromagnetic waves by a surrogate mine in soil has been investigated both numerically and experimentally.

The finite-difference time domain (FDTD) method is used to model the surrogate mine, which consists of a dielectric disk buried in dry sand. The surrogate also contains a metal pin representing the fuse of the mine. An electromagnetic plane wave is used to illuminate the object, and the heating pattern is calculated from the resultant E-field distribution and the dielectric properties. Comparison of the numerical and measured results can then be made. The latter are generated using a unique technique whereby an IR image is taken at 1cm intervals starting at the soil surface and working downwards. This is made possible by a series of wooden frames and plastic sheets that are buried with the surrogate at the desired interval spacing. As each layer is imaged, the overburden is quickly removed to expose the subsequent layer. Once digitized, these images can be numerically manipulated to establish a cross-sectional heating pattern anywhere in the soil. This is important because the IR image observed at the soil surface is composed of two parts. The first is a near-real time thermal image generated by electromagnetic scattering, and the second is a late-time effect resulting when the temperature gradients generated in and around the mine are thermally conducted upwards towards the soil surface. The time evolution of the thermal signature is a superposition of these two images.

In general, a good correlation is observed between the numerical and measured IR images both at the soil surface and at various cross-sections. As such, a parametric analysis as a function of: the mine composition, depth, pin orientation and soil composition can be

performed with confidence. A partial list of conclusions based on this analysis indicates that: 1) HPM/IR detection method can potentially be a powerful remote-sensing technique, particularly when used to complement conventional passive-IR detection and other detection technologies 2) the mine composition and depth have significant repercussions on the IR image and 3) polarization of the field with respect to the mine is important (for example, variations in pin orientation are clearly visible).

## 65.4

### Temperature Response of the Ground Near a Landmine

Carter, L.J.; Lee, M.-C.; Lu, A.I.-Y.; Deans, J.  
<sup>1</sup>University of Auckland, New Zealand

#### NOMENCLATURE

- a Thermal diffusivity of the soil (m<sup>2</sup>/s)
- h Convective heat transfer coefft (W/m<sup>2</sup> °C)
- k Thermal conductivity of the soil (W/m °C)
- T Temperature of the soil (°C)
- t Time (s)
- x Vertical distance from ground level (m)
- L Distance between top of mine and ground level.

#### INTRODUCTION

It has been known for some time that thermal imaging equipment can be used to detect the presence of buried landmines by observing surface temperature variations in soil which has been exposed to solar radiation. More recently there has been interest in a technique which uses microwave radiation to produce warming in the top layer of the soil [1,2]. The position of the mine is revealed by a 'cool spot' above it. This paper proposes a mechanism for the production of the cool spot, and compares simulation and measurement results.

#### THEORETICAL CONSIDERATIONS

The analysis examines the cooling down of the ground above and around the mine after the region has been heated by microwave radiation. We assume that heat flow in the soil above and in the region around the mine is one dimensional. By assuming that the ground temperature is initially uniform, that the energy conducted to the surface is convected away, and that the mine acts as a thermal barrier so that heat transfer between the mine and the surrounding soil is negligible during the test period, expressions for the surface temperature can be obtained [3]. For the surrounding soil,

$$\frac{T_{(ground\ surface, t)} - T_{initial}}{T_{\infty} - T_{initial}} = 1 - \left\{ \exp\left(\frac{h^2 \alpha t}{k^2}\right) \right\} \left\{ \operatorname{erfc}\left(\frac{h\sqrt{\alpha t}}{k}\right) \right\}$$

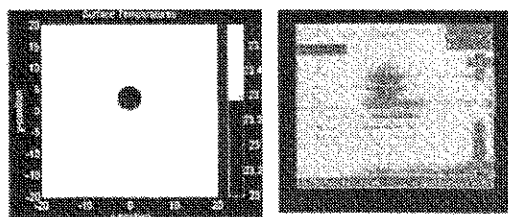
and above the mine,

$$\frac{T_{(ground\ surface, t)} - T_{initial}}{T_{\infty} - T_{initial}} = \sum_{n=1}^{\infty} \left( \frac{4 \operatorname{Sin} \xi}{2\xi + \operatorname{Sin}(2\xi)} \right) \left( \exp\left[-\xi^2 \left(\frac{\alpha t}{L}\right)\right] \right) (\operatorname{Cos} \xi)$$

where  $\xi \operatorname{Tan} \xi = \frac{hL}{k}$

#### MODELLING AND RESULTS

A computer model has been developed to predict the temperature variation of the soil surface above a landmine. The heating effect of the microwave energy on the soil and the landmine is first calculated [1]. Next, the above equations are used to determine the temperature of the soil surface above the landmine and elsewhere, and hence the temperature difference over time. Finally, these results are represented graphically in a form similar to that produced by a thermal imaging camera, with temperature shown as colour shading of a two-dimensional ground surface. The diagram compares a result obtained in this way with one obtained by measurement. By taking "snapshots" at intervals, the development of the thermal images can be observed.



#### CONCLUSIONS

Microwave stimulation of the soil, followed by thermal imaging of the surface, may be used to determine the location of completely non-metallic, shallowly buried objects such as antipersonnel landmines. Convection, producing a more rapid cooling of the soil above the mine, appears to be the main factor contributing to the formation of the 'cold spot'. Further work is needed to determine the range of operating conditions for which this technique might be useful in the field.

#### REFERENCES

1. Carter, L.J., Bryant, G.H.B., Le Fevre, M., and Wong, W.C., 'Moisture and landmine detection', Proc. EUREL/IEE International Conference on the Detection of Abandoned Landmines (MD96), Edinburgh, IEE Conference Publication Number 431, 83-87, 1996.
2. Carter, L.J., O'Sullivan, M.J., Hung, Y.J., and Teng, J.C.-C., 'Thermal imaging for landmine detection', Proc. IEE International Conference on the Detection of Abandoned Landmines (MD98), Edinburgh, IEE Conference Publication Number 458, 1998.
3. Mills, A.F., 'Heat Transfer', Irwin, 1992.

## 65.5

### Laser Method of UXO Disposal

*Garcia, C<sup>1</sup>; Sanchez, JA<sup>1</sup>; Rivera, T<sup>1</sup>; Muenchausen, R<sup>1</sup>; Brewer, R<sup>1</sup>*  
<sup>1</sup>Los Alamos National Laboratory, USA

A new process is under development in which a Nd:YAG laser is used to drill a small hole into a metal encased explosive, such as a UXO. An additional feature of this technique is the ability to observe the resulting plume spectroscopically to determine the exact location of the laser beam within the exposed piece in real time. The drilling can then be accomplished with a minimum disruption of the contents. The UXO can then be spectroscopically examined by utilizing this small hole to allow probing using laser spectroscopy to determine the UXO contents. There is a variety of methods that could be utilized for the spectral observation, two of these are laser-Raman and Laser-Induced Breakdown spectroscopy (LIBS). If the decision is made that the UXO is to be remediated, the UXO can be defuzed by utilizing the Nd:YAG laser as a cutting laser. We have recently shown that we can safely cut and drill into cased munitions by utilizing either a pulsed or a cw laser. Our experiments have included a wide range of energetic materials including TNT, composition B and other DoD and DOE explosives. Our studies also include a wide range of metals. The results are in qualitative agreement with a model of laser-HE interactions developed more than twenty years ago. Once the ordnance is defuzed and cut open by means of laser cutting, the ordnance can then be remediated in an environmentally acceptable manner. The energetic material could be rendered nonenergetic using base hydrolysis, a technique pioneered by this Laboratory. The base hydrolysate could then be treated using super critical water oxidation or by biodegradation of the hydrolysis products.

## 66.2

### Signal Processing for Low Metal Mine Detection and Identification: Results from a Blind Field Test

*Collins, L<sup>1</sup>; Gao, P<sup>1</sup>; Weaver, D<sup>2</sup>; Makowsky, L<sup>3</sup>*

<sup>1</sup>Duke University, USA; <sup>2</sup>JUXOCO, USA; <sup>3</sup>NVESD, USA

Electromagnetic induction (EMI) sensors have been used extensively to locate buried land mines. EMI sensors that utilize traditional detection algorithms based solely on the metal content suffer from large false alarm rates as a result of the often significant amount of metallic debris (clutter) present in the environment. Currently, the Joint UXO Coordination Office at Ft. Belvoir, VA is sponsoring a series of experiments designed to establish a performance baseline for mine and UXO detectors. This baseline will be used to measure the improvements in performance offered by advanced signal processing algorithms. In conjunction with this effort, data from low-metal content mines has been gathered using a variety of EMI sensors in a 50 meter by 20 meter plot at Fort A.P. Hill, VA as well as in a calibration area in an adjacent 5 meter by 25 meter plot. Approximately 100 mine targets were buried in the blind grid. The indigenous clutter was initially removed from the A.P. Hill site and then samples of the clutter were re-placed in the grids to provide discrete opportunities for false alarms. The ground truth associated with the calibration area is available; however, the ground truth associated with the main, or blind, test grid is sequestered. Algorithm developers provide the output of their algorithms for each grid square or "decision opportunity" to JUXOCO for scoring, thus simplifying the calculation of the detection and false alarm probabilities. We have implemented a series of algorithms in order to evaluate the tradeoffs between computational complexity and performance for several of the EMI sensors. We have developed statistical signal processing algorithms that operate only on the data measured at a single point as well as those that process spatially collected data. In addition, we have considered algorithms that specifically incorporate modeled signatures as well as those that utilize measured templates. We have also considered simple "energy detection". In this way, we can quantify the performance of a "baseline", which we consider to be single-point energy-based algorithms. Such a definition is typical of the type of signal processing that is currently used by fielded metal detectors. We can also quantify performance gains associated with using the entire signature, as well as incorporation of spatial information. Finally, we consider algorithms which not only distinguish between landmines and clutter, but which classify the landmine as to type. In this talk we will discuss the performance of the various algorithms for several EMI sensors and discuss the tradeoffs.

## 66.1

### Design of a Test Site for Mine/UXO Discrimination

*Weaver, R<sup>1</sup>*

<sup>1</sup>Joint UXO Coordination Office, USA

Fairly comparing the detection and discrimination performance of unexploded ordnance (UXO) and land mine sensors or systems is always difficult. A useful comparison is nearly impossible in uncontrolled test situations. The US Department of Defense (DOD) proposes measuring discrimination performance using a set of standard test locations, targets, and protocols that are administered by an impartial entity. This paper describes a pilot test site established to create performance benchmarks for hand-held metallic mine detectors. The Joint UXO Coordination Office (JUXOCO) created this pilot site under a US DOD initiative. Targets, site layout, methodology and some experimental results from electromagnetic induction (EMI) sensors are displayed and discussed using receiver operating characteristic (ROC) curves. Performance baselines are established for this site for several EMI sensors. This baseline is used to measure the potential improvements in performance offered by advanced signal processing algorithms. The effects of soil on target signatures is illustrated and discussed briefly. The Joint UXO Coordination Office (JUXOCO) is expanding this site to accommodate vehicle-mounted systems and additional types of sensors and targets. Additional data collections continue and data is available for analysis via a web site.

## 66.3

### Algorithms for Detecting and Identifying Landmines using the Time-Domain Electromagnetic Identification (TEMID) Sensor System

*Smith, D<sup>1</sup>; Nelson, C<sup>1</sup>; Sherbondy, K<sup>2</sup>; Huynh, J<sup>2</sup>*

<sup>1</sup>Johns Hopkins University Applied Physics Labs, USA; <sup>2</sup>U.S. Army, USA

The TEMID sensor system is an advanced prototype electromagnetic induction (EMI) landmine sensor system developed by The Johns Hopkins University Applied Physics Laboratory (JHU/APL) in conjunction with the U.S. Army CECOM Night Vision Electronic Sensors Directorate (NVESD). The self-contained, portable, prototype TEMID sensor system has demonstrated the capabilities to detect, identify and discriminate from metal clutter high and medium content metal landmines, as well as plastic cased landmines with metal parts. Compared to conventional EMI metal detectors, the TEMID sensor's discrimination feature results in a lower false alarm rate from metal clutter. The TEMID sensor system operates on the principle of eddy current time decay. A pulsed magnetic field excites eddy currents in a target. The time decay of the target's eddy currents is a function of the target's mechanical, electrical and magnetic properties. A target's identity can be determined by comparing accurately measured time decay characteristics of the target with a time decay characteristics of known mines.

This paper describes several data processing approaches for using the TEMID data for mine identification and clutter discrimination. These approaches include a template matching algorithm, time constant parameterization, and an adaptive neuro-fuzzy system. The paper presents results from applying these approaches to test objects from several recent field trials at the Ft. Belvoir mine lanes and Ft. A. P. Hill.

## 66.4

### SAR imaging of buried objects from computed scattered fields

Longstaff, J Dennis<sup>1</sup>; Wang, Yong<sup>1</sup>; Leat, Christopher J<sup>1</sup>

<sup>1</sup>CSSIP, University of Queensland, Australia

In this paper we compute Synthetic Aperture Radar (SAR) images of small resonant buried objects in the presence of ground clutter. We use the method of moments (MoM) to model scattered fields from a resonant buried conductor and model clutter as a Rayleigh amplitude distribution. A conventional SAR imaging technique is applied to the ultra-wideband waveforms to give a bipolar signal image (not the envelope image).

First, the induced currents on a target are calculated by a mixed potential integral equation (MPIE), with Formulation C, solved by the MoM using rooftop basis functions. The complex image method is applied to speed up the computation of the Green's functions.

To model the rough ground surface we represent this as a closely spaced linear array of point scatterers on the surface of the flat dielectric, each scatterer having random amplitude drawn from a Rayleigh distribution, and with uniform random phase.

The fields radiated from the target and point scatterer are then calculated by using the asymptotic technique based on the stationary phase method. The time domain responses are obtained by the inverse fast Fourier transform (IFFT).

To form the SAR image we assume the height of the radar and the permittivity of the ground are known and included in the imaging algorithm. The algorithm then computes the propagation delay from each point in the scene to each antenna point, including the effects of the dielectric ground. The scattered fields at the antenna points are then summed with these delays removed. A number of examples have been computed to illustrate the combined effects of SAR processing with resonant targets and clutter.

Fig.1 shows range profiles computed at 100 cross-range antenna positions with 2cm spacing. The target is a conducting plate of length 30cm and width 6cm buried in a dielectric half-space with  $\epsilon_r=5$  at depth 30cm. The hyperbolic response from the target can just be seen, embedded in range-dispersed ground clutter.

Figure 2 shows the computed SAR image. We see the effect of processing gain in improving signal to clutter ratio, and interestingly clutter is now smeared upwards only from the ground plane in the image, further improving visibility of the target. The resonance of the target is clearly seen and may assist with identification.

In summary, this simulation method is seen as useful tool for investigating the interesting features seen in SAR images of small buried objects

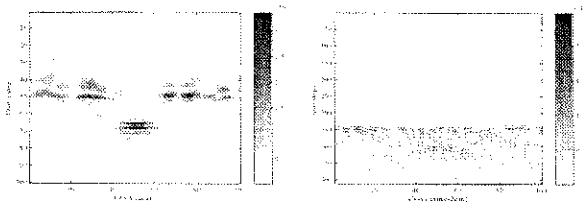


Fig.2 SAR image (rectified) of target and clutter Fig.1 Unprocessed range/azimuth data.

## 67.1

### Control of Chaos in a Plasma Filled Diode

Chen, X<sup>1</sup>; Lindsay, P A<sup>1</sup>; Zhang, J<sup>1</sup>

<sup>1</sup>Queen Mary Westfield College, UK

A plasma-filled diode is frequently used as a model for the interaction space of a virtual cathode oscillator (vircator). A vircator is capable of generating two types of oscillations: powerful and often ill-defined oscillations based on successive appearance and disappearance of a virtual cathode, and weaker but better defined oscillations due to a flip-flop action of the space-charge. In both cases the interaction process is highly nonlinear and the system is liable to slip into a chaotic range of operation. We propose to discuss methods for preventing.

We have been able to show that chaos is strongly affected by two important parameters of a plasma-filled diode: the reduced separation of the electrodes  $x_L$  and the electron/ion charge density ratio at the entrance electrode  $\alpha$ . In general some values of  $x_L$  are particularly conducive to the generation of chaos and should be avoided. Similarly the choice of  $\alpha > 1$  appears to be better in avoiding chaos than  $\alpha < 1$ . Chaos can also be controlled by a suitable choice of a load, although the influence of a load is far less dramatic than that of  $x_L$  or  $\alpha$ . In most cases a resistive component of the load tends to suppress chaos, although when too large it may quench the oscillations as well. An inductive component has a somewhat similar effect and there is little gain in its addition. The effect of a capacitive component is more involved, since in some case it may enhance both chaos and oscillations and has to be treated with some care. All these points will be discussed in more detail with help of suitable bifurcation diagrams.

## 66.5

### Phase Angle Based Clutter Reduction and 2D Imaging using Data From a Commercial Differential Two Frequency EMI System

Bruschini, C<sup>1</sup>; Sahli, H<sup>2</sup>

<sup>1</sup>EPFL VUB, Switzerland; <sup>2</sup>VUB, Belgium

The EPFL and the VUB have been investigating for some time the response of metal detectors for humanitarian demining<sup>1</sup>, in particular CW systems. A simple circuit model as well as a more complete model (full response of a sphere in the field of a circular coil) point to the possibility, as has also been stressed by others, of identifying some metallic objects based on their characteristic phase response. In addition, the phase shift of the received signal turns out to be a continuous function of the object size; this leads to the idea of imposing a "phase threshold" in order to reduce the amount of detected clutter. This approach is less ambitious than object identification, but is likely to be more robust, and to work best when looking for larger metallic objects such as those contained in non minimum-metal mines (e.g. PMN, PMN2) or UXO.

A first series of measurements were carried out using a Foerster Minex 2FD differential two-frequency metal detector. We have recorded the detector's in-phase (I) and quadrature-phase (Q) component at each frequency, as well as the difference of the two quadrature-phase components and the final audio signal. The latter is here directly derived from the difference signal. (Series of parallel) Linear scans have been carried out with a high density of points in the scan direction. The collection of data as a function of movement allows to analyse the data in the complex, or impedance, plane (I-Q). This method was inspired from Non-Destructive Testing, and puts in evidence global object properties rather than only local ones<sup>2</sup>. Results are presented for mines and mine components, as well as a few reference objects and clutter, buried in an indoor test system varying different parameters (material type, object distance, axial offset, orientation in the horizontal plane, etc.). The limits of such discrimination/identification approaches are also briefly outlined.

The parallel scans were also used to obtain bidimensional images of some metallic objects. Their resolution is limited by the detector's size, but can be ameliorated with image processing techniques such as deconvolution with the detectors intrinsic response, or PSF (Point Spread Function). The PSF, which is a function of the object's depth, can be obtained either theoretically (modelling) or experimentally via direct measurements on small objects for example<sup>3</sup>. Some example images are shown and the limits of this approach, such as sensitivity to noise and to ground inhomogeneities, are detailed.

- 1 C Bruschini, "Metal detectors in civil engineering and humanitarian de-mining: overview and tests of a commercial visualising system", INSIGHT - Non-DestructiveTesting and Condition Monitoring 42(2), pp 89-97, Feb 2000
- 2 P Szyngiera, "A Method of Metal Object Identification by Electromagnetic Means", in Proc. MINE'99 (Mine Identification Novelties Euroconference), pp, 155-160, Florencem Italy, Oct 1-3, 1999
- 3 L Merlat, M Acheroy, "Improving quality of information from metal detectors", in Proc 1999 ARIS Technical Workshop on Ground Survey for Humanitarian Demining, Brest, France, 26-27 Oct 1999



## 67.2

**Metastable Chaos Excitation in Highly-Susceptible Microwave Receiver and Digital Devices in the Conditions Interferences of Fractal Sequences Ultrashort Electric Pulses**

*Magda, J<sup>1</sup>; Novikov, V<sup>1</sup>; Pashchenko, A<sup>1</sup>; Shapoval, I<sup>1</sup>*  
<sup>1</sup>*Kharkov Institute of Physics Technology, Ukraine*

The study permits to conclude that the very high level of interference-related effects and potential danger of ultra-short pulse signals for the wide range of modern electronic devices, especially for highly-susceptible circuit of communication equipment, radio signals reception, rendering systems and digital devices.

The study demonstrates feasibility of scaling chaos excitation in the real electronic devices by means of the low-amplitude complex signals. The novel mechanisms of chaos excitation in the electronic devices are studied from the physical standpoint. These mechanisms are based on the unsteadiness of the boundary conditions and the mismatch of the electronic equipment components, while from the mathematical point of view they are partially based on IFS (Iterated Function System) concept. As distinct from ordinary mechanisms this latter one deal with the low-amplitude signals domain. The methods was developed can be applicable for the diagnostics and maintenance of the complex electronic equipment in the conditions of the modern electromagnetic environment. Two kinds of the high-power electric (electromagnetic) pulses generation for diagnostic investigations are suggested. Generation of pulses is performed during the switching of electron loop in the circuit, fed by the inductive storage. In the first schematic generation process is controlled by the nonlinear electronic circuit possesses the strange attractor. The above scheme permits to make the generated pulse sequence of a fractal character.

The principle of an operation of the secondary generation scheme is based on drop effect of a space charge at bifurcation transitions at some condition in an electron flow through the diode. Sequences of electric pulses produced by these generators may be transformed into sequences of electromagnetic pulses.

## 67.4

**Ray Splitting and Chaos in electromagnetic Resonators**

*Blumel, Reinhold<sup>1</sup>*  
<sup>1</sup>*Wesleyan University, USA*

Flat, cylindrical resonators of nonintegrable shapes are excellent systems for studying electromagnetic wave chaos. In this case, due to a formal equivalence of the stationary Maxwell equations and the quantum Schroedinger equation, flat cavities are also suitable for the study of quantum chaos in mesoscopic devices, important components for the next generation of super computers. Partially filled with dielectric substances, such as teflon, ray-splitting phenomena can be studied. For example, the Fourier transform of the frequency spectrum of a ray-splitting cavity shows peaks that correspond to the periodic orbits of a novel non-Newtonian mechanics that forms the semiclassical backbone of ray-splitting systems in the short-wavelength limit. In addition, ray splitting contributes novel universal terms to the Weyl formula that counts the number of modes in an electromagnetic resonator. This talk briefly reviews theoretical an experimental ray-splitting research carried out over the past ten years at the Universities of Maryland, Freiburg and Marburg, the State University of New York, the Polish Academy of Sciences and Wesleyan University. Experimental and numerical results on classically chaotic dielectric-loaded microwave cavities and analytical results on ray-splitting corrections to the Weyl formula will be presented.

## 67.3

**An Application of Chaos Theory to the High Frequency RCS Predication of Engine Ducts**

*MacKay, AJ<sup>1</sup>*  
<sup>1</sup>*DERA, UK*

The prediction of radar cross section (RCS) of electrically large structures is a topic of major interest for a number of applications. One particularly difficult problem is the accurate prediction of the RCS of engine ducts and other large cavities. Most general purpose methods employ shooting-and-bouncing ray tracing since more accurate modal and finite element methods are too computationally expensive for this purpose. However, using well established chaos theory we may show that numerical convergence is generally impossible using such ray tracing. We focus on straight ducts, terminated by a flat conductor, and show that there is a bound on the duct length, for a given incidence angle, in terms of the Lyapunov exponent for which convergence is not feasible. The Lyapunov exponent can be estimated from the average ray divergence using the Deschamps formulation or more directly using a tangent plane method from quantum mechanics.

Although special ray and hybrid-modal methods can probably be used to ensure numerical convergence this may not be necessary. We investigate the use of random fields to describe the RCS properties of a long stadium cross section duct in a regime where shooting-and-bouncing ray tracing can not achieve convergence. RCS distributions constructed in this way appear to have most of the features required of an exact prediction.

## 68.4

### Computer Aided Design of a Large Induction Heating System

Sazak, B.A.<sup>1</sup>

<sup>1</sup>Pamukkale Üniversitesi Muhendislik, Turkey

The analysis and development of electromagnetic devices is often difficult when the electromagnetic field is strongly coupled to the other quantities. In this case, conventional analytical methods give only rough approximation for the desired solution. Especially, if a precise determination of input values is needed, the classical methods often fail (Conraths, 1993). Additionally, with the increasing of system power as well as the operating frequency, the traditional investigation method on the basis of experiment becomes more and more difficult, even impossible in a laboratory condition. Consequently, circuit simulation packages Accusim and Design Architect have been used, which have been proven effective for power electronic system simulation compare with experimental results (Sazak, 1997). It can be used as an ideal tool to investigate power quality driven from mains supply. These package programmes allow the user both improvement an existing system and designing a new system.

Before starting to design of the coil some of the heater parameters have to be decided which effect the coil design, such as total power requirement, heating type, coil frequency, physical parameters of coil and the work piece. In this paper, output power was chosen as 85 kW at 4kHz resonant frequency and steel was chosen as working piece. Having defined these parameters, other parameters were calculated by using equivalent circuit coil-design method and then the coil together with workpiece was simulated. For simulating the complete induction heating system Design Architect and Accusim, which are the package programmes of Mentor Graphics were used. Initially, the complete induction heating system was designed for simulation by using Design Architect. After completion of design the circuit is transferred to another package program called Accusim. This is an analogue simulator that allows the user to test an analogue hardware design. Additionally, by using different probes a wide range of values such as voltage, current, frequency, maximum and minimum level of a wave have been measured.

A large induction heater was simulated with the real coil and the working piece parameters instead of simulating just a resistor and an inductance as coil parameters. Total Harmonic Distortion (THD) and Power Factor (PF) of input current were also plotted. Furthermore, a comparison study was made between actual value and computer simulation. For getting actual operation values a number of measurements were made on a large induction heater at an induction heater factory by using spectrum analyzer and then compared with the results of the computer simulation. Simulation of induction heater coil was found particularly useful for seeing the circuit behaviors in all operation conditions. By using these technique, the induction heater can be simulated at any kind of operation and load conditions (empty, half loaded, full loaded, cold load, hot load) and also for different load (steel, aluminum, nickel...) This helps the designer to see many circuit parameters before creation. This paper presents that computer simulation was quite close to the actual values. The simulation found useful for those applications, which requires high input power and also it helps to see the circuit condition for different load and operation mode.

Conraths H.J. Numerical Simulation of Induction Heating: A Finite Element Approximation, ETEP, Vol.3, No.5, 1993, pp.339-345. Sazak B.S. 1997 A New Unity Power Factor Quasi-Resonant Induction Heater, Doktora Tezi, University of Glamorgan, U.K.

## 68.5

### Field Pattern Simulation of High Power Plant for Microwave Drying of Wood

Boiko, P.; Galdetskiy, A.<sup>1</sup>; Korolev, A.<sup>1</sup>

<sup>1</sup>SRPC "Istok", Russia;

Materials processing is one of the prospective applications of high power microwaves. Microwave drying of wood allows to create relatively compact and mobile plants having drying cycle duration less than 48 hours. Now the microwave plant for wood drying having average power 50 kW and frequency 0.915 GHz is underdevelopment in "Istok". The key performances of such set-ups are the uniformity of electromagnetic energy density through a wood pile and good matching of magnetron generator with microwave chamber at various humidity of wood and chamber filling. Our previous attempts to solve these problems failed.

We consider new design of microwave coupler. In this structure the generator feeds long transmission line (waveguide) having distributed load in the form of a set of coupling loops (thus microwave power is distributed along X axis). Output of each loop feeds distributed radiator (Frankline antenna), transporting power along Z axis and radiating it along Y axis. Total radiation field should be close to the pattern of plane wave propagating in Y direction. Distributed loading of waveguide implies good matching of the generator with variable load.

The results of the simulation of such feeding system are presented. VSWR and microwave energy density were calculated. Variations of dielectric constant of wood and chamber filling don't increase VSWR in the waveguide more than value 1.2. Variation of microwave energy density is less than 50%. This value can be further diminished by using movable radiators. Averaged dissipated power is uniform within margins 10%. Thus considered design is quite suitable for use in industrial microwave plants.

## 71.1

### Evaluation of Several GPR Signal Processing Schemes

Rhebergen, J.<sup>1</sup>

<sup>1</sup>TNO Physics and Electronics Laboratory, Netherlands

Ultra wideband GPR is a technology appearing in most plans for advanced multi-sensor land-mine detection systems. The development and advancement of this technology is pursued at many laboratories. Together with infra-red and pulse-induction systems it is a suitable candidate for a multi-sensor system.

The TNO-FEL HOM2000 program, for example, is aimed at combining commercially available versions of the aforementioned sensors for sensor-fusion, producing one single output. All of these sensors have their false alarm rate (FAR), i.e., a buried object is detected but there is ambiguity involved in determining the nature of the detected object.

To be able to significantly reduce the FAR and speedup land mine detection, suitable signal processing algorithms need to be developed with the aim of real-time target identification (classification). This will improve the process of de-mining considerably.

GPR signal processing can be divided into a preprocessing/conditioning part and a identification/classification part. This study looks at the performance of several existing signal processing schemes, on data collected with our own experimental UWB GPR and data collected with commercial systems.

Currently simple preprocessing schemes like filtering, background subtraction, average removal, etc. are being implemented. We will also look at more advanced algorithms for imaging and identification like SAR/ISAR and EMSIM (electromagnetic singularity identification method).

## 71.2

### Landmines Detection using Higher-Order Spectral Analysis on Ground-Penetrating Radar Data

*Perrin, S<sup>1</sup>; Duflos, E<sup>1</sup>; Nivellet, F<sup>2</sup>; Vanheeghe, P<sup>3</sup>*

<sup>1</sup>ISEN, France; <sup>2</sup>Thomson CSF Detexis, France; <sup>3</sup>Lab d'automatique et Informatique de Lille, France

In the field of humanitarian demining, improvement of performances in term of landmines detection and identification are expected from the use of a multisensors system. Such a system implies a multisensors fusion task in order to benefit from complementarity of individual sensors. Heterogeneity of data often imposes a features extraction step prior to the fusion. Because of its good complementarity with the usually used metal detector, the ground-penetrating radar (GPR) is widely expected to be integrated to the future multisensors system. Therefore, numerous different methods have been proposed for features extraction from ground-penetrating radar data. The more commonly used methods are the correlation, the spectral analysis, the time-frequency analysis and the time-scale analysis.

In this study, a new method to analyse GPR data is proposed. This method is based on the Higher-Order Spectral Analysis (HOSA). This quite recent analysis is based on the computation of the higher-order moments. It allows to obtain information which can't be given by means of a classical spectral analysis. For instance, it allows the test of some properties of the analysed signal such as linearity and gaussianity and therefore HOSA is a well adapted tool for the analysis of non-linear and non-gaussian signals which is the case of ground-penetrating radar signals, as it will be shown.

In the first part of the article we define the higher-order cumulants and the bispectrum which are the main notions of HOSA that are used in this study. In the second part we describe a method to analyse the gaussianity and the linearity of GPR signals: the main result is that these signals are non-gaussian and non-linear. This result is very important as it means that parametric modeling of GPR data must be made from non-linear models. We also give some non-linear models which could be candidate for the modeling. In the third and last part of the paper we describe a new, HOSA derived method for

the analysis of GPR signals. This method is based on the analysis of the singular values of a specific matrix, the coefficients of which are computed from the third order cumulants. This method has been tested in simulation on measured GPR data. The results will be described and analysed in the paper. The main result is that the value of the significative singular value seems to be linked to the presence of a mine in the GPR signals.

## 71.3

### Bayesian Statistical Signal Processing Algorithms for Subsurface Target Detection and Identification

*Collins, L<sup>1</sup>; Tantum, S<sup>1</sup>*

<sup>1</sup>Duke University, USA

There are many sensor modalities, such as electromagnetic induction (EMI), magnetometers, radar, and seismic sensors, utilized for detection and identification of buried targets. EMI systems sense the currents induced in a metallic target by the incident field, and thus, are essentially metal detectors. The time domain response of pulsed electromagnetic induction (EMI) systems is often modeled as a sum of decaying exponential signals. Under this model, the characteristic decay rates, or poles, for a particular target are a function of the target's composition and geometry, and are independent of the target/sensor orientation. Therefore, the EMI signature for a given target may be parameterized by its intrinsic decay rates, regardless of the target/sensor orientation. Since the targets of interest (i.e., landmines and/or UXO) form a finite set whose decay rates can be determined a priori, either experimentally or through physical models, decay rate estimation has been proposed as a viable technique for detection and discrimination of landmines and UXO. Since the basis for this approach to target detection and discrimination is that targets are uniquely characterized by their decay rates, discrimination performance is dependent upon the performance of the decay rate estimation procedure. Although the decay rates are intrinsic to the target and are independent of the target/sensor orientation, the contribution of each decaying exponential to the total signal is a function of the target/sensor orientation. The orientation of subsurface targets relative to the sensor is rarely known a priori, and the uncertainty concerning this parameter may degrade detection and discrimination performance if it is not considered when developing signal processing algorithms. The uncertainty in the target/sensor orientation may be rigorously accounted for within a Bayesian construct. In this paper, the target detection and discrimination performance of several Bayesian statistical signal processing algorithms is compared. Specifically, algorithms which process the entire time domain signal are compared to algorithms which process the estimated decay rates. In addition, the effects of uncertainty in the target/sensor orientation on performance are investigated. Results are presented for both simulated and real data.

## 71.4

### Analysis of Forward-Looking Ground Penetrating Radar (GPR) Data for Mine Detection

*Rosen, E<sup>1</sup>; Sherbondy, K<sup>2</sup>*

<sup>1</sup>Institute for Defense Analyses, USA; <sup>2</sup>US Army CECOM, USA

To date, most of the vehicular-mounted mine detection systems employing ground penetrating radar are down-looking in the sense that the array of radar antennas are approximately 1-meter forward of the vehicle and pointed straight down. Advantages of systems that are able to look forward of the vehicle by more than 10 meters include the ability to make detections at earlier times, and to use multiple looks at targets in order to discriminate mines from clutter. Data collected by two such systems at two different sites provide a means by which these two advantages can be assessed. Although the two systems differ in many ways, each are stepped-frequency GPR's operating in nearly the same band.

We present, in this paper, a brief description of the two forward-looking GPR systems and the data collection exercises they underwent. Analysis of the raw GPR sensor data is then presented with an emphasis on comparing signal strengths reflected from targets with signals reflected in the absence of targets. We arrive at similar measures of performance despite the significant differences in signal processing techniques used for the two systems. Where applicable, the ability to track a target before passing over it is demonstrated. Detection trends as a function of incident frequency and target type are examined.

## 71.5

### Detection of Non-Metallic Antipersonnel Land Mines

*Brooks, J<sup>1</sup>; Adhami, R<sup>2</sup>; Biggs, A W<sup>2</sup>*

*<sup>1</sup>Brooks Enterprises International Inc. USA; <sup>2</sup>University of Alabama in Huntsville, USA*

This paper describes a method of detecting non-metallic antipersonnel land mine (NM APL) using certain attributes of wavelets and wavelet packets applied to GPR signal processing. A number of measurement data sources are used, including 1 and 10 GHz pulse GPR data, and a 6 GHz frequency-stepped GPR. Targets are chosen to include real APLs and also rocks, metallic clutter and other non-lethal clutter, which normally present false targets to the GPR. The GPR signals are first denoised with an adaptive wavelet packet denoising method, then the shape features of the APL are determined from exploiting the regularity properties of wavelets. Results are shown which indicate that the method may be applied to pulse GPR processing, but not for frequency-scanned GPRs.

Preprocessing the GPR signal for clutter reduction is not always necessary, thus simplifying the detection process. In addition to the technical contributions, the paper emphasizes several issues regarding practical land mine detection/clearance. The first author traveled to Cambodia in 1997 to participate in GPR data collection at the HALO Trust compound in Thmar Pouk. He was able to experience first-hand the difficulties of humanitarian demining with a metal detector and has developed a set of criteria to be applied to the design of high-tech mine detection equipment; details are provided in the paper.

## 6.5

### Mechanism of Spontaneous Pulse Shortening and Methods of Pulse Lengthening in Gigawatt Relativistic BWO

Batrakov, A V<sup>1</sup>; Karlik, K V<sup>1</sup>; Kitsanov, S A<sup>1</sup>; Klimov, A I<sup>1</sup>; Kononov, I N<sup>1</sup>; Korovin, S D<sup>1</sup>; Pegel, I V<sup>1</sup>; Polevin, S D<sup>1</sup>; Proskurovsky, D I<sup>1</sup>; Sukhov, M Yu<sup>1</sup>; Mesyats, G A<sup>2</sup>

<sup>1</sup>Institute of High Current Electronics SD RAS, Russia; <sup>2</sup>Institute of Electrophysics UD RAS, Russia

Spontaneous pulse shortening occurring in the relativistic BWO at gigawatt power levels it studied in experiment and theory.

In first experiments with a 3-GW relativistic BWO, spontaneous microwave pulse width limitation at 6 ns was observed. It is now experimentally demonstrated that this phenomenon is accompanied by formation of explosive-emission plasma at the surface of a corrugated slow wave structure and appearance of intense electron flows between the SWS ripples. Termination of microwave emission is explained in terms of the increase of the BWO starting current due to the partial absorption of the operating electromagnetic wave by electrons emitted from the plasma, while the intensity of absorption radically increases owing to the presence of positive ions emitted from the plasma.

To improve the electric strength of BWO electrodynamic system, treatment of its surface with low-energy, high-current electron beam (LEHCEB) is proposed. Effectively smoothing the metal surface and removing dielectric inclusions from the surface layer, such treatment allows suppression of the explosive emission.

A Penning discharge LEHCEB source with a plasma anode was developed having a pulse width 2.5 - 3  $\mu$ s. Treatment of slow-wave structure parts was made consequently in two regimes, the first one with energy deposition 8 - 10 J/cm<sup>2</sup> (evaporation of surface layer of ~0.4  $\mu$ m and melting to a depth of ~4  $\mu$ m), the second one at 5 - 6 J/cm<sup>2</sup> (melting to ~0.3  $\mu$ m with no evaporation). The first regime caused the removal of surface contaminants and dissolved gases, the second one provided smoothing of the surface.

## 19.3

### Quasi-Optical Methods for High Power Microwave Beam Control

Petelin, M I<sup>1</sup>

<sup>1</sup>Institute of Applied Physics, Russia

At higher powers and frequencies, especially at millimetre waves, standard (single mode) components used to canalise and control microwave energy at relatively low frequencies should be substituted with oversized, in particular, quasi-optical ones being low-loss, breakdown- and overheating-proof.

A part of such components can be developed for high power information (communication and radar) systems basing on experience gained in the frame of the controlled fusion program where 30-170 GHz wave flows of quasi-CW MW power are efficiently transmitted at tens meters. In these experiments various types of mode converters, waveguide bends, RF windows, mirror lines, wave polarisers, wave dividers, mutually coherent wave combiners and other elements with stationary or quasi-stationary parameters are used.

In addition to the components mentioned, the high power information systems may need some specific units to control high power microwave flows. In particular, some quasi-optical components with agile parameters can operate as wave beam switches receiver protectors and pulse compressors; the electrically controlled media being gas discharge tubes or laser illuminated semiconductors. A number these components contain periodic structures (gratings and Bragg reflectors) providing mode selectivity (in particular, polarisation sensitivity) and frequency dispersion. These elements can compose phase controlled beam switches-combiners, polarisation separators, and antenna transmit-receive duplexers.

There are some versions of quasi-optical multiplexers for multi-channel operation of high power communication systems and for high range resolution radar with synthesised frequency band.

Most of these components were proposed in the frame of collaboration of IAP with Stanford and Yale universities and GEC-Marconi. In the report submitted, new details of theoretical and experimental studies would be presented.

When running experiments on high-current electron accelerator SINUS-7 (pulse length 50 ns, max 20 kA and 2 MeV), arrangements were taken to provide cleaner vacuum conditions (oil-free evacuation, installation of liquid nitrogen traps, use of inert gas filling instead of air when opening the system). Just these measures (without LEHCEB treatment) combined with electrochemical polishing of SWS surface provided pulse lengthening up to 26 ns at a peak power of 3 GW (microwave pulse energy ~80 J). However, untimely termination of the microwave pulse did occur. Adding LEHCEB treatment resulted in further pulse length increase to 29 ns (pulse energy ~90 J). In this case, no untimely pulse termination was observed (the fall of the microwave pulse was coincident with the fall of the feeding e-beam current pulse).

The obtained results prove the hypothesis about explosive-emission nature of spontaneous pulse shortening in HPM sources.

## 25.3

### The High Power Microwave Facility: ORION

Spark, S N<sup>1</sup>; Kerr, B A<sup>1</sup>; Parkes, D M<sup>1</sup>; Harbour, M I<sup>1</sup>; Douglas, S C<sup>1</sup>

<sup>1</sup>DERA Malvern, UK

The ORION high power microwave facility was designed and constructed by Physics International (PI), San Leandro, California, USA, to a design specification which arose within the UK. This presentation will provide an overview of the system capabilities and describe in detail the operating principles of the pulsed power modulator.

The ORION system is now fully operational in the UK. The system has been commissioned and now meets all of its original design specifications generating HPM radiation across a continuous tuneable bandwidth from 1GHz to 3GHz. This system is based on a high performance, adaptable and highly engineered pulse power system. When coupled to the relativistic magnetrons ORION represents one of the most versatile HPM systems in the world today

## 28.3

### A Method of 3-D Scanning Pulsed Wave Beam for Subsurface Objects Location

*Kolchigin, N<sup>1</sup>; Egorov, M<sup>1</sup>; Pivnenko, S<sup>1</sup>*

<sup>1</sup>*Kharkov National University, Ukraine*

One of problems in subsurface radar is the detection and recognition of natural and artificial inhomogeneities in layered media. The existing devices for detection and recognition of small insertions in a subsurface layer are ineffective when investigating large area and vice versa, the devices for large area scanning are of little use when identifying small-sized insertions.

In this report, we present a method in which both electronic scanning a pulsed radar beam along the searching surface in two dimensions and controlling the location of the beam focus inside the search layer are realized. This results in enhancement of the efficiency of large area searching as well as allows to solve the problem of detection and following recognition of the detected small sized insertions.

In order to form the pulsed wave beam with the opportunity of the three-dimensional scanning we propose to employ an antenna system consisting of two orthogonal printed antenna arrays of special design. The arrays featured with an opportunity of controlling time delay distribution of pulsed excitation on the array elements. Such controlling, in turn, allows to vary both the location and the sizes of the focus for receiving and transmitting antennas.

A theoretical model of scanning and focusing the pulsed wave beam is developed which is based on the problem of transient field radiation by a rectangular aperture under non-synchronous excitation and specified amplitude distribution. Theoretical and experimental modeling are carried out to ascertain the dependence of the focus location in a subsurface layer on a shape of time distribution of electromagnetic fields on antenna array elements.

In order to perform the experimental part of the work, a complex calculational and experimental approach was applied which

incorporates theoretical investigation with laboratory and field experiments and takes into account the real conditions of interaction between fields and objects - transient character of the signals, losses in media, and interaction locality. The method of three-dimensional scanning increases the reliability of detection of subsurface objects and allows to increase the efficiency of their recognition. Based on the results of the work, industrial portable devices for search and recognition of various subsurface objects such as tubes, cables, cavities, unexploded ordnance, antipersonnel mines could be developed.

## 32.2

### Physical Models of Electromagnetic Ground Environment in the Nuclear Source Region

*Kouprienko, V M<sup>1</sup>; Ostaphiychuk, R M<sup>1</sup>; Ostaphiychuk, N A<sup>1</sup>*

<sup>1</sup>*Science Research Centre of 26 CSRI, Russia*

The EMP source region of a surface nuclear explosion is about 2 km in radius. The EMP is represented as a sequence of three time phases - the wave phase, the diffusion phase and the quasistatic phase. This paper describes a physical simulation of processes occurring in the diffusion and quasistatic phases.

An adequate and comprehensive reconstruction of the external EM environment is the key factor for the designing and testing of research techniques for a postulated physical model. The physical models of EM environment simulators totally depend on their application (research or test models), the object under study, the number of details to be reproduced, the EMP composition, and the space geometry to be simulated. In the model suggested the receptors are located in the ground under the EMP source area with a radius of several kilometers from the explosion center to a depth of 600 m. To reproduce adequately the EM environment in this space region in terms of the unambiguous solution of Maxwell's equations and EMP generation theory, it is necessary and sufficient to simulate the boundary conditions properly.

This paper discusses requirements on the set of initial data to be used for the solution of engineering problems for constructing appropriate physical models. Numerical estimations of parameters of the simulated systems and their design are presented. We also describe some small-scale models to study physical processes in the entire source region and models for EMP reconstruction in a limited space. Some experimental results of studies made by using the physical models suggested are presented.

## 40.5

### High Power Subnanosecond Generator for UWB Radar

*Prokhorenko, V<sup>1</sup>; Boryszenko, A<sup>2</sup>*

<sup>1</sup>Engineer of Research Comp. Diascarb, Ukraine; <sup>2</sup>Principal Engineer of Research Comp. Diascarb, Ukraine

Performance of the Ultra-Wide Bandwidth (UWB) radar is hardly dependence from pulse generator parameters. One of the most serious limitations of the UWB radar applications for subsurface and air surveying is too small peak power of the pulse generator. There are step recovery diodes, avalanche diodes or transistors used for subnanosecond pulse generation. Unfortunately achievable peak power such generator does not exceed several hundreds watts. As a matter of fact this power level is usually enough in most of cases for subsurface sounding applications but not for air UWB radar aims. Generator based on gas-discharge tube can provide high power impulse. But repetition rate of the generator is too little (a few Hertz) and generated pulse parameters (shape and peak power repeatability) do not under control.

A new sort of step-recovery mode has been discovered in Russia at the 80th beginning. This mode is observed into power rectifier diode structure. Such diodes, so-called drift step recovery diode (DSRD), are able to make high power step voltage sharpening. The DSRD structure seriously rivals among existent active elements for high power impulse generation especially for achievement of peak power beyond of kilowatt level. Really achievable power level is only limited by power supply and driver electronics availability. Thanks to using of step-recovery principle based on DSRD structure a pulse generator has wide possibilities to impulse shape and amplitude control. It has been reported about 1.6-Megawatt peak power 5-nanoseconds impulse generation. Repetition rate (100 Hz) with has been limited by power supply availability only. Instability has not been exceeded of 100-picosecond value.

Experimental set for power with nanosecond rise-time pulse generation is described at this work. Special attention has been devoted to numerical simulation and optimisation of the current drive circuit based on developed mathematical model of device.

Investigation results for peak power more than 5 kilowatts and rise time less than 2-nanosecond generation are reported. It has been shown abilities of application of some types of commercial available power rectifier diodes in a drift step recovery mode. DSRD generator can operate with low impedance antennas and forms nanosecond and subnanosecond high-power pulses preferable for subsurface and air sounding. Results on DSRD generator testing in UWB radar arrangement will be presented and discussed too.

## 41.3

### Measurement of Layered Dielectric Parameters in Wide Angular Sector Making use of Pulsed Wave Beam

*Pivnenko, S<sup>1</sup>; Kolchigin, N<sup>1</sup>*

<sup>1</sup>Kharkov National University, Ukraine

Determination of inner structure of opaque inhomogeneous and layered materials is an actual problem for a number of applications. This is subsurface exploration of minerals, measurement and checking parameters of composite layered materials, search and identification of subsurface objects like antipersonnel mines, unexploded ordnance, cavities, tubes, etc. Among various possible methods of investigation of inhomogeneous media, an employment of short electromagnetic pulses is the most informative and visual one. It is also worth to mention that for measurements in free space an account for the spatial structure of pulsed field radiated by an antenna (non-plane waves) in most cases is not only the necessary condition but allows also to improve accuracy and to accelerate measurements.

The aim of this work is modeling of pulsed wave beam scattering on inhomogeneous layered and absorbing materials and determination of parameters of the material through measured characteristics of scattered pulsed field.

In order to substantiate the method of measurement and to develop an algorithm of experimental data processing we use the solution to the problem of scattering of restricted in space pulsed field on layered lossy medium. Solution to the problem is based on application of integral Fourier transform and making use of layered medium reflection coefficient for time-harmonic plane waves. The obtained solution takes into consideration a few reflected waves and is valid for the case of small losses.

The developed and assembled experimental set for the investigations in free space using videopulses of hundreds of picosecond duration is described. The set allows to measure transient responses of objects in free space. Tapered slot antennas on dielectric substrate are employed as receiving-transmitting ones.

The results on experimental investigations of pulsed wave beam scattering on layered dielectric materials and absorbing materials are given. According to the obtained data, parameters of a dielectric layer placed on the perfectly conducting surface such as thickness and permittivity are calculated; frequency-angular dependences of the reflection coefficient for several types of radioabsorbing materials are obtained from the measured time-angular dependences of scattered field. The experimental results are in good agreement with actual parameters as well as with theoretical results.

The experimental investigations prove correctness of the obtained theoretical solution as well as reliability and accuracy of an algorithm of fast measurement of material and dimensional parameters of layered media in wide angular sector of incident angles without turn of radiating antenna proposed in (N. N. Kolchigin, S. N. Pivnenko, Proc. of Int. Conf. on MMET, 346-348. 1998. Kharkov, Ukraine).



## 54.1

### Generation and Radiation of Powerful Nanosecond and Subnanosecond Pulses at High Pulse Repetition Rate for UWB Systems

*Kardo-Sysoev, A<sup>1</sup>; Brylevsky, V<sup>2</sup>; Zazulin, S<sup>2</sup>; Smirnova, I<sup>2</sup>*  
*<sup>1</sup>Ioffe Physico-Technical Institute (Ioffe PTI), Russia; <sup>2</sup>Pulse Systems Group (PSG), Russia*

The best form of coherent signals for UWB systems is a short pulse of sub or nanosecond length, which strongly simplifies correlation procedure at receiving end.

The most critical element of sources of such pulses is a switch. Only semiconductor switch has practically unlimited number of shots, small sizes, can operate at pulse repetition frequency (PRF), exceeding dozens kilohertz and has high time stability. The most known devices are bipolar (BT) or field effect (FET) transistors, step recovery devices (SRD) can operate at high PRF up to megahertz, but their peak and average powers quickly decrease with decrease of switching times, going to peak watts and average milliwatts levels. Optically driven GaAs switches (BASS, BOSS) and avalanche transistors assembling have short life times <10E8 shots for MW power level and low PRF < 10 kHz.

The most promising semiconductor pulser technology which is able to provide both high peak (>10E5 W) and average powers (> 100 W) at high PRF (10E6 Hz) with low jitter (<10ps) is based on new devices Drift Step Recovery Diodes (DSRD) and Drift Step Recovery Transistors (DSRT). Both these devices are opening switches and energy is stored in inductors. So when switch breaks current in pulser there is high voltage multiplication and high voltage exists only during short pulse time, which prevents stray breakdowns and simplifies design.

At lower PRF (>100 kHz) other new closing switches Silicon Avalanche Shapers (SAS) are used, which has less than 100 ps rise times at tens kV, but need high  $dU/dt > 10E12$  V/sec to be triggered. Such high  $dU/dt$  is supplied by a stage on DSRD. The physics of operation of SAS is delayed ionisation.

## 54.2

### Ultrawideband Pulsed Synchronized Antenna Array

*Kardo-Sysoev, A<sup>1</sup>; Flerov, A<sup>2</sup>; Frantsuzov, A<sup>2</sup>; Zazulin, S<sup>2</sup>*  
*<sup>1</sup>Ioffe Physico-Technical Institute (Ioffe PTI), Russia; <sup>2</sup>Pulse Systems Group (PSG), Russia*

The most promising sources of coherent ultrawideband short pulsed (UWB-SP) signals are based on semiconductor devices. The most powerful fast switches are Drift Step Recovery Devices (Transistors - DSRT, Diodes - DSRD) and Silicon Avalanche Shapers - SAS. But well known rule "the shorter turn on/off time is less switching power" is valid still. So to increase output power, it is necessary to combine power of many devices. Parallel or/and series tight connections of many devices provides internal synchronization and is widely used in pulsers design. But such internal synchronization fails when distance between the remotest devices becomes comparable with electromagnetic wave's travel distance during pulse rise time. This and heatsink deterioration limit the maximum power. In this case a special external synchronizing system is needed to compensate possible difference of delays between devices.

But having external synchronization for the case of pulse radiation it is natural to use antenna array to combine the power of many pulses in space. Such array has been designed. It consisted of 8 horns (2 in H plane, 4 in E plane) fed by 4 pulsers, each of which generates 20 kW peak power pulses with 200 ps FWHM, 70 ps rise time at 12 kHz PRF. Initial delays between pulser's triggering input and output are around ~200 nanoseconds, dispersion of the delays is 6 nanoseconds. Jitter is less than 20 picoseconds, but there was slow temperature drift-100ps/10 minutes after initial drift ~1.5 during the first 20 minutes. Four independent feedback loops were used to lock the position of each pulse to the reference time point. Initial positions (the feedbacks loops are opened) were shifted from the reference point up to 30 ns. After closing of the loops the pulses locked onto the reference point during 0.1 sec with precision better than 30 ps. Radiated pulses in far zone are close to derivative of feeding ones. The first zero-zero half period width is 200 ps, efficient voltage is more than 12 kV. The field intensity is proportional to a number of pulsers locked with tolerance better than 10 %. The beam width is: H plane - 18 degrees E plane - 12 degrees.

As a rule, when a pulse is a subject to be radiated into the space, the main problem is to keep the length of radiated pulse as close as possible to length of pulse fed into an antenna. Such radiator may be represented as antenna with uniformly exited aperture. To get high gain the size of the aperture should be large to compare with the pulse length. The best realisation of aperture antenna is a horn. But the horn with uniformly exited aperture and high gain should have very large length - fare larger than aperture size, which makes such the best theoretically radiator unpractical.

We have suggested an approach called "folded" horn allowing to make it many times shorter. Such horn consists of several arrays of subhorns, placed on different levels. This approach may be applied to both flat horns (one dimensional) with fan like pattern and to usual two dimensional with needle like pattern. The ratio of high frequency to low frequency is higher than 20. Phase centre does not depend on the frequency.

## 56.2

### UXO Test Sites at YUMA Proving Ground and Eglin AFB: Layouts, Soils, Targets and Ground-Truth Data

*Kolodny, Michael<sup>1</sup>; DeLuca, Clyde<sup>1</sup>; Marinelli, Vincent<sup>1</sup>*  
*<sup>1</sup>US Army Research Laboratory, USA*

The U.S. Army Research Laboratory has installed extensive unexploded ordnance (UXO) test sites at the U.S. Army Yuma Proving Ground, Arizona, and Eglin Air Force Base, Florida. The two test sites were created under the sponsorship of the Strategic Environmental Research and Development Program to support ARL experiments to determine the applicability of stand-off ultra-wideband radar for the detection of UXO. Now that ARL has completed its experiments, the test sites are available to others who are interested in conducting UXO detection experiments at calibrated test sites.

Each site contains approximately 500 inert ordnance test targets of various types: submunitions, mines, mortars, artillery shells, rockets, and bombs. To give researchers a rich database from which to understand the phenomenology associated with UXO, targets were placed at varying depths and orientations and detailed ground-truth information (target ID number, photo of target in placement position, target orientation, and precisely surveyed location coordinates) was carefully measured and/or recorded.

The two sites are quite different in terms of soil, vegetation, and man-made clutter. The majority of the test site at Yuma is located within the Phillips Drop Zone, where the soil has been turned over to a depth of about 2 ft and is virtually free of vegetation; an almost homogeneous soil layer. This feature permits the investigation of electromagnetic wave propagation studies in a realistic but relatively easily definable soil. In contrast, the test site at Eglin-located at test area C-62, an active bombing range-is normally much wetter than Yuma and contains fast-growing ground cover and numerous subsurface UXO (training bombs) left behind from training activities; thus, the clutter environment is much more challenging.

## 57.4

### The Technique of Electron Beam Stabilization in Microwave Tubes with Cold Field Emitting Cathodes

Galdetskiy, A<sup>1</sup>

<sup>1</sup>SRPC "Istok", Russia

Field effect cathodes are very attractive for electron beam formation in vacuum microwave devices. The last achievements in technology of diamond-like carbon films deposition made it possible the obtaining of emitters capable to operate in technical vacuum ( $10^{-6}$  Torr) with average current density 1-2 /sq. at macroscopic electric fields on the cathode 6-7 kV/mm. This discovers the opportunities of creation of new class of electron guns for industrial microwave tubes (TWTs, klystrons) having unique features: instant turn-on time, absence of heating power, high time of life, increased electrodes stability and absence of cathode sputtering.

However beam current (and output microwave power) in such simple diode gun is not quite stable and is very sensitive to the cathode voltage due to small influence of space charge in the gun with field effect cathode and strong dependence of field emission current on electric field (cathode voltage).

We investigated the opportunities of currents stabilization by using the new gun design with two anodes. The first anode has variable potential (0.3-0.5 kV more negative than second anode) which is determined by a negative feedback circuit (solid-state or passive) and depends on beam current. In the simplest case the first anode is just biased from the second anode through a resistor and has the output aperture dimensions very close to the beam diameter in crossover. Potential of the first anode is determined by a small intercept current of electron beam. For such gun design having voltage  $U_c = 14$  kV and current 180mA the calculated sensitivity of the beam current to cathode voltage variations (transconductance) was decreased by 2 orders of magnitude at increasing of biasing resistance from 0 to 1 MOhm. We also investigated stability of beam current with respect to the fluctuations of emission. Beam current fluctuations (noise) were depressed by factor 110.

Feeding of the first anode through high resistance also protects the gun against possible discharges. Now experimental specimen of the gun with carbon cathode is fabricated.

## 58.1

### Biological Effects of Repetitively-Pulsed High-Power Microwave Radiation

Bol'shakov, M A<sup>1</sup>; Evdokimov, E V<sup>1</sup>; Goncharik, A O<sup>1</sup>; Bugaev, S P<sup>2</sup>;

Gunin, A V<sup>2</sup>; Klimov, A P<sup>2</sup>; Korovin, S D<sup>2</sup>; Pegel, I V<sup>2</sup>; Rostov, V V<sup>2</sup>

<sup>1</sup>Tomsk State University, Russia; <sup>2</sup>Institute of High Current Electronics SD RAS, Russia

Using a repetitively pulsed HPM source based on the Relativistic Backward Wave Oscillator driven by high-current electron accelerator SINUS-6, experimental study of biological effects of X-band nanosecond microwave pulses was made. The radiation wavelength was 3 cm, the pulse width was ~10 ns, and the pulse repetition rate was varied from units to 100 p.p.s. The radiating electrodynamic system formed a Gaussian microwave beam with linear polarization. The RF electric field strength was ~  $1.5 \times 10^4$  V/cm in the irradiation zone (spot diameter 25 cm at  $0.7 \times E_{max}$ ) and 1.5 times higher immediately behind the output vacuum window. To minimize the action of bremsstrahlung on the objects tested, lead X-ray protection was used decreasing the dose to ~  $10^6$  Rad/pulse.

The objects to test were: *E. Coli* bacteria, *Fusarium* fungus, and *Drosophila melanogaster* at different stages of development. Exposition to microwave pulses with the above parameters did not cause death or notable division deceleration of *E. Coli* cells that obviously indicates no electroporation of membranes as in the case of application of short high-voltage pulses. For the *Fusarium* fungus, at any pulse repetition rate, definite decrease in the growth rate of fungi immediately in course of irradiation was observed. The experiments demonstrated no notable difference in the growth rate for giphae oriented parallel and perpendicularly to electric field vector. Observation of post-action evidenced acceleration of growth for irradiated cultures.

*Drosophilas* flying from irradiated eggs demonstrated increased percentage of interrupted development, morphoses in a form of wrong segmentation of body, sterility, and untimely death of imagoes. The existence of biologically significant pulse repetition rate bands was confirmed.

## 57.5

### Operation of High-Power Planar FEM with Two-Dimensional Bragg Reflectors

Arzhannikov, A<sup>1</sup>; Agarin, N V<sup>1</sup>; Bobylev, V B<sup>1</sup>; Burdakov, A V<sup>1</sup>;

Burmasov, V S<sup>1</sup>; Ivanenko, V G<sup>1</sup>; Kalinin, P V<sup>1</sup>; Kuznetsov, S A<sup>1</sup>;

Sinitsky, S L<sup>1</sup>; Stepanov, V D<sup>1</sup>; Diankova, E V<sup>2</sup>; Petrov, P V<sup>2</sup>;

Ginzburg, N S<sup>3</sup>; Peskov, N Yu<sup>3</sup>; Sergeev, A S<sup>3</sup>

<sup>1</sup>Budker Institute of Nuclear Physics, Russia; <sup>2</sup>RFNC-VNIITF, Russia;

<sup>3</sup>Institute of Applied Physics, Russia

Free Electron Maser (FEM) driven by a sheet electron beam with a large transverse size can be considered as a promising device to generate microsecond microwave pulses with energy content 102-103 J. One of the main physical problems for operation of such device is to provide spatial coherence of radiation from different parts of electron beam when its width exceeds wavelength of the radiation in more than one order. We investigate two-dimensional distributed feedback in a planar FEM theoretically and experimentally as a method to solve this problem. The experimental studies are carried out at the Budker Institute of Nuclear Physics on the ELMI device. The ELMI device consists of the accelerator U3 (1 MeV, 5 kA, 5 mcs), an undulator magnetic system (longitudinal component is up to 1.4 T, transverse undulating one is up to 0.15 T), a planar resonator formed by two Bragg-reflectors with double corrugated inner surfaces, and diagnostics of beam and microwave radiation. First operation of the FEM with 2-D distributed feedback was recently demonstrated at this device (Agarin N.V., Arzhannikov A.V., Bobylev V.B. et al. Abstracts of 21st Int. FEL Conf., Hamburg, Germany, 1999, p.Mo-O-03). Studies on novel scheme of powerful FEM are developed in two directions. The first one is optimisation of geometry of the planar resonator and corrugation profiles of 2-D Bragg reflectors to increase efficiency and to improve spatial coherence of generated radiation. The second one is studying on mechanism of microwave pulse shortening that restricts pulse duration on the level of one microsecond and correspondingly limits energy of radiation pulse.

Results of investigations on the pointed objectives will be presented in this paper.

## 58.4

### Biological Effect of Non Heating Millimeter Wave Doses Radiation and its Using for Treatment of Animals

*Murav'ev, V. V.<sup>1</sup>; Tamelo, A. A.<sup>1</sup>; Fedosova, N. H.<sup>2</sup>*

<sup>1</sup>Belarusian State University, Belarus; <sup>2</sup>Belarusian Agricultural Academy, Belarus

ABSTRACT NOT AVAILABLE

## 58.5

### The Using of Laser and mm-range Radiation in Biomedical Diagnostics and Therapy

*Savenko, Y.<sup>1</sup>; Zinkovskiy, Y.<sup>1</sup>; Bogomolov, N.<sup>1</sup>*

<sup>1</sup>Kiev Polytechnic Institute, Ukraine

In recent time it is increased the interest in medical practice to use of laser methods of diagnostics and therapy. It requires a further research of mechanisms of effect of laser radiation for biological objects and organism of the man in whole. We carried out researches on effect of lowenergy radiation of the He-Ne laser (output power up to 2 mW) on blood of the man, on points acupuncture, and also on therapeutic operation on an organism of the man, in particular on the immune system, combined irradiation of acupuncture points by lowenergy laser radiation and by lowenergy noise radiation of mm-range. It was developed the mathematical model to researching of effect of laser radiation on blood of the man. Such model adequately reflects the mechanism of scattering and absorption of laser radiation by blood. The analysis of scattering allows obtaining the rather full information on the system of blood of the man, and also about other systems of the man, for example about the immune system. For experimental researches on laser diagnostics the original instrument (Y. V. Savenko, Abstracts URSI XXVI GA, 652, 1999) was developed which allows carrying out the analysis of blood with exception of test or intravascular. We had also designed original combine multifunctional irradiator in optical and mm-ranges. The device provides separate and combined operating modes of the He-Ne laser and the mm-range noise electromagnetic radiation source. The irradiator can be used in practical medicine as well as in scientific researches. Using the combine multifunctional irradiator made investigations on therapeutic effects for such medical applications: the stimulating of the human's immunity system by combined action on the biologically active points of the lightwave and mm-range electromagnetic radiation; intravascular blood treatment to biostimulate the human's organism. The preliminary clinical researches have confirmed efficiency of both applications in medical practice.

## 61.2

### Some Problems of GPR Soft- and Hardware Improving in Mine Detection and Classification Task

*Astanin, L.<sup>1</sup>*

<sup>1</sup>Pulse Systems Group, Russia

#### Unexploded Ordnance Detection and Range Remediation

The algorithms for mine detection and classification by using portable UWB ground probing radar are considered. The method based on surface reflection and direct-coupling signals subtraction from common signal is developed. The deducted signal is interpolated in advance. It is done for increase matching exactitude (from here term "precise subtraction"). The algorithm work with use of correlation matching for more precise signal from a surface arrival moment determination. The classification methods are based on representation signal as an image, which is created as bitmap-matrix appropriate to an intensities matrix of space-time signal. The segmentation is applied to an obtained image. The hidden objects classification methods are created based on the separate segments descriptions analysis. The geometric type features are used: square, perimeter, lengths of the circumscribed rectangle sizes; parametrical features of an object contour; curvature features, camber and concavity features of the selected object contour. The classification procedures are based on discriminant analysis methods, fuzzy logic and neural nets. The experimental researches were conducted with use of portable UWB GPR with 1GHz centre frequency antenna and different kinds of GPR hardware including mono- and biposition antennae crosspolarization mode etc are discussed.

## 61.3

### Evaluation of Potentials and Efficiency of Ultrawideband Radars for Remote Probing (GPR and/or FOLPEN) with use of Short Pulses at High Repetition Frequencies

*Kardo-Sysoev, A.<sup>1</sup>; Astanin, L.<sup>2</sup>*

<sup>1</sup>Ioffe Physico-Technical Institute, Russia; <sup>2</sup>Pulse Systems Group, Russia

Usually, ultrawideband (UWB) long rang radars exploit nano and picosecond pulses of peak power 1-10 MW and low pulse repetition frequency (PRF) less than 1 kHz. Such signals are easy to be processed at the receiving end (received signal represents a pulse response of the target) but they cause a lot of such problems, as to prevent breakdowns of feeders and antenna as well as to prevent interference with surrounding electronic equipment.

In recent years, small power UWB short pulse signals at high PRF > 10 MHz have been used in communication systems. The most promising coding for this application is time-position coding.

Such signals are very promising, as well, for long range UWB radars: FOLPENS and GPRs. But the absence of pulse sources with needed powers, PRF and very high time stability constrained development of such radars.

The current work is dedicated to evaluation of the potential of such signals for GPRs and FOLPEN UWB radars, based on the last achievements in the art of all solid state short pulse high PRF generation.

It was shown that very high energy potentials may be realized in this case, providing lower interferences with other electronic equipment. Far lower peak powers lead to simplification of a transmitter and antenna design, as well as improvement of ecology environment. The use of time-position coding and antennae aperture synthesis are considered. Active antenna array with developed synchronized set of pulsers provides needed antenna power and pattern.

## 68.1

### Sectioned Microwave Oscillators with Frequency Tuning

Abubakirov, E<sup>1</sup>; Denisenko, A<sup>1</sup>; Soluyanov, E<sup>1</sup>; Yastrebov, V<sup>1</sup>  
<sup>1</sup>Institute of Applied Physics, Russia

The possibility to control output parameters of high-power microwave (HPM) sources driven by relativistic electron beams is of great interest for a wide range of science and technical applications. The main difficulty is that the methods for changing output power, spatial structure, frequency and phase characteristics of microwave radiation, which are used in traditional microwave devices, can be hardly combined with an extremely high field strength and intensive electron beams in relativistic sources. Short duration of microwave pulses also limits the possibilities of such a control.

HPM amplifying systems seem to be the most suitable way to solve this problem. However, development of such devices is a very complicated task. Tunable microwave oscillators, which are an alternative to HPM amplifiers, can become a trade-off solution. A possible way to develop such oscillators is to use sectioned schemes. Longitudinal (with respect to the direction of electron beam propagation) sectioning of an oversized microwave system with mode-selective coupling between its sections provides coherence of the output radiation along with high efficiency of microwave device operation. (E. Abubakirov et al., Proc. of 8 Int. Conf. on High-Power Electron Beams, World Scientific, 1991, vol.2, p.1105-1110).

A simplest version of the sectioned oscillator is a relativistic travelling-wave amplifier (TWA) with a selective feedback channel formed by two Bragg waveguide reflectors (resonant TWTs) (Fig.1). The operating frequency of the resonant TWT is determined mainly by frequency properties of the reflectors, so we can tune the operating frequency of the oscillator by changing the frequency position of the reflector bandwidth. This can be realized by using periodically corrugated waveguide reflectors with phase irregularity of the corrugation. An interference of two parts of the reflector produces a frequency shift of the reflector bandwidth. The value of the shift depends on the phase mismatch and its maximum is approximately equal to the bandwidth. In the case of helical corrugation of the reflectors the shift can be realized by mutual rotation of the reflector parts.

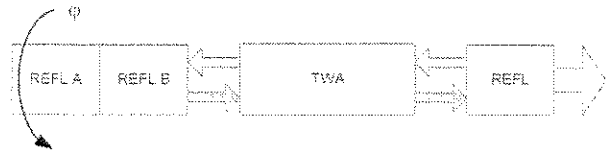


Fig. 1 Frequency-tuned resonant TWT

Another possibility to control oscillation frequency is associated with reactive properties of a magnetized electron beam, which are observed in the vicinity of the magnetic field corresponding to resonance interaction of the operating wave and the fast cyclotron wave of the beam. In the case of a rectilinear electron beam the main effect of the interaction is suppression of microwave generation.

However, when the values of the guiding magnetic field correspond to the wings of the absorption line, the reactive part of the high-frequency conductivity of the electron beam is rather high and can shift the oscillation frequency significantly. The scheme can be applied most efficiently to the sectioned cascade oscillator, where the first section is a relatively low-power master oscillator, and the second section is a TWA amplifier excited by the electron beam modulated in the first section. In this scheme strong changes of modulation due to cyclotron absorption in the first section are compensated by amplification of the TWA section, so frequency tuning can be combined with small changes of the output microwave power.

The both schemes were realized and tested experimentally in the X-band with a 1.2 MeV/6 kA/100 ns electron beam. Microwave pulses with a gigawatt level of peak power were produced. The mentioned methods of frequency tuning made it possible to reach an approximately 5% change of the carrying frequency with less than 3dB changes of the output power.

## 68.2

### Generation of Powerful Electromagnetic Pulse under Collision of Plasma Clot with a Target

Stupitsky, E<sup>1</sup>; Repin, A<sup>1</sup>; Kiuttu, G<sup>2</sup>

<sup>1</sup>Central Institute of Physics & Technology, Russia; <sup>2</sup>Air Force Research Laboratory, USA

In the present time in the number of countries the installations are used for generation and acceleration of plasma clots with high specific power capacity ~ 1MJ (Stepanov A.E. et al, Plasma Physics (in Russian), V.15, No.8, 1000-1007, 1989; Degnan J.H. et al, Physics of Fluids, No.2, 2938-2959, 1993). Under collision of such clot with a target the sharp plasma heating is occurred (up to ion temperature of the order of 10keV) and the powerful pulse of electromagnetic radiation is generated. The plasma itself as well as the generated pulse may effect on the environment.

Usually, the experimental conditions for particle density in clot are what in collision of clot with a target the interaction of incoming and re-flected flows takes place in the penetration regime, since ion free path length  $l_i \geq R$ , where R is the characteristic clot size. By this means a three-liquid type of plasma flow is realized: ions of incoming flow, ions of reflected flow and electrons. Such movement of interpenetrating plasma flows requires detail study of collisional processes under flows interaction, since it determine the temperatures of ion flows and electrons and, consequently, the plasma ionization and radiation. On the other hand, the currents generated in clot and electromagnetic pulse parameters depend on these processes.

In the present work the physical model of three-velocity plasma flow under collision of clot with target is given and the two-dimensional code was developed to calculate the parameters of the flow: electron and ion temperatures, ionization degree and coefficients of linear radiation in the range from x-ray up to visible. Simultaneously, the two-dimensional current distribution inside the interpenetrating plasma flows is calculated and then the electromagnetic pulse characteristics are determined. The ion temperatures in the interaction zone is up to 10 keV and magnetic field near clot

boundary is up to 10 MGs. By this means, the developed physical model and numerical algorithm allow one to determine plasma characteristics in the region of interaction of incoming and reflected flows as well as characteristics of electromagnetic pulse in microwave and x-ray radiation region.

## 68.3

### Single-Electrode Multipactor - Effective Mechanism of Electrons' Bunching and Amplification of Microwaves

*Galdetskiy, A<sup>1</sup>*

<sup>1</sup>SRPC "Istok", Russia

Multipactor discharge is usually considered as extremely harmful phenomena in high power vacuum microwave systems: vacuum tubes, satellite antennas, etc. However recently several works were performed considering two-electrode multipactor discharge as a source of bunched electron beam for accelerators and vacuum tubes. Electrons launched from one electrode in dynode structures in a proper phase of microwave field are accelerated and arrive to the other electrode in decelerating phase. Thus they become the source of secondary electrons which in turn come back to the first electrode. This process is accompanied by electrons bunching in time (in contrast to bunching in space occurring in klystrons or TWTs). As result the buncher stage length, magnetic system and power supply voltage can be made much less than in conventional O-type devices. Such structure possesses instant turn on time. However two-electrode multipactor put severe limitations on transit time through the gap which restrict working frequencies to units of GHz.

We considered slightly different mechanism of single-electrode multipactor occurring in a gap between flat electrodes (the grid and reflector) at applying dc and microwave fields. In such structure the interelectrode spacing can be made much larger than amplitude of electrons oscillations. As result operation in millimeter wave band can be achieved. We simulated operation of such structure at frequency 35 GHz (gap is equal to 1 mm), average current density of bunched beam is more than 10 A/sq.cm. The using of materials with small first critical potential of secondary emission (Ag Pd, carbon) ~ 20 V will allow the development of very attractive design of microwave sources.



**Euro Electromagnetics**  
30 May - 2 June 2000, Edinburgh

# **Poster Presentations**

## P3

**Stimulated Microwave Radiation of Classical Oscillators Gas in Collisions Conditions (at Explosion of Condensed High Explosives)**  
*Shumilin, V<sup>1</sup>; Cherepenin, V<sup>2</sup>*  
<sup>1</sup>High Energy Density Research Center RAS, Russia; <sup>2</sup>Institute of Radio Engineering Electronics, Russia

In the paper (V A Cherepenin V P Shumilin, Proc of the EUROEM'98 Int Symp) the mechanism explaining origin of a broadband microwave radiation at explosion of charges of condensed high explosives was offered. There was shown that products of detonation on the initial stages of the expansion are highly non-equilibrium. In these situation realisation of necessary conditions for development of radiation instability in gas of classical non-linear oscillators on principle is possible. However these conditions were obtained (see, for example, (A V Gaponov M I Petelin V K Yulpatov, Izv Vuzov Radiophysics (Russian) 10, 1414-1453, 1967)) only for collisionless gas. In products of a detonation on initial stages of the expansion substantially different situation takes place. The density of gas is so high, that the collisions play an essential role.

It is shown that in gas of classical oscillators in an external field, full chaotic character of free oscillations phase after collisions does not take place. The collisions in this situation bring to some phasing of oscillators. This influence essentially to characteristics of the stimulated microwave radiation.

## P7

**Matching of the MFC with the Pulsed Power Vircator System with the Aid of Transformer**  
*Mintsev, V B<sup>1</sup>; Ushnurtsev, A E<sup>1</sup>; Dudin, S V<sup>1</sup>; Fortov, V E<sup>1</sup>; Leontyev, A A<sup>2</sup>; Shurupov, A V<sup>2</sup>; Zherlitsyn, A G<sup>3</sup>; Kanaev, G G<sup>3</sup>; Melnikov, G V<sup>3</sup>; Tsvetkov, V P<sup>3</sup>*  
<sup>1</sup>Institute of Problems of Chemical Physics, Russia; <sup>2</sup>Shatura Dept of High Temperature Institute, Russia; <sup>3</sup>Nuclear Physics Institute of Tomsk, Russia

ABSTRACT NOT AVAILABLE

## P6

**Two-Stage Magnetic Flux Compressors for Generation of Electron Beam and High Power Microwaves**  
*Mintsev, V B<sup>1</sup>; Ushnurtsev, A E<sup>1</sup>; Fortov, V E<sup>1</sup>; Leontyev, A A<sup>2</sup>; Shurupov, A V<sup>2</sup>*  
<sup>1</sup>Institute of Problems of Chemical Physics, Russia; <sup>2</sup>Shatura Department of High Temperature Institute, Russia

ABSTRACT NOT AVAILABLE

## P8

**Multimodal Nonlinear Analysis of Beam-Plasma Instability in Periodic Plasma-Filled Waveguide**  
*Zaginaylov, G<sup>1</sup>; Raguin, J Y<sup>2</sup>*  
<sup>1</sup>Kharkov National University, Ukraine; <sup>2</sup>Technical University Hamburg-Harburg, Germany

Introducing background plasma into the high-power microwave tubes can significantly increase the bandwidth, efficiency and output power of the microwave electron devices (Y Carmel et al, Phys Rev Lett 62, 2389-2392, 1989). However, the mechanisms of plasma influence on the operation of high-power microwave sources are still unclear. Presence of plasma drastically changes the electromagnetic properties of microwave tubes. At the frequencies below plasma one a new type of a spectral behaviour is formed. It is the so-called "dense" spectrum (W R Lou et al, Phys Rev Lett 67, 2481-2485, 1991).

The conventional analysis usually used for corrugated vacuum waveguide and based on spatial harmonic expansion and Rayleigh hypothesis was unsuccessful for the treatment of the "dense" spectrum either due to the poor convergence of the spatial harmonic series or due to the unacceptability of such an approach at all (K Ogura et al, J Phys Soc Japan 61, 4022-4032, 1992).

Quite recently (I L Verbitskii & G I Zaginaylov, IEEE Plasma Sci 27, 1101-1104, 1999), the issue of applicability of conventional analysis for this case has been considered in a mathematically correct manner on the basis of integral equation approach. The necessary and sufficient conditions for its validity have been obtained. Further, the new approach has been applied for investigation of the linear stage of the beam-plasma instability in the periodic plasma-filled waveguide (G I Zaginaylov et al, Phys Rev E 60, No 5, 1999). The analytical solution of the problem has been obtained in quasi-static approximation on the basis of analytical regularization (A Nosich, IEEE Antenn Prop Magazine 41, 34-49, 1999) which was frequently used before in the problems of computational electromagnetics. Results showed that the beam excitation of plasma waves which form "dense" spectrum is much more efficient than that predicted on the basis of conventional analysis and can influence on operation of plasma-filled electronic devices more strongly than it was expected before.

In present report the integral equation approach is extended to analyze the nonlinear regime of the beam-plasma instability in the periodic plasma-filled waveguide which is more close to the experimental situation. The beam assumed to be monoenergetic and nonrelativistic. The beam current assumed to be rather low in order to neglect its influence on dispersion properties of the system. Numerical results show that efficiency of the beam-wave energy transfer is higher than that predicted in the scope of the single mode nonlinear theory of beam-wave interaction. This can be attributed to the influence of the highest plasma and beam harmonics taken into account rigorously by the new approach in contrast with the single mode nonlinear analysis.



## P9

### High-Harmonic Large Orbit Gyrotron with Thermionic Electron-Optical System

*Kalynov, Y. K<sup>1</sup>; Bratman, V. L<sup>1</sup>; Ofitserov, M. M<sup>1</sup>; Samsonov, S. V<sup>1</sup>*  
<sup>1</sup>Institute of Applied Physics, Russia

Selective excitation of modes TE<sub>4,2,1</sub> and TE<sub>3,2,1</sub> of a traditional gyrotron cavity at the 4th and 3rd cyclotron harmonics, respectively, has been obtained in the configuration of Large Orbit Gyrotron (LOG). In the electron-optical system of the LOG first a thin rectilinear beam with the maximal electron energy of 250 keV and current of 10 A is formed in a diode quasi-Pierce gun with a spherical thermionic cathode immersed in a tapered magnetic field which lines are parallel to the particle trajectories. After the motion in an increasing magnetic field the electron beam is pumped in a kicker, which is formed by four rectangular current loops generating a perpendicular component of magnetic field. As a result, in the operating magnetic field of 1.6–2.0 T the electron beam has a thickness of about 0.6 mm and electrons gyrate around the axis with a pitch factor up to  $g=1.1-1.5$ .

Stable excitation of the operating modes, TE<sub>4,2</sub> and TE<sub>3,2</sub>, is clearly observed at magnetic fields 1.67–1.75 T and 1.92–1.99 T, respectively. A maximum efficiency, 4.0% for the TE<sub>4,2</sub> mode and 4.8% for the TE<sub>3,2</sub> mode, is achieved at the current of 4–6 A. A maximum power is 70–80 kW at the efficiency of 3.5% for the both modes.

It is important that the described electron-optical system has allowed testing the possibility of stable selective generation of the operating mode TE<sub>4,2</sub> at the 4th cyclotron harmonic for lower electron energy down to 130 keV. Simulations predict a selective generation even for further decrease of the electron energy down to a typical gyrotron value of 80 keV. The developed method will be used for generation of powerful submillimeter wavelength radiation.

## P11

### Development of Transverse-Wave Type Microwave tubes

*Savvin, V<sup>1</sup>*  
<sup>1</sup>Moscow State University, Russia

New types of high-quality vacuum microwave devices were successfully developed in Russia last years. Their operating principle is based on transverse grouping of homogeneous (non-bunched) electron beam in circularly polarised electromagnetic fields of slow-wave structures and resonant cavities. The use of transverse (cyclotron and synchronous) waves of electron beam gives possibility to realise efficient energy exchange mechanisms with HF fields, to achieve perfect wave selection and to minimise non-linear influence of space charge fields on output characteristics resulting in the unique qualities of transverse-wave microwave vacuum devices: - outstanding linearity and low-noise level of input amplifiers combined with super-high self-protection against microwave impact, - high level of efficiency of powerful microwave tubes combined with improved phase characteristics.

One of the distinctive features of transverse-wave interaction is relatively low level of space charge density of the beam. As against well-known microwave tubes with space charge waves the transverse-wave devices use HF structures forming spatially disjointed areas of accelerating and decelerating electric field in each cross-section of interaction channel simultaneously. Thus grouping of electrons in proper phase of HF field is implemented at the expense of transverse deviation of electrons in each cross-section of uniformly charged (non-bunched) beam in corresponding direction. As a result the electron beam acquires the spiral shape maintaining thus a low level of space charge density.

The advanced theory of transverse-wave interaction was developed using improved 3-D models of electron beam for computer analysis, academic research was tightly combined with experimental investigations. It was shown that relatively low level of space charge density and therefore relatively small electron velocity spread in powerful transverse-wave devices enable noticeable improvement of resulting efficiency using beam energy recuperation in one-stage

## P10

### Perspectives of Creation High Power Pulse Systems Based on the Plasma-Filled TWT

*Perevodchikov, V<sup>1</sup>; Zavalov, M<sup>1</sup>; Shapiro, A<sup>1</sup>; Yu, K<sup>1</sup>; Shevchuk, V<sup>1</sup>; Yagolnikov, S<sup>1</sup>*  
<sup>1</sup>All-Russian Electrotechnical Institute, Russia

There was information in the previous publications [V. Perevodchikov et al., EUROEM Proc., Tel-Aviv, 1998] about high-power plasma-filled TWT for continuous operation mode developed at VEI. Researches have shown that presence of plasma in the decelerating structures increases essentially efficiency of electron beam energy conversion into energy of electromagnetic oscillation and expands the band of working frequencies. This effect is defined by several factors: by expansion dispersion characteristics because of plasma presence, by compensation the space electron charge with electron beam bunching, by an opportunity to change electromagnetic wave propagation velocity along the beam due to plasma density changing. Researches of plasma-filled TWT have shown high quality of signals amplification because of gain-transfer characteristic linearity, stability of phase characteristics and low level of noise in the working frequency band and on the highest harmonics. It opens broad perspectives for application plasma-filled TWT in communication and radiolocation systems. It is possible to mark the following important advantages of plasma-filled TWT in comparison with existing vacuum TWT on a triad of main characteristics: high radiated power (up to 10–20kW in the continuous operating mode and over 100kW in the pulse operating mode), high efficiency (20%–30%), wide frequency bandwidth (20% of carrier frequency) which allow to use them in radar systems as output amplifiers of wide-band and super wide-band signals. It will allow not only to provide high accuracy of coordinates measurement for target range and velocity, but also to increase jamproof of radar stations and to reduce requirements for transmitter pulse power by base message value. Due to this the security of radar station is increased. Besides the application of plasma-beam devices will ensure a possibility of creation of multifunctional stations, for example, joining function of radar station and jamming system. The use of uniform noise signal in such station as sounding and interference signal ensures parallel radar-tracking and radio-jamming. In the report the perspectives of creation pulse plasma-filled TWT and possibility of addition signals generated by several plasma-filled TWT are considered during transportation and on site, and also possibility compression of signals in time. Such method generation of high-power signals simplifies solution of extremely difficult protection problem of microwave systems output tracts from breakdowns.

depressed collector. Moreover, it is possible to use slow gyration of the beam around its axis under the action of space charge field and thus to compensate influence of heterogeneity of HF field across the beam cross-section, which can be one of factors limiting resulting efficiency of the device.

Improved 3-D models of electron beam were designed for the analysis and optimisation of transverse-wave devices. Development of 3-D models with partial beams of finite cross-section ensured improvement noticeable (in 5–10 times better) accuracy of calculation of space charge field in comparison with filamentary beam models.

The results of fulfilled investigations are used for design of powerful microwave devices with improved efficiency (transverse-wave TWT, cyclotron-wave converters, gyrocons and magnicons

P12

Full Wave Analysis of the Mode Conversion in Overmoded Periodic Structures of Finite Extent

Zaginaylov, G<sup>1</sup>; Gandel, Y<sup>1</sup>; Turbin, P<sup>2</sup>  
<sup>1</sup>Kharkov National University, Ukraine; <sup>2</sup>Scientific Center of Physical Technologies, Ukraine

Using the overmoded periodic structures as the slow wave structures (SWS) in high-power microwave (HPM) sources can become a new key technology in producing HPM radiation. This allows us to substantially reduce the probability of breakdown on the conducting walls increasing power-handling capabilities of HPM sources. Several kinds of HPM sources based on the overmoded SWS with the record output power levels (S P Bugaev et al, IEEE Trans Plasma Sci 18, 518-536, 1990) have been elaborated up to date attracting the universal attention of HPM community. However, increasing the diameter of the structure may introduce mode competition as unwanted side effect. There are two main reasons for appearance of the multimode operation. The former of them is due to the multimode beam-wave interaction and can be suppressed by the proper choice of the beam parameters (D K Abe et al, IEEE Trans Plasma Sci 26, 591-604, 1998). The latter one is due to the spatial mode conversion at the ends or irregularities of the overmoded structure which can strongly affect the efficiency and output power (M P Deichuly et al, J Commun Technol Electronics 41, 1996) and hardly can be suppressed to the negligible level.

Different methods of theoretical description of overmoded structures for HPM sources applications use simplified treatments of mode conversion effects assuming the total reflection or total matching conditions at the ends of the structure what is rather far from reality.

Here we report on the systematic investigations of mode conversion effects in finite length overmoded SWS based on the singular integral equation (SIE) method (G I Zaginaylov et al, Microwave Opt Technol Lett 16, 50-54, 1997). The numerical results show that the effects of mode conversion and reflection at the ends of overmoded SWS are quite different from those for the conventional single mode SWS. In the latter case substantial mode reflections from the ends cause the quantization of the wave number and formation of axial resonant modes (S Kobayashi et al, IEEE Trans Plasma Sci 26, 947-954, 1998). In contrast, in the overmoded finite length SWS the formation of the axial resonant modes is hardly possible. This follows from the behaviour of transmission coefficient for the fundamental mode versus frequency. It has not sharp resonant peaks inherent to single mode SWS. There is the only maximum near the  $\pi$ -type frequency for the corresponding infinite periodic structure. The levels of reflection and conversion into the higher modes are minimal in this regime what is of great interest for HPM sources. The fundamental mode mainly transforms into the next radial one (15-25 %) what is in good agreement with experimental investigations.

P14

Full-Wave of the Chiral Microstrip Lines

Mayouf, A<sup>1</sup>; Djahli, F<sup>1</sup>  
<sup>1</sup>University Ferhat Abbas, Algeria

The monolithic microwave integrated circuits have been designed to perform multiple functions at higher frequencies. However, in addition to higher frequency requirements, smaller and more densely packed circuits are being designed in order to reduce cost. Then, more complex structures are inevitable. One reason why monolithic circuits are becoming more elaborate is the use of a class of nonplanar interconnects, which may be described as microstrip structures printed on chiral substrates. These materials, which are usually bi-isotropic, have been investigated for antenna radomes, as polarization transformers, and as microstrip circuits materials, among other uses (George W. Hanson, IEEE, TMTT, 1996, vol. 44, n° 1, 144-151) and (PLAZA G. & al., IEEE, TMTT, 1998, vol. 46, n° 8, 1150-57).

This paper studies the characteristics of chiral planar microstrip lines including the possible frequency dependence of the chiral parameters. For characterizing the chiral microstrip line using a full-wave approach, we have developed our exact dyadic Green's function for planar bianisotropic media. This development has been based on the integral equation approach of Hanson (George W. Hanson, IEEE, TMTT, 1996, vol. 44, n° 1, 144-151).

We have formulated, in our original approach, an integral matrix equation in the spectral domain based on the electrical surface current density. We have applied our algorithm of the two-dimensional Galerkin's method to solve this last for the phase and attenuation constants. In addition, we have extracted the effective propagation constant and permittivity and the characteristic impedance of the chiral microstrip line.

We have obtained results concerning the phase and attenuation coefficients of several microstrip structures. In addition, we have calculated the characteristic impedance and effective relative permittivity and effective propagation constant with respect to geometrical and electrical parameters of microstrip line and as function of frequency. The quality of these results, compared to those of other approaches, proves the efficiency and the high accuracy of the developed theoretical model.

P13

Full-Wave Characterizations of the Open-End and Gap Discontinuities of Chiral Microstrip Lines

Mayouf, A<sup>1</sup>; Djahli, F<sup>1</sup>  
<sup>1</sup>University Ferhat Abbas, Algeria

Applications of monolithic microwave integrated circuits and their discontinuities continue to extend farther into the millimeter-wave range, approaching terahertz frequencies. In addition to higher frequency requirements, smaller and more densely packed circuits are being designed in order to reduce cost. This further increase coupling necessitate the use of many discontinuities. The characterization of microstrip discontinuities on chiral dielectric substrate requires an accurate theoretical full-wave model accounting for electromagnetic coupling, space wave radiation and surface wave excitation.

In this paper, we have developed an original theoretical model and an accurate CAD tool to characterize the open-end and gap microstrip discontinuities on chiral substrate and carefully studies the effects of this dielectric structure on circuit performances.

In this model, we have developed our exact dyadic Green's function for planar bianisotropic media. This development has been based on the integral equation approach of Hanson (George W. Hanson, IEEE, TMTT, 1996, vol. 44, n° 1, 144-151). We have formulated a set of integral equations, for each type of studied discontinuities, in the spectral domain based on the electrical surface current density. We have applied our algorithm of the two-dimensional Galerkin's method to solve this last for the reflected and transmitted components of the current.

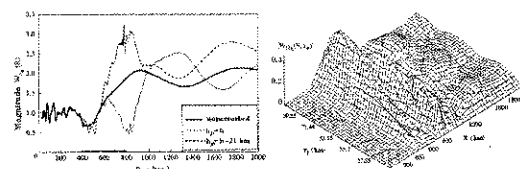
Obtained results concerning the reflection and transmissions coefficients (phase and magnitude) and losses due to the excitation of surface waves and to the radiation of space waves as function of frequency. The quality of these results, compared to those of other approaches, proves the accuracy of the developed model, even for the high frequencies and for the arbitrary structures of substrates.

P16

VLF and LF Radiowave Propagation under a Strong Lower Ionosphere Disturbance

Soloviev, O V<sup>1</sup>  
<sup>1</sup>St Petersburg State University, Russia

This paper presents the latest results pertaining to the theory of radio wave propagation in the irregular Earth-ionosphere waveguide (EIWG). The particular attention is given to the effects of 3D large-scale perturbations of environment when first-order scattering theory is not valid. Among natural disturbances, we can mention those due to polar cap, earthquakes, magnetic storms, lightning-induced electron precipitation, sporadic E-layer. Such disturbances may be hundreds or thousands of kilometres in extent and may cause noticeable changes in amplitude and phase of electromagnetic field. Some disturbances may be attributed to rocket launches, nuclear explosions, etc. The parameters of inhomogeneous surface impedance model of the irregular EIWG (tensor impedances  $\delta_{10}$ ,  $\delta_{20}$  and waveguide heights  $h$ ,  $h_p$ ) are calculated from given electron density  $N_e(r, \varphi, z)$ ,  $N_{ep}(r, \varphi, z)$  and collision frequency  $\nu_e(r, \varphi, z)$ ,  $\nu_{ep}(r, \varphi, z)$  height profiles, unperturbed and perturbed. The radiation of a point vertical electrical source problem is reduced to the system of four coupled surface integral equations for  $E_z$ ,  $H_z$ ,  $E_\varphi$ ,  $H_\varphi$  field components. The solution is based on preliminary asymptotic integration of the rigorous two-dimensional integral equations (O.V.Soloviev & V.V.Agapov, Radio Science, 32, 515-524, 1997). An original computational algorithm is proposed to invert approximate equations after diagonalization of the set of equations. The figures below illustrate the behaviour of the magnitudes of the attenuation functions  $W_{H0}$  (primary field component) and  $W_{H2}$  (secondary field component arising as a result of radiation scattering by 3D perturbation) as functions of the distance  $R$ . The frequency of the signal was assumed to be 16.8 kHz. The elliptic cross section of the cylinder disturbance  $[(x - x_p)/a]^2 + [(y - y_p)/b]^2 \leq 1$  is characterized by the values



$a = 2b = 200 \text{ km}$ ,  $x_p = 600 \text{ km}$ . For left-hand figure  $y_p = 0$ , for right-hand figure  $h_p = h - 21 \text{ km}$ ;  $\delta_{10}^{(e)} = 0$ ,  $\delta_{20}^{(e)} = (1 - 0.5i) \times 10^{-3}$ ; daylight conditions:  $\delta_{10}^{(e)} = (0.358 + 0.177i)$ ,  $\delta_{20}^{(e)} = (2.317 - 1.502i)$ ,  $h = 59.3 \text{ km}$ .

## P17

### The Possibility of Focusing of Wave Beams into Sub-Wavelength Area

*Petrov, N<sup>1</sup>*

<sup>1</sup>All-Russian Electro-technical Institute, Russia

The possibility of super-resolution (restoration of details of objects within the diffractive limit) in images is of great interest for various problems of near-field microscopy, nano-optics, etc. In this paper the minimal sizes of focusing area of wave beam in a graded-index medium limited by nonparaxial and polarization effects are determined. The possibility of focusing of substantial part of beam energy into an area with linear sizes less than the wavelength is shown.

Coherent states method is used for the consideration of a gaussian beam propagation in an inhomogeneous medium (N.I. Petrov, Phys. Letts. A, 234, 239-250, 1997). It is shown, that the nonparaxial effects limit the possibility of focusing a beam into sub-wavelength area. It is found that the distances of focus plane determined from the calculations of minimal width of a beam and maximum intensity of light on the waveguide axis are not the same. It is more important to consider the light intensity distribution both in transverse and longitudinal directions from the point of view of resolution criterion.

It is obtained that the ring structure of light intensity distribution with the bright spot in the center is formed in the focusing plane. The intensity of this central spot may be 100 times as high as the intensity of light in a surrounding area. Linear sizes of the central spot may be substantially less than the wavelength of radiation, but the energy concentrated in a spot decreases with decreasing of its size. So at the spot size of the order of one tenth of wavelength only 57% of the total energy is concentrated in the central spot. It is shown that the longitudinal distribution of the field intensity in the focusing area has a fine structure with linear sizes, which are comparable to the wavelength of radiation. It is found that the increase of the refractive index on the axis of waveguide leads to the decrease of the size of focusing area due to decreasing of influence of nonparaxial effects. So, at the refractive index of 10 the

central spot has the size of one tenth of wavelength with 88% of total energy inside.

The possibility of focusing of substantial part of light energy into an area with linear sizes less than the wavelength of radiation is shown in longitudinally inhomogeneous waveguide consisting of the collection of graded-index lenses connected one after another.

## P18

### Modelling of Electromagnetic Wave Propagation Through Lightning Region

*Vorgul, I<sup>1</sup>*

<sup>1</sup>Kharkov State University, Ukraine

Theoretical modeling of electromagnetic wave propagation through lightning region is presented. Lightning is modeled here as an electrical discharge leading to time-splash of conductivity. One considers electromagnetic field transformation in a medium with time-splashing conductivity. This splash is assumed as a continuous one without an approximation of abrupt changes. Its form corresponds to that under a condenser discharge with arbitrary duration and amplitude. It can be a splash in the positive values of conductivity as well as in the negative ones.

The problem is studied by solving Volterra integral equation for the field in transient medium in one-space-dimensional case. It is solved by resolvent techniques Exact solution for the field is obtained. In the analytical solution no restrictions on the time and spatial (one-dimensional) dependence of the incident field assumed. Numerical analysis is carried out for the incident field taken as a plane harmonic wave.

The numerical analysis shows that when the splash is large, the incident field amplitude reduces very quickly and before the conductivity starts decreasing it already is equal to zero. In this case the field completely disappears during the conductivity splash and does not appear after the conductivity becomes zero again. In the opposite case of a small time-splash of conductivity, the field is decreasing before the conductivity reaches its maximum value and increasing after this. When the conductivity has completely disappeared the field takes its initial form.

In the intermediate case, the field was calculated by the exact formula for different values of  $x$ . The field time dependence here has a very short splash. Its maximum value is more than 4 times as much as the initial field amplitude. It reduces to the initial value before the conductivity reaches its maximum. These results are for  $x = 0$ , that is

for the points where the initial field had its maximum at the zero time moment. For  $x = p/2$  the field time dependence shape seems to have the same form, but the field values here are hundred times less and do not reach the values of initial field at the corresponding moments for constant conductivity. For  $x = p/4$ , the field splash having the same form as two ones mentioned above, is about one and a half times less than for  $x = 0$ .

Thus the field under the influence of intermediate value time-splash of conductivity is focused in the planes where  $x$  is divisible by  $p$  that is where the initial field was maximal at the moment the nonstationarity turns on.

## P19

**Physical Mechanisms of High-Altitude Lightning Discharges Development***Petrova, G N<sup>1</sup>; Petrov, N I<sup>1</sup>*<sup>1</sup>All-Russian Electrotechnical Institute, Russia

Investigation of the physical mechanisms of the development of discharges between storm-cloud and ionosphere which have been found recently from artificial satellite and called as high-altitude lightning is important for the elucidation of their influence on ionosphere characteristics. The streamer propagation in quasi-electrostatic field of a storm-cloud (A.I. Sukhorukov, et.al., Geophys. Res. Letts., 23, 1625-1628, 1996) and the runaway electron breakdown (A.V. Gurevich, et.al., Phys. Letts. A, 165, 463-468, 1992) are usually considered as a foundation for the mechanisms of high-altitude lightning development.

In this paper the influence of the variation of the atmosphere pressure with the height and geometry of storm-clouds on the development of a lightning propagating upward to ionosphere has been investigated. For the modeling of lightning trajectory the fractal approach taking into account intra-cloud discharges is used. Computer simulations show that lightning develops to the ground or it propagates only from the cloud-top to the ionosphere in the dependence on the distribution of charges inside the storm-cloud, distance between the lower part of cloud and ground. Usually discharge developing from the cloud-top has a positive polarity due to the smaller values of the critical electric field for the developing of a positive leader than for a negative leader. Measurements of the electric field inside the streamer zones of leaders in a long air gaps show (N.I. Petrov, et.al., Tech. Phys., 39, 546-551, 1994), that the electric field in the streamer zone of a positive leader is 5 kV/cm, and for negative leader - 10 kV/cm. Besides, an air density in upper layers of atmosphere decreases that also makes the developing of a leader easier. Blue jets observed may be considered as the streamer zone of a positive leader discharge. It is known that the velocity of upward propagation of jets is of the order of 100 km/s and the jets have the form of upward expanding beams of luminosity with cone angle. The streamer zone of leader also has a cone form and the

minimum velocity of streamer corona propagation in atmosphere is equal to 100 km/s. Red sprites may be considered as the streamer zone of a negative leader. Note that the negative streamer corona has the plasma clot formations analogically to the red sprites. It has been found that the high-altitude lightning formation is conditioned by a decrease in pressure with distance from earth and is possible only from storm-clouds situated at large heights.

## P20

**On the Spiral Structure of a Lightning Discharge Channel***Petrov, N I<sup>1</sup>*<sup>1</sup>All-Russian Electro-technical Institute, Russia

Mechanisms of the stability of the helical modes of the return stroke current are considered. It is shown that the lightning channel may be considered as a spiral antenna. As the experiments have shown the spark discharge channel in long air gaps is a spiral structure with the step and diameter of spiral of the order of a few cm, i.e. there is a longitudinal magnetic field inside the spiral breakdown channel. The step of spiral trajectory is equal to 1.5-2.5 cm, the diameter of spiral is about 3 cm (N.I. Petrov, Proc. 24th ICLP, 1, 252-257, 1998). Longitudinal magnetic field evaluated from the measured return stroke current is equal to one tenth of MA/m. Measurements were carried out in rod-plane discharge gap with length up to a few ten meters under application of high-voltage impulses (N.I. Petrov, et.al., Proc. ISH'93, 1, 9-12, 1993). Impulses were formed on an outlet of high-voltage generator of an outdoor installation with the total charging voltage 9 MV and energy capacity 1.35 MJ.

In lightning discharge the longitudinal magnetic field may reach the values of the order of MGs. Note that the inductance of a spiral channel of lightning is less than the inductance of a straight discharge channel.

Peculiarities of the electromagnetic radiation field created by spiral lightning channel are considered. In the area of decimeter and meter wavelength the observation of discrete spectra of radiation of lightning caused by the effect of spatial resonance is possible. The same effect leads to the spatial directionality of lightning radiation. It is known that the spiral antennas have the narrow diagram of directionality, the axis of which is directed at some angle to the antenna axis. Such antenna has a spatial resonances determined by the parameters of spiral structure.

In lightning the diameter of the spiral channel is bigger than in a laboratory spark. Therefore effects predicted here should be observed in the decimeter range.

## P21

**Influence of High-Energy Electron Beam on the Orientation of Positive Leader to Earthed Structures***Petrov, N I<sup>1</sup>; Bulatov, M U<sup>1</sup>; Rassadin, B M<sup>1</sup>; Gurevich, A V<sup>2</sup>*<sup>1</sup>All-Russian Electro-technical Institute, Russia; <sup>2</sup>Lebedev Physical Institute, Russia

The necessity of increasing the efficiency of objects protection against lightning raises a problem of creation a new lightning protection system. The creation of a system allowing to influence on the trajectory of lightning of positive polarity is of particular interest.

In this paper the experimental investigations of influence of high-energy electron beams on the trajectory of leader in long air gaps at atmospheric conditions are carried out.

Pulsed electron beam with duration of 30 ns and energy 350 keV was injected into the long air discharge gap with length of 6 and 12 meters. Impulse voltage in a gap was formed by 9 MV high-voltage generator. The duration of the front of voltage impulse was 45 microseconds, the duration of impulse - 7500 microseconds. The delay of electron beam launching relative to the high-voltage generator was fixed 50 microseconds or more. Trajectories of discharges were registered from the two perpendicular planes. Comparison of the trajectories of discharges with the presence of electron beam and without it in a gap showed that the electron beam influences substantially on the orientation of leader channel to earthed structures. So the earthed rod placed at 1 m distance from the axis line of the electron beam was been struck more frequently when the electron gun was launched. If the probability of stroke of earthed rod without electron beam was 10%, then at synchronized switching of electron gun the striking probability of the rod became 90%.

Note, that usual lightning rods are not effective against positive lightning discharges. The same takes place also for laser beam. Therefore the effect of influence of electron beam on the attraction of positive lightning leader may be used in the design of lightning protection systems. Thus the efficiency of high-power electron beams in protection of earthed structures against positive leader is substantially higher than the efficiency of usual Franklin rods.

## P22

### Search of Runaway Electrons at High Voltage Discharge in Atmosphere

*Petrov, N<sup>1</sup>; Apanasenko, A V<sup>2</sup>; Gurevich, A V<sup>2</sup>*

<sup>1</sup>All-Russian Electro-technical Institute, Russia; <sup>2</sup>Lebedev Physical Institute, Russia

There is no doubt that the observed X-ray and gamma radiations during the thunderstorms in atmosphere are generated with the high-energy electrons. It is supposed (A.V. Gurevich, et al., Phys. Letts.A, 165, 463-468, 1992) that the lightning at high altitudes is caused by high-energy priming electrons created by cosmic rays. However this mechanism has not yet been verified experimentally. Therefore modeling of conditions arising in a storm-cloud and detection of runaway electrons in laboratory experiments are of great interest. In this paper the results of the experiments devoted to the search of runaway electrons, X-ray and gamma radiations in a long discharge air gap are presented. Investigation of the effects of external electric field influence on the penetration of electrons into atmospheric air is carried out. Electric field was created in a discharge plane-plane gap with length of 6 and 12 meters under application of pulse voltage with amplitude of 4 MV. The primary electrons with energy 350 keV were created by the electron gun placed under metallic earthed plane. The cathode current was 0.5 kA and the duration of electron beam was 30 ns. Before the measurements two generators were joined and synchronized. The nuclear emulsion was used for registration of runaway electrons and high-energy photons connected with them. Plate-holders with nuclear emulsion were placed in a discharge gap at different distances above the electron gun. Experiments with and without the external electric field were carried out at identical conditions. Three layers in every cassette were placed between copper and leaden absorbers with different thickness. So each subsequent layer of emulsion registered more hard radiation than previous. Nuclear emulsions were developed at identical conditions and investigated using the microscope. The analysis of the tracks in the emulsion has shown that their number depends on the distance between the cassette with emulsion and electron gun. Besides the number of the tracks depends on the availability the external electric field in a discharge

gap. So the number of the tracks is twice as big as the number of tracks without external field. This shows that the electric field influences on the penetration of the electrons in air which indicates that the effect of the acceleration of electrons in a field  $E > 2$  kV/cm takes place. Note that there are not any effects observed at the external electric fields  $E < 2$  kV/cm.

## P23

### Generation of High Power Microwaves Using Superlight Source of Electron Current

*Petrov, P<sup>1</sup>; Lazarev, Y<sup>1</sup>*

<sup>1</sup>Russian Federal Nuclear Center, Russia

The power produced by existing sources of microwave radiation falls off with decreasing wavelength. To solve this problem a new concept is proposed for generating microwave radiation, based on the use superlight source formed when electrons are emitted into vacuum from a medium and the emission front propagates along the surface with a speed greater than that of light. Such generators are shown to have a number of completely unique properties: they radiate extremely short videopulses (as short as picoseconds); their power exceeds that of existing sources by orders of magnitude; and unlike existing sources, it increases as the wavelength is reduced.

## P24

### MCG-Based Device for Transmission Line Charging

*Nesterov, E<sup>1</sup>; Chernykh, E<sup>1</sup>; Fortov, E<sup>1</sup>; Stroganov, V<sup>1</sup>; Gorbachev, K<sup>1</sup>; Mikhailov, V<sup>1</sup>; Plaksina, S<sup>1</sup>; Gorbachev, K<sup>1</sup>; Mikhailov, V<sup>1</sup>; Plaksina, S<sup>1</sup>*

<sup>1</sup>High Energy Density Research Centre, Russia

At present, MCGs are the most powerful energy sources. Existing level of high technology as well as numerical simulation methods allow to create MCGs with characteristics varying over a wide range of values, which gives new prospects for creation of compact MCGs for different pulsed power applications.

A device based on MCG capable of charging a transmission line up to 450 kV voltage during ~200 ns is discussed in the report. The line has a few Ohms impedance and electrical length 5 ns. Short charging time allows to reduce significantly storage volume and to diminish requirements for high water purification. The unit consists of MCG of 4 cm in diameter, pulsed transformer and EEOS. Specific feature of this design is connection of EEOS into the primary winding of transformer.

## P25

### Generation of Ultra Short Unipolar Electromagnetic Pulses by Quasi-Planar Electron Bunchs

*Savilov, A<sup>1</sup>; Bratman, V<sup>1</sup>; Samsonov, S<sup>1</sup>; Jaroszynski, D<sup>1</sup>*  
<sup>1</sup>Russian Academy of Sciences, Russia

The use of photoinjectors in the modern accelerator technology allows the formation of dense bunches of relativistic electrons with very short pulse durations (shorter than one picosecond) and very high power (up to 109-1013 W). Evidently, such electron bunches can be used for producing short powerful pulses of coherent electromagnetic radiation. On this way, the most attractive possibility is producing electromagnetic pulses, those duration is comparable or even shorter than the duration of the electron pulse; in particular, producing short unipolar videopulses.

It is evident from general principles that in order to produce an unipolar electromagnetic videopulse, one should provide an analogous pulse of the electron current. One of the simplest method on this way is the synchrotron radiation of a relativistic electron bunch moving along a finite curvilinear trajectory. In this case, the polarization and unipolarity of the radiated pulse are determined by the form of the electron trajectory. In order to provide a high directivity (mode pattern) of the radiation, one can use quasi-planar bunches with transverse dimensions, which are much larger than the longitudinal dimension of the bunch (the dimension in the direction of the translational motion of the bunch). In this paper, the proposed method is clarified by a simplest example of an infinitely-thin charged plane performing an imposed transverse motion. After that, it is studied in detail for a realistic quasi-plane electron bunch with taking into account both radiative and Coulomb interaction of its different "slices". It is shown that the existing technique allows generation of powerful electromagnetic videopulses (including unipolar pulses) with the duration of the order of 1 ps.

## P27

### On the Darwin's Description of Dynamics of Many Charged Particle System

*Zhukov, A<sup>1</sup>*  
<sup>1</sup>Kharkov National University, Ukraine

Following the Darwin's approach (H. Esse, Journ. of Phys. A: Math. Gen. 32, 1999, 2297 ; H.Essen, Phys. Rev. E 56, 1997, 5858) of describing dynamics of system of many charged particles, influence of magnetic effects on the relaxation processes in low-dimension (1D or 2D) electron systems is studied. Possible experimental realisations of found effects are discussed.

## P26

### Spin-Orbit Term at Fully Relativistic Interaction with External Field

*Bondarenko, N<sup>1</sup>; Shul'ga, N<sup>2</sup>*  
<sup>1</sup>Kharkov National University, Ukraine; <sup>2</sup>Kharkov Institute of Physics and Technology, Ukraine

A new approach of treating spin-orbit interaction term of electron with external field is discussed, which principally differs from two common ones - so-called elimination method ( W.Pauli. Die allgemeinen Prinzipien der Wellenmechanik, in S.Flugge, ed., Encyclopedia of Physics(Springer, Berlin, 1958) Vol. 5/1, p. 160); A. I. Akhiezer, V. B. Berestetskii. Quantum Electrodynamics, Interscience, New York, 1965 ) and from the Foldy-Wouthuysen transformation method ( L.L.Foldy and S.A.Wouthuysen, Phys. Rev. 78, 1950, 29 ; E.Eriksen, Phys. Rev. 111, 1958, 1011 ). We consider a scattering problem and start from the squared Dirac equation, which we then transform to equation with first derivative in the direction of incident electron momentum versus "Hamiltonian" operator containing a fully relativistic generalisation of spin-orbit interaction term in the known Darwin Hamiltonian. This obtained equation provides correspondence between semi-relativistic and high-energy frameworks (N. Bondarenko and N. Shul'ga In: Proceedings of EDS-99 International Conference (VIIIth 'Blois Workshop') on Elastic and Diffractive Scattering, June 28 - July 2, 1999, Protvino, Russia ), that finds certain applications.

## P28

### On the Elimination of Electromagnetic Field from Equations of Motion of Charged Matter

*Bondarenko, N<sup>1</sup>*  
<sup>1</sup>Kharkov National University, Ukraine

We propose a method of continuous charged medium, interacting with the electromagnetic field. We obtain the Lagrangian and derive equations of motion of the matter and the field. We show that the field can be eliminated (in a fully relativistic way). The resulting differential equation for the charged matter alone is discussed and its special solutions are obtained.

## P29

### Generation of Powerful Ultrashort Microwave Pulses in Millimetre Wave Band Based on Superradiance

*Ginzburg, N<sup>1</sup>; Zotova, I V<sup>1</sup>; Sergeev, A S<sup>1</sup>; Phelps, A D R<sup>2</sup>; Cross, A W<sup>2</sup>; Wiggins, S M<sup>2</sup>; Ronald, K<sup>2</sup>; Shpak, V G<sup>2</sup>; Yalandin, M I<sup>2</sup>; Shunailov, S A<sup>3</sup>; Ulmaskulov, M R<sup>3</sup>; Tarakanov, V P<sup>4</sup>*

<sup>1</sup>Institute of Applied Physics, Russia; <sup>2</sup>University of Strathclyde, UK; <sup>3</sup>Institute of Electrophysics, Russia; <sup>4</sup>High Energy Research Center, Russia

Experimental results of the observation of superradiant emission from the intense, subnanosecond electron bunches moving through a periodic waveguide and interacting with a backward wave TM01 are presented. The short microwave pulses in Ka, W and G bands were generated with repetition frequencies up to 25 Hz. Modification of subnanosecond slicer of the accelerator RADAN allowed us to increase the voltage pulse amplitude up to 300 kV and electron bunch current up to 2 kA. As a result peak power of the 300 ps Ka band microwave pulses increased in 2 times with respect to those reported in the paper (N.S.Ginzburg et al Phys.Rev.E, 1999 V.60, P.3297) and achieved about 140 MW. Rather high level of radiation power was indicated by the illumination of a neon bulb panel as well as observation of RF breakdown of ambient air. The initial experiments on generation of 75 GHz, 10-15MW radiation pulses with duration less than 150 ps, and of 150 GHz microwave spikes with the front of 75 ps are also reported. The experimental data are compared with numerical simulations using pic code KARAT.

## P31

### Ka-Band Gyro-TWT with a Helically Grooved Waveguide

*Samsonov, S V<sup>1</sup>; Bratman, V L<sup>1</sup>; Denisov, G G<sup>1</sup>; Ofitserov, M M<sup>1</sup>*

<sup>1</sup>Institute of Applied Physics, Russia

Experimental results are presented of Ka-band gyrotron traveling wave tubes (gyro-TWTs) based on a new microwave system in the form of a cylindrical waveguide with a helical corrugation of the inner surface. The corrugation radically changes the wave dispersion resulting in appearance of an operating eigenwave of constant group velocity in the region of close-to-zero axial wavenumber. For a gyro-TWT such a dispersion characteristic permits operation with significantly increased bandwidth, reduced sensitivity to electron-beam axial velocity spread and higher stability to the spurious oscillations. A gyro-TWT with a moderately relativistic short-pulse electron beam (290 keV, 36 A, 20 ns) operating at the second cyclotron harmonic has produced an output power of 2.8 MW and a gain of 33 dB corresponding to an efficiency of 27% at a frequency of 36.5 GHz. A theoretically predicted frequency bandwidth amounts to about 20%, but it has not been measured yet. An experiment on the gyro-TWT with a low relativistic long-pulse electron beam (80 keV, 20 A, 10 microsec.) has been started. Designed output parameters are as follows: central frequency of 36 GHz, mode TE<sub>1,1</sub>, power of 0.5 MW, efficiency of 30%, gain of >30 dB, bandwidth of 15%.

## P30

### A Gyrodevice Based on Simultaneous Excitation of Opposite and Forward Waves (Gytron BWO-TWT)

*Eddotov, A<sup>1</sup>; Bratman, V<sup>1</sup>; Savilov, A<sup>1</sup>*

<sup>1</sup>Russian Academy of Sciences, Russia

In spite of a very attractive opportunity for a wideband frequency tuning a gyrotron variety of Backward Wave Oscillator (gyro-BWO) is not significantly spread. It is explained by problems of selective excitation for opposite waves and by low efficiency of gyro-BWO as compared to the gyrotron. The latter is caused by the following reasons: 1) electron axial momentum increases at the excitation of the opposite wave (recoil); 2) axial field structure decreasing along the interaction region is unfavorable for obtaining high efficiency; 3) a significant Doppler broadening of cyclotron resonance line for running waves because of spread in electron velocity. At the same time, it is well known that these factors are absent in the gyro-TWT being a CRM-amplifier with a traveling (forward) wave. In this device the RF field structure being favorable for high efficiency builds-up automatically. Since the radiation of the forward wave results in a decrease of the electron longitudinal momentum, the wave extracts not only the transverse electron energy but also, unlike the gyrotron, a part of the longitudinal energy.

It would be attractive to combine the advantages of the gyro-BWO and the gyro-TWT (a high efficiency and a broadband frequency tuning) in a single device. Such a device (gyro-BWO-TWT) can be realized by means of arranging the simultaneous (inside a single waveguide) interaction of electrons with opposite and forward waves at the same frequency but at different cyclotron harmonics; in particular, at the second cyclotron harmonic for the backward wave and at the fundamental one for the forward wave. An effective interaction (coupling) between the waves is provided by the use of a phase-synchronized beam of gyro-rotating electrons; in the unperturbed state of this beam, all particles of any beam cross-section have the same gyro-phases. Since electron bunches, which are created in the phase-synchronized electron beam by the both waves, have strictly identical structures, the beam provides a strong coupling of the waves.

According to simulations, the use of the proposed method allows significant increasing the efficiency of gyro-BWO (from 10% up to 20-30%) with the possibility for a wide (5-20%) frequency tuning. In a smooth-wall circular waveguide such second-harmonic gyro-BWO with simultaneous fundamental-harmonic excitation of the forward wave can not be realized due to the undesired fundamental-harmonic excitation of the gyrotron or the usual gyro-BWO. This mode competition can be avoided in a helically corrugated waveguide.



## P33

### Prospects for Gamma-ray Laser on Radiative Transition of Free Nuclei

Zadernovskiy, A<sup>1</sup>

<sup>1</sup>Moscow State Institute of Radio Engineering, Russia

Gamma-ray laser attracts attention of researchers for many years. The unique possibility for building of gamma-ray laser give the excited isomeric states of nuclei with the energies from tens of keV to tens of MeV and lifetimes from a few microseconds to tens of years. Inverse medium prepared by photochemical separation of the excited long-lived isomeric nuclei from unexcited ones could be, in principle, used for achieving amplification of stimulated gamma radiation. However, large Doppler broadening of emission lines for gamma transitions (Doppler width is proportional to the square root of recoil energy of a nucleus) brings to catastrophic fall of the stimulated emission cross section and the process of amplification turns out to be unlikely.

In majority schemes proposed for nuclear gamma-ray laser the Messbauer recoilless transitions in crystals are suggested to use in order to remove Doppler broadening and thus reduce radiative linewidth to its natural value. Unfortunately, the Messbauer effect can exist only for short-lived nuclear states with lifetimes less than approximately 10 microseconds what is absolutely not enough for separation of excited nuclei and preparation of them the inverse crystal medium. Despite of a variety of numerous suggestions to bypass this obstacle (G.C.Baidwin, J.C.Solem, Rev. Mod. Phys., 69, 1085, 1997), the difficulties with developing a selfconsistent scheme for Messbauer gamma laser are not surmounted up to now.

In this report we consider in detail an alternative way to achieve gain for stimulated gamma radiation based on the recently proposed concept for recoil assisted gamma-ray laser (L.A.Rivlin, Quantum Electronics, 6, 467, 1999) on cooled (monokinized) beam of free isomeric nuclei.

As is well known, the centers of emission and absorption lines of a free nucleus are displaced by the double nuclear recoil energy.

Modern methods for laser cooling of atoms containing isomeric nuclei allow to reduce the Doppler broadening of nuclear transitions to the extent sufficient for appearing the spectral splitting of emission and absorption lines of radiative gamma transitions. This brings about formation of spectral-local population inversion in a cooled nuclear beam without excess of the number of excited nuclei over unexcited ones and leads to arising the amplification of stimulated radiation.

For discussion of nuclear gamma decay we consider a three level system. The nucleus is initially in the isomeric state from which it decays very slowly to its ground state. Under the influence of an external broadband x-ray radiation we can induce a two step decay to the nuclear ground state through an intermediate short-lived level. These triggering two-quantum transitions is accompanied by the absorption of x-ray photons with simultaneous emission of gamma-quanta. We present the cross section for the stimulated anti-Stokes scattering with quanta of different multipolarity as well as the gain for stimulated gamma radiation in a cooled nuclear beam with spectral-local population inversion. Numerical estimations, executed for the nucleus <sup>179</sup>Hf (the energy of isomeric level 1105,84 keV, lifetime 25,05 days, energy of nearest intermediate level 1105,91 keV) yields the threshold ratio 10(-3) for concentration of isomeric nuclei to overall nuclear concentration in the beam and the pumping threshold spectral photon flux density 10(8)-10(10) photons/(cm(2) c Hz) attainable, for instance, with plasma sources of x-ray radiation.

## P34

### Application of Finite-Difference Time-Domain Method for Investigation the Microwaves Penetration into Cavities

Goncharov, A N<sup>1</sup>; Kiselev, V V<sup>1</sup>; Kondratiev, V M<sup>1</sup>; Kondratieva, A I<sup>1</sup>; Panteleev, S V<sup>1</sup>

<sup>1</sup>Central Institute of Physics and Technology, Russia

Investigation of Microwaves-objects interaction, in particular, penetration into cavities through slots and apertures of various forms is of great practical interest in the problem of electromagnetic compatibility. The studying of this interaction can be accomplished using experiments as well as numerical methods. This report presents the numerical study of the Microwaves penetration into cavities through the apertures in a metal casing.

To solve the three-dimensional Maxwell equations system depicting the interaction of EMP field and objects of complex shape the FDTD method has been used. We have created a set of programs to calculate the EM environment in the vicinity of perfectly conductive objects as well as for objects with real electrophysical characteristics (I.B. Bakholdin, N.I. Kozlov, A.I. Kondratieva, Mathematical Modeling, vol. 6, No.8, 1994). Several program variants have been developed: for objects in a free space, at the ground surface, some objects in a counting volume, narrow slots on the objects surface.

The report describes the opportunity of applying the available programs to investigate the Microwaves interaction with different objects, in particular, its penetration into cavities through apertures and slots of various forms. The numerical procedure accuracy is estimated by using the available experimental data.

A metal cylinder of 20 cm in diameter has been tested. The Microwaves with wave length of 4 cm fall on the cylinder head along its axis. In one case the cylinder head is opened, in another case it is closed by a metal cover with a slot hole of 12x30 mm<sup>2</sup> displaced for 30 mm relative to the cylinder axis. The Microwaves flux power relation at the opened and covered head has been measured during the experiment inside the cylinder at a distance of 7 cm from its head. For calculation the cylinder was simulated by the cubic cells in Cartesian system at the maximum approximation to the real object form. The investigations resulted in obtaining amplitude-time characteristics of the Microwaves electric and magnetic fields in different points inside the cylinder with the opened and covered head.

## P35

### EMF Induced in Power Systems by MHD-EMP and Geomagnetic Storms

Garanyishkin, N V<sup>1</sup>; Kondratiev, V M<sup>1</sup>; Sokovikh, V V<sup>1</sup>

<sup>1</sup>Central Institute of Physics and Technology, Russia

It is known that low-frequency electromagnetic fields at the Earth surface generated by geomagnetic storms reveal as electromotive force (EMF) sources creating quasi-dc electric currents in long power lines. These currents give rise to fluctuations of active and reactive power, voltage drop, frequency shift, relaying problems and, in some cases, transformer failures. Magnetohydrodynamic electromagnetic pulse (MHD-EMP) of high-altitude nuclear burst can cause similar impact on power systems. Since the experimental data on MHD-EMP fields and their impact on power systems are insufficient, it is necessary to use mathematical simulation methods to investigate this problem. The report presents the results of calculating EMF induced by MHD-EMP between the grounded power systems points in comparison with EMF generated by severe geomagnetic storms. At comparable EMF values the observed facts of failures under the impact of geomagnetic storms can be extrapolated on MHD-EMP impact.

The Earth surface electric field distributions arisen from long-time geophysical observations were used as the initial data for calculating EMF induced by geomagnetic storms. MHD-EMP fields of high-altitude nuclear burst calculation has been made according to three-dimensional procedure with due account of all main physical factors effecting their formation, in particular, the real inclination of geomagnetic field lines and tensor character of ionospheric plasma conductivity (V.M. Kondratiev, V.V. Sokovikh, Proc. of Int. Symp. on EMC, Sept 14-18, 1988, Rome, Italy). This procedure has been tested on the experimental data. It allows to depict accurately the spatial distribution of MHD-EMP amplitude and form near the Earth surface, which is of great importance for assessment of its impact on long power lines. Several scenarios of MHD-EMP impact on a really existing power system have been considered. Amplitudes and forms of EMF pulse were obtained for each scenario. Pulse parameters dependency on mutual location of the power system and the burst epicenter has been analyzed. It was shown that EMF magnitudes induced in power systems by MHD-EMP are commensurable or exceed the corresponding EMF arising during severe geomagnetic storms. The obtained results can be applied to the indirect test procedures of MHD-EMP impact on separate power system components.

P36

Transverse Inductance in Coaxial Structures with Conductive Dielectrics

Badic, M<sup>1</sup>; Marinescu, M J<sup>1</sup>

<sup>1</sup>Research Institute for Electrical Engineering-ICPE, Romania

Coaxial disk resistors are used in measuring high intensity impulse currents having  $\mu s$  rise time or less. In coaxial structures, they may appear as conductive dielectrics in measuring shielding effectiveness ( $SE_{dB}$ ) of materials by means of TEM coaxial cells. The paper deals with inductance evaluation of conductive dielectrics mounted in coaxial structures, knowing that characteristic parameters are extremely important in the material (having  $\mu, \epsilon, \sigma$ )-electromagnetic field interaction. Authors demonstrate that inductance of such disk tends to 0 when  $d \ll \delta$  ( $d$ =sample thickness,  $\delta$ =skin depth).

Demonstration starts from the classical scheme of elementary lossy transmission line and it is analysed the suitability of introducing a transverse inductance, based "a priori" on the fact that if there is a transverse current it should exist a corresponding inductance.

The calculus uses Shelkunoff's equation that defines shielding effectiveness:

$$SE_{dB} = 8.6859 \frac{d}{\delta} + 20 \log \left| \frac{(1+K)^2}{4K} \right| + 20 \log \left| \frac{(K-1)^2}{(K+1)^2} e^{-2(1+j)\frac{d}{\delta}} \right|$$

where  $K = \frac{Z_c}{(1+j)R_s} \frac{d}{\delta} = \frac{Z_c}{\sqrt{j\omega\epsilon\mu} R_s d}$ ;  $R_s = \frac{L}{cd}$ ;  $Z_c = 376.7 \Omega$  in the case of plane waves, or a certain value for the Fresnel zone.

If there is a transverse inductance, it should be found in the  $SE_{dB}$  expression because this one has to cover the whole phenomenon in a coaxial structure considered transmission line ( $SE_{dB} = ABSORPTION + REFLECTION + RE-REFLECTION$ ). On the other hand it is well known that, inductance, as physical amount, has to include magnetic permeability  $\mu$ . Considering all of these, authors propose an original algorithm in order to obtain another equation for shielding effectiveness:

$$SE_{dB} = 20 \log \left\{ \frac{Z_c cd}{2} \left[ 1 + \frac{32}{6!} \left( \frac{d}{\delta} \right)^4 + \frac{512}{10!} \left( \frac{d}{\delta} \right)^6 + \dots \right]^2 \right\}$$

It may be observed that the first term containing  $d/\delta$  is multiplied by 0.044, the second 0.000141, a.s.o., while the corresponding exponents rise by 4 units.

Because inductance is expressed in the above equation only by skin depth  $\delta$  and not by conductivity ( $\sigma$ ), it means that this equation allows an accurate evaluation of the weight of inductance in the conductor/semiconductor disk impedance, function of its thickness and frequency.

The paper also describes the magnetic field configuration in electrically thick samples, assumed to produce the disk inductance in the specified conditions. When  $d \ll \delta$ , meaning that the disk is electrically thin, it may be considered that its inductance tends to vanish.

P39

Measurement of High-Amplitude Pulsed Currents with Nanosecond Rise Time

Ivanov, L N<sup>1</sup>; Kovalenko, S A<sup>1</sup>; Krokhavev, D I<sup>1</sup>; Sidoryuk, P A<sup>1</sup>; Shkurin, E V<sup>1</sup>

<sup>1</sup>Central Institute of Physics Technology, Russia

When testing the objects on lightning protection (MIL-STD 1757, IEC-60) and immunity to electromagnetic factors of artificial origins (IEC 1000-2-10, 1996), it is needed to measure pulsed currents with amplitude of tens-hundreds kiloamperes and time characteristics from tens nanoseconds to several milli-seconds. When creating required for that measuring means, main problem is absence of calibrating facilities, forming precision pulsed currents with rise time of 5-10 ns. The use of pulses with short rise time by the calibration is needed to reduce dynamic error.

The creation of such calibration facilities, forming currents up to few hundreds kiloamperes, is restrained by high cost of their development.

We realized less high-priced approach, allowing to solve the problem of measuring means calibration by the way of using the facilities with limited amplitude range. By the use of the facility, forming calibration pulses with rise time of 5 ns and amplitude of current up to 1 kA, a device for measuring pulsed currents up to 250 kA is designed in our organizations.

Principle of action of the measuring device is based on splitting full current onto equal parts by means of N elements (conductors).

A number of the elements is chosen with taking into account the need to provide both measurement of full current with required amplitude, and possibility of calibrating single element of the device with mentioned above calibration facility within the range of 10 A to 1 kA.

To determine full current by means of the measuring device, it is sufficient to register a current in one of its elements, equipped

P38

Variable Bandwidth Filter on Base of Gratings-Polarizers

Arzhannikov, A<sup>1</sup>; Kuznetsov, S<sup>1</sup>; Sinitsky, S<sup>1</sup>

<sup>1</sup>Budker Institute of Nuclear Physics, Russia

A new type of the interference filter operating in the range of millimeter-centimeter waves is described. Such a filter consists of a set of flat gratings of parallel metallic wires, which operate as polarizers of the electromagnetic wave.

A mathematical model and a computer code are developed for calculation of spectral properties of the interference system consisting of an arbitrary number of parallel gratings and an arbitrary orientation angle of wires in the plain of each grating (counting from orientation of the first grating). Nonideality of gratings as polarizers is also taken into account. It is shown that the spectral properties of the filter consisting of 3 gratings are close to the ones of the Fabry-Perot interferometer. For operation this device like a Fabry-Perot interferometer the edge gratings must have the same orientation angle and the incident wave must be H-wave for the gratings (electric field vector is perpendicular to wires). The orientation angle of the middle grating F defines dependency of filter transparency on wavelength of incident wave and therefore its transparency bandwidth. As a result, changing selective properties of the filter can be realized by varying of the angle F. The high spectral resolution regime occurs for the case of almost crossed gratings ( $F - \pi/2 \ll 1$ ,  $\pi = 3.14159$ ). At these conditions for ideal polarizers and identical gaps between gratings the resolution R is proportional to the inference order m and inverse deviation ( $F - \pi/2$ ) in square. The value of R tends to infinity for F tending to  $\pi/2$ . The upper limitation on the resolution is connected with nonideal properties of gratings as polarizers. For instance, the resolution limit is about 1000 (m~1) for gratings consisting of metallic wires with diameter ~ 0.1 mm and separated by the same distance. In the opposite case, when orientation angles of the middle grating and the edge ones are close ( $F \ll 1$ ) the filter reveals an ability to select narrow peaks of nontransparency (reflection) with a relative width proportional to F in square.

Spectral properties of multigratings interference filters obtained in the theory have been successfully confirmed by experimental measurements. It opens perspectives of application of such filters for spectral analysis and spectral selection of waves in the microwave region.

to this purpose by induction transducer (Rogovsky's ring), which does not have galvanic contact with the circuit under measurement.

Development of the pulsed currents measuring device was based on the results of theoretical and experimental studies of such processes as: the influence of neighbouring grounded surfaces upon fast-acting of the device; the influence of magnetic field of the device's elements on induction transducer; the influence of induction transducer on current on the circuit under measurement; the influence of reverse current lead on equality of current dividing between the device's elements.

Achieved characteristics of developed measuring device allow using it to determine characteristics of pulsed currents with rise time down to 50 ns and duration up to 1 ms within amplitude range of 2,5-250 kA. Error of transfer coefficient of the measuring device does not exceed  $\pm 10\%$ .

## P40

### Universal Optoelectronic System for Measurement of Pulsed Electromagnetic Fields

Bzyta, V I<sup>1</sup>; Ivanov, L N<sup>1</sup>; Rekin, I B<sup>1</sup>; Sidoryuk, P A<sup>1</sup>; Farafonov, O A<sup>1</sup>  
<sup>1</sup>Central Institute of Physics Technology, Russia

The measurement devices, protected from EMP noises effects and not introduced distortions into a measured fields structure and also ensured non interference output of measuring data, are necessary for carrying out of certification tests of technical facilities on stability to powerful pulsed electromagnetic influences (EMP, HPM). Optoelectronic measuring systems satisfy that requires.

An optoelectronic measuring system was designed and produced in CIPT. The system consist of the measuring channels, the control unit, the recorders and the program. Each measuring channel consist of the transmitter, optical fiber line for data transmission, photo receiver, and also set of the sensors for transformation of various electromagnetic influences.

Since at a last time the problem of determination of nanosecond pulsed electromagnetic influences parameters was appear, it is necessary to provide a rapidity of the measuring channel's components order 200 ps.

The measuring converters of capacitance and induction types, and also coaxial dividers of a voltage, wave guide current shunts and detection HPM-section was used as the sensors of electromagnetic fields, currents and voltages. Sensor's singularity is agreement of its signals circuits and universal input cascade of the optoelectronic transmitter on a wave resistance. The transmitter realizes transformation of electrical signal into light by means of the one mode semiconductor DBR-laser, which has rise time of the transient characteristic of 70 ps. Transformation of optics signal into electric ones is realized by photo receiver unit on the base of the InAsGa pin-photo diode and the amplifier with rapidity of 50 ps. The signal circuits of the transmitter and the photo receiver are based on micro strip lines and coordinated to wave resistance. To decrease a measuring error the remote controlled built-in calibrator, which permit to determine parameters of the optoelectronic channel before and after a measurement, is placed in the transmission unit.

## P41

### Attenuators for Measuring of High Voltage Nano- And Subnanosecond Pulses

Kriklenko, A<sup>1</sup>; Efanov, V<sup>1</sup>; Yarin, P<sup>1</sup>  
<sup>1</sup>FID Technology, Russia

Several Types of high voltage attenuators for short pulses are developed. The N-connector symmetrical resistive attenuator with dimensions 20x20x74mm has a 150ps resolution. Its maximum voltage is 20kV and 1ns wide pulse, the maximum average power is 0,25W.

The attenuator for 50kV 20ns pulses with 0,5ns resolution has a specially designed connector. The average power is 100W (with oil pumping). The dimensions are 80x80x240mm.

The same connectors are used for 50kV directional couplers with 8ns time slot. The resolution is 0,5ns, dimensions are 55x85x850mm, the coupling factor is 30dB.

All devices operate at 500 Ohm load.

Designed methods of measurements and technical solutions allow to create the system for measurements of amplitude and time parameters of the video pulses and envelopes of radio pulses with the rise time of 0.5 ns, the duration up 1 mks in amplitude range up to 500 kV/m and 1500 A/m for electromagnetic fields, and up to 50 kA and 100 kV for pulsed currents and voltages. The system able to include up to 64 measuring channels. Control of channels and processing of measuring results is realized by means of computer and special software.

## P44

### The Time-Dependent Dynamics of Processes of Radiation Antagonism, Synergism and Self-Radioprotection During Separated and Combined Irradiation of Biological Systems

Vysotskii, V<sup>1</sup>; Pinchuk, A A<sup>1</sup>; Kornilova, A A<sup>2</sup>  
<sup>1</sup>Kiev Shevchenko University, Ukraine; <sup>2</sup>Moscow State University, Russia

Among a variety of actual problems of radiobiology the problem of radiation viability of DNA's seems to be the most important. The main result of action of irradiation to biological system is the creation of double breaks of DNA macromolecules. Other results of radiation action are generation of hydrated electrons and heavy ions in intercellular salt-aqueous medium. The force of interaction between the end-pairs of nucleotides on the opposite sites of a break is totally under control of the width of the break L as well as of both nucleotides

electric charge distribution (Coulomb interaction) and dispersion features of dielectric permeabilities  $\epsilon_3(\omega)$  of intercellular salt-aqueous medium and nucleotides  $\epsilon_4(\omega)$  through all the range of frequencies  $\omega$  (Van-der-Waals-like forces). From the one hand, the action of irradiation leads to additional DNA breaks and DNA degradation. From the other one it leads to the phenomena of both controlled nucleotides pairs interaction and possible breaks autorepairing. It has

been for the first time established that at the low concentration of hydrated electrons ( $\eta \leq 10^{-9}$ ) the energy of the mutual interaction of the some end-pairs of nucleotides (e.g., AT(Adenin-Thymine)-AT(Adenin-Thymine) has a repelling barrier with value  $V(L_0, \eta) \approx (1-3) KT$  at  $L_0 \approx 7-8 \text{ \AA}$  (fig.1) and corresponds to attraction between them at  $L < L_0$ . If in the result of radiation J action the concentration  $\eta$  is increasing, the barrier is reducing and  $V(L_0, \eta(J)) \approx V_0(1-cJ)$ .

At  $\eta \geq 10^{-7}$  the barrier disappears. All other transversal end-pairs of DNA nucleotides experience only attraction. The layout of the process of depolymerisation and

autorepairing of DNA at combined action of two kinds  $J_1$  and  $J_2$  of ionizing radiation and action of free radicals W is shown on the fig. 2. Here  $\tau$ ,  $T_1$  and  $T_2$  are the times of total, reversible and irreversible DNA double breaks relaxation. The time-dependent dynamics of birth and destruction of double breaks of DNA and dynamics of controlled DNA depolymerisation and autorepairing are described by the system of kinetic equations for concentrations of reversible ( $n$ ) and irreversible ( $m_i$ ) double breaks. The solutions of DNA radiation antagonism problem (the number of DNA double breaks caused by radiation  $J_1$  is decreasing with growing the intensity of radiation  $J_2$ ) at separated and combined action of slight and intensive irradiation (including "the problem of low-dose" for cases of short-time intensive irradiation and long-time slight irradiation and the phenomenon of "hormesis") are studied.

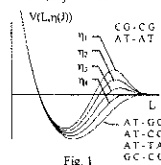


Fig 1

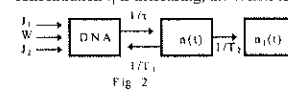


Fig 2

P45

Numerical Study of Electric-Discharge Facilities EMP Impact Parameters on Bioobjects

Gavrish, N N<sup>1</sup>; Davydov, A A<sup>1</sup>; Kondratieva, A I<sup>1</sup>; Kondratiev, V M<sup>1</sup>; Mokochnin, V L<sup>1</sup>; Nikulin, P V<sup>1</sup>; Plygach, V A<sup>1</sup>  
<sup>1</sup>Central Institute of Physics and Technology, Russia

Sanitary-hygienic standardization of EMP fields impact on bioobjects is nowadays an urgent problem in providing electromagnetic safety of a man. One of the ways of solving this problem is to accomplish purpose biological experiments on animals. However such experiments are complicated and expensive. Therefore, the calculated methods are of great importance in planning experiments, analysis of the obtained results and their extrapolation on a human. The report presents the calculated data on EMP field impact on bioobjects. Calculation technique means the numerical solving of Maxwell equations system by using FDTD method. Homogeneous cylindrical models with electrophysical characteristics corresponding to biological tissue with a large content of water are applied for animals and human simulation. The choice of electrophysical constants has been made according to resonance frequency.

Current density is taken as a main parameter of EMP field impact on biological objects in numerical modeling. This choice is stipulated by nonthermal effect of electric-discharge facilities powerful single pulses. Numerical study of impact parameters was carried out in three trends. The first trend includes an experimental examination of the calculation technique and substantiation of the primary assumptions in bioobject simulation. The second trend is aimed at the calculation of the average current density induced in animal models by EMP fields of electric-discharge facilities. The purpose of this study is to compare the calculated impact parameters with the results of medical examination of experimental animals and to determine the impact parameter threshold causing functional disturbances. The third trend is the calculation of the average current density in a human model under the impact of EMP fields with different time parameters. The purpose of the study is the receiving of the initial data to determine EMP field characteristics allowing to reach the critical level of a human impact parameters.

P49

Electromagnetic Eddy-Current Shielding

Zinkovskiy, Y<sup>1</sup>; Klimenko, V<sup>1</sup>; Savenko, Y<sup>1</sup>  
<sup>1</sup>Kiev Polytechnic Institute, Ukraine

The development of the information technologies determines the necessity of increasing of the level of electromagnetic and information protection of electronic devices and computers. Shielding is a principal engineering estimate of an electromagnetic protection. Rising of the shielding efficiency is the main task at increasing of the production size and computer using, because the market price of shielded computer is more on the order. The authors offer a calculation techniques of the electromagnetic shields that enable essentially to increase their efficiency on executable functions. Expenses simultaneously are reduced at designing, production of maintenance of the shielded computers. According to the offered technique are calculated the electromagnetic shielded fields, main effects of their interaction with materials of shields, constructions of shields and their main goal functions by the numerical methods with using of the appropriate software, developed by the authors. An analytical basis - device of systems of the integrated Fredholm equations in a combination to shielding effects "of secondary sources" rather half-chaotic poorly canalization of eddy currents. With use of the offered method the accuracy of account of shields (unit of percents) raises, the saving of expensive shielding metal materials, is improved electromagnetic and information security of computers.

P48

Influence of Modulated Low-Energy High Frequency Fields on Biological Subjects

Germanovitch, O P<sup>1</sup>; Pavlovski, V F<sup>2</sup>

<sup>1</sup>North-West Politechnical Institute; <sup>2</sup>Influenza Institute, Russia

The unique fact of influence of electromagnetic fields (EMF) modulated in the window of internal brain frequency spectrum, upon the intra-cell concentration of Ca<sup>++</sup> ions is well known now. This fact, in turn, presents the opportunity of controlling the Ca-dependent processes. It was shown that the effect of exposition to modulated EMF could be explained with facilitation or, sometimes, inhibition of Ca<sup>++</sup> ions penetration into a cell, and/or Ca<sup>++</sup> flow from the cisterns. That could be a trigger to turn on the cascade of biochemical processes in a cell, which result in integrating neurons' activities.

Our research is based on the previously adopted mathematical model of generating of the electroencephalogram (EEG) of animals that were exposed to hypoxic hypoxia of different extent. This model describes EEG with non-linear electronic oscillator equation

$$\Theta'' = (-gA(x)) \sin \Theta \tag{1}$$

Where  $g$  – a constant of EMF of the Earth,  
 $A(x)$  – functional, which depends upon parameter  $x$  and gives out the frequency and amplitude of oscillator,  $\Theta$  – the phase slope and differential equation of type

$$x'(t) = \int_0^{\alpha(t)} p(t, \tau) x(t - \tau) d\tau + f(t) \tag{2}$$

where  $p(t, \tau)$  – multiplier, defining the influence of past on future,  
 $x(t - \tau)$  – position of subject in concrete past,  
 $f(t)$  – factor of individual dependence of the subject.  
 To understand the non-linear oscillator model, let us imagine the mathematical pendulum of changeable length, i.e.  $A(x)$ , where  $x(t)$  changes spontaneously. Then, if the energy was constant the changes of amplitude will change the frequency (if lower, - then higher).

The electronic oscillator equation describes the EEG-signal pattern quite well, but cannot define the time dependence of the process. That is why it is necessary to find the  $x$  parameter, which is time-dependent. This parameter is to be found from the equation (2), the starting point of which is the previous history of the process, and the velocity of the process depends on external influences at the moment, previous history and pattern of the process in the past.

Thus calculating the epoch  $t1$  of the EEG of an animal being in an initial point, we can predict the development of the process on the epoch  $t2$  keeping in mind the previous history of the process and taking in account the factor of biosystems reactions' delay to external influences.

The not-steady-state processes and delay characteristics of EEG of the animals being exposed to different levels of hypoxic hypoxia were studied using the mathematical model. The results were used to elaborate the modulation programs, aimed to:

1. trigger resonance effects at frequencies 0.2 – 80 Hz,
2. change cAMP and cGMP level up to 160%, beta-endorphine level – up to 150%, calmoduline level – up to 180% vs control,
3. to restore the sensitivity of opiate receptors,
4. change psycho-emotional status, that could be useful treating narcomania.

P50

Thermal Transient in ICs due to HEMP Action of Nanosecond Duration

Zhuravliov, V<sup>1</sup>; Alexeev, V<sup>1</sup>

<sup>1</sup>Belarusian State University, Belarus

The high electromagnetic pulse (HEMP) action on integrated circuits may cause sufficiently great overfalls of temperature in crystal, which lead to different breakdown types of ICs. The temperature transients can reach more than one hundred of degrees at some regions of die sometimes, that are due to short duration of HEMP action.

By the theoretical and experimental data phenomenologic model of IC heating under HEMP action is developed that takes into account material's thermophysical properties. IC is presented as half-limited body with heated region at metallization configuration (fig.1). The temperature gradient, originating in die bulk, depends direct via HEMP duration and energy:

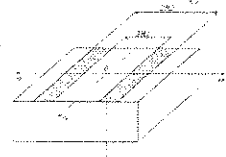


Fig.1

$$\Delta T = \frac{P_0}{2b\sqrt{\pi}} \int_0^{\tau} \frac{\exp\left[-\frac{a^2}{4a^2(\tau - \tau_0)}\right]}{\sqrt{\tau - \tau_0}} \left\{ \operatorname{erf} \left[ \frac{R - x}{2\sqrt{a^2(\tau - \tau_0)}} \right] - \operatorname{erf} \left[ \frac{R - x}{2\sqrt{a^2(\tau - \tau_0)}} \right] \right\} d\tau_0$$

where  $\tau_0$  is moment time;  $P_0$  is absorbed pulse energy;  $\tau$  is duration of EMP,  $a = (K/b)^2$  is temperature conductivity;  $K$  is material thermal conductivity.

As result, thermal transient distributions are calculated for HEMP with  $\tau = 10$  ns (fig.2) and  $\tau = 500$  ns (fig.3) at equal energy. It is shown, that thermal transient at  $\tau = 10$  ns of HEMP more sleeper considerable, than one at 100 ns.

Thus, HEMP with nanosecond duration can also initiate considerable thermal gradient and more, as one with more durations.

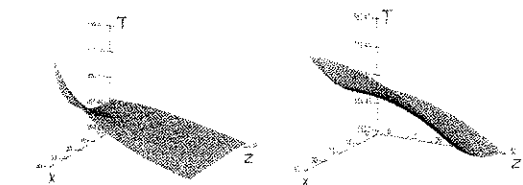


Fig.2

Fig.3

## P52

### Potential Possibilities of use of GPR for Detection of Subsurface Layers Polluted by Petroleum

*Sugak, V'*

*'National Academy of Science of Ukraine, Ukraine*

One of important task of environment monitoring nowadays is ecological task of detection and mapping of subsurface zones polluted by oil and petroleum products with use of ground penetrating radar (GPR). The potential possibilities of GPR use for monitoring of subsurface layers down to a level of ground waters (zone of aeration) for this purpose is determined by distinction of soil electrical characteristics at natural distribution of humidity on depth from the case of presence of various kind of inhomogenates (saturation by petroleum).

Results of measurements of dependence of dielectric constant of typical subterranean rock's samples of zone of aeration (clay loam and sand) upon humidity and degree of saturation by petroleum, carried out as in laboratory conditions as well as at natural their stratification in lizimeter in the radio-frequency band of 40...150 MHz are represented. For this purpose it was developed the special sensors, which could be immersed in a researched soil without essential mechanical destruction of its structure.

It is shown, that saturation of damp soil samples by petroleum results in essential increase of their dielectric constants. A hypothesis, explaining obtained effects, is offered.

It was experimentally estimated the potential possibilities of detection of subsurface layers saturated by petroleum with use of GPR model, based on sweep generator in the frequency band of 100-180 MHz and special method of signal processing based on high order spectral estimation to obtain more high depth resolution and to compensate the dependence of soil electrical constants upon frequency (dispersion). The results of detection of subsurface layer polluted by petroleum is presented.

## P54

### Experimental Investigation of Multi Element Impulse Radiating Antenna

*Ostashev, V.E'; Yankovskii, B.D'; Ul'yanov, A.V'; Lebedev, Ye.F'; Syzranov, V.S'; Fedorov, V.M'*

*'Russian Academy of Sciences, Russia*

Generator of subnanosecond pulses was designed with the use of the semiconductor technology. It excited multi element IRA (~100 elements) in repetitive mode (up to 1 kHz). The total peak power of generator was 10 MW. Rise time of unipolar impulse of bell form was  $\tau = 0.3$  ns. For experimental study of parameters of matching the generator and antennas, EM field of radiation and its spectral particularities two antennas on 54 radiating elements was designed. Radiating surface of one of the antennas was like chess board, formed by plane radiator elements with the size of 3.3 cm and square slots of similar form. The excitation of radiating elements was produced by coaxial 50-Ohm cables connected to corners of nearby elements. The plane metal EM reflector of about 0.6\*0.6 m was installed on the distance of  $ct/2 \gg 4-5$  cm. Reflector closed the current of excitation of antenna elements. The front view of the second IRA was identical the first one. But in this antenna each feeder was connected to quasi horn antenna. There was no reflector in this antenna. The results of experimental measurements of parameters of pulse of excitation, EM field of pulsed radiation, spatial distribution of radiation, as well as analysis of evolution of spectral composition of pulse in process of its carrying and transformations in system will be presented.

## P53

### Radiation of Electromagnetic Pulse Signals with Variable Pulse Width

*Pochanin, G'*

*'National Academy of Sciences of Ukraine, Ukraine*

The ground penetrating radars with antenna systems, matched with fixed pulse width, use usually for subsurface sounding realization. Wideband dipoles with impact excitation relate to these antenna systems. Such antennas provide the best radiation of signals the pulse width of which is nearly equal to the propagation time of the exciting signal in radiating elements. The fixed pulse duration restricts possibilities of extending the penetration depth and increasing the resolution.

In order to increase the penetration depth we need to replace an antenna system by one that radiates signals with longer pulse duration. But if we need to increase a resolution we must use a small antenna that radiates short pulses. However, the problem of subsurface objects detection at larger depth often appears when sounding. And it is very inconvenient to change an antenna system every time. Thus, the creation of a new antenna, which is able to radiate different duration signals, is a burning question.

The promising approach to the development of the antenna with variable pulse width is based on the Harmuth's Large Current Radiator (LCR) idea. LCR is inherently a non-resonant radiator, so it can radiate a signal with arbitrary time dependence and with different durations.

This report presents result of the investigation of the antenna for radiation of the pulse signals with duration from range of 3 to 5 ns. Measured spatial and time domain characteristics of the LCR are discussed in the presentation.

\* This work was supported by Prof. Henning. F. Harmuth of Catholic University of America, Washington DC and by Geophysical Survey System Inc. of North Salem, NH (USA) and by AetherWire and Location, Inc. of Nicasio CA (USA).

## P55

### Radiator for Pulsed Electromagnetic Field Standard

*Ostashev, V.E'; Lebedev, E.F'; Fedorov, V.M'; Fortov, V.E'; Tarakanov, V.P'; Ul'yanov, A.V'; Yankovskii, B.D'*

*'Russian Academy of Sciences, Russia*

The diagnostics of parameters of UWB EM pulses of nanosecond duration is a difficult problem both due to the lack of an approved technical facilities, and verified algorithms of processing, registered by them data. So the development of standard radiator of UWB electromagnetic pulses is an actual problem. The accumulation of coordinated experimental and simulation data will allow to create and to check the facility of reliable diagnostics of EMP radiation.

Offered standard UWB radiator consists of the fine coil antenna which radius is equal to  $\rho_d = 0.3$  m. Semiconductor pulse generator with a peak electric power 10 MW, impulse rise time  $\tau = 0.3-0.4$  ns and repetition frequency up to 1 kHz was used for antenna excitation. Antenna was excited simultaneously in many of its points and quicker than generated EM wave moved along diameter of the coil. Amplitude of excitation current - 40 A. Far field was formed 2 ns after the beginning of antenna excitation. On a distance of 1 m from the center of antenna and in 15 grad from its main axis electric field was equal to 11-12 kV/m.

Unlike cone-shaped, proposed coil IRA is excited in many points (~100), that permits to radiate the total power with more high level. The matching the time of testing and longitudinal size of testable object is realized at the expense of variation the length of cables from generator to elements of coil IRA but at no charge to size of antenna.

Advantages of proposed generator of standard pulses of EM radiation consist in the following:

- simplicity of antenna's geometry allows to calculate parameters of a EM field of its radiating on the measured current of excitation exactly;
- multipoint excitation of antenna allows to generate the greater power, than at single point excitation;
- quick excitation of antenna ( $\tau < \rho_d/c$ ) leads to its high energy efficiency in UWB range;
- time of existence/measurement of a standard EM pulse of radiation is limited by the reflections on the ends of cables from generator to antenna, i.e. length of cables, but not the size of antenna;
- time-amplitude and spectral parameters of generated pulses may be changed by turn of antenna's plane;
- lasting life (hours) and stable generation of nanosecond pulses of radiating in the repetition frequency up to 1 kHz vastly simplifies a registration of parameters of electromagnetic field and raises the validity of results.

## P56

### Dielectric Structures for Kerr-lens Mode Locking in Solid-state and Fiber Lasers.

*Romanova, E<sup>1</sup>*

<sup>1</sup>*Saratov State Agrarian University, Russia*

Kerr-lens mode locking is a powerful technique for ultra-short pulse generation in solid-state and fiber lasers. The Kerr-lens mode locking can be understood as an effect of the intensity-dependent loss in the laser cavity produced by the simultaneous action of self-focusing and aperturing (radially varying gain).

Through the Kerr-effect the laser beam parameters become power dependent. If the laser cavity elements are arranged correctly, the high-intensity beam experiences lower diffraction losses than the low-intensity beam.

In this work, transmittance of various intracavity dielectric structures with the Kerr-like nonlinearity is evaluated using the generalized method of moments suitable not only for the Kerr medium but for the active transversely inhomogeneous gain-guided medium. Homogeneous medium, parabolic-index guiding as well as anti-guiding structures are considered.

Input pulse temporal shape is supposed to be Gaussian. The pulse compression coefficient is estimated for each structure and presented as the surface plot versus the input beam width and radius of the aperture.

The system based on the polarization ellipse rotation is also considered. The pulse compression coefficient is plotted versus the mutual orientation of the system elements.

The novel type of structures for Kerr-lens mode-locking is proposed. It is the nonadiabatic connection of two step-index fibers with different radii. Nonlinear transmittance of the structure is shown to depend on the characteristic frequencies of the fiber segments resulting in broadening or compression of the input pulse. The range of the fiber segments radii suitable for the pulse compression is

evaluated. The estimations are verified by numerical simulations of the total field propagation along the fiber axis. The Finite-Difference Beam Propagation Method is used to solve the scalar wave equation for the slowly varying amplitude of the total field in the weakly-guiding approximation.

The maximum value of the pulse compression coefficient for all these structures is shown to be restricted by the magnitude of nonlinear part of the refraction coefficient. To obtain this limit one has to use sufficiently narrow input beams and apertures, being constrained however by the growing intracavity losses. The irregular fiber structures proposed in the work occur to be more efficient and easily adjustable being applied as the intracavity elements of the fiber lasers.

## P57

### Repetitive All-Solid-State Short Pulse Generators

*Rukin, S<sup>1</sup>; Darznek, S A<sup>1</sup>; Lyubutin, S K<sup>1</sup>; Slovikovskiy, B G<sup>1</sup>; Tsiranov, S N<sup>1</sup>*

<sup>1</sup>*Institute of Electrophysics RAS, Russia*

The recently detected effect of the subnanosecond interruption of high-density currents in SOS-diodes opens up fresh opportunities in generation of powerful high-voltage short pulses. The study of the SOS-diodes showed that the current interruption time decreased to 500-600 ps when the reverse pumping time was reduced to 10-15 ns. A subnanosecond SOS-diode, which cuts off a 1-kA current in 600 ps, served as the basis for development of a pulse generator that produces pulses having the amplitude of 150 - 250 kV, the half-height duration of 3 to 4 ns, and the repetition frequency up to 5 kHz in a 30-second burst. A more powerful generator produces pulses having the duration of 5 to 6 ns, the power of 400 to 500 MW, the voltage of up to 400 kV, and the repetition frequency up to 2 kHz in the burst mode. These generators do not contain gas-discharge switches. As a result, they combine a high repetition frequency and stability of pulses, boast of virtually unlimited (solid-state) service life, and offer a high specific average power. These properties are especially important for high-power short-pulse generators intended for commercial applications. Physical processes that take place in the semiconductor structure of the SOS-diodes operating for subnanosecond interruption of currents are discussed. The circuitry and design of the short-pulse generators are described. Results of the tests performed on the said generators are reported.

Another method for additional sharpening of the pulse rise time was examined. For this purpose, one more switch was connected in series in the load circuit. This device functions as a closing switch and uses fast filling of the semiconductor structure with plasma produced by an ionization shock wave. Initial experiments showed that a reverse-biased SOS-diode, which operates under these conditions, withstands a voltage increasing up to 400 kV in about 6 ns and then is broken down. A voltage rise time of 500 to 600 ps long (0.1 to 0.9 of the amplitude) is formed at the load. The maximum current rise rate at the load is 3 kA/ns. The report presents results of experiments on formation of powerful high-voltage pulses with a subnanosecond rise time.

## P58

### Glagoleva-Arkadyeva's Impulse Source of High-Power Wide-Band Microwave Radiation

*Cherepenin, V<sup>1</sup>; Shumilin, V<sup>2</sup>; Vdovin, V<sup>1</sup>*

<sup>1</sup>*Institute of Radio Engineering Electronics RAS, Russia; <sup>2</sup>High Energy Density Research Center, Russia*

The high-power sources of quasi-coherent or non-coherent radiation having a sufficient power in specific frequency band are necessary for some researches. As an example it is possible to name well known discharge microwaves generators of a noise, or fuse sources of an optical radiation. However, their spectral power density, especially in radio frequencies, is usually insignificant. There is large interest to create high-power impulse sources of such radiation in a microwave range of wavelengths. The construction of a Glagoleva-Arkadyeva's high-power impulse wide-band source of a microwave radiation is represented. This idea for the first time was offered in (A Glagoleva-Arkadyeva, Zeitschrift für Physik 24, 153-154, 1924). As is known, in Glagoleva-Arkadyeva's generator as an active medium the metal sawdust located in oil was used between which there were electrical discharges. In the offered device - the same idea, however, as a source of voltage is used high-power nanosecond generator of impulse voltages. The mixture pass between electrodes, on which impulse voltage with amplitude 100-150 kV and repetition frequency of 50 Hz is applied. In this mixture the numerous breakdowns between conducting particles happen, as results in excitation of electromagnetic oscillations. The maximum of a spectral power density of a radiation depends on an average size of the particles and permittivity of the oil and is selected to correspond to a microwave range. This search may be used for testing of wide-band microwave probes.

## P59

### Pulsed Power Electron Beam Penetration into Atmosphere

*Petrov, N<sup>1</sup>; Bondar, Yu F<sup>2</sup>; Mheidze, G P<sup>2</sup>; Gurevich, A V<sup>3</sup>*  
<sup>1</sup>All-Russian Electro-technical Institute, Russia; <sup>2</sup>General Physics Institute, Russia; <sup>3</sup>Lebedev Physical Institute, Russia

Modeling of the conditions arising in a storm-cloud at the availability of priming electrons in laboratory experiments is of practical interest.

In this paper the experimental setup for modeling of runaway breakdown phenomenon in atmosphere is described. The priming electrons were injected into a long air plane-plane discharge gap under application of high-voltage impulses. Impulses were forming on outlet of a high-voltage outdoor generator with the total charging voltage 9 MV and energy capacity of 1.35 MJ. The duration of the front of impulses was 45 microseconds and the half-decay of the impulse was 7500 microseconds. The results of experimental and theoretical investigations of electron beam propagation in air at atmospheric conditions are presented. The sources of priming electrons on 200-250 and 350-400 keV are designed. The duration of electron beam pulse was 30 ns. High-voltage generator and electron beam gun were joined together and synchronized.

The parameters of priming electron beam are investigated with the help of the Monte-Carlo method taking into account the elastic and inelastic collision. The energy losses of a beam in an exit window of high-voltage diode and in air are determined. The minimum energy of electrons which is needed to penetrate them into atmosphere is determined. The specific distribution of ionization losses in air is obtained. It is shown that the number of electrons is modicum at the distances of 130 cm and there are not any primary electrons on the distances more than 150 cm. Therefore the electrons detected on such distances may be identified as runaway electrons.

## P61

### Development of High-Power Pulsed REB Accelerator Based on the Forming Line Supplied with Current

*Fortov, E<sup>1</sup>; Stroganov, V<sup>1</sup>; Nesterov, E<sup>1</sup>; Roschupkin, S<sup>1</sup>; Mikhailov, V<sup>1</sup>; Petrov, V<sup>1</sup>; Plaksina, S<sup>1</sup>*  
<sup>1</sup>High Energy Density Research Centre, Russia

Inductive storage technique offers high voltage pulses generation when high current capacitive storages or MCG are used as primary sources of energy.

Application of inductive storages is limited by the low quality of the generated beam. Replacement of traditional coil with a piece of forming line allows to integrate the advantages of inductive storages (small sizes) with these of forming lines (active output impedance and rectangular pulse waveform) as well as to increase conversion efficiency.

On the basis of previous design the new accelerator was developed and created, which was designed to operate in one of the three basic operation modes:

1 mode:  $U_{max} = 800$  kV, beams power  $P_{max} = 24$  GW, impedance of the line  $Z = 250\Omega$ , pulse duration  $t = 80$  ns.

2 mode:  $U_{max} = 600$  kV,  $P_{max} = 15$  GW,  $Z = 250\Omega$ ,  $t = 250$  ns.

3 mode:  $U_{max} = 600$  kV,  $P_{max} = 30$  GW,  $Z = 12,50\Omega$ ,  $t = 250$  ns.

Accelerator is power supplied by either up to 4 pulsed current generators with capacitance 1.6 microF each charged up to 100 kV or specially designed MCG.

The possibility of accelerator utilisation for various types of microwave oscillators load is provided.

## P60

### Pulse Power Generator for Dynamic Material Property Testing

*Krivosheev, S<sup>1</sup>*  
<sup>1</sup>St. Petersburg State Technical University, Russia

The pressure pulses with control parameters are necessary for dynamic materials testing. Magneto-pulsing method allows to form such pressure pulse with short time duration and large amplitude and measure the pulse parameters. The main component of this method is the pulse current generator.

The pulse current generator with storage energy about 12 kJ was developed for dynamic testing of materials. The generator aggregated from two modules, collector and load. Each module consist two capacitors with total capacity 6 mF and charge voltage up to 50 kV. Special low-inductive multichannels dischargers were developed and used for module current commutation into load. The nonlinear resistance installed in the discharge circuit of module for current pulse parameters control. The volume buss system was used for buses of module.

This generator can form the pulse current about 1 MA amplitude and 2,5 mks duration in the 45 nH load. The amplitude of pressure pulse is about 1000 MPa.

The using of this generator for material testing make for the experimental definition of threshold fracture mechanical load for specimens with macro-defects and the structure time of failure for PMMA.

## P62

### Ultra Wideband Pulses Forming by Compact Generators

*Dubrov, E A<sup>1</sup>; Ivanov, L N<sup>1</sup>; Kovalenko, S A<sup>1</sup>; Krokhalev, D I<sup>1</sup>*  
<sup>1</sup>Central Institute of Physics Technology, Russia

When undertaking the studies on electromagnetic compatibility of technical facilities and biological objects, the need to form high-voltage pulses with nanosecond and sub-nanosecond duration appears. Generators, forming such pulses, include, as a rule, a source of high voltage, in consequence of which sizes of such generators achieve several metres, and their weights - hundreds of kilograms.

In the paper, the studies are described, which are aimed on ultra-wideband high-voltage pulses forming by compact generators and defining amplitude-time characteristics of the pulses. With that end in view, we develop a generator on the base of piezoelectric element with the weight of 10 grams and sizes within 10\*10\*30 mm.

It is known, that when piezoelectric element is exposed to mechanical impact, electrical charges arise on its faces. To get voltage pulse, experimental facility was designed. A charge, appearing by the mechanical hit with the force of 30 N, is sufficient to break down air gap up to several millimetres, which indicates the presence of high voltage.

However, the difficulties, connected with high inductance of the spark gap, mismatch of power source and transmitting line, dissipating part of energy into surrounding space, and imperfection of measurement methods and means, did not allow to form and detect high-voltage pulses with sub-nanosecond time characteristics.

To overcome arising difficulties, we developed low-inductive air switching device, means for screening dissipating energy and matching generator with transmitting line, as well as fast-acting strip measurement means.

As a result of carried out work, high-voltage pulses with amplitude more than 2,5 kV, rise time of 0,3 ns and half-amplitude duration of 0,5 ns were formed.



P65

Explicit Conditions for Virtual Boundaries for the Problems of Non Harmonic Wave

Yashina, N<sup>1</sup>; Sirenko, Y<sup>1</sup>; Perov, A<sup>1</sup>; Yildiz, E<sup>1</sup>  
<sup>1</sup>Institute of Radiophysics Electronics of NAS, Ukraine

The efficient limitation of computation domain in analysis of initial boundary value problems in infinite domains is one of the principal items while dealing not only with FDTD schemes but also in other numerical methods and algorithms, close ideologically to FDTD. The known versions of the solution to this problem are based on several approaches, various in principal. The first one that is the most widely spread in applied computations based in introduction of so called ABC. It supposes that the region where the sources and the part of scatterers that is of interest are located is surrounding with virtual boundaries where absorbing boundary conditions (ABC) are fulfilled. These conditions are derived from rather clear physical perception about propagation of the beam of complex plane waves in the free space. Such ABC provides the zero reflection for the partial components of the beam that are of normal incidence to the virtual boundary. Naturally the reflection coefficient increases with the rise of deviation of incident angle of partial components from normal one. The higher is the order of ABC the slower is the increase of reflection coefficient. It is clear that real physical situation has much more various sources of distortions, then ideal theoretical models, within the frames of which the local classic ABC have been derived. That the reason that make the application of original ABC for rather rare. The modifications into ABC are introduces in accordance with the situation under consideration: the accepted and expected accuracy of numerical results, the acceptable dimension of the computational domain, the degree of heterogeneity of the media parameters in virtual boundaries. The base of modification is mostly created by three heuristic suggestions about the structure of the field that is "interacting" with virtual boundary. The validity of the statements presumed is to be proved indirectly during numerical experiments. Such experiments are used also for testing algorithm's accuracy and efficiency, for proper choice of "optimal" magnitudes of the free parameters of the method.

The examples of other approaches to the problem of the limitation of computational domain that differ in principal from mentioned above, give the papers where instead of ABC the rigorous radiation condition are applied to the scattered fields that are related to certain virtual boundaries. These boundaries are often of coordinate shape and surround efficient scatterers (compact discontinuities in free space or in wave guiding structure). Not being based on any of heuristic suggestions about subtle structure of the field in the vicinity of boundary and being in complete concord with physical nature of process mathematically simulated these conditions do not distort the wave scattering processes (at least theoretically) and have no connection with such inconvenient free parameter as the dimension of computational domain.

Several new radiation conditions are suggested in present paper. They result from representations of transport operators describing time-space transformations of the elements of the evolutionary basis of signals propagating from the region where the sources and scatterers are located. These conditions have been incorporated in a correct way into the finite-difference schemas, verified in numerical experiments for model problems of the theory of periodic and waveguide resonators. The results of the experiments are to be presented in the presentation. They proved high efficiency of conditions suggested, possibility of radical solving of the computational domain limitation in finite difference methods for various model problems of the theory of non harmonic wave scattering.

P66

The Restoration of Signal Form with Using of System Invariance Property

Stoukatch, O. V<sup>1</sup>  
<sup>1</sup>TUCSR, Russia

In many practical problems, in particular, for underground penetration radar system designing the decision of incorrect problem of restoration of the true signal form on measured signal is necessary. By mathematics kind this problem is convolution of required signal  $s(t)$  with registration antenna system apparatus function or pulse characteristic  $g(t)$ :

$$\int_{-\infty}^{\infty} g(t) s(t-T) dT = u(t), \quad (1)$$

where  $u(t)$  is target signal. Well-known methods for decision of this problem assumes, that  $g(t)$  is known. However in the many practical cases it strongly depends on many factors, is rather unstable or has a complexity kind. It make a large errors in the results. To exclude obvious definition of function  $g(t)$ , frequently signal is restored by results of two measurements in different time, or double-channel system.

The accuracy of this method is also insufficient, because of it requires exact knowledge of  $s(t)$  and  $u(t)$  form for "trial response", that is initial measurement  $g(t)$  at known  $s(t)$  and  $u(t)$ . At the same time the signal  $s(t)$  cannot be defined with a small error even in case of width of the directivity and registration system impulse characteristic, essentially distinguished from measurement signal form.

We shall decide the problem of signal reduction on the basis of double its measurement by system with the adjustable amplitude-frequency characteristic (AFC) and phase-frequency characteristic (PFC) invariance to AFC. A number of transformations of equation (1) in the frequency domain by means of Fourier transformation is carried out for this purpose. PFC of system is considered stable and does not change by essential form during measurements. In this case the decision of (1) is reduced to operations above signals, which can be executed on a computer. Initial data for reduction of signal will be the information about AFC of system in two conditions and two measured responses of the phase-invariance system.

There are many examples of the model problems decision of the true signal form restoration, deformed by pulse characteristic of the elementary phase-invariance systems. The examples proven the opportunity of decision of the signal restoration problem in case of signal processing by the phase-invariance system.

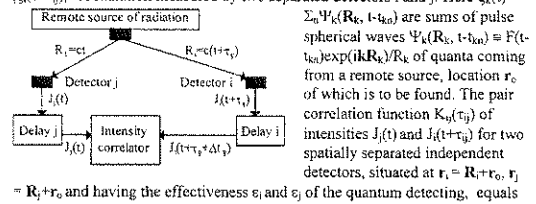
This method can be used in case of impossibility of the decision of problem by method of trial response, as well as by use of two-channel systems with different AFC and identical PFC. Improvement of this method in view of the strong measurement errors is hereinafter offered.

P67

The Problem and Method of Spatial 3-D Detecting of Remote Radiation Sources By Correlation of Intensity of Radiation

Vysotskii, V<sup>1</sup>  
<sup>1</sup>Kiev Shevchenko University, Ukraine

The intensity correlation method of spatial and angular (three-dimensional) location of solitary or remote sources of VVV, X-, and gamma-radiation is suggested and studied. The main idea of the method is based on the phenomenon of pair correlation of intensities  $J_i(t) = \epsilon_i |\xi_i(t)|^2$  and  $J_j(t+\tau_{ij}) = \epsilon_j |\xi_j(t+\tau_{ij})|^2$  of radiation measured by two separated detectors  $i$  and  $j$ . Here  $\xi_k(t) = \sum_{\mathbf{R}_k} \Psi_k(\mathbf{R}_k, t - t_{k0})$  are sums of pulse spherical waves  $\Psi_k(\mathbf{R}_k, t - t_{k0}) = F(t - t_{k0}) \exp(i\mathbf{k}\mathbf{R}_k) / R_k$  of quanta coming from a remote source, location  $\mathbf{r}_0$  of which is to be found. The pair correlation function  $K_{ij}(\tau_{ij})$  of intensities  $J_i(t)$  and  $J_j(t+\tau_{ij})$  for two spatially separated independent detectors, situated at  $\mathbf{r}_i = \mathbf{R}_i + \mathbf{r}_0$ ,  $\mathbf{r}_j = \mathbf{R}_j + \mathbf{r}_0$  and having the effectiveness  $\epsilon_i$  and  $\epsilon_j$  of the quantum detecting, equals



$$K_{ij}(\tau_{ij}) = \langle J_i(t) J_j(t + \tau_{ij}) \rangle - \langle J_i(t) \rangle \langle J_j(t + \tau_{ij}) \rangle$$

Here  $\tau_{ij} = (R_i - R_j)/c$  is the time-delay of measured intensities  $J_i(t)$  and  $J_j(t + \tau_{ij})$  in different detectors  $i$  and  $j$  from the same remote detected source of radiation.

For the studied case of quasi-stationary source of radiation and for the usual case of the random Gaussian process of quanta detecting  $\xi_k(t)$  the correlation function of intensity has the form

$$K_{ij}(\tau_{ij}) = \epsilon_i \epsilon_j \{ \langle \xi_i(t) \xi_i^*(t) \rangle \langle \xi_j(t + \tau_{ij}) \xi_j^*(t + \tau_{ij}) \rangle + \langle \xi_i(t) \xi_j(t + \tau_{ij}) \rangle \langle \xi_j^*(t + \tau_{ij}) \xi_i^*(t) \rangle - \langle \xi_i(t) \xi_i^*(t + \tau_{ij}) \rangle \langle \xi_j^*(t) \xi_j(t) \rangle - \langle J_i(t) \rangle \langle J_j(t + \tau_{ij}) \rangle = \langle n_i \rangle \langle n_j \rangle + \int_{-\infty}^{\infty} F(\omega)^2 \exp(-i\omega \tau_{ij}) d\omega \}^2$$

Here  $F(\omega) = \int_{-\infty}^{\infty} f(t) \exp(-i\omega t) dt$ ;  $|F(\omega)|^2$  is the spectral intensity (having the spectral half-width  $\delta\omega$ ) of the single detected quantum after detector;  $\Delta\omega$  - the spectral band of the intensity correlator (signal acquisition and processing system);  $\langle n_i \rangle$  and  $\langle n_j \rangle$  are the averaged quantity of detected quanta in the detectors  $i$  and  $j$ . For the usual case  $\Delta\omega \ll \delta\omega$  we have  $K_{ij}(\tau_{ij}) \approx 4 \langle n_i \rangle \langle n_j \rangle |F(0)|^2 \sin^2(\Delta\omega \tau_{ij}) / \tau_{ij}^2$ . The maximum value of equals  $K_{ij}(0) = 4 \langle n_i \rangle \langle n_j \rangle |F(0)|^4 \Delta\omega^2$  and corresponds to the additional delay  $\Delta t_{ij} = -\tau_{ij}$  of the registered intensity signal  $J_i(t + \tau_{ij})$  from one of the detectors (i) or both detectors (i and j) introduced in the correlator.

For three-dimensional location of the remote source of VVV, X- or gamma-radiation it is necessary to use three or more spatially separated independent detectors, situated at  $\mathbf{r}_1, \mathbf{r}_2, \mathbf{r}_3, \dots$ , and three or more independent intensity correlators. For this case the position of the detected remote source  $\mathbf{r}_0 = \{x_0, y_0, z_0\}$  of X-radiation may be calculated using the system of equations  $[(x_i - x_0)^2 + (y_i - y_0)^2 + (z_i - z_0)^2]^{1/2} + c\Delta t_{ij} = [(x_j - x_0)^2 + (y_j - y_0)^2 + (z_j - z_0)^2]^{1/2}$ , for maximum values of correlation functions  $K_{ij}(0)$  for different pairs  $ij$  ( $i, j = 1, 2, 3, \dots$ ) of detectors.

**P68**

**The Scattering of Electromagnetic Waves by Rectangular-cell Double-periodic Magnetodielectric Layer**

*Yachin, V<sup>1</sup>; Ryazantseva, N<sup>1</sup>*

<sup>1</sup>*Institute of Radio Astronomy, Ukraine*

In the paper the vector problem of electromagnetic wave scattering by a double-periodic magnetodielectric layer is solved by a method based on the rigorous 3-D integro-differential equations. The Galerkin method is applied to reduce these equations to a set of second-order differential ones with constant coefficients in functionals.

Formulation of the problem is as follows: an arbitrarily polarized plane electromagnetic wave is incident at an arbitrary angle on the double-periodic infinite layer. The periods of the layer are divided onto M and N segments in the X and Y direction, respectively. Thus, the periodic cell of the structure consists of M\*N rectangular parallelepipeds placed closely together. Each of parallelepipeds are characterized by the arbitrary complex relative permittivity and permeability and the layer has the thickness h. We have to obtain the transmitted and reflected fields in the immediate vicinity of the layer.

The functionals for the field of each parallelepiped in the periodic cell can be expressed through the field functionals of one certain parallelepiped and the problem under consideration reduces to the problem already been solved for a magnetodielectric double-periodic grating (Yachin Ryazantseva, *Microwave Opt. Technology Lett.* 5, 177-183, 1999).

For some particular layers the calculated transmission and reflection coefficients are presented. The validity of the method was confirmed by comparing our results with the published results.

In microwave engineering the periodic magnetodielectric structures have application to tunable selective filters, polarizers, electromagnetic absorbers, various types of shields as well as to laser accelerators etc.

**P72**

**An Interaction of Electromagnetic Field with a Collapsing Plasma Layer**

*Yemelyanov, K<sup>1</sup>; Nerukh, A<sup>2</sup>*

<sup>1</sup>*Kharkov National University, Ukraine;* <sup>2</sup>*Kharkov Technical University of Radio Electronics, Ukraine*

It is known that temporal variations in medium parameters cause alterations in the frequency and amplitude of the electromagnetic wave propagating in the medium. The wave reflection from a moving boundary of the medium results in the same effect. These effects can be used for a generation of high power microwaves and ultra wide band pulses. The purpose of the paper is to consider the interaction of an electromagnetic wave with a flat plasma layer whose boundaries starting from a zero moment of time move one to another so that after a certain temporal interval the collapse of the layer takes place.

The problem is formulated in terms of the Volterra integral equation of the second kind and its solution is found by the resolvent method. The resolvent operators for both the steady layer and the layer with collapsing boundaries are obtained. The resolvent obtained allows to consider the transformation of an arbitrary initial electromagnetic field.

It has been shown that because of the motion of the plasma layer boundaries, such a relation between the parameters, which enables the energy accumulation is possible. This process is accompanied by the excitation of packets of electromagnetic pulses outside the layer. The duration of pulses decreases to zero with the approaching to the moment of the layer collapse. The frequency of the electromagnetic field within the pulse infinitely increases. The field energy in the pulse also increases unlimitedly in the approximation of an infinitely powerful mechanism for the rapprochement of the boundaries. The same phenomena is also in a resonator with moving wall.

**P71**

**Electrodynamic Properties of Gradient Conducting and Semiconducting Media**

*Bashkuev, Y<sup>1</sup>; Gantimurov, A<sup>1</sup>; Angarkhaeva, L<sup>1</sup>*

<sup>1</sup>*Buryat Scientific Center of Siberian, Russia*

In the report the results of an investigation of the gradient conducting and semiconducting media are considered. They may be useful in synthesis of media with determined electrodynamic characteristics (reflection coefficient, transmission coefficient, surface impedance and so on).

In the report is shown that determined electrodynamic characteristics of conducting and semiconducting media may be synthesized in the class of gradient media (in particular, on the basis of Rayleigh solution), in which conductivity and dielectric permeability vary in inverse proportion to the square of the distance from air-conductive medium interface. The media with constant and real impedance in the wide frequency range are proposed.

The relationships between dielectric permeability and conductivity corresponding to constant real impedance are established. It is shown that the electric-field component in the medium damps out very weakly with depth (A.G. Gantimurov Yu.B. Bashkuev, *Journal of Communications Technology and Electronics* V.39, N 7, 1057-1060, 1994). The impedance of the medium becomes purely real and constant and medium is without frequency dispersion in the wide frequency range. This property is important, in particular, when transmitting a noise-similar signals in information transmission digital systems.

Thus in the report the generalization of Rayleigh solution to the cases of conducting and semiconducting media on the semi-infinite interval and for three-layer medium is made (Yu.B. Bashkuev, A.G. Gantimurov L.Kh. Angarkhaeva, *Journal of Communications Technology and Electronics* V.39, N 7, 1060-1065, 1994).

The equation for magneto-inhomogeneous medium allowing analytic Rayleigh solution is obtained.

The results of the work can be used in acoustics, optics, heat-physics by virtue of identity of equations.

**P73**

**Boundary and Transport Operators in the Space of Signal's Evolutionary Basis. TD Analogue of Generalized Scattering Matrix Technique.**

*Yashina, N<sup>1</sup>; Sirenko, Y<sup>1</sup>*

<sup>1</sup>*Institute of Radiophysics Electronics of NAS, Ukraine*

The analogue of scattering matrix technique developed for the wave scattering problems in TD is the subject of the presentation. This technique makes possible the creation of electromagnetic system (software) for design of complicated electromagnetic structures build of waveguide and grating units accordingly to the requirements to real antenna and pulse radar systems.

The modification of scattering matrix method for TD heavily relies on the accurate, efficient and reliable solution of initial boundary value problems of wave scattering by certain generic structures. Generic structures are those type of waveguide or grating units, that can not be decomposed into the more simple configurations and that are free of resonant features.

Every of the generic structures is described by its own transform operators, valid in the space of evolutionary basis of signals and resulting from the solution of the canonic initial boundary value problems (see Yu.K. Sirenko and N.P. Yashina. "Accurate solution of canonic initial boundary value problems for the theory of open periodic and waveguide resonators." Submitted to the section 44 "New Canonical Problems Benchmark Solutions").

These operators describe completely the scattering properties of the generic structures. Introduction in the explicit or accurate numerical form of transport operators in regular regions, that serve as an interaction domain between generic structures' scattered fields, accomplishes the procedure of receiving the operators, necessary for assembling compound structures, made of generic ones as building blocks. This assembling results in the necessity to solve a system of matrix equations of the second kind respectively unknown vector-functions, forming the transform operators of compound structure. Characteristic feature of original hyperbolic boundary value problems is the finite velocity of field perturbation propagation. This feature allows to avoid the inversion of matrix operator while solving the resulting matrix equation and, increasing the efficiency of final algorithm, makes possible to reduce the problem to the direct schema: straightforward moving along "time layers".

## P75

### Transformation of Plane Monochromatic Wave with Pulse-Periodic Modulation in Unbounded Medium.

*Slipchenko, N.P.; Rybin, O.N.*

*<sup>1</sup>Kharkov State Technical University, Ukraine*

The exact solution of the plane monochromatic electromagnetic wave conversion with the time-finite identical sequences of rectangular periodic pulses of permittivity and conductivity of the unbounded region has been obtained. These sequences have random periods, porosities and amplitudes of pulses. In this case the sequence of conductivity pulses lags behind the permittivity pulses sequence in time by a random shift. The solution of this problem is performed using the integral equations method according to which the interaction of the electromagnetic field with the non-stationary medium is described with Volterra integral second order equation solved in this work by means of resolvent.

The performed numerical-analytical analysis of the obtained solution has shown that the transformed field at any point on the positive time semiaxis represents the sum of the direct and backward monochromatic waves, whose absolute value of the wave numbers coincides with the absolute value of the wave number of the primary wave and the amplitudes and frequencies are step functions of time. Moreover, the direct wave amplitude in absolute value exceeds, as a rule, the background wave amplitude on the time intervals, where the medium parameters have the initial values. The numerical investigations have also shown that the amplitude of the formed waves can exceed in absolute value the primary wave amplitude with some values of the medium parameters and the primary wave frequency on these time intervals. As this takes place, the given superiority can be reached both at the expense of the permittivity variation and the conductivity variation in the passive media for narrow perturbation pulses.

## P77

### New Approach in Construction of the Electromagnetic Field Theory

*Virchenko, V.; Vadim, D.*

*<sup>1</sup>Usikov Institute for radiophysics Electronics, Ukraine*

In the construction of the theory of an electromagnetic field the new approach with use of algebra of quaternions and theory of analytical functions is applied. In comparison with a vector algebra  $V_3$  of dimensionality  $n=3$  the quaternion algebra has the advantage that it is a division algebra. It has allowed to construct the theory of the analysis of functions quaternion variable and to prove the basic theorem of the analysis, according to which the complete analysis of any analytical function is possible only in fields of real, complex numbers and skew field of quaternions above a field of real numbers. As the complete analysis of any analytical function we term a mutually reversibility of operations of derivation and integration of function, if accordingly derivative and integral of this function exist.

In outcome we have received the equations of an electromagnetic field by the analysis of functions quaternion variable [1]. The system of the obtained equations is much wider than a set of the Maxwell's equations and contains a series of new magnitudes and constants. In particular obtained set of equations contains the equations for an irrotational electric field connected a vectorial potential with a scalar potential describing this field. These equations contain constants. The constant  $b$  characterizes a density of forces of a tension of a vector, which is required for a variation of a potential in time. The constant  $h$  connects an electric field strength and velocity of a variation of a potential in time.

We have termed constants as constants of an electric field displacement. The Maxwell's theory does not contain constants and their values are nondeducible in this theory. The problem of radiation of a monopole oscillating electrical charge is decided and it is shown that such source radiates a longitudinal spherical electrical wave. Thus the longitudinal electrical wave is present at any electrodynamic system containing electrical charges varying in time. In particular, it is shown that the dipole radiates a pure longitudinal electrical wave

## P76

### Axial Symmetric Electromagnetic Field in a Plate Waveguide Filled by a Time-Varying Plasma

*Nerukh, A.; Sakhnenko, N.; Scherbatko, P.*

*<sup>1</sup>Kharkov Technical University of Radio Electronics, Ukraine*

The problem of an excitation and propagation of electromagnetic waves in a plane waveguide filled by a homogeneous cold time-varying plasma is considered. An initial electromagnetic field is created by an arbitrary axial symmetric source that can begin work before time changing of a plasma as well as after it. The plasma is characterised by the time dependent plasma frequency and begins to change by jump at zero moment of time.

The problem is described by a four-dimensional integral Volterra equation of the second kind. The solution to this integral equation is constructed by the resolvent method. The axial symmetric distribution of an electromagnetic field is considered. To obtain the resolvent in this case the polar coordinate system is used. By virtue of Fourier expansions with respect to the lateral coordinate and the axial angle and Hankel transformation with respect to the polar radius a system of one-dimensional integral equations with respect to the time variable is obtained for coefficients of the field expansion. Though these equations connect the coefficients with different subscripts it is succeeded in finding such combinations of these coefficients that are indifferent to the index of the expansion. That allows to obtain an exact and explicit expression for the resolvent of the integral equation and consequently for the solutions for the integral equation.

The transformation of an electromagnetic radiation of an axial source in the plane waveguide caused by a time variation of plasma frequency is considered by virtue of the obtained resolvent. The expression for the field shows that a transformed field consists of two time dependent parts the first of which is determined by a plasma characteristic and the second one is determined by mixed characteristics of a plasma and a waveguide. The obtained expression allows to consider a transformation of an initial electromagnetic field generated by a source with an arbitrary time dependence. These expressions are convenient especially for consideration of pulse sources.

in a direction of the axis. We guess that quantum properties of the electromagnetic fields become apparent on the frequencies higher Hz and structure of a quantized electromagnetic field is determined by some source of a field as the distributed dipole moment. Thus the charge of the quantum field source is a fundamental constant of the nature, where  $h$  is the Planck's constant,  $\epsilon$  is a dielectric constant,  $l$  is a light velocity.

1. V. L. Virchenko and V. N. Derkach. *Int. J. Infrared and Millimeter Waves* 20, 1327(1999).

## P78

### Accurate Solution of Canonic Initial Boundary Value Problems in the Theory of Open Periodic and Waveguide Resonators.

*Yashina, N<sup>1</sup>; Sirenko, Y<sup>1</sup>*

<sup>1</sup>*Institute of Radiophysics Electronics of NAS, Ukraine*

The accurate (sometime explicit) solutions of canonic problems in time domain electro-magnetic theory are of special interest and importance. Their existence makes proper methodological background for development of numerical and heuristic methods, for estimation limits of validity for various approximate approaches. Finally, their existence provides us with upper limits of the possible insights while investigation the electromagnetic features of simple canonic model problems that might be expected and then extended for complicated problems of applied importance.

In this paper we present the solutions of initial boundary problems for such canonic structures as bifurcation of circular waveguide, infinitely thin iris in circular waveguides and infinitely thin stripe gratings.

For all problems the analogue of FD mode matching technique is developed for TD. In this case the transient field is presented in form of the expansion over evolutionary basis and transverse eigen basis functions of corresponding structure. Such field's representation being subjected to boundary conditions with relevant initial conditions provides the analogue of mode matching method in TD. Applying this technique we arrive to the matrix equation of the first kind (for the waveguide bifurcation and grating of infinitely thin semi planes) or of the second kind (for infinitely thin irises). The implementation of the idea of semi inversion for the convolution type matrix operators in the matrix equation of the first kind (that is the version of analytical regularization technique) reduces the problems to the solving in general case the Fredholm equation of the second kind with all following advantages in accuracy and convergence. Moreover for special cases like iris and bifurcation, considered herein, the direct schema (straightforward time layers moving) can be applied clearly for solving the operator equations of the second kind.

Solutions of the canonic problems considered, had been thoroughly tested analytically and numerically. Such tests included the transform of TD results into FD and further comparison with known accurate rigorous solution obtained in FD for such canonic problems.

## P79

### Mutual Coupling of the Wave-Oscillation Eigenfields and Local Evolution Equations

*Yatsik, V<sup>1</sup>*

<sup>1</sup>*Usikov Institute for Radiophysics and Electronics, Ukraine*

For a laterally inhomogeneous dielectric layer, the dispersion equations and laws of the irregular dynamics of the spectra near the Morse critical point (MCP) are reported. This knowledge permits the square-law representation and furnishes the local equations of the time-space evolution of the wave-oscillation fields. The findings give insight into nonlinear evolution processes, they may be useful in diagnosis problems, wave propagation in a layered dielectric waveguide, linear and nonlinear dielectrics, semiconductor superlattice, in the design of transmission lines of communication systems.

The dispersion laws (spectral characteristics) considering the MCP are developed from the rigorous solution of the elementary homogeneous boundary value problem of a laterally inhomogeneous dielectric layer. The knowledge of the anomalies of the spectra near the MCP, feasibility of their analytical treatment by the both direct numerical analytical method and alternative approach based on experimental results, and dispersion equations of the free oscillations provide the basis on which the local equations of the space-time evolution of the layer field are furnished near the MCP of irregular dispersion.

The solution results of this problem in conjunction with alternative approach to the MCP search and the obtained square-law representation of the irregular behaviour of the dispersion curves in the MCP vicinity with characteristic features of the irregular dynamics of the spectra have formed the basis for the derivation of one-dimensional dispersion equations of eigenoscillations and two-dimensional dispersion equations of wave-oscillation fields. On this basis, the local (near the MCP) evolution equations of a laterally inhomogeneous dielectric layer have been deduced.

The obtained evolution equations of wave-oscillation fields and eigenoscillations conditioned by the dispersion features of the corresponding fields in their "mutual coupling" demonstrate a new mathematical apparatus giving insight into the evolution processes of the field pulses (signals) at the layer interface and evolution of the initial spatial distributions of the disturbances. Referred to the Kowalewska-type equations, they are particularly appropriate for the processes with a finite propagation velocity. With the knowledge of the layer eigenfields, the initial boundary value problem of the processes presented by these equations can be reduced to the Cauchy-Kowalewska problem describing the evolution of amplitude characteristics of the corresponding electromagnetic fields of the laterally inhomogeneous dielectric layer in the area of the irregular behaviour (near the MCP) of their phase components.

## P80

### Explosives' Detection Based on UHF Radio-Waves Spectroscopy

*Kuznetsov, A<sup>1</sup>*

<sup>1</sup>*Applied Physics Laboratory, Russia*

There exist techniques that employ radio waves and radio-spectroscopy for structural analysis of substances, qualitative and quantitative analysis of complex compounds and mixtures. To identify explosives, we propose to carry out the analysis of electromagnetic waves (EMW) spectra in the ultra-high frequency (UHF) region (2-60 GHz).

To allow explosive's identification in presence of organic-rich consumer goods by employing radio-spectroscopy, the selective absorption and characteristic EMW spectral bands and narrow lines which are "footprints" of explosive materials (characteristic of the molecules of the explosive substances) will be determined. Characteristic absorption lines and bands in UHF range exist due to the following effects: oscillation and rotation spectra of complex molecules; specific intermolecular interaction; Seemann split of electron and nuclear levels in the internal molecular magnetic field.

In the framework of ISTC Project 1050 "Development of Methods and Building a Mobile Device for Explosives Detection", it was proposed to develop a new method of reliable explosive's identification in presence of consumer goods and other materials by using selective absorption of EMW radiation in UHF range and secondary characteristic emission in UHF range, induced by EM waves or a flux of ionizing particles. This method promises to be very informative: in this range the number of the resolved lines exceeds 100000. The method also has low sensitivity threshold and, unlike nuclear-based methods, it is sensitive to molecular structure and intermolecular interaction. The secondary characteristic radiation is governed by different set of selection rules and can also be used for explosives identification. This radiation can be induced by electromagnetic waves (analogue in optical range - Raman scattering), or by ionizing radiation.

First experimental results of studying absorption lines and bands in UHF range (3.5-8.5 and 26-38 GHz) by irradiation of various consumer goods (cotton, nylon, leather, ham, rice) and the materials with the same granularity (rice, sugar, ammonium nitrate NH<sub>4</sub>NO<sub>3</sub>) will be presented.

## P82

### A Geo-Radar for Detection, Control and Diagnostics of Subsurface Objects

*Stoukatch, O V<sup>1</sup>; Lukjanov, S P<sup>1</sup>; Semenchuk, V E<sup>1</sup>; Karaush, A S<sup>1</sup>;*

*Zagoskin, V V<sup>1</sup>; Potemin, R V<sup>1</sup>*

<sup>1</sup>*TUCSR, Russia*

During the last years new scientific and engineering trend as remote sensing of objects and media with electromagnetic short-pulses has been forming in radioelectronics. This technique is based on analysis of the investigated medium response caused by probing pulse with wide spectrum. The pulse impact leads to exciting all possible eigen-modes of the object or medium that allows to significantly increase information content of the diagnostics. In this connection, engineering systems for diagnostics and control of subsurface objects have become qualitatively new class of searching-prospecting equipment.

The georadar methods are based on analysis of subsurface object response caused by ultra-wideband (UWB) electromagnetic radiation. The width of used signals spectra equals to hundreds of MHz (or more), therefore the UWB-signal impact leads to excitation of all possible modes of investigated object. It essentially increases informative ability of radar diagnostics of disturbances in media.

Theoretical and experimental investigations in the field of subsurface radar systems designing, which were carried out in Siberian Physical and Technical Institute and Tomsk University of Control Systems and Radioelectronics during last years, have shown good prospects of sub-nanosecond radar methods for searching, detection and recognition of small-sized, low-contrast dielectric inhomogeneities in subsurface media.

High information content of the radiophysical methods of investigations has lead to their intensive use for solution of a wide range of fundamental and applied problems. Once an engineering possibility to radiate high-amplitude UWB-signals has been acquired, the radiophysical probing of semi-conducting media has become one of the efficient methods of investigation of natural processes in different media and objects.

To date, sufficient theoretical and practical experience for designing both individual functional units, and transmitting-receiving devices of georadar systems has been accumulated. Principles of designing antennas, video-pulse generators were studied, receiving and processing designs of reflected signals were approved. Alternates of logarithmic amplifiers and digital processing units were designed and manufactured.

An mock-up of the georadar system including dual-channel antenna, dual-channel stroboscopic receiver, synchronizer and microprocessor unit for data processing has been designed. The most of units are original ones. There is a significant theoretical and practical margin regarding the UWB subsurface radar systems.

The further investigations direction will be connected with complex studies of the influence which is rendered by the permittivity and conductivity of such complex composition and structure media as rocks, grounds and soils, building materials, on the characteristics of geo-radar system as an engineering tool for prospecting subsurface objects and media of interest. It is expected that the developed investigations will ensure a high efficiency of subsurface objects prospecting by geo-radar. The system being developed for diagnostics of subsurface media will allow to improve the efficiency of resolution, detection and identification (due to increasing the informative ability) of small-sized and low-contrast objects (with dimensions of order 7-30 cm) at several (2-5 m) meters depth under surface.

## P81

### The Landmines Identification by Nuclear Quadrupole Resonance (NQR)

*Mozjoukhine, G<sup>1</sup>*

<sup>1</sup>*Kaliningrad State University, Russia*

The main problems in remote NQR for landmines detection are: ii) a small ratio a signal to noise; ii) the difficulties of creation of the homogenous magnetic field in the sample space; iii) the complicate structure of NQR 14N lines in low frequency band (5 Mhz). Although, NQR spectra is more simpler than spectra of NMR (nuclear magnetic resonance), there exists the problem of identification of chemical compounds. The one of the main features of any substance is full spectrum of NQR. The using two-frequency method is possible for the identification of type of explosive. The two-frequency (NQR) method consists of two-frequencies excitation of NQR of spin system. (V.S.Grechishkin, N.Ya.Sinyavski. *Uspehi Fiz.Nauk*(Russia), v.163, 10, 95-119,1993.)

For resonance of 14N nuclei in explosives is possible to use two- and three-frequency excitation. The main substance in landmines are hexahydro-1,3,5-trinitro-s-triazine C<sub>3</sub>H<sub>6</sub>N<sub>6</sub>O<sub>6</sub> (RDX) (S.M.Klainer, T.B.Hirschfeld, R.A.Marino. *Fourier Transform in Chemistry*. Fourier, Hadamard and Hilbert Transform in Chemistry. N.-Y.:Plenum,1982.-p.147-181) and trinitrotoluene C<sub>7</sub>H<sub>5</sub>N<sub>3</sub>O<sub>6</sub> (TNT) (R.A.Marino, R.F.Connors. *J.Mol.Structure*, 111, 323-328, 1983). Often the mixture of these substances is using for landmines. In the case of landmines with high percentage of RDX there are nine lines of frequency spectrum in range of 1.7 MHz to 5.24 MHz. The lines resolution is high. For detection it is used the transition with frequency 5.2 MHz or 3.4 MHz. Although the presence of masking effects of the influence of piezo-electric resonance ringing and transition ringing processes in equipment decrease a assurance of landmines detection by NQR. Usually the multiple pulse NQR sequences is using for detect

ion of signal. The echo is essential component of the NQR signal. Two frequency experiments in RDX allow observe successfully only the so-called "lock effect", it is the effect of reducing intensity of spin-echo signal on the frequency n+ within the influence of pulse excitation on nearby transition with the frequency n-. This effect is result of spin coherency break under the influence on adjacent transition. The offset frequency dependence of echo signal is investigated for this method.

The NQR spectrum of TNT has 24 lines in range of 730 kHz to 895 kHz. The frequency resolution is low. The industry samples of TNT has a big intrinsic piezo-resonances in this range. To avoid the piezo-electric ringing of sample and to identify signal it is possible use multiple frequency NQR too. The coherency transfer in two frequency method allows to get signal on third frequency in 14N nuclei system. The behaviour of this signal with frequency offset is analysing, too.

## P83

**Selective Properties of Planar Bragg Reflectors with Various 2-D Surface Corrugations**

*Arzhannikov, A V<sup>1</sup>; Kalinin, P V<sup>1</sup>; Kuznetsov, A S<sup>1</sup>; Sinitsky, S L<sup>1</sup>; Stepanov, V D<sup>1</sup>; Ginzburg, N S<sup>2</sup>; Peskov, N Yu<sup>2</sup>; Sergeev, A S<sup>2</sup>; Diankov, E V<sup>3</sup>; Petrov, P V<sup>3</sup>*

*<sup>1</sup>Budker Institute of Nuclear Physics, Russia; <sup>2</sup>Institute of Applied Physics, Russia; <sup>3</sup>RENC-VNIITF, Russia*

In order to generate 4-mm radiation in a narrow spectral band at the ELMI-device (BINP, Novosibirsk) a planar resonator consisting of a regular wave-guide and two selective reflectors is used. Such a reflector is composed of two parallel Bragg gratings, which are manufactured of a copper plate with a small corrugation on its surface. We will describe our studies on selective properties of such reflectors with various types of surface corrugation. Reflectivities of them were measured in a wide bandwidth on a special testing bench. Different computer simulations were used to obtain the structure of electromagnetic waves and the radiation modes composition between the gratings of reflectors. It was turned out that mode transformation on a thread of the gratings had influence on a width of the spectral interval of the reflected radiation and on a modes ratio in this interval. Experimental investigations confirmed this fact. As a main result of these studies we ascertained the basic principles of radiation modes forming in the reflectors with different types and parameters of the gratings thread. Using this principles we have designed 2-D gratings with chessboard and round-holes corrugations which will allow us to obtain the most effective 2-D distributed feedback for the further development of the experiment.



**Euro Electromagnetics**  
30 May - 2 June 2000, Edinburgh

# **Plenary Sessions**



## PL3

### Development of Wavelength-Resolution Synthetic Aperture Radar in the Metric Radio-Band: A New Tool for Remote Sensing

*Ulander, Lars M H<sup>1</sup>*

<sup>1</sup>Swedish Defence Research Establishment (FOA), Sweden

During the last two decades a new class of synthetic-aperture radar (SAR) systems have been developed operating at frequencies below 100 MHz. The foremost example of such a system is the CARABAS VHF-band SAR developed and operated by the Swedish Defence Research Establishment (FOA). The driving force has been their obvious military application but a number of key civilian application have also been proven. In this paper, we will address some of the basic design considerations and challenges which have been solved to make this into a new tool available for the remote sensing and business community to exploit, as well as to show illustrative examples.

The CARABAS SAR have been developed to approach the fundamental resolution limit which at the same time reduces the deleterious speckle effect. Hence both the bandwidth and beamwidth are pushed to their limits of what is possible, ie a relative bandwidth of 1 and a beamwidth of 180 degrees. Subsequent processing of the imagery reveal image details down to a resolution of about a quarter of the centre wavelength. The CARABAS spatial resolution is typically measured to 2.5m as compared with its theoretical value of 2 m. Incomplete calibration of the antenna response is the single most important contributor to the phase errors responsible for not reaching the theoretical resolution.

The CARABAS images have a quite different appearance compared with microwave SAR images with similar resolution, ie bandwidth. The reason is that the electromagnetic wavelength is about 10-100 times larger than conventional microwave systems, and only meter-scale structures and larger contribute to the image. For example, a grass field or an agricultural field have a very low backscatter response since their surface roughness is much smaller than the wavelength. Dominating image structures are instead man-made objects, eg vehicles, houses, telephone and power cables, and fences. The backscatter from natural terrain is dominated by forested areas as well as topographic features in rugged terrain.

It has been shown that the forest response in CARABAS images can be accurately related to forest stem volume (m<sup>3</sup>/ha). Stem volume is defined as the volume of the tree trunks including bark but excluding branches and stumps per unit area. The trunks act like Rayleigh scatterers in the CARABAS band since both the diameter-to-wavelength as well as diameter-to-length ratio is small. This implies that the image amplitude response is proportional to trunk volume and independent of the exact shape of the trunk. The image response is produced by the dihedral corner formed by between the ground and trunk when the ground is horizontal. The mechanism becomes more complicated when the ground surface is sloping which results in a strong aspect angle dependency. The response is periodic in aspect angle similar to the backscatter from the ocean surface. A complete knowledge of the aspect angle dependency is expected to give information on topography besides the stem volume.

A canopy layer is essentially transparent to the CARABAS frequencies and the attenuation is typically measured to be less than 3 dB. In combination with the low backscatter response from the forest, the net result is that the image response to forest stem volume is linear even for very dense forest. This enables stem volume retrieval with an accuracy of about 10%. The point of saturation, ie loss of sensitivity, is probably somewhere between 500-1000 m<sup>3</sup>/ha although no measurements above 400 m<sup>3</sup>/ha have yet been performed. Also, the results have been obtained in rather homogeneous forest typical of Scandinavia and there is need to verify the capability over mixed forests.

These excellent results is expected to open up opportunities for both environmental monitoring as well as commercial forest inventory and management.

## PL4

### Microwave Solutions: the Ultimate High-intensity Ultrafast Pulse

*Arnold, J M<sup>1</sup>*

<sup>1</sup>University of Glasgow, UK

In the search for the ultimate high-intensity electromagnetic pulse with spectral content over a wide range of frequencies, two fundamental physical constraints are always encountered: high intensity eventually drives nonlinearities in the media in which the electromagnetic wave propagates, and dispersion eventually limits the rise time of the pulse.

It is possible under certain circumstances to engineer the propagation environment so that these two limiting mechanisms actually cooperate with each other in sustaining a self-stabilising pulse which does not suffer dispersion spreading, but maintains its temporal shape intact over long propagation distances. The circumstances under which this happens, leading to a so-called "solitary wave", have long been understood, and such phenomena were first observed in a natural environment by the Scottish marine engineer John Scott Russell in 1834 while riding a horse alongside the Union Canal near Edinburgh, in a celebrated piece of scientific folklore. It was realised in the late 1960s that the solitary wave was a manifestation of a universal physical phenomenon that can occur in a large variety of wave types, including electromagnetic waves. Also it became understood that there exist particularly robust forms of solitary waves, generally called solitons. Now many natural phenomena are understood in terms of a solitary wave, including some quite spectacular ones such as the Great Red Spot of Jupiter, large-scale ocean drift waves, Alfvén waves in plasma and charge transfer processes in polymer chains. It is a particular curiosity that the names of many Scottish scientists are connected with fundamental discoveries in this area, including Russell, Kerr, Maxwell, Kelvin and others.

In recent years a determined effort has been made by many scientists to actually engineer the appearance and properties of solitary waves in fabricated environments such as electromagnetic waveguides. This effort has been most successful in the field of optics, where picosecond solitons in optical fibres have been propagated over enormous distances at very modest power. Far less work has been done to reproduce soliton behaviour experimentally in the microwave. Achievement of this objective in the microwave or millimetre-wave domain would greatly enhance the performance of systems relying on the transmission of high-intensity ultrafast pulses, since it would become possible to convey them over significant distances without experiencing the deleterious effects referred to earlier.

In this talk the potential of microwave solitons will be addressed, along with structures which can be engineered to support them.

## PL5

### Ultra-Wideband Antennas

*Farr, E.G.<sup>1</sup>*

<sup>1</sup>*Farr Research Inc, USA*

We consider here a selection of Ultra-Wideband (UWB) antennas that are currently available. We consider both the older designs, such as TEM horns and log periodic designs, as well as the newer designs with focused apertures, referred to as Impulse Radiating Antennas (IRAs). These newer designs include full IRAs, half IRAs, lens IRAs, solid dielectric lens IRAs, and IRAs with feed point lenses. We also discuss the sensors that are used to detect the signals radiated by these antennas. We provide tradeoffs of the various antennas, concerning such issues as gain, bandwidth, dispersion, weight, cost, and voltage breakdown.

UWB antennas can be used in a number of applications that lie outside the area of RF effects. One area is broadband communications, which may be either in the frequency or time domain. Another area is mine detection, which can take advantage of the symmetries of manmade targets to discriminate between manmade objects and clutter. Yet another area is space-based applications, in which a single antenna may be needed to serve multiple missions on many different frequency bands.

A number of new technologies have recently been demonstrated that will affect UWB antenna design. Enhanced versions of standard reflector IRAs are now available that can withstand mechanical shock and vibration. An IRA is also available with a collapsible design. IRAs with multiple polarizations and multiple channels have now been demonstrated. UWB waveguide bends have now been demonstrated that can withstand very high voltages, with low dispersion. Finally, the emergence of time domain antenna ranges promises to reduce significantly the cost of making antenna patterns, when compared to frequency domain ranges.

Looking forward, we can see a number of problems will be addressed within the next few years. New variations of reflector IRAs have been proposed that will address existing limitations on gain, polarization purity, high-end bandwidth, sidelobe level, and mechanical durability. Time domain antenna ranges will continue to develop and will provide an economical alternative to frequency domain ranges. Finally, there is a consensus emerging on definitions of standard terms that can be used to describe this class of antenna.

## PL6

### Future Directions in Ultra-Wideband Electromagnetic Modeling and Signal Processing

*Carin, L.<sup>1</sup>*

<sup>1</sup>*Duke University, USA*

This talk will review recent developments and future directions for UWB electromagnetics, with a focus on modeling and signal processing issues. Concerning the former, we will discuss developments in both time- and frequency-domain modeling, with discussions of their relative merits. Models to be addressed include finite difference time domain (FDTD), multi-resolution time domain (MRTD), method of moments (MoM), and the multi-level fast multipole algorithm (MLFMA). We will also demonstrate how fundamental electromagnetic modeling can be transferred to state-of-the-art signal processing. In this context, significant attention will be directed toward the general use of hidden Markov models (HMMs) in target classification. A broad range of applications will be discussed, including the use of UWB electromagnetics for ground-penetration (land mines and unexploded ordnance) and foliage penetrating (sensing vehicles in foliage) radar sensors.



**Euro Electromagnetics**  
30 May - 2 June 2000, Edinburgh

# **Author's Index**

# Author's Index

Name	Abstract	Page No.		
Abramson, E	53.2	73	Camp, M	18.2
Abubakirov, E+	68.2	91	Cangelaris, A C+	37.4
Adballah, C T	1.1	5	Capozzoli, A	4.5
Adhami, R	71.5	94	Carin, L+	24.4, 39.2, 56.5, PL6
Agarin, N V	57.5	99	Carlsson, J	23.1
Agee, F J	7.1	12	Carlisten, B	1.3
Akduman, I+	26.5, 37.1	36, 52	Carroll, C E	23.2
Aksoy, S	7.2, 17.2	13, 24	Carroll, TL+	62.1
Al-Asadi, M+	19.4	27	Carter, D+	29.4
Alexeev, V	P50	115	Carter, L+	65.4
Aillsopp, D	46.4	65	Carter, N+	31.1
Alp Azizoglu, S+	21.3	29	Carter, R J+	8.5
Altman, Z	7.5, 49.2	13, 68	Caryotakis, G	1.3
Amazeen, C+	46.5	65	Casey, Jeffrey	44.4
Anada, T+	19.1	26	Cattin, V+	51.3
Andreadis, T+	29.5, 62.5	40, 84	Cerri, G	53.3
Andrews, J R+	47.2	66	Chai, J C+	32.1
Andrieu, J	5.1, 59.2	10, 79	Chassay, G	39.3
Angarkhaeva, L	P71	120	Chen, C+	52.2
Apanasenko, A V	P22	109	Chen, X+	67.1
Arfin, B	1.3	5	Cheney, M+	22.1
Arnold, J M+	PL2, 55.3	126, 75	Cheong, H	9.2
Arter, W+	1.5	6	Cherepenin, V+	P3, P58
Arzhannikov, A+	57.5, P38, P83	99, 113, 124	Chernykh, E	P24
Astanin, L	61.2, 61.3	100, 82	Chew, W C+	14.1
Audhuy, M	2.1, 2.2	6	Chiarandini, S	53.3
Bacherikov, A	53.4	73	Chignell, R+	46.2
Backstrom, M	8.4	14	Christodoulou, C G	1.1
Badic, M+	50.4, P36	69, 113	Chuanming, Z	26.4
Baker, G H+	13.4	22	Cizmic, J	36.5
Banna, S+	52.5	72	Clark, T+	38.4
Baranowski, S+	41.1	57	Clemens, M	19.2
Barber, G D M+	7.3	13	Cloude, S	17.3, 34.1, 39.1, 46.3
Barrall, G	65.2	87	Coburn, W+	18.4, 45.1, 50.1
Bashkuev, Y+	P71	120	Collins, L+	66.2, 71.3
Batrakov, A V	6.5	95	Corre, Y	28.2
Baum, C E+	9.3, 13.1, 23.3, 24.2, 24.3, 32.4, 34.3, 34.4, 39.2, 44.3, 54.3, 50.5, 55.1, 59.4 63.4, 64.1	16, 21, 32, 33, 45, 47, 48, 55, 62, 69, 74, 75, 80, 86	Courtney, C	32.6
Beamish, D+	42.3	59	Cripp, G N	46.3, 59.5
Beason, Charles	58.3	79	Cross, A W	1.2, 52.3, 57.1, P29
Beillard, B	5.1, 59.2	10, 79	Cumming, T	38.4
Benford, G	6.4	12	Dabis, H	46.2
Benford, J+	6.4	12	Dagys, M+	7.1
Berry, M	18.4	26	Daniel, J-P+	30.4
Bertuol, S	23.4	32	Daniels, D+	46.1
Bigelow, W S+	22.5	31	Darznek, S A	P57
Biggs, A W	71.5	94	Dauchy, J W	56.3, 61.
Birbir, F	15.1	23	Davydov, A	P45
Bishay, S T+	37.2, 37.5	52, 53	Dawson, J F	31.4
Bishop, PK+	51.5	71	De Leo, R+	53.3
Blaise, G	2.3	6	De Pasquale, G	46.3
Blumel, Reinhold+	67.5	99	De, N C+	12.5
Bobylov, V B	57.5	99	Deans, J	65.4
Boerner, W+	34.1	47	D'Elia, G	4.5
Bogomolov, N	58.5	100	DeLuca, Clyde	56.2
Bohi, J	11.4, 12.1, 18.1, 35.3	19, 20, 25, 49	Demoulin, B	41.1
Boiko, P	68.5	92	Deng, Q	11.3, 43.1
Boling, R+	28.1	38	Denisenko, A	68.2
Bolomey, J Ch	7.5	13	Denisov, G G	52.3, P31
Bol'shakov, M A	58.1	99	Diankov, E V	P83
Bonan, D	26.4	36	Diankova, E V	57.5
Bondar, Yu F	P59	118	Dickson, D	29.4
Bondarenko, N+	P26, P28	110	Didenko, A+	6.1
Booker, S+	62.2, 62.3	83, 84	Djahli, F	P13, P14
Boryszenko, A	5.5, 26.1, 40.5	11, 35, 97	Dogaru, T	24.4
Boryszenko, O	5.5	11	Domarkiene, S	53.2
Boulay, F	23.4	32	Dong, Y	56.5
Bowen, L	26.2, 34.4, 47.1, 64.1	35, 48, 65, 86	Douglas, S	6.3
Bowers, J R+	61.1	82	Douglas, S C	25.3
Brasile, J P+	35.1, 35.2	48, 49	Drozd, A L+	23.2
Bratman, V	57.2, 62.2, 62.3, P9, P25, P30, P31	72, 78, 105, 110, 111	Dubrovin, E A	P62
Brennan, P	62.2, 62.3	83, 84	Dudin, S V	P7
Bretones, A R	43.3, 60.4, 60.5	61, 81, 82	Duffy, A	19.4, 63.5
Brewer, R	65.5	89	Duffos, E	71.2
Britting, A O	32.1	44	Duzdar, A+	5.2
Brooks, J+	71.5	94	Eastwood, J	1.4, 1.5, 6.3
Brouaye, F	7.5	13	Efanov, V	40.2, 44.2, P41
Bruschini, C+	51.3, 66.5	70, 90	Egorov, M	28.3
Brylevsky, V	54.1	98	Ehlen, T+	11.4, 12.1, 18.1, 35.3
Bucci, O M+	4.5	9	Elizondo, J	44.3
Buchenauer, J	47.4	66	Elliott, J R+	19.5
Bugaev, S P	58.1	99	Engheta, N+	9.4
Bulatov, M U	P21	108	Erinmez, A+	38.2
Bullcock, R	62.2, 62.3	83, 84	Evdokimov, E V	58.1
Bunger, R	27.3	37	Fabregas, X	39.5
Burch, I+	46.4	65	Fan, J	52.2
Burdakov, A V	57.5	99	Fanbao, M+	26.4
Burmasov, V S	57.5	99	Farafonov, O A	P40
Büyükkaksoy, A	15.1	23	Farr, E+	22.5, 26.2, 34.4, 44.3, 47.1, 64.1, PL4
Bzyta, V I	P40	114	Fazi, C	30.1, 63.3
Calahan, K	13.4	22	Fazio, M+	1.3
			Fedorov, V M	P54, P5
			Fedosova, N H	58.4
			Fedotov, A+	P30
			Felsen, L B+	9.1
				25
				52
				9
				33, 55, 77, 126
				31
				5
				31
				83
				40
				88
				42
				15
				5
				63
				70
				73
				44
				55
				71
				90
				29
				15
				104, 117
				109
				22
				73
				64
				5
				36
				51
				54
				27
				24, 47, 54, 65
				26, 63, 68
				89, 93
				38
				45
				65, 80
				5, 72, 77, 111
				54
				64
				12
				41
				64
				117
				77, 83
				115
				43
				73
				65
				21
				88
				9
				98
				57
				19, 60
				91
				72, 111
				124
				99
				40
				11
				106
				33
				73
				77
				12
				95
				31
				118
				104
				27, 86
				93
				10
				5, 6, 12
				57, 62, 114
				96
				19, 20, 25, 49
				62
				28
				16
				53
				99
				56
				71
				36
				114
				31, 35, 48, 62, 65, 86, 126
				40, 85
				5
				116
				100
				111
				15

# Author's Index

Fenical, G+	31.5	44	Israaelevich, P	53.2	73
Ferencz, C S+	22.2	30	Issac, F	23.4	32
Fischer, J	18.5	26	Ittel, J M	51.3	70
Flerov, A	54.2	98	Iudin, D I	15.2, 32.3	23, 44
Fliermans, C B+	51.4	70	Ivanenko, V G	57.5	99
Foley, J+	61.5	83	Ivanov, I E	57.3	78
Fontana, R+	10.2, 10.3	17	Ivanov, L N+	P39, P40, P62	113, 114, 118
Fortgang, C	1.3	5	Jaeger, D	18.3	25
Fortov, E	3.1, 8.3, P24, P61	7, 14 109, 118	Jancewicz, B	4.3	9
Fortov, V E	P6, P7, P55	104, 116	Jansen, F+	33.1	46
Fortuny, J	39.5	56	Jansson, L	8.4	14
Fourestié, B+	7.5, 49.2	13, 68	Jaroszynski, D A	57.1, P25	77, 110
Frantsuzov, A	54.2	98	Jecko, B	5.1, 59.2	10, 79
Frazier, S	29.2, 29.3, 29.4	39, 40	Jordan, David L	34.2	47
Friedhoff, H	18.2	25	Jousse, D	35.1	48
Friedrich, J	10.5	18	Jui-Pang, H	19.1	26
Frost, N	46.2	64	Juli, E+	9.2	15
Fujiwara, O+	41.4	58	Kalediene, R	53.2	73
Gabbay, U	53.2	73	Kálin, A	8.2, 37.3	14, 52
Galdetskiy, A+	57.4, 68.3, 68.5	99, 102, 92	Kalinin, P V	57.5	99
Gallais, F	5.1, 59.2	10, 79	Kalynov, Y K+	P9	105
Galstjan, E+	21.2, 40.4	28, 57	Kami, Yoshio+	41.5	58
Gandel, Y	P12	106	Kanaev, G G	P7	104
Gantimurov, A	P71	120	Kancleris, Z	7.1	12
Gao, P	66.2	89	Kappenman, J	38.1, 42.4	53, 60
Garanyishkin, N V	P35	112	Karacuha, E	7.2	13
Garbe, H+	41.2	58	Karakus, C+	26.5	36
Garcia, C+	65.5	89	Karaush, A S	P82	123
Gardiner, P	46.4	65	Kardo-Sysoev, A+	54.1, 54.2, 61.3	98, 82
Gardner, R L	3.2, 13.2, 13.3	7, 21	Karlik, K V	6.5	95
Gaudreau, Marcel P J+	44.4	63	Karlsson, T+	23.1	31
Gavrilov, S	17.1, 17.2	24	Karpowicz, J+	53.5, 58.2	74, 78
Gavrish, N N	P45	115	Karzas, W J+	3.4	8
Germanovitch, O P+	P48	115	Kashyap, S	65.3	88
Geronimo, R J	2.2	6	Kawakami, Y	36.4	51
Gilbert, J+	32.5, 42.2	45, 59	Kawaiko, S F	19.5	28
Giner, V	60.3	81	Kawasaki, F+	36.4	51
Ginzburg, N S	1.2, P29, P83	5, 111, 124	Kazanskyi, L	40.4	57
Gleisner, H+	42.1	59	Kehs, R A	25.5	35
Glen, S	64.1	86	Kempkes, Michael A	44.4	63
Goncharik, A O	58.1	99	Kerr, B	6.3, 25.3	12, 95
Goncharov, A N	P34	112	Kesler, M	30.5	41
Gonschorek, K H+	27.1, 27.2	36, 37	Khanna, S M	65.3	88
Gonzalez Garcia, S+	43.3	61	Khizhnyak, A N	55.5	76
Gooding-Williams, G+	17.3	24	Kiselev, V V	P34	112
Gorbachev, K	P24	109	Kitsanov, S A	6.2, 6.5	12, 95
Griffiths, H	39.3	55	Kiuttu, G	68.3	101
Grothus, M	29.4	40	Klimenko, V	P49	115
Grünfeld, Mr	31.2	42	Klimov, A I	6.2, 6.5, 58.1	12, 95, 99
Gryz, K	53.5, 58.2	74, 78	Knowles, T	6.4	12
Gu, J	49.3	68	Kohiberg, I	2.3, 8.5, 24.1, 63.3	6, 15, 32, 85
Gunin, A V	58.1	99	Kolchigin, N	28.3, 41.3	96, 97
Gurevich, A V	P21, P22, P59	108, 109, 118	Kolodny, Michael+	56.2	98
Haase, A	1.3	5	Kompa, G	5.2	10
Haase, H	8.1	14	Kondratiev, V M	P34, P35, P45	112, 115
Habiger, K	1.3	5	Kondratieva, A I+	P34, P45	112, 115
Hambrook, J L	53.1	72	Kone, L	41.1	57
Hannigan, AB+	30.2	41	Konoplev, I V V+	1.2	5
Harbour, M	6.3, 25.2	12, 95	Konovalev, I N	6.5	95
Harlacher, B L	18.5	26	Kornilova, A A	58.4	100
Harris, H	6.4	12	Korolev, A	68.5	92
Harrison, Michael+	29.1, 29.4	38, 40	Korovin, S D+	6.2, 6.5, 58.1	12, 95, 99
Hastedt, R+	31.2	42	Korovkin, N V	15.2, 32.3	23, 44
Hatfield, L L	2.4, 35.4	7, 49	Koshelev, V+	5.4, 26.3	10, 36
Hawkins, K	1.4, 6.3	5, 12	Kositsky, Joel	46.5	65
Hayakawa, H+	15.2	23	Kotchetov, S V	32.3	44
Hayakawa, M+	32.3	44	Kouprienko, V M+	32.2	96
He, W	1.2, 52.3, 57.1	5, 72, 77	Kovalenko, S A	P39, P62	113, 118
Heard, J	29.4	40	Kriklenko, A+	40.2, 44.2, P41	57, 62, 114
Hegeler, F	1.1	5	Kristiansen, M	2.4, 35.4	7, 49
Hemmert, D	2.4	7	Krivoshchev, S I+	P60	118
Henderson, M	29.4	40	Krokhalev, D I	P39, P62	113, 118
Hernández-López, M A	43.3	61	Krompholz, H+	2.4, 35.4	7, 49
Heyman, Ehud+	4.4, 21.1	9, 28	Kuanr, A V	2.5	7
Heynderickx, D+	33.3	46	Kuanr, B K+	2.5	7
Hibbs, A	65.2	87	Kudelya, A	17.	24
Hiraoka, T	19.1	26	Kurkan, I K	6.2	12
Hjelmstad, J+	56.4	77	Kurtovic, M	36.5	51
Hodge, K	19.4	27	Kutenkov, O P	6.2	12
Holden, S+	53.1	72	Kuznetsov, A S	57.5, P38, P80, P80	99, 113, 123, 124
Hongge, M	26.4	36	Lahart, M J	63.3	85
Hook, M+	1.4, 6.3	5, 12	Lassas, M	22.1	29
Huang, J S+	11.3, 43.1	19, 60	Latess, J	3.2, 13.2, 13.3	7, 21
Hui, N+	12.3	20	Lazarev, Y	P23	109
Huilong, Y	26.4	36	Le Goff, M	5.1, 59.2	10, 79
Hunter, R+	33.5	47	Leat, Christopher J	66.4	90
Huynh, J	51.2, 66.3	70, 89	Lebedev, E F	P54, P55	116
Ianoz, M	8.2, 63.2	14, 85	Lee, M-C :	65.4	88
Iezekiel, S	43.5	61	Lehr, J+	44.3, 50.5, 59.4	62, 69, 80
Imbs, Y+	5.1, 59.2	10, 79	Lemaire, J+	33.2	46
Immoriev, I I	10.1	17	Leontyev, A A	P6, P7	104
Inns, RH	53.1	72	Levitas, B	17.2	24
Isaacson, D	22.1	29	Lewis, Gareth D+	34.2	47
Ishida, H	36.4	51	Lger, J M	51.3	70
Islam, N E+	40.3	57	Libefo, L F	62.5	84

# Author's Index

Lighthart, L P	5.3	10	Parfenov, Yu	3.1, 8.3	7, 14
Lindell, Ismo+	4.3	9	Parkes, D M	25.3	95
Lindsay, CD	53.1	72	Parmantier, J P+	23.4	32
Lindsay, P A	67.1	90	Pashchenko, A	67.2	91
Lishchenko, A	5.5	11	Pavlovski, V F	P48	115
Litz, M+	25.5, 30.1, 45.1, 50.3	35, 40, 63, 69	Payment, T+	10.4	18
Liu, F	11.3, 43.1	19, 60	Pegel, I V	6.2, 6.5, 58.1	12, 95, 99
Liu, G	52.2	71	Pennock, S+	16.1, 16.2, 30.2	23, 24, 41
Lo Vetri, J	12.4	20	Perala, R A	19.5	28
Loborev, V+	3.1, 8.3	7, 14	Perevodchikov, V+	P10	105
Lomakin, V	21.1	28	Perov, A	34.5, P65	48, 119
Longstaff, I Dennis+	66.4	90	Perrin, S+	71.2	93
Lostanlen, Y+	28.2, 39.3	38, 55	Peskov, N Yu	1.2, P83	5, 124
Loubriel, G M	40.3	57	Petelin, M I+	19.3	95
Louie, A	65.3	88	Petrauskienė, J	53.2	73
LoVetri, J+	11.2	18	Petrov, N I+	P19, P20	108
Lövstrad, K G+	31.3	43	Petrov, N+	P17, P21, P22, P59	107, 108, 109, 118
Loza, O T+	57.3	78	Petrov, P V	57.5, P83	99, 124
Lu, A I-Y	65.4	88	Petrov, P+	P23	109
Lubell, J	11.5	19	Petrov, V	P61	118
Lucic, R+	36.5	51	Petrova, G N+	P19	108
Luhh, F+	44.1	62	Peyeri, P	10.5, 46.3	18, 65
Lui, F	43.1	60	Phelps, A D R	1.2, 52.3, 57.1, 57.2, P29	5, 72, 77, 78, 111
Luiken ter Haseborg, J	36.2	50	Phillipakis, M	46.1	64
Lukjanov, S P	P82	123	Pietrzyk, M+	22.3	30
Lyubutin, S K	35.5, P57	49, 117	Pinchuk, A A	58.4	100
Ma Pierre, J+	11.5	19	Pirjola, R+	38.3	53
Maack, J	18.2	25	Pivnenko, S+	28.3, 41.3	96, 97
MacKay, AJ	67.3	91	Plaksina, S	P24, P61	109, 118
Madrid, M	32.5	45	Plygach, V A	P45	115
Magda, I+	6.1, 67.2	11, 91	Pochanin, G+	P53	116
Makowsky, L	66.2	89	Polevin, S D	6.2, 6.5	12, 95
Mallepeyre, V	5.1, 59.2	10, 79	Poljak, D	43.4	61
Maloney, J+	30.5	41	Potemin, R V	P82	123
Manuel, J	39.5	56	Poyedinchuk, A E+	55.5	76
Mar, A	40.3	57	Prather, W	26.2, 34.4, 59.4 64.1	35, 48, 80, 86
Marinelli, Vincent	56.2	98	Primak, S L+	12.4	20
Marinescu, M J	50.4, P3	69, 113	Prokhorenko, V+	5.5, 40.4	11, 97
Martel, C	46.1	64	Proskurovsky, D I	6.5	95
Martin, R G	43.3	61	Puikkinen, A	38.	53
Martynov, L	63.2	85	Rachidi, F+	63.2	85
Maruyama, X K+	56.1	76	Radasky, W+	3.3, 3.5, 42.4	8, 60
Matthews, R+	65.2	87	Raguin, J Y	P8	104
Mattsson, J+	65.1	87	Rassadin, B M	P21	108
Mayouf, A+	P13, P14	106	Ratcliffe, J A+	46.3	65
McGowen, A	43.4	61	Rauschenbach, P	10.5	18
McQuilton, D	7.3	13	Redfern, M	16.1, 16.2	23, 24
Meadows, E	29.2	39	Reiter, J	27.3	37
Melnikov, G V	P7	104	Rekin, I B	P40	114
Menvielle, M+	33.4	46	Repin, A	68.3	101
Merih Büyükdura, O	21.3	29	Rhebergen, J+	71.1	92
Merritt, James H+	58.3	79	Rice, P	53.1	72
Mesyats, G A	6.5	95	Riggs, L+	24.5	34
Mheidze, G P	P59	118	Ritter, J+	27.3	37
Mikhailov, V	P24, P61	109, 118	Rivera, T	65.5	89
Miletta, J	45.1	63	Robinson, J	31.1	42
Miller, J R	23.2, 50.2	31, 69	Romanova, E+	P56	117
Milyaev, P+	47.5	67	Ronald, K	1.2, 52.3, 57.1, P29	5, 72, 77, 111
Mintsev, V B+	P6, P7	104	Rooney, M	11.5	19
Mo, C	13.4, 36.3	22, 51	Roschupkin, S	P61	118
Mokochunin, V L	P45	115	Rosen, E+	51.1, 71.4	70, 93
Moncho, S	35.1, 35.2	48, 49	Rosberg, M	10.5	18
Monos, S	32.1	44	Rostov, V V	6.2, 58.1	12, 99
Morgan, M+	12.2	20	Rothenhaeusler, M+	18.3	25
Mozjoukhine, G+	P81	123	Rowley, Ray	59.5	80
Muenchausen, R	65.5	89	Roy, J	12.4	20
Mulvaney, J Michael	44.4	63	Ruffing, K+	11.1	18
Murav'ev, V V+	58.4	100	Rukin, S N	35.5, P57	49, 177
Murphy, Michael R	58.3	79	Russo, P	53.3	73
Murso, M	27.3	37	Ryazantseva, N	P68	120
Naus, R	11.2	18	Rybin, O N	P75	121
Nelson, C	51.2, 66.3	70, 89	Sabatier, J	51.1	70
Nelson, E	1.3	5	Sachs, J	10.5, 46.3	18, 65
Nerukh, A+	43.5, P72, P76	61, 120, 121	Saethre, E+	38.5	54
Nesterov, E	P24, P61	109, 118	Sagues, L+	39.5	56
Neuber, A	2.4	7	Sahli, H	46.3, 66.5	65, 90
Nicoara, B+	8.2	14	Sakhnenko, N	P76	121
Nicol, D	38.4	54	Salman, A O	17.1	24
Nikulin, P V	P45	115	Saimoria, G V+	2.1, 2.2	6
Nimtz, G+	21.5	29	Sami, G M	37.2, 37.5	52, 53
Nitsch, D+	18.2	25	Samsonov, S V	52.3, 57.2, P9, P25, P31	72, 78, 105, 110, 111
Nitsch, J	8.1, 23.5	14, 32	Sanchez, JA	65.5	89
Nivelle, F	71.2	93	Sancho, M	60.3	81
Novikov, V	67.2	91	Sarajcev, I	63.1	85
O'Bryon, J F	8.5, 25.1, 29.4 36.6	15, 34, 40	Sarjeant, W	2.3	6
Ofitserov, M M	P9, P31	105, 111	Sasse, H+	63.5	86
Ohnstad, T M	38.5	54	Sato, M+	39.4	55
Okhmatovsky, V	37.4	52	Savenko, Y	58.5, P49	100, 115
Ostaphiychuk, N A	32.2	96	Savilov, A	57.2, P25, P30	78, 110, 111
Ostaphiychuk, R M	32.2	96	Savvin, V+	P11	105
Ostashev, V E+	P54, P55	116	Sazak, BA+	68.4	92
Oughstun, K E+	22.4, 47.3	30, 66	Schachter, L	52.5	72
Oulmasculov, M R	35.5, 40.1	49, 56	Schamiloglu, E	1.1, 40.3, 7.1	5, 57, 12
Pande, D C+	12.5	21	Schantz, H+	21.4, 59.3	29, 79
Panteleev, S V	P34	112	Schätzing, W	44.1	62

# Author's Index

Scheibe, H P	44.1	62	Tsvetkov, V I	P7	104
Scheitrum, G	1.3	5	Tuchkin, Y+	55.2, 60.1	75, 80
Scherbatko, I	P76	121	Turbin, P	P12	106
Schieber, D	52.5	72	Turchin, V	54.5	74
Scholfeld, DW	59.4	80	Turner, T	18.4	26
Schultz, S	18.3	25	Tyo, S+	47.4, 54.4	66, 74
Scott, W	18.5, 36.3	26, 51	Uguen, B	28.2, 39.3	38, 55
Sebastian, J L+	60.3	81	Ulander, Lars M H+	PL3	126
Seida, O A+	37.2	52	Ulmaskulov, M R	P29	111
Selina, E E	15.2, 32.3	23, 44	Ul'yanov, A V	P54, P55	116
Semenchuk, V E	P82	123	Ulyanov, D	52.4	72
Sencer Koç, S	21.3	29	Ushnurtsev, A E	P6, P7	104
Seow, T S+	8.4	14	Uslenghi, P+	9.5	16
Serafin, D+	25.4	34	Vadim, D	53.4, P77	73, 121
Seregelyi, J S+	65.3	88	Valder, K	56.3	77
Sergeev, A S	1.2, P29, P83	5, 111, 124	Van Bladel, J+	4.1	9
Shapiro, A	P10	105	Van Genderen, P	5.3	10
Shapoval, I	67.2	91	Van Thielen, B+	36.1	50
Shepherd, PR	30.2	41	Vandenbosch, Guy	15.3	23
Sherbatko, I+	43.5	61	Vanderbosch, G	36.1	50
Sherbondy, K	51.1, 51.2, 66.3, 71.4	70, 89, 93	Vanheeghe, P	71.2	93
Shevchuk, V	P10	105	Vdovin, V	P58	117
Shipilov, S	5.4	10	Velychko, L+	34.5	48
Shkurin, E V	P39	113	Venet, D	35.1, 35.2	48, 49
Shlivinski, A	4.4, 30.6	9, 42	Vertiy, A+	17.1, 17.2	24
Short, B	35.4	49	Viljanen, A	38.3	53
Shpak, V G	35.5, 40.1, P29	49, 56, 111	Vinogradov, S	30.3, 30.4	41
Shul'ga, N	P26	110	Vinogradova, ED+	60.2	81
Shumilin, V	P3, P58	104, 117	Virchenko, V+	P77	121
Shunailov, S A	35.5, 40.1, P29	49, 56, 111	Vodopianov, G	63.2	85
Shurupov, A V	P6, P7	104	von Siemens, C F	27.1	36
Shvartsburg, A B+	43.2	60	Vorgul, I+	P18	107
Sidoruk, P A	P39, P40	113, 114	Voss, D	32.6	45
Silva Paula, M M	2.2	6	Voynovskiy, I	17.1, 17.2	24
Simniskis, R	7.1	12	Vucak, S	63.1	85
Sini, L	3.1	7	Vysotskii, V+	58.4, P67	100, 119
Sinitsky, S L	57.5, P38, P83	99, 113, 124	Wallace, C+	62.4	84
Sirenko, Y	34.5, P65, P73, P78	48, 119, 120, 122	Wang, Yong	66.4	90
Sizranov, V+	8.3	14	Wasylikiwskiy, W	50.1	68
Skulkin, S+	54.5	74	Watkins, S P+	7.4	13
Slipchenko, N I+	P75	121	Weaver, D	66.2	89
Slovikovskiy, B G	35.5, P57	49, 117	Weaver, R	66.1	89
Smirnova, I	54.1	98	Weber, T+	36.2	50
Smith, D+	51.2, 66.3	70, 89	Wei, L	26.4	36
Smith, G	30.5	41	Weiland, T	19.2	27
Smith, K	42.4	60	Whyman, N L+	31.4	43
Smith, P	30.3, 60.2, 62.2, 62.3	41, 81, 83, 84	Whyte, C G	1.2, 52.3, 57.1	5, 72, 77
Sokovikh, V V	P35	112	Wiert, J	7.5	13
Soluyanov, E	68.2	91	Wieting, T	29.5, 62.5	40, 84
Song, Z	52.2	71	Wiggins, S M	P29	111
Sonnemann, F	12.1, 18.1, 35.3	20, 25, 49	Wik, M+	3.3, 3.5	8
Spark, S	6.3, 25.3	12, 95	Wilbers, A+	11.2	18
Stahlhofen, A A	21.5	29	Wilke, M+	19.2	27
Steinberg, B Z	21.1	28	Willis, A	19.4	27
Steinmetz, T	23.5	32	Wioland, R	6.2	12
Stepanov, V D	57.5, P83	99, 124	Wollenberg, Ing G	44.1	62
Stepanuyk, V	17.2	24	Wu, D-H+	62.5	84
Stephen, W	46.2	64	Xiao, H	47.3	66
Stewart, R W+	18.5	26	Yachin, V+	P68	120
Stone, A+	55.1	75	Yaghjian, A D+	9.1	15
Stoudt, D C+	3.2, 13.2, 13.3	7, 21	Yagolnikov, S	P10	105
Stoukatch, O V+	P66, P82	119, 123	Yakovenko, V+	52.1	71
Stoupei, E G+	53.2	73	Yakubov, V	5.4	10
Streikov, P+	52.4	72	Yalandin, M I	35.5, 40.1, P29	49, 56, 111
Stroganov, V+	P24, P61	109, 118	Yaldiz, E	34.5, P65	48, 119
Stupitsky, E+	68.3	101	Yankovskii, B D	P54, P55	116
Sturm, A+	27.2	37	Yapar, A	37.1	52
Sugak, V+	P52	116	Yarin, P	40.2, 44.2, P41	57, 62, 114
Sukhov, M Yu	6.5	95	Yarovoy, A G+	5.3	10
Sulkes, J	53.2	73	Yashina, N+	P65, P73, P78	118, 120, 122
Sullivan, A	56.5	77	Yastrebov, V	68.2	91
Sunderland, K V	23.2	31	Yatsik, V+	P79	122
Svezhentsev, A Y+	15.3	23	Yemelyanov, K+	P72	120
Syzranov, V S	P54	116	Yeo, P C	8.4	14
Tamelo, A A	58.4	100	Younan, N+	49.3	68
Tantum, S	71.3	93	Young, A	57.1	77
Tarakanov, V P	6.2, P29, P55	12, 111, 116	Young, A R	52.3	72
Tattersall, JH	53.1	72	Yu, K	P10	105
Taylor, C	49.3	68	Zadernovsky, A+	P33	112
Taylor, J D+	10.1	17	Zaginaylov, G+	P8, P12	104, 106
Tayyar, I H+	7.2, 15.1	13, 23	Zagoskin, V V	P82	123
Tesche, F M	8.2, 37.3	14, 52	Zange, R	44.1	62
Tesny, N	45.1	63	Zavialov, M	P10	105
Tham, C Y+	43.4	61	Zazulin, S	54.1, 54.2	98
Thomsen, K+	56.3	77	Zelic, I+	63.1	85
Thomsen, Kurt O	61.4	83	Zhang, J	67.1	90
Thomson, A	38.4	54	Zherlitsyn, A G	P7	104
Thornhill, C	39.1, 59.5	54, 80	Zhoubing, Y	26.4	36
Tijhuis, A+	49.1, 60.4, 60.5	67, 81, 82	Zhukov, A+	P27	110
Timmons, M+	32.6	45	Zhuravliov, V+	P50	115
Tkachenko, S	63.2	85	Zinkovskiy, Y+	58.5, P49	100, 115
Towers, M S	43.4	61	Zotova, I V	P29	111
Trakhtengerts, V Y	15.2	23	Zucco, C	2.1	6
Tretyakov, O+	55.4	76	Zutavov, F J	40.3	57
Tsiranov, S N	P57	117	Zwamborn, P	49.1	67